

REPORT DOCUMENTATION PAGE

Form Approved
OMB No. 0704-0188

Public reporting burden for this collection of information is estimated to average 1 hour per response, including the time for reviewing instructions, searching existing data sources, gathering and maintaining the data needed, and completing and reviewing the collection of information. Send comments regarding this burden estimate or any other aspect of this collection of information, including suggestions for reducing this burden to Washington Headquarters Services, Directorate for Information Operations and Reports, 1215 Jefferson Davis Highway, Suite 1204, Arlington, VA 22202-4302, and to the Office of Management and Budget, Paperwork Reduction Project (0704-0188), Washington, DC 20503

1. AGENCY USE ONLY (Leave Blank)

2. REPORT DATE
DECEMBER 1995

3. REPORT TYPE AND DATES COVERED
Final: July 1994 - 30 Sept. 1995

4. TITLE AND SUBTITLE

RECOMBINATION, ELECTRON-EXCITED ATOM COLLISIONS
AND ION-MOLECULE REACTIONS

5. FUNDING NUMBERS

AFOSR
~~F49620-94-1-0379~~
61102F
23011DS

6. AUTHOR(S)

M. R. Flannery

7. PERFORMING ORGANIZATION NAME(S) AND ADDRESS(ES)

School of Physics
Georgia Institute of Technology
Atlanta, Georgia 30332-0430

8. PERFORMING ORGANIZATION REPORT NUMBER

GIT-94-001

AFOSR TR 96

9. SPONSORING/MONITORING AGENCY NAME(S) AND ADDRESS(ES)

AFOSR/NE
110 Duncan Avenue
Suite B115
Bolling AFB, D. C. 20332-0001

10. SPONSORING/MONITORING AGENCY REPORT NUMBER

0045
F49620-94-1-0379

11. SUPPLEMENTARY NOTES COR:

12. DISTRIBUTION/AVAILABILITY STATEMENT

Approved for public release.
Distribution is unlimited.

13. DISTRIBUTION CODE

14. ABSTRACT (Maximum 200 words)

This report summarizes all of the basic Physics research performed and published on the following topics:

- (A) Dissociative Recombination. (B) Electron-Excited Atom Collisions.
- (C) General Electron-Ion and Ion-Ion Recombination Processes and
- (D) Elastic Scattering: Classical, Quantal, and Semiclassical Theories.

19960206 070

15. SUBJECT TERMS

Recombination, Dissociative, Electron-Ion, Ion-Ion,
Excited Atoms, Elastic Scattering.

16. NUMBER OF PAGES

17. PRICE CODE

18. SECURITY CLASSIFICATION OF REPORT

Unclassified

19. SECURITY CLASSIFICATION OF THIS PAGE

Unclassified

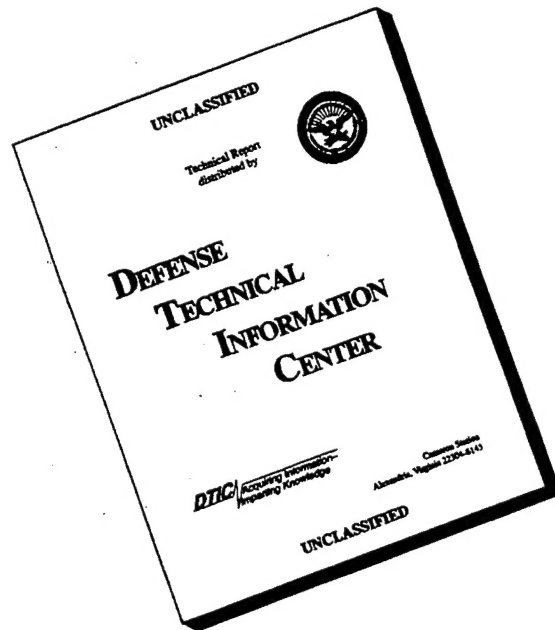
20. SECURITY CLASSIFICATION OF ABSTRACT

Unclassified

21. LIMITATION OF ABSTRACT

UL

DISCLAIMER NOTICE



**THIS DOCUMENT IS BEST
QUALITY AVAILABLE. THE
COPY FURNISHED TO DTIC
CONTAINED A SIGNIFICANT
NUMBER OF PAGES WHICH DO
NOT REPRODUCE LEGIBLY.**

Table of Contents

	Abstract	2
I.	Introduction	3
II.	Research Completed	3
III.	Research Published and In Press	4
IV.	Technology Transitions and Transfers	5
V.	Research Abstracts	7
VI.	PIADC Survey Form	10
VII.	Appendix A: Semiclassical Theory of Direct Dissociative Recombination	13
VIII.	Appendix B: The Semiclassical-Classical Path Theory of Direct Electron-Ion Dissociative Recombination and $e^- + H_3^+$ Recombination	38
IX.	Appendix C: Electron-Ion and Ion-Ion Recombination	53
X.	Appendix D: Rydberg Collisions: Binary Encounter, Born and Impulse Approximations	80
XI.	Appendix E: Elastic Scattering: Classical, Quantal and Semiclassical	105

**Annual Technical Report
(7/1/94 - 9/30/95)**

Abstract

This report is a summary of all the research performed on the project entitled "Recombination, electron-excited atom collisions and Ion-Molecule Reactions". Basic theoretical research was completed and published on the following topics:

- (A) Dissociative Recombination
- (B) Electron-Excited Atom Collisions
- (C) Electron-Ion and Ion-Ion Recombination Processes
- (D) Elastic Scattering: Classical, Quantal, and Semiclassical

I. Introduction

This report summarizes all of the basic Physics research performed and published on the project:

Title: Recombination, electron-excited atom collisions and Ion-Molecule reactions.

Grant Number: F49620-94-1-0379

Award Amount: \$105,000.

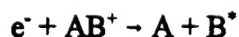
Award Period: 94/07/01 - 95/09/30

The objectives of this basic research program was to formulate, develop, and implement theoretical methods essential to the physics of electronic and atomic collision processes with relevance to various Air Force Missions.

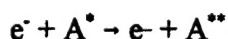
II. Research Completed

Research was completed on the following topics:

(A) Dissociative Recombination:



(B) Electron-(excited) Atom Collisions:



(C) General Electron-Ion and Ion-Ion Recombination Processes:

(D) Elastic Scattering: Classical, Quantal, and Semiclassical Theories.

III. Research Published and In Press

1. M. R. Flannery, "Semiclassical Theory of Direct Dissociative Recombination", in "Atomic Collisions", (D. R. Schultz, M. R. Strayer and J. H. Macek, eds.) AIP Press, 1995), pp. 53-75. Reprinted as Appendix A.
2. M. R. Flannery, "Semiclassical-Classical Path Theory of Direct Electron-Ion Dissociative Recombination and $e^- + H_3^+$ Recombination", Int. J. Mass Spectrom. (1996), in press. Reprinted as Appendix B.
3. M. R. Flannery, "Electron-Ion and Ion-Ion Recombination Processes", in Atomic, Molecular, and Optical Physics Handbook, AIP Press (1996), in press. Reprinted as Appendix C.
4. E. J. Mansky, "Rydberg Collisions: Binary Encounter, Born and Impulse Approximations", in Atomic, Molecular and Optical Physics Handbook, AIP Press (1996), in press. Reprinted as Appendix D.
5. M. R. Flannery, "Elastic Scattering: Classical, Quantal, and Semiclassical", in "Atomic, Molecular, and Optical Physics Handbook", AIP Press (1996), in press. Reprinted as Appendix E.
6. E. J. Mansky and M. R. Flannery, "Automatic Generation of Analytical Matrix Elements for Electron-Atom Scattering", Comput. Phys. Commun. 88 (1995) 278-292. 6 Reprints attached in separate Report GIT-94-003.
7. E. J. Mansky and M. R. Flannery, "The Multichannel Eikonal Theory Program for Electron-Atom Scattering", Comput. Phys. Commun. 88 (1995) 249-277. 6 Reprints attached in separate Report GIT-94-002.

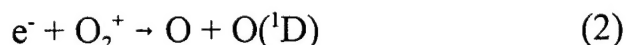
The abstracts of publications #6 and 7 are printed in Section V.

IV. Technology Transitions and Transfers with Phillips Laboratory Resulting from the Research Work of M.R. Flannery on Recombination.

A. Environmental connection: The present program on theoretical treatments of the rate and cross sections for the **Dissociative Recombination Process:**

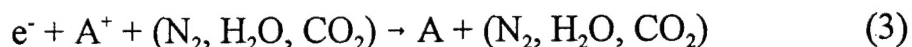


is very important to the environmental program of Dr. A.A. Viggiano and Dr. T. Miller at Phillips Laboratory, Hanscomb Air Force Base. Interactions of the neutral products of (1), particularly the excited state products e.g. $O^*(^1D)$ and N^* , with the greenhouse gases SF_6 and CF_4 are important to the physics of the Greenhouse Effect. The Greenhouse gases SF_6 and CF_4 have long lifetimes in the atmosphere. They are unreactive with the usual atmospheric ground state species and with the usual atmospheric cleansing agent OH. They, however, react strongly with $O(^1D)$, an excited metastable oxygen atom, which is produced in the dissociative recombination process



between the electrons e^- and molecular O_2^+ ions in the atmosphere. The dissociative recombination process (2) is the dominate source of metastable $O(^1D)$ which then react and cause fragmentation of the greenhouse gases SF_6 and CF_4 . How much $O(^1D)$ is produced and how fast it is produced is therefore of key significance. Examination of (1) provides the answer.

B. Re-Entry Flowfields: The present program on theoretical treatments of the **Three-Body Recombination Process:**



is very important to the program of Dr. R.A. Morris at Phillips Laboratory. It is key to the analysis of re-entry flowfields of spacecraft and the subsequent wake-neutralization. Here the positive ions A^+ are the alkali (ablated) contaminants in space craft materials and the third bodies (N_2, H_2O, CO_2) are atmospheric species. The wake-neutralization between electrons and positive ions occurs via (3) and is strongly dependent on the nature of the third bodies. Neutralization is also effected by **Dissociative Recombination**



with atmospheric ions NO^+ . Processes (3) and (4) control the electron concentration in the plasma. These processes have quite different physical mechanisms. Knowledge of the partitioning of electron depletion between processes (3) and (4) is extremely important and is addressed by Flannery's research.

IV. Research Abstracts

REPORT DOCUMENTATION PAGE

Form Approved
OMB No. 0704-0188

Public reporting burden for this collection of information is estimated to average 1 hour per response, including the time for reviewing instructions, searching existing data sources, gathering and maintaining the data needed, and completing and reviewing the collection of information. Send comments regarding this burden estimate or any other aspect of this collection of information, including suggestions for reducing this burden to Washington Headquarters Services, Directorate for Information Operations and Reports, 1215 Jefferson Davis Highway, Suite 1204, Arlington, VA 22202-4302, and to the Office of Management and Budget, Paperwork Reduction Project (0704-0188), Washington, DC 20503

1. AGENCY USE ONLY (Leave Blank)		2. REPORT DATE December 1995	3. REPORT TYPE AND DATES COVERED Reprint: 1 July 1994 - 30 Sept. 1995	
4. TITLE AND SUBTITLE AUTOMATIC GENERATION OF ANALYTICAL MATRIX ELEMENTS FOR ELECTRON-ATOM SCATTERING			5. FUNDING NUMBERS AFOSR F49620-94-1-0379	
6. AUTHOR(S) E. J. Mansky and M. R. Flannery				
7. PERFORMING ORGANIZATION NAME(S) AND ADDRESS(ES) School of Physics Georgia Institute of Technology Atlanta, Georgia 30332			8. PERFORMING ORGANIZATION REPORT NUMBER GIT-94-003	
9. SPONSORING/MONITORING AGENCY NAME(S) AND ADDRESS(ES) AFOSR/NE 110 Duncan Avenue Suite B-15 Bolling AFB, D. C. 20332-0001			10. SPONSORING/MONITORING AGENCY REPORT NUMBER	
11. SUPPLEMENTARY NOTES COR: Reprint: Computer Physics Commun. <u>88</u> (1995) pp. 278-292.				
12a. DISTRIBUTION/AVAILABILITY STATEMENT Approved for public release. Distribution is unlimited.			12b. DISTRIBUTION CODE	
13. ABSTRACT (Maximum 200 words) Abstract A code which can be used to automatically generate entire sets of analytical matrix elements of the instantaneous electrostatic interaction potential between the projectile electron and the target atom is described. The code can be used at present for both hydrogen and helium target atoms. In the case of hydrogen, the present code <i>V_{ij}</i> generalizes and extends an earlier code of Jamison [1]; while in the case of helium, Hartree-Fock frozen-core wave-functions are used to represent the two-electron wavefunctions. When an entire set of matrix elements is generated, a complete set of FORTRAN subroutines is produced which can be directly incorporated into the code MET_cross used to solve the multichannel eikonal theory (see accompanying paper). A principal application of the code <i>V_{ij}</i> is to aid the elucidation of the systematic trends observed in transitions among metastable states in electron-atom collisions by studying the functional form of the underlying interaction matrix elements.				
14. SUBJECT TERMS Keywords: interaction matrix elements, inelastic, analytical electron-atom matrix elements, Hartree-Fock, frozen-core, wavefunctions			15. NUMBER OF PAGES	
			16. PRICE CODE	
17. SECURITY CLASSIFICATION OF REPORT Unclassified	18. SECURITY CLASSIFICATION OF THIS PAGE Unclassified	19. SECURITY CLASSIFICATION OF ABSTRACT Unclassified	20. LIMITATION OF ABSTRACT UL	

Reprinted from

Computer Physics Communications

Computer Physics Communications 88 (1995) 278–292

Automatic generation of analytical matrix elements for electron–atom scattering

E.J. Mansky ¹, M.R. Flannery

School of Physics, Georgia Institute of Technology, Atlanta, GA 30332-0430, USA

Received 28 July 1994



COMPUTER PHYSICS COMMUNICATIONS

An international journal and program library for computational physics and physical chemistry

Honorary Editor: P.G. BURKE, Belfast

Principal Editors

Geerd H.F. DIERCKSEN

Max-Planck-Institut für Astrophysik, Karl-Schwarzschild
Strasse 1, D-85740 Garching bei München, Germany

James W. EASTWOOD

Culham Laboratory, Abingdon, Oxfordshire OX14 3DB, UK

J.E. INGLESFIELD

ESM, Department of physics, Catholic University of Nijmegen,
Toernooiveld, 6525 ED Nijmegen, The Netherlands

F. JAMES

CERN, Data Handling Division, CH-1211 Geneva 23,
Switzerland

Editors in specialist fields

The complete mailing addresses of all Editors in specialist fields are printed at the beginning of each volume.

Algebraic manipulation

J. CIZEK, Waterloo, Ont., Canada

J.P. FITCH, Bath, UK

A.C. HEARN, Santa Monica, CA

Astrophysics

D.G. HUMMER, München, Germany

M.L. NORMAN, Urbana, IL

W.M. TSCHARNUTER, Heidelberg,
Germany

Atomic and molecular dynamics

B.H. BRANSDEN, Durham, UK

D.C. CLARY, Cambridge, UK

T.H. DUNNING, Jr., Richland, WA

F.A. GIANTURCO, Rome, Italy

J.-M. LAUNAY, Meudon, France

H. NAKAMURA, Okazaki, Japan

J. READING, College Station, TX

G.C. SCHATZ, Evanston, IL

R.E. WYATT, Austin, TX

Atomic and molecular structure, spectra and properties

W. DUCH, Torun, Poland

Donald G. TRUHLAR

University of Minnesota, Department of Chemistry and
Supercomputer Institute, 207 Pleasant Street S.E., Minneapolis,
MN 55455, USA

Program Librarian

Miss C. JACKSON

Department of Applied Mathematics,
Queen's University of Belfast, Belfast BT7 1NN, N. Ireland

Program Library Director

P.G. BURKE

Department of Applied Mathematics,
Queen's University of Belfast, Belfast BT7 1NN, N. Ireland

C.F. FISCHER, Nashville, TN

I.P. GRANT, Oxford, England

I. SHAVITT, Columbus, OH

B.T. SUTCLIFFE, Heslington, UK

Algorithms, software and architectures

J.M. BOYLE, Argonne, IL

I.S. DUFF, Chilton, UK

Y. MURAOKA, Tokyo, Japan

W. SCHÖNAUER, Karlsruhe, Germany

N.S. SCOTT, Belfast, N. Ireland

Biophysics and biochemistry

B. MONTGOMERY PETTITT,
Houston, TX

Condensed matter physics

C.R.A. CATLOW, London, UK

D. FINCHAM, Keele, UK

R. HAYDOCK, Eugene, OR

O.H. NIELSEN, Lyngby, Denmark

S.B. TRICKEY, Gainesville, FL

Electromagnetics

D.A. McNAMARA, Pretoria,
South Africa

High energy physics

B. van ELJK, Amsterdam,
The Netherlands

C.B. LANG, Graz, Austria

J. LINNEMANN, East Lansing, MI

Y. OYANAGI, Tokyo, Japan

C. REBBI, Boston, MA

Nuclear physics

I.R. AFNAN, Adelaide, Australia

B.S. NILSSON, Copenhagen, Denmark

V.R. PANDHARIPANDE, Urbana, IL

Plasma physics

D.C. BARNES, Los Alamos, NM

D.F. DÜCHS, Garching bei München,
Germany

D.W. HEWETT, Livermore, CA

Statistical mechanics and many body physics

K. BINDER, Mainz, Germany

M. PARRINELLO, Stuttgart, Germany

Statistics and data analysis

F. JAMES, Geneva, Switzerland

J. LINNEMANN, East Lansing, MI

Aims and Scope

Computer Physics Communications is an international interdisciplinary journal in which computational physicists and physical chemists can record their computing research and express their views, and which they can consult for the most recent developments in computing techniques in their field. Two classes of papers are published:

(i) Papers in the general area of computational physics and physical chemistry, concerned with computational methods and the application of computers to physics and physical chemistry.

(ii) Write-ups describing programs to be held in the CPC Program Library.

Abstracted/Indexed in:

Chemical Abstracts; Current Contents: Engineering, Technology & Applied Sciences; EI Compendex Plus; Engineering Index; INSPEC.

Subscription Information 1995

Volumes 86-92 of *Computer Physics Communications* (ISSN 0010-4655) are scheduled for publication. (Frequency: monthly.) Prices are available upon request from the publisher.

Subscriptions are accepted on a prepaid basis only and are entered on a calendar year basis. Issues are sent by SAL (Surface Air Lifted) mail wherever this service is available. Airmail rates are available upon request. Please address all enquiries regarding orders and subscriptions to:

Elsevier Science B.V.

Order Fulfilment Department

P.O. Box 211, 1000 AE Amsterdam

The Netherlands

Tel. +31 20 4853642, Fax. +31 20 4853598

Claims for issues not received should be made within six months of our publication (mailing) date.

US mailing notice - Computer Physics Communications (ISSN 0010-4655) is published monthly by Elsevier Science B.V., Molenwerf 1, P.O. Box 211, 1000 AE Amsterdam, The Netherlands. Annual subscription price in the USA US\$ 2299.00 (valid in North, Central and South America only), including air speed delivery. Second class postage paid at Jamaica, NY 11431.

USA POSTMASTERS: Send address changes to Computer Physics Communications, Publications Expediting, Inc., 200 Meacham Avenue, Elmont, NY 11003. Airfreight and mailing in the USA by Publications Expediting.

© The paper used in this publication meets the requirements of ANSI/NISO Z39.48-1992 (Permanence of Paper).



North-Holland, an imprint of Elsevier Science

Printed in The Netherlands



ELSEVIER

Computer Physics Communications 88 (1995) 278–292

Computer Physics
Communications

Automatic generation of analytical matrix elements for electron–atom scattering

E.J. Mansky¹, M.R. Flannery

School of Physics, Georgia Institute of Technology, Atlanta, GA 30332-0430, USA

Received 28 July 1994

Abstract

A code which can be used to automatically generate entire sets of analytical matrix elements of the instantaneous electrostatic interaction potential between the projectile electron and the target atom is described. The code can be used at present for both hydrogen and helium target atoms. In the case of hydrogen, the present code *Vij* generalizes and extends an earlier code of Jamison [1]; while in the case of helium, Hartree–Fock frozen-core wave-functions are used to represent the two-electron wavefunctions. When an entire set of matrix elements is generated, a complete set of FORTRAN subroutines is produced which can be directly incorporated into the code *MET_cross* used to solve the multichannel eikonal theory (see accompanying paper). A principal application of the code *Vij* is to aid the elucidation of the systematic trends observed in transitions among metastable states in electron–atom collisions by studying the functional form of the underlying interaction matrix elements.

PROGRAM SUMMARY

Title of program: *Vij*

Catalogue number: ADAX

Program obtainable from: CPC Program Library, Queen's University of Belfast, N. Ireland (see application form in this issue)

Licensing provisions: none

Computers for which the program is designed and others on which it has been tested: IBM RS/6000 and HP/Apollo 9000 model 700 series workstations with a FORTRAN 77 compiler. With minor changes the program will also run on CDC 800 series mainframes and Cray supercomputers (see comment cards in code for details).

Computers: IBM RS/6000 model 520 and HP/Apollo 9000 model 730 workstations; *Installation:* School of Physics, Georgia Institute of Technology.

Operating systems: AIX 3.1.7, HP-UX 8.07, 9.01

Programming Language used: FORTRAN 77

Memory required to execute with typical data: 3848 words

No. of bits in a word: 32

Peripherals used: Terminal or card reader for data input. Terminal, line printer or magnetic disk for storage of output data.

No. of lines in distributed program, including test data, etc: 3022

Keywords: interaction matrix elements, inelastic, analytical electron-atom matrix elements, Hartree-Fock, frozen-core, wavefunctions

¹ E-mail address: mansky@eikonal.physics.gatech.edu.

Nature of physical problem

Generation of individual or complete sets of analytical interaction matrix elements for use in electron–atom scattering codes.

Method of solution

The core of the present program is a generalization of a hydrogenic interaction matrix elements code of Jamison [1] which has been extended to deal with both electron–hydrogen and electron–helium interaction matrix elements. In the case of He, the Hartree–Fock frozen-core wavefunctions of Cohen and McEachran and co-workers [2,3] are used in the representation of the Slater form of the two-electron wavefunctions required in the matrix element calculation.

Restrictions on the complexity of the problem

There are no limits on the number of individual matrix elements which can be generated at a given time. In generating complete sets of matrix elements the program is limited to orbitals with principal quantum number $n \leq 6$. The restriction $n \leq 6$ can be relaxed for H, but cannot at present be relaxed for He due to the use of the frozen-core Hartree–Fock wave-functions [2,3].

Typical running times: between 4 and 24 seconds

References

- [1] M.J. Jamison, Comput. Phys. Commun. 1 (1970) 437.
- [2] M. Cohen and R.P. McEachran, Proc. Phys. Soc. 92 (1967) 37.
- [3] R.P. McEachran and M. Cohen, J. Phys. B 2 (1969) 1271.

LONG WRITE-UP

1. Introduction

One of the central quantities in the formulation of both quantal and semiclassical scattering theories of the electronic excitation of atoms are the matrix elements of the instantaneous electrostatic interaction,

$$V_{nj}(\mathbf{R}) = \langle \Psi_n | V(\mathbf{R}, \{\mathbf{r}_i\}) | \Psi_j \rangle, \quad (1)$$

which characterizes the potential energy of the interaction between the projectile electron and the target atom. Over twenty years ago Jamison published in this journal [1] a code for the evaluation of (1) for hydrogenic wavefunctions. In this paper we generalize and extend Jamison's code for hydrogenic target wavefunctions to handle two-electron Hartree–Fock frozen-core wavefunctions and to automatically generate a FORTRAN code for the evaluation of the analytical expressions which result from [1]. The present code `v i j` can be used to generate individual matrix elements V_{nj} , or entire sets $\{V_{nj}\}$ suitable for direct incorporation into the multichannel eikonal scattering code `MET_cross` (see accompanying paper). Knowledge of the analytical behavior of the interaction matrix elements (1), with respect to the projectile–target relative separation \mathbf{R} , in addition provides insight into the mechanism for the direct electronic excitation in the bound–bound transition $j \rightarrow n$ and hence is important in elucidating the role various multipole terms play in electronic transitions among metastable states of H and He.

The remainder of this paper is organized as follows. Section 2 presents the functional form of the direct interaction matrix elements V_{nj} for the hydrogenic and two-electron atomic targets of interest to us. In Section 3 a description of the algorithm used to generate the matrix elements (1) is given, while a sample of the output produced by `v i j` is provided in Section 4. Unless otherwise noted, atomic units are used throughout the paper. Program names in this paper are indicated in `typewriter` type-set, while names of modules are given in **boldface**.

2. Theory

The basic theory for the hydrogenic case has been covered in detail by Jamison [1], while Flannery and McCann [2] have considered the two-electron case using the Hartree–Fock frozen-core wavefunctions of

Cohen and McEachran [3–6]. Here we simply collect together the central formulae and refer the interested reader to the atomic physics literature for details.

2.1. Hydrogen

In the case of hydrogen the matrix elements of the Coulomb interaction between the projectile and target electrons is expressed [1] as

$$V_{ji}^{(ee)}(\mathbf{R}) = \int \psi_j^*(\mathbf{r}) \frac{1}{|\mathbf{R} - \mathbf{r}|} \psi_i(\mathbf{r}) d\mathbf{r}, \quad (2)$$

where the hydrogenic wavefunctions for the initial and final states are given, respectively, by ψ_i and ψ_j , and the integration is over the coordinate \mathbf{r} of the electron bound to the H^+ core. Upon application of the multipole expansion [7] to the Coulomb interaction, the matrix elements $V_{nj}(\mathbf{R})$ can be expressed as analytical functions of the projectile–target distance \mathbf{R} . The resultant analytical expression (see below) facilitates the investigation of the underlying physics responsible for the systematic trends observed in metastable atom collisions [8,9]. After expressing the hydrogenic wavefunctions in terms of the associated Laguerre polynomials [10–13] $L_{n+\ell}^{(2\ell+1)}(2\beta r)$ ($\beta = Z/n$), and some algebraic manipulation, the following expression is obtained:

$$V_{ji}^{(ee)}(\mathbf{R}) = 4\pi \sum_{k=0}^{n+\ell} A_k^{(n\ell)} \sum_{k'=0}^{n'+\ell'} A_{k'}^{(n'\ell')} \sum_{L=|\ell-\ell'|}^{\ell+\ell'} \sum_{M=-L}^L \frac{(-1)^M}{2L+1} D(\ell, L, \ell'; m, -M, m') Y_{LM}(\hat{\mathbf{R}}) \\ \times \left[\frac{(K+2L+2)!}{\gamma^{K+2L+3}} \frac{1}{R^{L+1}} + e^{-\beta R} \left(R^L \sum_{p=0}^P \frac{(K+1)!}{\gamma^{K+2-p}} \frac{R^p}{p!} - \frac{1}{R^{L+1}} \sum_{q=0}^Q \frac{(K+2L+2)!}{\gamma^{K+2L+3-q}} \frac{R^q}{q!} \right) \right], \quad (3)$$

with $K \equiv \ell + \ell' + k + k' - L$, $Q = K + 2L + 2$, $P = K + 1$ and $\gamma = \beta + \beta'$ ($Z = 1$ for H).

The function $D(\ell, L, \ell'; m, -M, m')$ is the angular part of the matrix element and is given by

$$\int Y_{lm}(\hat{\mathbf{r}}) Y_{L,-M}(\hat{\mathbf{r}}) Y_{l'm'}^*(\hat{\mathbf{r}}) d\hat{\mathbf{r}} \\ = \left(\frac{(2\ell+1)(2\ell'+1)(2L+1)}{4\pi} \right)^{1/2} \begin{pmatrix} \ell & L & \ell' \\ 0 & 0 & 0 \end{pmatrix} \begin{pmatrix} \ell & L & \ell' \\ m & -M & m' \end{pmatrix} \\ \equiv D(\ell, L, \ell'; m, -M, m') \quad (4)$$

in terms of 3-j symbols and using the phase convention of Edmonds [14]. The remaining coefficients in (3) are given by

$$A_k^{(n\ell)} = \frac{(-1)^k}{k!} \frac{[(n+\ell)!(n-\ell-1)!]^{1/2}}{(n-\ell-k-1)!(2\ell+k+1)!} \frac{2^{\ell+k+1}}{n^{\ell+k+2}}. \quad (5)$$

A similar expression for $A_{k'}^{(n'\ell')}$ is obtained from (5) by replacing n , ℓ and k by their primed counterparts.

The 3-j symbols needed in (4) are obtained using an adaptation of a code of Tamura [15]. The subscripts i and j used in (2) are shorthand for the complete quantum numbers $\{n, \ell, m\}$ and $\{n', \ell', m'\}$ for the initial and final states, respectively. The expressions (5) are the products of the

normalization constants and the coefficients in the power series definition [12,13] of the associated Laguerre polynomials $L_{n+\ell}^{(2\ell+1)}(2\beta r)$ and $L_{n'+\ell'}^{(2\ell'+1)}(2\beta' r)$ which appear in the radial part of the hydrogenic wavefunctions $\psi_{n\ell m}(r)$ and $\psi_{n'\ell' m'}(r)$, respectively. The particular choice used here for the definition of associated Laguerre polynomials [12,13] results in the coefficient multiplying the highest power of r for a given n, ℓ being unity. Other choices are possible [16] and lead to expressions similar in functional form to (3) above. Note that our choice of associated Laguerre polynomials is the one most commonly used in the atomic physics literature [17,18] and differs from that used in applied mathematics [19].

2.2. Helium

The matrix elements of the Coulomb interaction between the projectile electron and the bound electrons in the target helium atom are written [2] as

$$V_{ji}^{(ee)}(R) = \int d\mathbf{r}_1 \int d\mathbf{r}_2 \Psi_j(\mathbf{r}_1, \mathbf{r}_2)^* \left(\frac{1}{|\mathbf{R} - \mathbf{r}_1|} + \frac{1}{|\mathbf{R} - \mathbf{r}_2|} \right) \Psi_i(\mathbf{r}_1, \mathbf{r}_2), \quad (6)$$

where the labels i and j are shorthand for the complete set of LS-coupled quantum numbers $n^{1,3}L_m$ and $n'^{1,3}L'_m$ for the initial and final states of the He atom, respectively. Since our primary interest lies in the development of scattering codes to describe the scattering of electrons, in the intermediate to high energy regime, by atoms *initially* in an excited or metastable state, a single-configuration frozen-core Hartree–Fock level of description for the two-electron wavefunctions $\Psi_i(\mathbf{r}_1, \mathbf{r}_2)$ is adequate. As shown by Cohen, McEachran and co-workers [20–22], the frozen-core Hartree–Fock level of the description of the wavefunctions yields systematic trends and dipole and quadrupole oscillator strengths in good agreement with the Hylleraas-type variational wavefunctions of Weiss and co-workers [23,24] and becomes increasingly accurate as both the principal quantum number n and orbital quantum number L increase. A resort to more sophisticated multi-configuration Hartree–Fock wavefunctions [25] or CI-wavefunctions [26] is only required if one is interested in electronic excitation near threshold or if one is studying the resonances in electron–atom scattering.

The two-electron wavefunctions $\Psi_{n\ell}(\mathbf{r}_1, \mathbf{r}_2)$ in the frozen-core approximation are written as

$$\Psi_{n\ell}^{(\pm)}(\mathbf{r}_1, \mathbf{r}_2) = N_{n\ell} [\phi_0(\mathbf{r}_1) \phi_{n\ell}(\mathbf{r}_2) \pm \phi_0(\mathbf{r}_2) \phi_{n\ell}(\mathbf{r}_1)], \quad (7)$$

where the superscripts (\pm) indicate the spin multiplicity ($+$: singlet, $-$: triplet) and $N_{n\ell}$ is the normalization constant for the two-electron wavefunction. The one-electron valence orbitals are given by [3–6]

$$\phi_0(\mathbf{r}) = 2Z^{3/2} e^{-Zr} Y_{00}(\hat{\mathbf{r}}), \quad (8a)$$

$$\phi_{n\ell}(\mathbf{r}) = (Zr)^\ell \sum_{j=2\ell+1}^{\mathcal{N}} a_j^{(n\ell)} L_{n+\ell}^{(2\ell+1)}(2\beta r) e^{-\beta r} Y_{\ell m}(\hat{\mathbf{r}}), \quad (8b)$$

where $Z = 2$ for He and again $\beta = Z/n$, while $\alpha = 2\ell + 1$. The coefficients $a_j^{(n\ell)}$ in the expansion (8b) over the associated Laguerre polynomials of the un-normalized valence orbital $\phi_{n\ell}$ are solutions of a generalized eigenvalue problem and have been tabulated in [3–5]. As shown by Flannery and McCann [2], it proves useful to transform the valence orbitals (8b) into Slater-type orbitals (STO),

$$\phi_{n\ell}(\mathbf{r}) = \sum_{N=\ell+1}^{\mathcal{N}-\ell} B_N^{(n\ell)} r^{N-1} e^{-\beta r} Y_{\ell m}(\hat{\mathbf{r}}), \quad (8b')$$

where the coefficients $B_N^{(n\ell)}$ are given in terms of the $a_j^{(n\ell)}$ coefficients,

$$B_N^{(n\ell)} = \sum_{j=N+\ell}^{\mathcal{N}} a_j^{(n\ell)} \frac{(-1)^{N-\ell} Z^\ell (2\beta)^{N-\ell-1} (j!)^2}{(N-\ell-1)!(N+\ell)!(j-N-\ell)!}, \quad (9)$$

and have been tabulated in [27].

In terms of the valence orbitals (8), the matrix elements (6) become

$$V_{ji}^{(ee)}(\mathbf{R}) = N_j N_i \sum_{k=1}^2 \left\langle \phi_j \left| \frac{1}{|\mathbf{R} - \mathbf{r}_k|} \right| \phi_i \right\rangle \pm \langle \phi_j | \phi_0 \rangle \left\langle \phi_0 \left| \frac{1}{|\mathbf{R} - \mathbf{r}_k|} \right| \phi_i \right\rangle \\ \pm \langle \phi_0 | \phi_i \rangle \left\langle \phi_j \left| \frac{1}{|\mathbf{R} - \mathbf{r}_k|} \right| \phi_0 \right\rangle + \langle \phi_j | \phi_i \rangle \left\langle \phi_0 \left| \frac{1}{|\mathbf{R} - \mathbf{r}_k|} \right| \phi_0 \right\rangle, \quad (10)$$

where the notation

$$\langle f | g \rangle = \int_0^\infty f^*(x) g(x) x^2 dx$$

is used, and the normalization constants are

$$N_{n\ell} = \frac{1}{[2(H_{n\ell} \pm G_{n\ell}^2)]^{1/2}}.$$

The overlap integral of the un-normalized valence orbitals is written in terms of the B coefficients as

$$\langle \phi_j | \phi_i \rangle \equiv G_{n\ell n'\ell'} = \delta_{\ell\ell'} \delta_{mm'} \sum_{N=\ell+1}^{\mathcal{N}-\ell} \sum_{N'=\ell+1}^{\mathcal{N}'-\ell} B_N^{(n\ell)} B_{N'}^{(n'\ell')} \frac{(N+N')!}{\gamma^{N+N'+1}} \quad (11a)$$

and equals $H_{n\ell}$ when $n = n'$. The remaining overlap integrals $\langle \phi_{n\ell} | \phi_{n\ell} \rangle$ and $\langle \phi_0 | \phi_{n\ell} \rangle = \langle \phi_{n\ell} | \phi_0 \rangle$ are determined using the expressions [2,27]

$$\langle \phi_{n\ell} | \phi_{n\ell} \rangle \equiv H_{n\ell} = \sum_{N=\ell+1}^{\mathcal{N}-\ell} \sum_{N'=\ell+1}^{\mathcal{N}'-\ell} B_N^{(n\ell)} B_{N'}^{(n'\ell')} \frac{(N+N')!}{(2\beta)^{N+N'+1}}, \quad (11b)$$

$$\langle \phi_0 | \phi_{n\ell} \rangle = \langle \phi_{n\ell} | \phi_0 \rangle \equiv G_{n\ell} = 2^{5/2} \delta_{\ell 0} \sum_{N=\ell+1}^{\mathcal{N}-\ell} B_N^{(n\ell)} \frac{(N+1)!}{(\beta+2)^{N+2}}. \quad (11c)$$

Upon replacing the Coulomb interactions in (10) with the multipole expansion, the first 3 terms in (10) yield expressions similar in form to Eq. (3) above, while the fourth term in (10) can be written in closed form. Collecting together the resultant expressions from (9) we get

$$V_{ji}^{(ee)}(\mathbf{R}) = 4\pi N_i N_j \sum_{L=|\ell-\ell'|}^{\ell+\ell'} \sum_{M=-L}^L \frac{(-1)^M}{2L+1} D(\ell, L, \ell'; m, -M, m') Y_{LM}(\hat{\mathbf{R}}) \\ \times \left[\left[\sum_{N=\ell+1}^{\mathcal{N}-\ell} B_N^{(n\ell)} \sum_{N'=\ell+1}^{\mathcal{N}'-\ell} B_{N'}^{(n'\ell')} \right] \frac{(N+N'+L)!}{\gamma^{N+N'+L+1}} \frac{1}{R^{L+1}} \right. \\ \left. + e^{-\gamma R} \left(R^L \sum_{p=0}^{P_1} \frac{P_1!}{\gamma^{P_1-p}} \frac{R^p}{p!} - \frac{1}{R^{L+1}} \sum_{q=0}^{Q_1} \frac{Q_1!}{\gamma^{Q_1-q+1}} \frac{R^q}{q!} \right) \right]$$

$$\begin{aligned}
& \pm 2G_i \delta_{L'L} \delta_{M,-m'} 2Z^{3/2} \sum_{N'=\ell+1}^{\mathcal{N}'-\ell} B_{N'}^{(n\ell)} \left[\frac{(N'+L+1)!}{(\beta'+Z)^{N'+L+2}} \frac{1}{R^{L+1}} + e^{-(\beta'+Z)R} \right. \\
& \times \left(R^L \sum_{p=0}^{P_2} \frac{P_2!}{(\beta'+Z)^{P_2+p+1}} \frac{R^p}{p!} - \frac{1}{R^{L+1}} \sum_{q=0}^{Q_2} \frac{Q_2!}{(\beta'+Z)^{Q_2-q+1}} \frac{R^q}{q!} \right) \Bigg] \\
& \pm 2G_j \delta_{L'L} \delta_{M,-m} 2Z^{3/2} \sum_{N=\ell+1}^{\mathcal{N}-\ell} B_N^{(n\ell)} \left[\frac{(N+L+1)!}{(\beta+Z)^{N+L+2}} \frac{1}{R^{L+1}} + e^{-(\beta+Z)R} \right. \\
& \times \left(R^L \sum_{p=0}^{P_3} \frac{P_3!}{(\beta+Z)^{P_3-p+1}} \frac{R^p}{p!} - \frac{1}{R^{L+1}} \sum_{q=0}^{Q_3} \frac{Q_3!}{(\beta+Z)^{Q_3-q+1}} \frac{R^q}{q!} \right) \Bigg] \Bigg] \\
& + 2N_i N_j G_{ji} \left[\frac{1}{R} - \left(\frac{1}{R} + Z \right) e^{-2ZR} \right], \tag{12}
\end{aligned}$$

where \mathcal{N} and \mathcal{N}' are the number of $a_j^{(n\ell)}$ coefficients in the expansion (8b) of the valence orbitals ϕ_{nl} and $\phi_{n'\ell'}$, respectively, and $\gamma = \beta + \beta'$. Typically [28] the number of terms varies from 9 to 22 for the ground state to the $6^{1,3}D$ states of He. The limits on the various inner summations in (12) are

$$P_1 = N + N' - L - 1, \quad P_2 = N' - L, \quad P_3 = N - L, \tag{13a}$$

$$Q_1 = N + N' + L, \quad Q_2 = N' + L + 1, \quad Q_3 = N + L + 1. \tag{13b}$$

Returning to (1), the full instantaneous electrostatic interaction is written as

$$V(\mathbf{R}, \{\mathbf{r}_i\}) = \frac{-Z}{R} + \sum_{i=1}^{(1 \text{ or } 2)} \frac{1}{|\mathbf{R} - \mathbf{r}_i|}, \tag{14}$$

composed of the Coulombic attraction between the projectile electron and the target nucleus (of atomic charge Z) and the mutual electronic repulsion between the projectile electron and electron(s) bound to the target atom. The matrix elements of the interaction (14) are then written as a sum of two terms,

$$V_{nj}(\mathbf{R}) = V_{nj}^{(\text{en})}(\mathbf{R}) + V_{nj}^{(\text{ee})}(\mathbf{R}), \tag{15}$$

where expressions for the electron–electron matrix elements are provided by Eqs. (3) and (12) for hydrogen and helium, respectively. The nuclear matrix elements in the case of H are particularly simple,

$$V_{ji}^{(\text{en})}(\mathbf{R}) \equiv \left\langle \psi_j \left| -\frac{1}{R} \right| \psi_i \right\rangle = -\frac{1}{R} \delta_{nn'} \delta_{\ell\ell'} \delta_{mm'}, \tag{16a}$$

while in the two-electron case, the nuclear matrix elements are written as

$$V_{ji}^{(\text{en})}(\mathbf{R}) \equiv \left\langle \Psi_j \left| -\frac{Z}{R} \right| \Psi_i \right\rangle = -\frac{1}{R} \langle \Psi_j | \Psi_i \rangle \tag{16b}$$

$$= -\frac{Z}{R} 2N_i N_j (G_{ji} \pm G_i G_j), \tag{16c}$$

where in (16c) we have used the analytical frozen-core Hartree–Fock wavefunctions (7) to express the two-electron overlap integrals, $\langle \Psi_j | \Psi_i \rangle$, in terms of the overlap among the un-normalized valence orbitals and the overlap between the un-normalized valence orbitals and the normalized core orbital. Combining (16c) with (12) we see that in the case of He ($Z = 2$), the nuclear matrix elements (16c) are cancelled *exactly* by corresponding terms in the electronic matrix elements (12). In particular, the first

Table 1
Number of matrix elements in full and reduced equation sets

n_{\max}	\mathcal{N}_r	\mathcal{N}_M	\mathcal{M}	$\mathcal{M}^{(\text{full})}$
2	4	1	11	15
3	10	4	65	105
4	20	10	265	465
5	35	20	840	1540
6	56	35	2226	4186

term in (16c) is cancelled by the summation of the $L = 0$ part of the first term in (12) and the long-range Coulomb part of the fourth term in (12). The second term in (16c) is likewise cancelled exactly by addition of the $L = 0$ part of the long-range multipole in the second and third terms of (12).

The cancellation of the nuclear matrix elements in the two-electron case is only *partial* in the ionic case with $Z \geq 3$ as expected. The incomplete cancellation of the nuclear matrix elements when $Z \geq 3$ can be seen clearly in the Z dependence of (12) and is facilitated by use of the analytical wavefunctions (7).

Handling the nuclear matrix elements in the one-electron case is simpler due to the orthogonality of the hydrogenic wavefunctions. Upon addition of (16a) to (3) we see that the hydrogenic nuclear matrix element is cancelled *exactly* by the $L = 0$ part of the long-range multipole term in (3).

Therefore, taking advantage of the exact cancellation of the nuclear matrix elements (16) we omit from the electronic matrix elements (3) and (12) the long-range $1/R$ Coulomb term arising from the $L = 0$ part of the multipole expansions. The resultant expressions for the electron–electron matrix elements for H and He from (3) and (12), respectively, can then be easily evaluated and output as analytical functions of R and inserted into the program MET_cross for use in semiclassical scattering calculations.

In the accompanying paper on the multichannel eikonal theory (MET), a key assumption is that the motion of the projectile electron about the target atom occurs in the plane of scattering. The assumption of central force motion is accurate for the small-angle long-range encounters in the intermediate to high energy region of primary interest to us in metastable atom scattering, and will generally be valid whenever explicit magnetic or spin-dependent forces are absent from the Hamiltonian. One consequence of central force motion is that the azimuthal-angle dependence of the matrix elements of the instantaneous electrostatic interaction (15) is concentrated in the $Y_{LM}(\hat{R})$ spherical harmonics. The resultant symmetry properties of the spherical harmonics (e.g. $Y_{L,-M} = (-1)^M Y_{LM}$) allow for a reduction in the number of coupled equations which need to be solved in the semiclassical MET due to independence of the radial part of the matrix elements (15) on the azimuthal angle. Details on the transformation, effected by the use of the azimuthal angle symmetry properties of the spherical harmonics, to reduce the number of coupled equations to be solved, can be found in [29]. In Table 1 are shown the numbers of matrix elements (15) which are needed for different size basis sets ranging from $n_{\max} = 1$ –6 for both the full (i.e. all M substates included) and reduced (i.e. $M \geq 0$) coupled equation sets. A general expression for the number of matrix elements needed in the reduced equation set is

$$\mathcal{M} = \frac{1}{2}\mathcal{N}_r(\mathcal{N}_r + 1) + \frac{1}{2}\mathcal{N}_M(\mathcal{N}_M + 1), \quad (17)$$

where \mathcal{N}_r is the number of coupled equations in the reduced set and \mathcal{N}_M are the number of equations in the reduced set with $M \geq 0$. The first term in (17) is simply the total number of matrix elements on and above the diagonal ² of the coefficient matrix of the reduced equations, while the second term in (17) is

² The matrix elements (15) are Hermitian.

Table 2
Number of lines of FORTRAN code generated by *vi j* with *iset* = 1 for H and He

n_{\max}	Hydrogen	Helium	
		singlet states	triplet states
2	187	409	250
3	1314	2723	2317
4	7274	7665	7044
5	28847	16005	15058
6	91031	28448	27133

the number of additional matrix elements required in the reduced equation set due to the transformation restricting the number of coupled equations to those with $M \geq 0$ (see [29] for details). The overall utility of the transformation from the full to the reduced equation sets is evidenced then by the reduction (ranging from 38% to 47% for basis sets with $n_{\max} = 3$ –6) in the number of matrix elements (15) needed. Table 2 shows the number of lines of FORTRAN code output by *vi j* for different size basis sets with $n_{\max} = 2$ –6. It is clear from Table 2 that the number and complexity of matrix elements (15) is a central issue in the design and implementation of an algorithm to solve the coupled amplitude equations of the multichannel eikonal theory. In the case of H the matrix elements are exact, while for He the choice of frozen-core Hartree–Fock wavefunctions represents a compromise between keeping the resultant code length tractable and incorporating the physics essential to describe metastable atom scattering into the problem.

3. Description of the code

The general logical structure of the code *vi j* is illustrated by the flowchart in Fig. 1. Figs. 2 and 3 show the details of the computational tasks preformed in modules **HYD** and **COFF**, respectively. At present the code is restricted to the targets H and He. In the two-electron case the Hartree–Fock frozen-core wavefunctions of McEachran and co-workers [3–6] are used, which in turn are limited by the tabulated values of the $a_j^{(n\ell)}$ coefficients [28] to states with $L \leq 2$ in both the singlet and triplet manifolds. Below is given a short description of each of the modules in *vi j*.

The output produced by *vi j* is the FORTRAN source code needed for the evaluation of the desired matrix elements and is suitable for direct incorporation into a scattering code (e.g. see the description of **MET_cross** in the accompanying paper) for the computation of cross sections, or into a program for the study of individual matrix elements. Standard ANSI FORTRAN 77 syntax is used and all code produced by *vi j* assumes 64-bit word lengths (i.e. calculations are done in double precision for 32-bit workstations). The original version of *vi j* (then called **Helium**) was written by K.J. McCann in 1974 using FORTRAN 66 syntax. The present code, *vi j* was first written in 1981 by the first author for use on mainframes, and has been in continual usage since, evolving under extensive testing on a number of mainframe computers and (starting in 1990) on workstations. Any questions regarding code usage and portability can be sent to the e-mail address of the first author.

VIJ. The main routine first reads in the input data (described in Section 4 below), initializes various quantities and then calls subroutine **HYD** (once in the case of H, four times in the case of He³) to generate the FORTRAN code necessary to evaluate the electronic matrix elements (3) and (12). If an

³ Four times in the case of He due to the four terms appearing in (10).

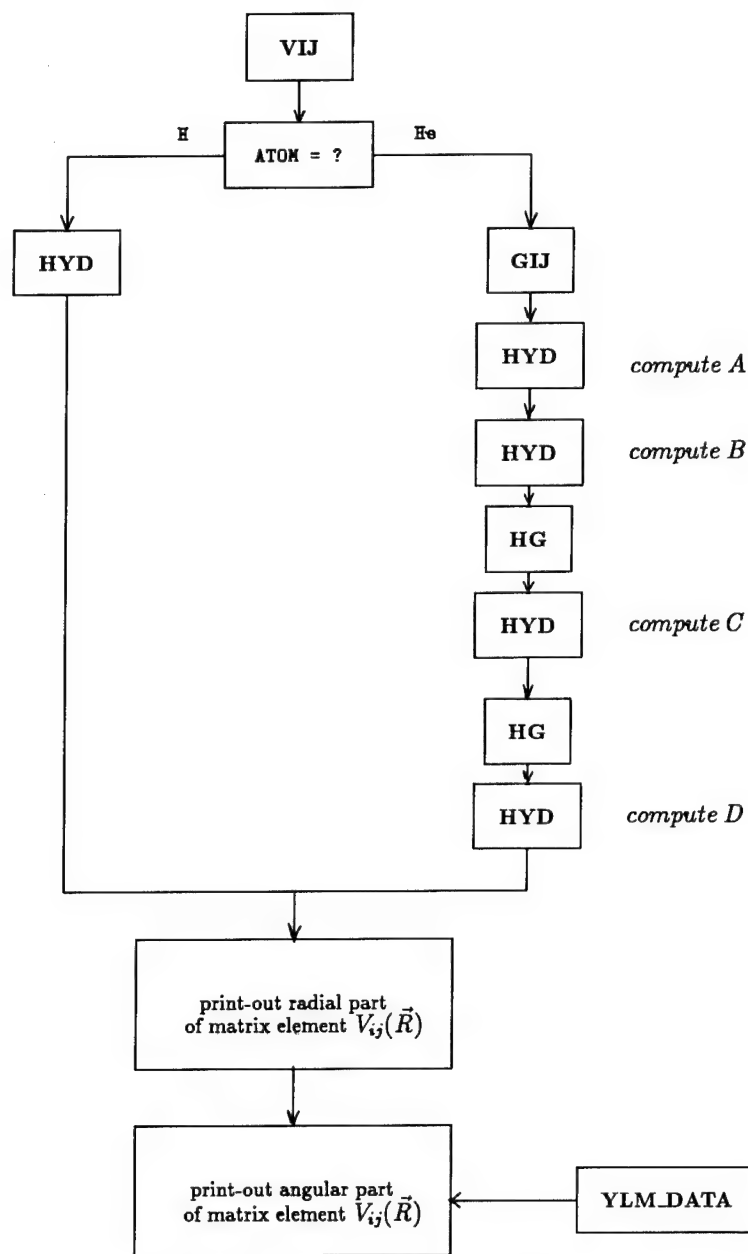


Fig. 1. Logical flowchart of program V i j.

entire set of matrix elements is required, the main routine also prints out the FORTRAN code needed to assemble the individual matrix elements computed by **HYD** into a coefficient matrix for use in the program **MET_cross**.

HYD. The principal module used to generate the FORTRAN code needed to evaluate an individual electronic matrix element. Once the coefficients for the initial and final state wavefunctions have been obtained from module **COFF**, the coefficients and powers of R needed in (3) and (12) are computed and

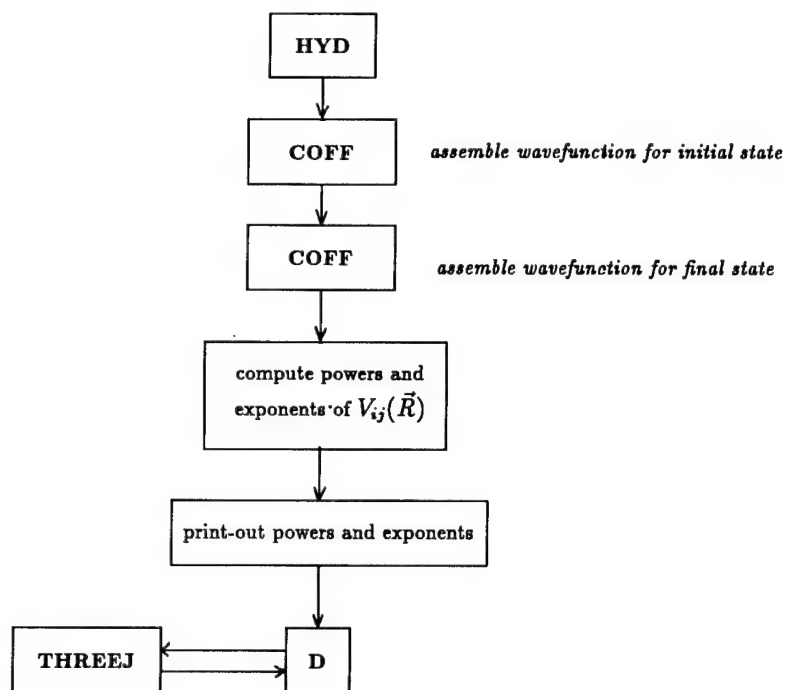


Fig. 2. Logical flowchart of module HYD used in program Vij.

then the FORTRAN code necessary for the evaluation of the radial part of the matrix element is output. Finally, before returning the control back to the main module **Vij**, the angular part of the matrix element is determined from the output of the function **D** and then the requisite FORTRAN code for its evaluation is output.

COFF. Given the quantum numbers and atomic charge Z of the atomic state desired, the coefficients in the power series (5) in the case of H, or the $B_N^{(n\ell)}$ coefficients (9) in the case of He, are computed and stored for use in subroutines **HYD**, **GIJ** and **HG**. When dealing with helium the normalization constants $N_{n\ell}$ are also computed. The coefficients stored, for further use elsewhere in the code, are actually the product $N_{n\ell} B_N^{(n\ell)}$. Further discussion about the product $N_{n\ell} B_N^{(n\ell)}$ can be found in Section 2 of [27].

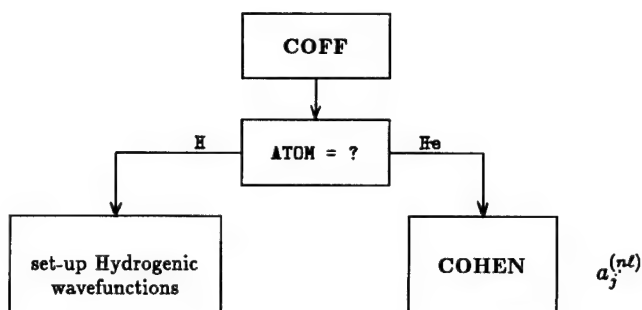


Fig. 3. Logical flowchart of module COFF used in program Vij.

GIJ. Given the atomic charges and quantum numbers of the two valence orbitals, this evaluates (11a) for the overlap $G_{n\ell n'\ell'}$ between the orbitals $\phi_{n\ell}(\mathbf{r})$ and $\phi_{n'\ell'}(\mathbf{r})$.

HG. Computes the overlaps $\langle \phi_{n\ell} | \phi_{n\ell} \rangle \equiv H_{n\ell}$ and $\langle \phi_0 | \phi_{n\ell} \rangle = \langle \phi_{n\ell} | \phi_0 \rangle = G_{n\ell}$ from (11b,c), respectively, given the quantum numbers of the valence orbital $\phi_{n\ell}(\mathbf{r})$.

COHEN. Respository of the wavefunction coefficients $a_j^{(n\ell)}$ in the frozen-core Hartree–Fock representation (8b) of the valence orbital $\phi_{n\ell}(\mathbf{r})$. The present tabulation, taken from [28], is more extensive than that published in [3–6] and yields two-electron overlap integrals $|\langle \Psi_j | \Psi_i \rangle| \leq 10^{-3}$ for all singlet and triplet states of He up to $n = 6$ and $L \leq 2$.

D. Evaluates Eq. (4) for the angular part of the electronic matrix element given the orbital and magnetic quantum numbers $\{\ell, \ell', L\}$ and $\{m, m', M\}$, respectively.

THREEJ. Evaluates the Wigner 3-j symbols [14] appearing in (4) by an adaptation of a code of Tamura [15].

YLM_DATA. Block data module of coefficients defining the spherical harmonics $Y_{LM}(\hat{\mathbf{R}})$ up to $L = 6$.

The original output of Jamison's [1] subroutine **HYD** has been replaced by **WRITE** statements which generate a **FORTRAN** code to evaluate the electronic matrix elements (3) and (12). The execution time of the code for generating entire sets of matrix elements is quite rapid – being in all cases less than 1 minute for all sets with $n_{\max} \leq 6$. However, the output created (see Table 2) can be extensive and care must be taken by the user in viewing the results or in obtaining hard copies.

At present only matrix elements with $n_{\max} \leq 4$ have been used in the DMET code (see accompanying paper). The overall algebraic structure of the polynomials in R in the matrix elements, involving alternating powers of R , will necessarily put practical limits on the value of n_{\max} which can be used in a scattering code. The practical limitations on the accuracy achievable with a given basis set in the DMET code is discussed in further detail in [8,9,30].

4. Description of input data and test runs

The amount of input data required depends on whether the user wishes to produce entire sets of matrix elements or just a select number of individual elements. The input variable **iset** governs the choice of whether individual matrix elements (**iset** = 0) or entire sets (**iset** = 1) are required by the user. Below are detailed the remaining input variables required by **Vij**:

Line 1: iset	
iset = 0:	iset = 1:
Line 2: NVIJ , Z1 , Z2	Line 2: NNMAX , Z1 , Z2
Line 3: ELEMENT	Line 3: ELEMENT
Line 4: if(ELEMENT = He) SPIN	Line 4: if(ELEMENT = He) SPIN
Line 5: LABEL	
Line 6: N1 , L1 , M1 , N2 , L2 , M2 , NL	
Line 7: (L(K), K=1, NL)	

When **iset** = 0, the remaining input variables are defined as follows:

NVIJ = number of matrix elements required by user.

Z1, **Z2** = atomic charges of the initial and final states of the target atom.

SPIN = integer variable indicating the spin multiplicity of He (SPIN = 1 indicates singlets and SPIN = 3 indicates triplets).

ELEMENT = character variable identifying the target atom (H for hydrogen and He for helium).

LABEL = character variable labeling the matrix element. See comment cards in code for a description of the labeling scheme used.

{N1, L1, M1, N2, L2, M2} = principal, orbital and magnetic quantum numbers for the initial and final states in the matrix element, respectively.

NL = number of terms in multipole expansion (3).

L(K) = value of L in the multipole expansion (3).

When $i \text{ set} = 1$, the amount of input data required is reduced considerably. The variables ELEMENT, SPIN and Z1, Z2 retain their meanings given above. The only new variable required is NNMAX, the principal quantum number of the largest shell the user wishes to include in the basis set. NNMAX is currently limited to values less than or equal to six.

4.1. Test runs

As an example of the use of V_{ij} , below are three sample test runs. In the first, we provide an example of the use of V_{ij} to generate a single electronic matrix element. In the second and third examples we show the use of V_{ij} to generate entire sets of matrix elements. In the latter two examples we choose $NNMAX \equiv n_{\max} = 3$. Below we exhibit only one of the 65 matrix elements generated, the full output is provided with the source code in the tape provided with this issue.

Example 1. Generate a single hydrogenic matrix element:

```
Line 1: 0
Line 2: 1, 1.0, 1.0
Line 3: H
Line 4: V2S3P0
Line 5: 2, 0, 0, 3, 1, 0, 1
Line 6: 1
```

Example 2. Generate an entire set of matrix elements for the singlet states of He:

```
Line 1: 1
Line 2: 3, 2.0, 2.0
Line 3: HE
Line 4: 1
```

Example 3. Generate an entire set of matrix elements for the triplet states of He:

```
Line 1: 1
Line 2: 3, 2.0, 2.0
Line 3: HE
Line 4: 3
```

4.2. Test run results

An example of the output produced by V_{ij} for the $V_{2s \rightarrow 3p_0}(R)$ hydrogenic matrix element and the $V_{2^{1,3} \rightarrow 3^{1,3}p_0}(R)$ matrix elements of He are given below. A full listing of the output produced by V_{ij} is provided with the code listing in the tape distributed with this issue.

Example 1. Hydrogenic matrix element $V_{2s \rightarrow 3p_0}(R)$:

```

C
C      V( 2, 0, 0; 3, 1, 0)
C
  A=0.0
  B=0.0
  C=0.0
  D=0.0
  E=0.0
  A =
$ .306481541E+01*R**( -2)
$+(( -.307920144E-01)*R**( 3)+( -.492672230E-01)*R**( 2)
$+( -.106417202E+01)*R**( 0)+( -.280823171E+00)*R**( 1)
$+( -.306481541E+01)*R**( -2)+( -.255401284E+01)*R**( -1))
$ *EXP(-R*( .833333333E+00))
  A =A *( 1.181635901)*Y10
  V2S3P0=A+B+C+D+E

```

Example 2. Helium singlet state matrix element $V_{2^1S \rightarrow 3^1P_0}(R)$:

```

C
C      V( 2, 0, 0; 3, 1, 0)
C
  A=0.0
  B1=0.0
  B2=0.0
  B3=0.0
  B4=0.0
  B5=0.0
  C=0.0
  D=0.0
  B1=
$ .161780700E+01*R**( -2)
$+(( -.120892841E-16)*R**( 21)+( .142382085E-14)*R**( 20)
$+( .104286194E-02)*R**( 6)+( -.358795234E-02)*R**( 7)
$+( .141343206E-02)*R**( 8)+( -.639241785E-03)*R**( 9)
$+( .198011762E-03)*R**( 10)+( -.494745544E-04)*R**( 11)
$+( .959744627E-05)*R**( 12)+( -.147964830E-05)*R**( 13)
$+( .179354810E-06)*R**( 14)+( -.170501952E-07)*R**( 15)
$+( .125246864E-08)*R**( 16)+( -.697870211E-10)*R**( 17)
$+( .284851904E-11)*R**( 18)+( -.807515692E-13)*R**( 19))
$ *EXP(-R*( .166666667E+01))
  B1=B1
$+(( -.266065271E-01)*R**( 5)+( -.556815780E-01)*R**( 4)
$+( -.224695416E+01)*R**( 0)+( -.125436008E+01)*R**( 1)
$+( -.530215296E+00)*R**( 2)+( -.209352558E+00)*R**( 3)
$+( -.161780700E+01)*R**( -2)+( -.269634499E+01)*R**( -1))
$ *EXP(-R*( .166666667E+01))
  B1=B1* 1.181635901*Y10
  C =
$ .117599923E-01*R**( -2)
$+(( .242273848E-11)*R**( 12)+( -.220062934E-09)*R**( 11)
$+( -.313599795E-01)*R**( -1)+( -.418133060E-01)*R**( 0)
$+( -.292217421E-01)*R**( 1)+( -.358987920E-02)*R**( 2)
$+( -.101038368E-02)*R**( 3)+( .155722428E-02)*R**( 4)
$+( -.617872512E-03)*R**( 5)+( .171257557E-03)*R**( 6)
$+( -.280582351E-04)*R**( 7)+( .303964573E-05)*R**( 8)
$+( -.209213963E-06)*R**( 9)+( .903397663E-08)*R**( 10)
$+( -.117599923E-01)*R**( -2))
$ *EXP(-R*( .266666667E+01))
  C =C * 1.181635901*Y10
  V2S3P0=A+B1+B2+B3+B4+B5+C+D

```

Example 3. Helium triplet state matrix element $V_{2^3S \rightarrow 3^3P_0}(R)$:

```

C
C      V( 2, 0, 0; 3, 1, 0)
C
      A=0.0
      B1=0.0
      B2=0.0
      B3=0.0
      B4=0.0
      B5=0.0
      C=0.0
      D=0.0
      B1=
      $ -.847865486E+00*R**(-2)
      $+((.711580370E-17)*R**(20)+(-.616120024E-15)*R**(19)
      $+(.141310914E+01)*R**(-1)+(.117759095E+01)*R**(0)
      $+(.666908328E+00)*R**(1)+(.293742385E+00)*R**(2)
      $+(.181267885E+00)*R**(3)+(.321201766E-01)*R**(4)
      $+(.234102036E-01)*R**(5)+(-.112747362E-02)*R**(6)
      $+(.168687521E-02)*R**(7)+(-.294687995E-03)*R**(8)
      $+(.858494145E-04)*R**(9)+(-.135847621E-04)*R**(10)
      $+(.200481943E-05)*R**(11)+(-.191252417E-06)*R**(12)
      $+(.123894395E-07)*R**(13)+(-.423321476E-10)*R**(14)
      $+(-.780479568E-10)*R**(15)+(.958880358E-11)*R**(16)
      $+(-.624436151E-12)*R**(17)+(.257452079E-13)*R**(18)
      $+(.847865486E+00)*R**(-2))
      $ *EXP(-R*(.166666667E+01))
      B1=B1+ 1.181635901*Y10
      C =
      $ -.180166309E-08*R**(-2)
      $+((-1.63320997E-18)*R**(12)+(.142370347E-16)*R**(11)
      $+(.480443491E-08)*R**(-1)+(.640591321E-08)*R**(0)
      $+(.409807247E-08)*R**(1)+(-.460096893E-09)*R**(2)
      $+(.388933740E-09)*R**(3)+(-.239424281E-09)*R**(4)
      $+(.630764242E-10)*R**(5)+(-.140214816E-10)*R**(6)
      $+(.198513510E-11)*R**(7)+(-.200807733E-12)*R**(8)
      $+(.133493330E-13)*R**(9)+(-.576006461E-15)*R**(10)
      $+(.180166309E-08)*R**(-2))
      $ *EXP(-R*(.266666667E+01))
      C =C + 1.181635901*Y10
      V2S3P0=A+B1+B2+B3+B4+B5+C+D

```

Acknowledgements

This research is supported by the US Air Force Office of Scientific Research under Grant no. F49620-94-1-0379.

References

- [1] M.J. Jamison, Comput. Phys. Commun. 1 (1970) 437.
- [2] M.R. Flannery and K.J. McCann, J. Phys. B 8 (1975) 1716.
- [3] M. Cohen and R.P. McEachran, Proc. Phys. Soc. 92 (1967) 37.
- [4] M. Cohen and R.P. McEachran, Proc. Phys. Soc. 92 (1967) 539.
- [5] R.P. McEachran and M. Cohen, J. Phys. B 2 (1969) 1271.
- [6] D. Crothers and R.P. McEachran, J. Phys. B 3 (1970) 976.

- [7] A. Messiah, *Quantum Mechanics*, Vol. 1 (North-Holland, Amsterdam, 1964) pp. 496, 497.
- [8] E.J. Mansky and M.R. Flannery, *J. Phys. B*, in preparation.
- [9] E.J. Mansky and M.R. Flannery, *J. Phys. B*, in preparation.
- [10] E.U. Condon and P.M. Morse, *Quantum Mechanics* (McGraw-Hill, New York, 1929) pp. 62–66.
- [11] L. Pauling and E.B. Wilson, *Introduction to Quantum Mechanics* (McGraw-Hill, New York, 1935) pp. 129–150.
- [12] E.C. Kemble, *The Fundamental Principles of Quantum Mechanics* (McGraw-Hill, New York, 1937) Appendix G.
- [13] H. Margenau and G.M. Murphy, *The Mathematics of Physics and Chemistry* 2nd Ed. (Van Nostrand, Princeton, NJ, 1956) pp. 77–78, 126–131.
- [14] A.R. Edmonds, *Angular Momentum in Quantum Mechanics*, 2nd Ed. (Princeton Univ. Press, Princeton, NJ, 1960).
- [15] T. Tamura, *Comput. Phys. Commun.* 1 (1970) 337.
- [16] H. Schull and P. Löwdin, *J. Chem. Phys.* 30 (1959) 617.
R.T. Brown and P.R. Fontana, *J. Chem. Phys.* 45 (1966) 4248.
M. Rotenberg, *Ann. Phys. (NY)* 19 (1962) 262.
- [17] E. Schrödinger, *Ann. Phys. (Germany)* 80 (1926) 483.
- [18] H.A. Bethe and E.E. Salpeter, *Quantum Mechanics of One- and Two-Electron Atoms* (Plenum/Rosetta, New York, 1977) Section 3.
- [19] M. Abramowitz and I.A. Stegun, eds., *Handbook of Mathematical Functions* (NBS, Washington, 1964) chap. 22.
- [20] S. Cameron, R.P. McEachran and M. Cohen, *Can. J. Phys.* 48 (1970) 211.
- [21] M. Cohen, R.P. McEachran and M. Cohen, *J. Phys. B* 5 (1972) 184.
- [22] M. Cohen and R.P. McEachran, *Can. J. Phys.* 50 (1972) 1363.
- [23] A.W. Weiss, *J. Res. NBS Sect. A* 71 (1967) 163.
- [24] W.L. Wiese, M.W. Smith and B.M. Glennon, *Atomic Transition Probabilities* (NBS, Washington, 1966).
- [25] C.F. Fischer, *Comput. Phys. Commun.* 43 (1987) 355.
- [26] A. Hibbert, *Comput. Phys. Commun.* 9 (1975) 141.
- [27] E.J. Mansky and M.R. Flannery, *J. Phys. B* 23 (1990) 4573.
- [28] M. Cohen, private communication with M.R. Flannery (1975).
- [29] M.R. Flannery, *Phys. Rev.* 183 (1969) 241.
E.J. Mansky, Ph.D. thesis, Georgia Institute of Technology (1985) chap. 3, Appendix A.
- [30] E.J. Mansky, *J. Comput. Phys.*, in preparation.

COMPUTER PHYSICS COMMUNICATIONS

Instructions to Authors (short version)

(A more detailed version of these instructions has been published in the preliminary pages of volume 83.)

Submission of papers

Manuscripts (one original + two copies), accompanied by a covering letter, should be sent to one of the Editors indicated on page 2 of the cover.

Original material. By submitting a paper for publication in Computer Physics Communications the authors imply that the material has not been published previously nor has been submitted for publication elsewhere and that the authors have obtained the necessary authority for publication.

Refereeing. Submitted papers will be refereed and, if necessary, authors may be invited to revise their manuscript. If a submitted paper relies heavily on published material, it would be helpful to have a copy of that material for the use of the referee.

Type of contributions

Two classes of papers are published by Computer Physics Communications:

- (i) Papers in the general area of computational physics and physical chemistry including research papers, notes conference proceedings, review papers and feature articles.
- (ii) Write-ups describing programs to be held in the CPC Program Library together with descriptions of new versions of existing programs and erratum notices. (A description of the CPC Program Library is given in Comput. Phys. Commun. 42 (1986) xxv-xxvii.)

Manuscript preparation

All manuscripts should be written in good English. The paper copies of the text should be prepared with double line spacing and wide margins, on numbered sheets. See notes opposite on electronic version of manuscripts.

Structure. Please adhere to the following order of presentation: Article title, Author(s), Affiliation(s), Abstract, PACS codes and keywords, Program summary*, Main text, Acknowledgements, Appendices, References, Test Run Input* and Output*, Figure captions, Tables. (Items marked with * are only requested for program descriptions; see more detailed Instructions to Authors.)

Corresponding author. The name, complete postal address, telephone and fax numbers and the e-mail address of the corresponding author should be given on the first page of the manuscript.

PACS codes/keywords. Please supply one or more relevant PACS-1995 classification codes and 6-8 keywords of your own choice for indexing purposes.

References. References to other work should be consecutively numbered in the text using square brackets and listed by number in the Reference list. Please refer to the more detailed instructions for examples.

Illustrations

Illustrations should also be submitted in triplicate: one master set and two sets of copies. The *line drawings* in the master set should be original laser printer or plotter output or drawn in black india ink, with careful lettering, large enough (3-5 mm) to remain legible after reduction for printing. The *photographs* should be originals, with somewhat more contrast than is required in the printed version. They should be unmounted unless part of a composite figure. Any scale markers should be inserted on the photograph, not drawn below it.

Colour plates. Figures may be published in colour, if this is judged essential by the Editor. The Publisher and the author will each bear part of the extra costs involved. Further information is available from the Publisher.

After acceptance

Notification. You will be notified by the Editor of the journal of the acceptance of your article and invited to supply an electronic version of the accepted text, if this is not already available.

Copyright transfer. You will be asked to transfer the copyright of the article to the Publisher. This transfer will ensure the widest possible dissemination of information.

Computer programs. After acceptance of the description of a computer program, you will be asked to send the program file to the CPC Program Library.

Electronic manuscripts

The Publisher welcomes the receipt of an electronic version of your accepted manuscript (*encode in LaTeX*). If you have not already supplied the final, revised version of your article (on diskette) to the Journal Editor, you are requested herewith to send a file with the text of the accepted manuscript directly to the Publisher by e-mail or on diskette (allowed formats 3.5" or 5.25" MS-DOS, or 3.5" Macintosh) to the address given below. Please note that no deviations from the version accepted by the Editor of the journal are permissible without the prior and explicit approval by the Editor. Such changes should be clearly indicated on an accompanying printout of the file.

LaTeX papers

If the electronic file is suitable for processing by the publisher, the article will be published without rekeying the full text. The article should be encoded in LaTeX, preferably using the Elsevier document style 'elsart' or alternatively the standard document style 'article' or the document style 'revtex'.

The Elsevier LaTeX package (including detailed instructions to authors) can be obtained using anonymous FTP from the Comprehensive TeX Archive Network (CTAN) from the directory: /tex-archive/macros/latex/contrib/supported/elsevier.

The participating hosts in the Comprehensive TeX Archive Network are: ftp.shsu.edu (TX, USA), ftp.dante.de (Germany), ftp.tex.ac.uk (UK). Questions concerning the LaTeX author-prepared article project and requests for the booklet with instructions to authors should be directed to the address below.

Author benefits

No page charges. Publishing in Computer Physics Communications is free.

Free offprints. The corresponding Author will receive 50 offprints free of charge. An offprint order form will be supplied by the Publisher for ordering any additional paid offprints.

Discount. Contributors to Elsevier Science journals are entitled to a 30% discount on all Elsevier Science books.

Contents Alert. Theoretical and High-Energy Physics papers scheduled for publication in Computer Physics Communications are included in Elsevier's pre-publication service Contents Alert.

Further information (after acceptance)

Elsevier Science B.V., Computer Physics Communication
Desk Editorial Department
P.O. Box 103, 1000 AC Amsterdam
The Netherlands
Tel.: +31 20 4852517
Fax: + 31 20 4852319
E-mail: physdesk@elsevier.nl



North-Holland, an imprint of Elsevier Science



**A CURRENT AWARENESS SERVICE
FREE OF CHARGE
VIA ELECTRONIC MAIL**

FOR SCIENTISTS WORKING IN THE FIELD OF SURFACES, INTERFACES AND THIN FILMS

**FOR SCIENTISTS WORKING IN THE FIELD OF MATHEMATICAL & THEORETICAL
METHODS IN PHYSICS**

As the number of scientific publications grows daily it becomes increasingly important to trace the most interesting publications in a way that costs as little time as possible.

Elsevier Science Publishers now provides CONTENTS-Alert, **a free electronic service** that can assist you in carrying out time-saving searches on a regular, two-weekly basis.

CONTENTS-Alert is a current awareness service which delivers, through e-mail, the tables of contents of a selected group of journals. Not only will you receive these tables of contents **before or upon publication** of the journals but you can also browse through these tables of contents **at your own terminal**, in your own time. A survey carried out among researchers using CONTENTS-Alert has shown that this free service is very convenient and time-effective.

We offer two versions of CONTENTS-Alert each covering a specific field. One version of CONTENTS-Alert includes journals on Surfaces, Interfaces and Thin Films, and one includes journals on Mathematical and Theoretical Methods in Physics.

Journals covering the field of Surfaces, Interfaces and Thin Films

Applied Surface Science
Chemical Physics Letters
Materials Science and Engineering: R: Reports
Nuclear Instruments and Methods in Physics Research: Section B
Surface Science (including Surface Science Letters)
Surface Science Reports
Thin Solid Films
Vacuum

Our e-mail for this version is:
RFC-822: C-ALERT@ELSEVIER.NL
X.400: C=NL;A=400NET;P=SURF;O=ELSEVIER;S=C-ALERT

Journals covering the field of Mathematical and Theoretical Methods in Physics

Computer Physics Communications
Journal of Geometry and Physics
Nuclear Physics B
Physica A
Physica D
Physics Letters A
Physics Letters B
Physics Reports
Wave Motion

Our e-mail for this version is:
RFC-822: C-ALERT.MATHPHYS@ELSEVIER.NL
X.400: C=NL;A=400NET;P=SURF;O=ELSEVIER;
S=MATHPHYS; G=C-ALERT

Subscribe now to this **free pre-publication service** and find out how useful CONTENTS-Alert really is. Just send your full address to the e-mail number quoted above that corresponds with the CONTENTS-Alert version you wish to receive, or send it by post and we will make sure you will receive CONTENTS-Alert every two weeks. Please allow three weeks processing time for your free subscription.

**Yes, please add my name to the circulation list of
CONTENTS-Alert.**

Version: ☐ Surfaces, Interfaces and Thin Films
☐ Mathematical and Theoretical Methods in Physics

Return to:

ELSEVIER SCIENCE PUBLISHERS B.V.,
Att: Mr. M. Stavenga,
P.O. BOX 103, 1000 AC Amsterdam, The Netherlands
Fax 31 20 5862580

Name _____
Initials _____ Title _____ ☐ Male ☐ Female
Institute _____
Department _____
Street/ PO Box _____
City _____
Country _____
Tel: _____ Fax: _____
E-mail _____

REPORT DOCUMENTATION PAGE			Form Approved OMB No. 0704-0188	
<small>Public reporting burden for this collection of information is estimated to average 1 hour per response, including the time for reviewing instructions, searching existing data sources, gathering and maintaining the data needed, and completing and reviewing the collection of information. Send comments regarding this burden estimate or any other aspect of this collection of information, including suggestions for reducing this burden to Washington Headquarters Services, Directorate for Information Operations and Reports, 1215 Jefferson Davis Highway, Suite 1204, Arlington, VA 22202-4302, and to the Office of Management and Budget, Paperwork Reduction Project (0704-0188), Washington, DC 20503</small>				
1. AGENCY USE ONLY (Leave Blank)		2. REPORT DATE December 1995		3. REPORT TYPE AND DATES COVERED Reprint: 1 July 1994 - 30 Sept. 1995
4. TITLE AND SUBTITLE THE MULTICHANNEL EIKONAL THEORY PROGRAM FOR ELECTRON-ATOM SCATTERING			5. FUNDING NUMBERS AFOSR F49620-94-1-0379	
6. AUTHOR(S) E. J. Mansky and M. R. Flannery				
7. PERFORMING ORGANIZATION NAME(S) AND ADDRESS(ES) School of Physics Georgia Institute of Technology Atlanta, Georgia 30332			8. PERFORMING ORGANIZATION REPORT NUMBER GIT-94-002	
9. SPONSORING/MONITORING AGENCY NAME(S) AND ADDRESS(ES) AFOSR/NE 110 Duncan Avenue Suite B115 Bolling AFB, D. C. 20332-0001			10. SPONSORING/MONITORING AGENCY REPORT NUMBER	
11. SUPPLEMENTARY NOTES COR: Reprint: Computer Physics Commun. <u>88</u> (1995) pp. 249-277.				
12a. DISTRIBUTION/AVAILABILITY STATEMENT Approved for public release. Distribution is unlimited.			12b. DISTRIBUTION CODE	
13. ABSTRACT (Maximum 200 words) Abstract The operation of the code MET_cross for the solution of the semiclassical multichannel eikonal theory for electron-atom scattering is described. Also described is a second code, MET_states, which utilizes the results produced by MET_cross to generate a complete set of state multipoles and coherence and alignment parameters needed to characterize the polarization properties of the radiation emitted in the decay of the metastable atomic states excited in the collision. Included also is a discussion of the relationship between the present codes used to solve the semiclassical multichannel eikonal theory and codes used to implement other semiclassical and quantal scattering theories of electron-atom scattering.				
14. SUBJECT TERMS Keywords: Hamilton-Jacobi equation, Schödinger's equation, semiclassical, partial differential equations, inelastic cross sections, electron-atom scattering			15. NUMBER OF PAGES 28	
			16. PRICE CODE	
17. SECURITY CLASSIFICATION OF REPORT Unclassified	18. SECURITY CLASSIFICATION OF THIS PAGE Unclassified	19. SECURITY CLASSIFICATION OF ABSTRACT Unclassified	20. LIMITATION OF ABSTRACT UL	

Reprinted from

Computer Physics Communications

Computer Physics Communications 88 (1995) 249–277

The multichannel eikonal theory program for electron–atom scattering

E.J. Mansky¹, M.R. Flannery

School of Physics, Georgia Institute of Technology, Atlanta, GA 30332-0430, USA

Received 28 July 1994



COMPUTER PHYSICS COMMUNICATIONS

An international journal and program library for computational physics and physical chemistry

Honorary Editor: P.G. BURKE, Belfast

Principal Editors

Geerd H.F. DIERCKSEN

Max-Planck-Institut für Astrophysik, Karl-Schwarzschild
Strasse 1, D-85740 Garching bei München, Germany

James W. EASTWOOD

Culham Laboratory, Abingdon, Oxfordshire OX14 3DB, UK

J.E. INGLESFIELD

ESM, Department of physics, Catholic University of Nijmegen,
Toernooiveld, 6525 ED Nijmegen, The Netherlands

F. JAMES

CERN, Data Handling Division, CH-1211 Geneva 23,
Switzerland

Editors in specialist fields

The complete mailing addresses of all Editors in specialist fields are printed at the beginning of each volume.

Algebraic manipulation

J. CIZEK, Waterloo, Ont., Canada

J.P. FITCH, Bath, UK

A.C. HEARN, Santa Monica, CA

Astrophysics

D.G. HUMMER, München, Germany

M.L. NORMAN, Urbana, IL

W.M. TSCHARNUTER, Heidelberg,
Germany

Atomic and molecular dynamics

B.H. BRANSDEN, Durham, UK

D.C. CLARY, Cambridge, UK

T.H. DUNNING, Jr., Richland, WA

F.A. GIANTURCO, Rome, Italy

J.-M. LAUNAY, Meudon, France

H. NAKAMURA, Okazaki, Japan

J. READING, College Station, TX

G.C. SCHATZ, Evanston, IL

R.E. WYATT, Austin, TX

Atomic and molecular structure, spectra and properties

W. DUCH, Torun, Poland

C.F. FISCHER, Nashville, TN

I.P. GRANT, Oxford, England

I. SHAVITT, Columbus, OH

B.T. SUTCLIFFE, Heslington, UK

Algorithms, software and architectures

J.M. BOYLE, Argonne, IL

I.S. DUFF, Chilton, UK

Y. MURAOKA, Tokyo, Japan

W. SCHÖNAUER, Karlsruhe, Germany

N.S. SCOTT, Belfast, N. Ireland

Biophysics and biochemistry

B. MONTGOMERY PETTITT,
Houston, TX

Condensed matter physics

C.R.A. CATLOW, London, UK

D. FINCHAM, Keele, UK

R. HAYDOCK, Eugene, OR

O.H. NIELSEN, Lyngby, Denmark

S.B. TRICKEY, Gainesville, FL

Electromagnetics

D.A. McNAMARA, Pretoria,
South Africa

Donald G. TRUHLAR

University of Minnesota, Department of Chemistry and
Supercomputer Institute, 207 Pleasant Street S.E., Minneapolis,
MN 55455, USA

Program Librarian

Miss C. JACKSON

Department of Applied Mathematics,
Queen's University of Belfast, Belfast BT7 1NN, N. Ireland

Program Library Director

P.G. BURKE

Department of Applied Mathematics,
Queen's University of Belfast, Belfast BT7 1NN, N. Ireland

High energy physics

B. van EIJK, Amsterdam,
The Netherlands

C.B. LANG, Graz, Austria

J. LINNEMANN, East Lansing, MI

Y. OYANAGI, Tokyo, Japan

C. REBBI, Boston, MA

Nuclear physics

I.R. AFNAN, Adelaide, Australia

B.S. NILSSON, Copenhagen, Denmark

V.R. PANDHARIPANDE, Urbana, IL

Plasma physics

D.C. BARNES, Los Alamos, NM

D.F. DÜCHS, Garching bei München,
Germany

D.W. HEWETT, Livermore, CA

Statistical mechanics and many body physics

K. BINDER, Mainz, Germany

M. PARRINELLO, Stuttgart, Germany

Statistics and data analysis

F. JAMES, Geneva, Switzerland

J. LINNEMANN, East Lansing, MI

Aims and Scope

Computer Physics Communications is an international interdisciplinary journal in which computational physicists and physical chemists can record their computing research and express their views, and which they can consult for the most recent developments in computing techniques in their field. Two classes of papers are published:

(i) Papers in the general area of computational physics and physical chemistry, concerned with computational methods and the application of computers to physics and physical chemistry.

(ii) Write-ups describing programs to be held in the CPC Program Library.

Abstracted/Indexed in:

Chemical Abstracts; Current Contents: Engineering, Technology
& Applied Sciences; Ei Compendex Plus; Engineering Index;
INSPEC.

Subscription Information 1995

Volumes 86-92 of *Computer Physics Communications* (ISSN 0010-4655) are scheduled for publication. (Frequency: monthly.)

Prices are available upon request from the publisher.

Subscriptions are accepted on a prepaid basis only and are entered on a calendar year basis. Issues are sent by SAL (Surface Air Lifted) mail wherever this service is available. Airmail rates are available upon request. Please address all enquiries regarding orders and subscriptions to:

Elsevier Science B.V.

Order Fulfilment Department

P.O. Box 211, 1000 AE Amsterdam

The Netherlands

Tel. +31 20 4853642, Fax. +31 20 4853598

Claims for issues not received should be made within six months of our publication (mailing) date.

US mailing notice - Computer Physics Communications (ISSN 0010-4655) is published monthly by Elsevier Science B.V., Molenwerf 1, P.O. Box 211, 1000 AE Amsterdam, The Netherlands. Annual subscription price in the USA US\$ 2299.00 (valid in North, Central and South America only), including air speed delivery. Second class postage paid at Jamaica, NY 11431.

USA POSTMASTERS: Send address changes to Computer Physics Communications, Publications Expediting, Inc., 200 Meacham Avenue, Elmont, NY 11003. Airfreight and mailing in the USA by Publications Expediting.

© The paper used in this publication meets the requirements of ANSI/NISO Z39.48-1992 (Permanence of Paper).



North-Holland, an imprint of Elsevier Science

Printed in The Netherlands



ELSEVIER

Computer Physics Communications 88 (1995) 249–277

Computer Physics
Communications

The multichannel eikonal theory program for electron–atom scattering

E.J. Mansky¹, M.R. Flannery

School of Physics, Georgia Institute of Technology, Atlanta, GA 30332-0430, USA

Received 28 July 1994

Abstract

The operation of the code `MET_cross` for the solution of the semiclassical multichannel eikonal theory for electron–atom scattering is described. Also described is a second code, `MET_states`, which utilizes the results produced by `MET_cross` to generate a complete set of state multipoles and coherence and alignment parameters needed to characterize the polarization properties of the radiation emitted in the decay of the metastable atomic states excited in the collision. Included also is a discussion of the relationship between the present codes used to solve the semiclassical multichannel eikonal theory and codes used to implement other semiclassical and quantal scattering theories of electron–atom scattering.

PROGRAM SUMMARY

Title of program: `MET_cross`

Catalogue number: ADAW

Program obtainable from: CPC Program Library, Queen's University of Belfast, N. Ireland (see application form in this issue)

Licensing provisions: none

Computers for which the program is designed and others on which it has been tested: IBM RS/6000 and HP/Apollo 9000 model 700 series workstations with a FORTRAN 77 compiler. With minor changes the program will also run on CDC 800 series mainframes and Cray supercomputers (see comment cards in code for details).

Computers: IBM RS/6000 model 520 and HP/Apollo 9000

model 730 workstations; *Installation:* School of Physics, Georgia Institute of Technology

Operating systems: AIX 3.1.7, HP-UX 8.07, 9.01

Programming language used: FORTRAN 77

Memory required to execute with typical data: 13 776 words

No. of bits in a word: 32

Peripherals used: Terminal or card reader for data input. Terminal, line printer or magnetic disk for storage of output data.

No. of lines in distributed program including test data, etc.: 4631

Keywords: Hamilton–Jacobi equation, Schrödinger's equation, semiclassical, partial differential equations, inelastic cross sections, electron–atom scattering

¹ E-mail address: mansky@eikonal.physics.gatech.edu.

Nature of physical problem

Calculation of the complex scattering amplitudes, differential and integral cross sections for the elastic and inelastic scattering of electrons by atoms in the intermediate to high energy regime. In addition, a characterization of the orientation and alignment of the atomic charge clouds via calculation of the coherence and correlation parameters.

Method of solution

The semiclassical multichannel eikonal theory (MET) [1,2] is used to solve the Schrödinger equation describing the electron-atom scattering using an impact-parameter representation for the system wavefunction, for the complex amplitude functions. In the present paper the design of the algorithm used to implement the MET, for the case of straight-line trajectories and electron exchange neglected is described. The resulting set of Hamilton–Jacobi coupled partial differential equations for the amplitude functions is solved using the rational extrapolation technique of Bulirsch and Stoer [3]. Evaluation of the complex scattering amplitudes, differential and integral cross sections for each of the states in the basis set is then achieved by Gaussian quadrature.

Restrictions on the complexity of the problem

At present the MET code is limited to a maximum of 10 states in the basis set and 1600 points in the Z -integration of the coupled Hamilton–Jacobi equations. Furthermore, the maximum number of impact parameters ρ and electron scattering angles θ which can be considered is 250 and 126, respectively. All of the above limits are easily changed by adjusting the appropriate array lengths in the PARAMETER statements in the code (see instructions in the comment cards for details).

Typical running times: 1–3 CPU hours (depending on the energy)

References

- [1] M.R. Flannery and K.J. McCann, J. Phys. B 7 (1974) 2518.
- [2] E.J. Mansky and M.R. Flannery, J. Phys. B 23 (1990) 4549, 4573.
- [3] R. Bulirsch and J. Stoer, Num. Math. 8 (1966) 1.

Program Summary

Title of program: MET_states

Catalogue number: ADAY

Program obtainable from: CPC Program Library, Queen's University of Belfast, N. Ireland (see application form in this issue)

Licensing provisions: none

Computers for which the program is designed and others on which it has been tested: IBM RS/6000 and HP/Apollo 9000 model 700 series workstations with a FORTRAN 77 compiler. With minor changes the program will also run on CDC 800 series mainframes and Cray supercomputers (see comment cards in code for details).

Computers: IBM RS/6000 model 520 and HP/Apollo 9000 model 730 workstations; *Installation:* School of Physics, Georgia Institute of Technology

Operating systems: AIX 3.1.7, HP-UX 8.07, 9.01

Programming language used: FORTRAN 77

Memory required to execute with typical data: 1549 words

No. of bits in a word: 32

Peripherals used: terminal or card reader for data input. Terminal, line printer or magnetic disk for storage of output data

No. of lines in distributed program, including test data, etc.: 2531

Keywords: state multipoles, orientation, alignment tensor, scattering amplitude, magnetic substate coherences, Stokes parameters

Nature of physical problem

Given the complex scattering amplitudes $f_i \rightarrow n(\theta)$ for excitation of atomic states $|n\rangle$, by intermediate to high energy electrons, calculate the state multipoles $\langle T(JJ)_{KQ}^+ \rangle$ characterizing the coherence among the magnetic substates and the correlation between the scattered electron and the photon emitted in the decay of the state $|n\rangle$ under the influence of the Q -component of a tensor \mathbf{T} of rank K . Also, completely determine the degree of polarization of the emitted radiation by computing the Stokes parameters P_i and density matrices ρ_{in} .

Method of solution

At present the program applies the formulae of Fano and Macek [1,2] for the orientation vector $O_{Q\pm}$ and alignment tensor $A_{Q\pm}$, the state multipoles of Blum and Kleinpoppen [3] and the Stokes parameters P_i of Andersen and co-workers [4–6], to the complex scattering amplitudes $f_i \rightarrow n(\theta)$ generated by the multichannel eikonal theory code.

Restrictions on the complexity of the problem

The program is presently limited to using the semiclassical scattering amplitudes obtained from the companion program in the spin-averaged versions of the formulae for the above physical observables in [1–6]. Future versions of the code will: (a) incorporate the use of the full, spin-dependent formulae

for the state multipoles, coherence and correlation parameters and the Stokes parameters, and (b) allow the user to input complex scattering amplitudes obtained from other theories (e.g. R-matrix, distorted-wave).

Typical running times: less than 30 seconds

References

- [1] U. Fano and J.H. Macek, *Rev. Mod. Phys.* 45 (1973) 553.
- [2] J.H. Macek and D.H. Jaecks, *Phys. Rev. A* 4 (1971) 2288.
- [3] K. Blum and H. Kleinpoppen, *J. Phys. B* 10 (1977) 3283; *Phys. Rep.* 52 (1979) 203.
- [4] N. Andersen and S.E. Nielsen, *Adv. At. Mol. Phys.* 18 (1982) 265.
- [5] H.W. Hermann and I.V. Hertel, *Comments At. Mol. Phys.* 12 (1982) 61, 127.
- [6] N. Andersen, J.W. Gallagher and I.V. Hertel, *Phys. Rep.* 165 (1988) 1.

LONG WRITE-UP

1. Introduction

A large number of computer codes for the theoretical study of excitation processes in electron–atom scattering have been published during the past twenty years. The types of codes published, using algorithms designed to implement various theories for electron–atom collision processes, can be characterized in general by the energy regime of the projectile electron. At low energies, from threshold to (approximately) the first ionization threshold, codes like the R-matrix [1], NIEM [2], IMPACT [3] and the general algebraic variational [4], optical potentials [5] and non-iterative partial differential equation [6] methods (among many others) allow one to treat electron–atom scattering processes, with atomic wavefunctions of varying sophistication, using an eigenfunction expansion technique. In the codes published in [1–4] both the projectile and target are treated quantum mechanically and the eigenfunction expansion techniques used lead numerically to a matrix diagonalization problem. The size of the Hermitian matrix to be diagonalized is a function of the number of atomic states in the basis set and the number of partial waves needed to characterize the relative motion of the projectile. The latter quantity is necessarily a sensitive function of the energy of the colliding electron and hence the size of the matrix diagonalization problem grows dramatically with energy. Addition of the $n = 5$ manifold to the basis set in helium for example, results in a doubling of the maximum size of the Hamiltonian matrix to be diagonalized in the R-matrix code [7] from 1433×1433 to 3363×3363 . A major impediment to the continued extension of codes like the R-matrix [1] (for example) to incorporate additional continuum orbitals into their basis sets is therefore the memory requirements of, and the numerical stability characteristics attendant with, the direct techniques [8] needed to solve the matrix diagonalization problem. Hence balancing the task of including the physics essential to describing electron–atom scattering in the intermediate to high energy regime, whilst keeping the algorithms, resulting from the dual treatment of both projectile and target quantum mechanically, tractable, is difficult in eigenfunction expansions.

In order to handle the intermediate energy regime (roughly from one to several times the ionization threshold) to the high energy regime (wherein the Born approximation is valid), a number of perturbative [9] and semiclassical [10–12] techniques have also been developed over the past two decades. In perturbative methods an expansion in the matrix elements of the instantaneous electrostatic interaction $V(\mathbf{R}, \{\mathbf{r}_i\})$, between the projectile electron and the bound electrons in the target atom, results in Born, Bethe or distorted-wave types of series in powers of V for the scattering amplitude to be summed. Semiclassical methods avoid the difficulties associated with explicitly summing over partial waves, as required when both projectile and target are treated quantum mechanically [1–4], by employing a coordinate representation in the eigenfunction expansion wherein the projectile electron is treated

classically and the target atom quantum mechanically. The use of a coordinate representation in semiclassical methods like the multichannel eikonal theory [12] therefore maps discrete variables such as the orbital angular momentum of the scattered electron into a continuous impact-parameter variable ρ , thereby converting summation over partial waves l into integration over ρ . The mapping from l to ρ therefore allows for the incorporation of the physics important in the intermediate to high energy regime to be accounted for in semiclassical theories in a manner more tractable numerically due to the reformulation of the core numerical problem of the algorithm from one of matrix diagonalization to that of solving systems of differential equations in the plane.

The mapping $l \rightarrow \rho$ done in semiclassical scattering theories necessarily involves making trade-offs between the accuracy to which the cross sections are desired against the numerical effort required to achieve that level of accuracy. The original objective in developing the multichannel eikonal theory (MET) was to formulate a means of computing *integral* cross sections for electronic excitation of atoms *initially* in an excited or metastable state. Hence the differential cross sections for excitation only needs to be accurate for scattering angles $\theta \leq 40^\circ$ wherein the majority of the contribution to the integral cross section is made. Furthermore, the region wherein electron exchange effects are expected [14,15,33] to contribute significantly to the integral cross section is reduced when dealing with transitions between metastable states, when compared to excitation out of the ground state, due to the much smaller threshold energies involved and the consequent increased importance of long-range interactions such as polarization. Therefore, the neglect of electron exchange effects and the use of straight-line trajectories is justified when interest lies primarily in predicting cross sections for the electronic excitation of atoms initially in an excited state. Hence the trade-off in the MET of restricting the validity of the amplitude equations to the small-angle-high-energy regime allows for the computation of integral cross sections for the excitation of atoms initially in metastable states with only a small loss of accuracy and with a considerable reduction in the numerical effort required. When interest lies in resonance phenomena in the region near threshold, a quantal treatment of the motion of the projectile electron is required due to the low relative speed of the projectile electron, as compared to the electrons bound in the target atom, and hence with the increased probability of strong deflections of the scattered electron through large angles due to close encounters with the target atom. In this case a large number of codes have been developed [1–4] which may be used to deal with excitation out of the ground state as well as a limited number of excited states. However, application of the codes which decompose the relative motion of the projectile in terms of partial waves is necessarily limited to the near threshold region due to the growth rate of the matrix diagonalization problem as a function of impact energy. To cover the entire energy regime from threshold to the high energy limit generally requires a hybrid code which uses a partial wave description in the near threshold regime and an impact parameter description in the high energy regime. A future paper will detail the design and operation of such a hybrid code. The intermediate energy R-matrix theory of Burke and co-workers [34] is an example of another such hybrid code developed within the R-matrix theory.

In this paper the design and use of the algorithm which implements the multichannel eikonal theory [12] is described. The present version of the multichannel eikonal theory assumes that the motion of the projectile electron occurs in the scattering plane (central force motion) via a rectilinear trajectory and that electron exchange can be omitted. In a separate paper [13] we describe the detailed numerical properties (e.g. convergence rates, grid selection, etc.) of the algorithm. Here we provide a guide to the actual use and underlying design of the code. The results of the present MET code for electron scattering by hydrogen and helium appears elsewhere [14,15] and largely updates and supercedes the earlier work in [12].

The remainder of the paper is organized as follows. Section 2 provides an overview of the general logical structure of the algorithm and details the method used to solve the coupled system of differential equations which arise in the MET. It also contains a discussion of the quadrature grids employed in the

evaluation of the scattering amplitudes and the differential and integral cross sections. Section 3 describes the type of output produced by the algorithm, while Section 4 provides a test run. Unless otherwise noted, atomic units are used throughout the paper. In this and the accompanying paper [16] the names of actual computer codes are indicated in *typewriter* type-set, while the names of specific modules constituting a given code are given in **boldface**. Variable names within a module are in turn denoted by CAPITAL letters in the text and *typewriter* type-set in the tables.

2. Description of the code

The algorithm described in this paper implements numerically the multichannel eikonal theory using a semiclassical coordinate representation to formulate and solve the resultant coupled differential equations for the amplitude functions. The basic design is to minimize the required input data (see Section 4 below) and user intervention as much as possible by separating the algorithm into two principal parts: **MET_cross** and **MET_states**. The code **MET_cross** solves the coupled amplitude equations, performs the necessary quadratures to obtain the complex scattering amplitudes, differential and integral cross sections, and then outputs the results for **MET_states** to generate the state multipoles and Stokes parameters. The two codes have been used principally [12,14,15] to study electron scattering by H and He. The modifications needed to treat other target atoms are detailed in Section 3 under the appropriate modules which require editing. In addition to the input data described in Section 4, the user must supply **MET_cross** with energy levels of the target atom being studied and the values of the matrix elements,

$$V_{in}(\mathbf{R}) = \langle \Psi_n | V(\mathbf{R}, \{\mathbf{r}\}) | \Psi_i \rangle_r, \quad (1)$$

of the instantaneous electrostatic interaction between the projectile electron and the target atom's bound electrons. The matrix elements (1) may be provided by the user as analytical functions of the projectile–target distance \mathbf{R} , or interpolated from numerical tables. In the accompanying paper [16], a code **vij** is described which can be used, for the cases of H and He, to generate the required matrix elements (1) for entire basis sets as analytical functions of \mathbf{R} . Fig. 1 illustrates the overall logical relationship between the three codes **MET_cross**, **MET_states** and **vij**. A general flowchart showing the logical arrangement of the modules and a breakdown of the computational tasks performed in **MET_cross** appears in Figs. 2 and 3. Fig. 4 provides a similar illustration of the order of the tasks performed in **MET_states**.

Here in this paper we simply quote the basic equations of the MET and refer the reader to the atomic

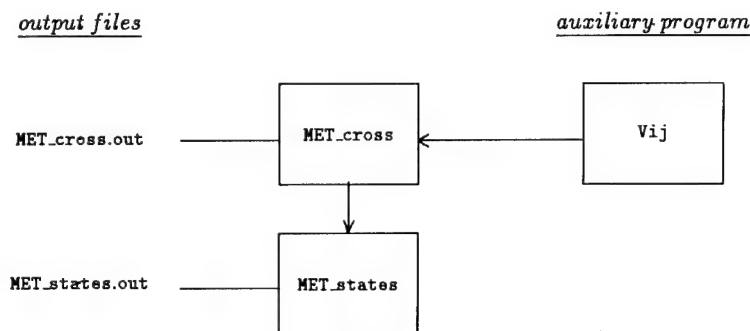


Fig. 1. Logical ordering of programs **MET_cross** and **MET_states**.

physics literature for details [12,14,15]. The coupled differential equations to be solved in `MET_cross` for the complex amplitude functions $C_n(\rho, Z)$ are

$$\begin{aligned} i \frac{\hbar^2}{\mu} \kappa_n(\rho, Z) \frac{\partial C_n(\rho, Z)}{\partial Z} + \left(-\frac{\hbar^2}{\mu} \kappa_n(\rho, Z) [\kappa_n(\rho, Z) - k_n] + V_{nn}(\rho, Z) \right) C_n(\rho, Z) \\ = \sum_{j=1}^{\mathcal{N}} V_{nj}(\rho, Z) C_j(\rho, Z) \exp[i(k_j - k_n)Z], \end{aligned} \quad (2)$$

where the local and asymptotic wavenumbers, $\kappa_n(\rho, Z)$ and k_n , in channel n are given by

$$\kappa_n(\rho, Z) = \left(k_n^2 - \frac{2\mu}{\hbar^2} V_{nn} \right)^{1/2}, \quad k_n^2 = k_i^2 - \frac{2\mu}{\hbar^2} (\epsilon_n - \epsilon_i)$$

and where k_i is the wavenumber of the incident electron and the ϵ_n are the eigenenergies of the target atom. The \mathcal{N} coupled equations (2) are solved subject to the asymptotic boundary conditions

$$C_n(\rho, Z \rightarrow -\infty) = \delta_{ni}$$

over a rectangular grid: $0 \leq \rho \leq \rho_{\max}$ and $-Z_{\max} \leq Z \leq Z_{\max}$. The choice of grid limits ρ_{\max} and Z_{\max} are determined by the constraints

$$\sum_{n=1}^{\mathcal{N}} |C_n(\rho, Z = Z_{\max})|^2 - 1 \leq 0.10, \quad (3a)$$

$$\max_n \left(\frac{|Q_n(\rho_2) - Q_n(\rho_1)|}{Q_n(\rho_1)} \right) \leq \epsilon, \quad \rho_2 - \rho_1 \equiv \Delta\rho, \quad 0 \leq \rho \leq \rho_{\max}, \quad (3b)$$

where ϵ is a user-supplied tolerance (generally $\frac{1}{2}\%$) and $Q_n(\rho_j)$ is the usual impact-parameter expression for the integral cross section for the $i \rightarrow n$ excitation in terms of the probabilities,

$$Q_n(\rho_j) = 2\pi \int_0^{\rho_j} |C_n(\rho, Z)|^2 \rho \, d\rho = 2\pi \sum_{k=1}^{\mathcal{N}_j^{(GL)}} \varphi_k |C_n(\rho_k, Z)|^2 \rho_k, \quad (4)$$

where the ρ -integration in (4) is done using an $\mathcal{N}_j^{(GL)}$ -point Gauss–Legendre quadrature. By choosing the ρ -grid used in solving the coupled equations (2) to be the pivot points, in succession of 1-, 2-, 4- and 10-point Gauss–Legendre quadratures [17] a progressive refinement is made in the evaluation of $Q_n(\rho_j)$ until two such evaluations of the impact-parameter cross section differ by less than a specified amount (ϵ) for *each* of the \mathcal{N} states in the basis set.

Once the solutions to the coupled equations (2) are obtained, subject to the constraints (3), the MET expression for the complex scattering amplitude $f_{i \rightarrow n}(\theta)$,

$$f_{i \rightarrow n}(\theta) = -(i)^{\Delta+1} \int_0^\infty J_\Delta(q'\rho) [I_1(\rho, \gamma(\theta)) - iI_2(\rho, \gamma(\theta))] \rho \, d\rho, \quad (5)$$

is evaluated, with q' , Δ and $\gamma(\theta)$ being given by

$$q' = k_n \sin \theta, \quad \Delta = m_i - m_n, \quad \gamma(\theta) = k_n(1 - \cos \theta).$$

The differential and integral cross sections are then given by the usual expressions

$$\frac{d\sigma_{ni}}{d\Omega} = \frac{k_n}{k_i} |f_{i \rightarrow n}(\theta)|^2, \quad (6a)$$

$$\sigma_{ni} = 2\pi \int_0^\pi \frac{k_n}{k_i} |f_{i \rightarrow n}(\theta)|^2 \sin \theta \, d\theta. \quad (6b)$$

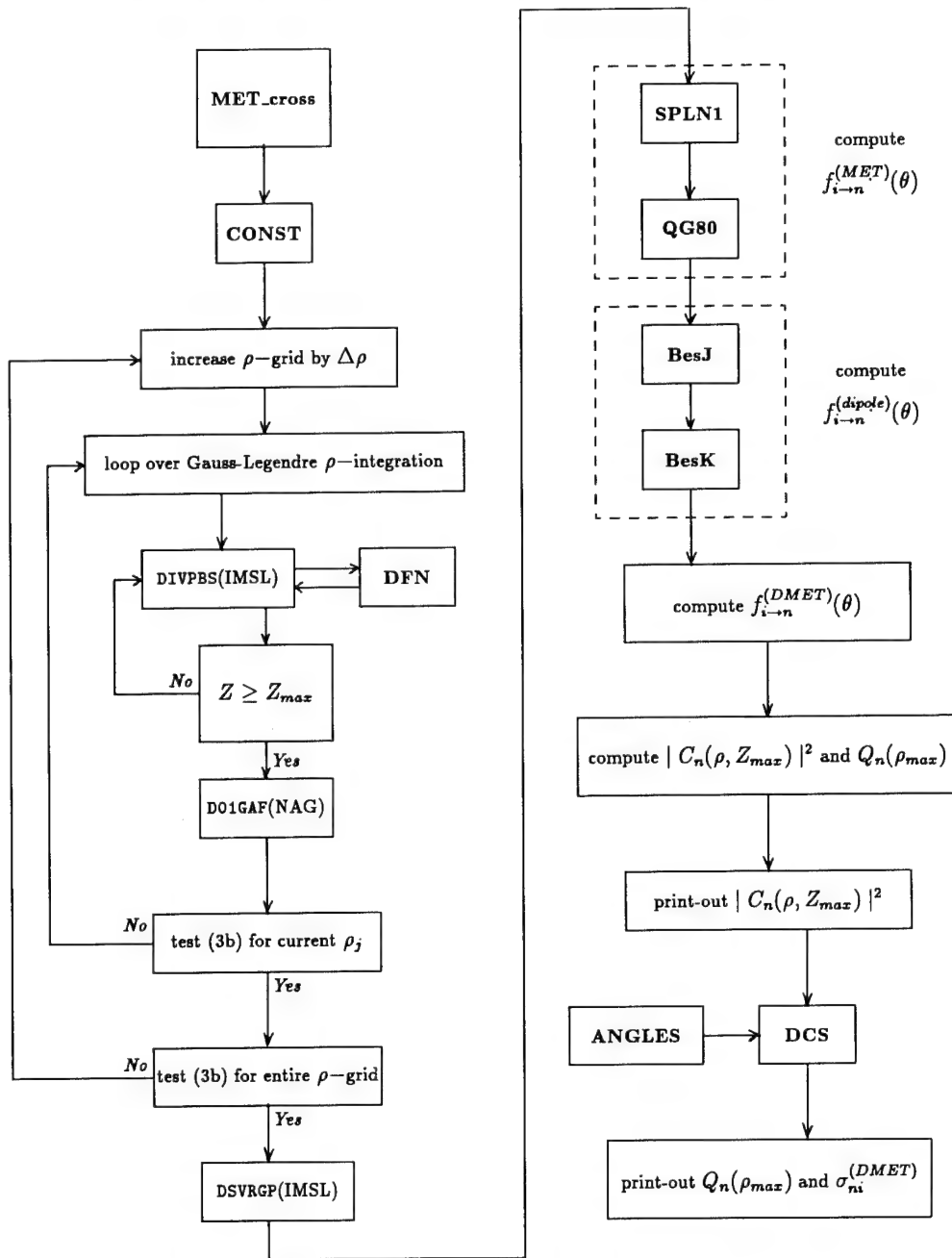


Fig. 2. Logical flowchart detailing computational tasks in program MET_cross.

The integrals I_1 and I_2 in (5) are defined as

$$I_1(\rho, \gamma(\theta)) = \int_{-\infty}^{\infty} dZ \kappa_n(\rho, Z) \frac{\partial C_n(\rho, Z)}{\partial Z} \exp[i\gamma(\theta)Z], \quad (7a)$$

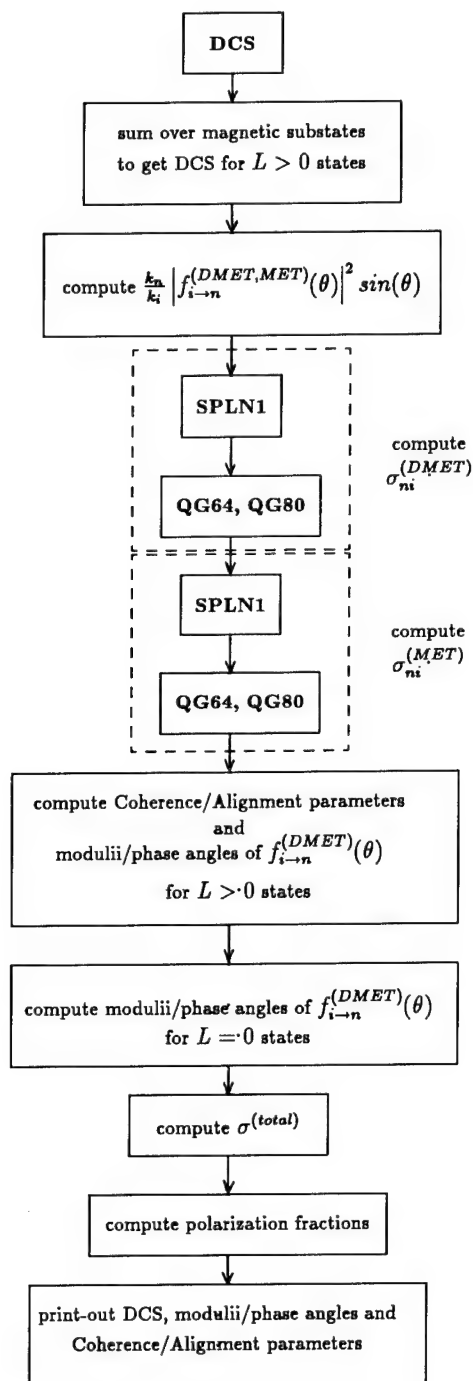


Fig. 3. Logical flowchart of module DCS in program MET_cross.

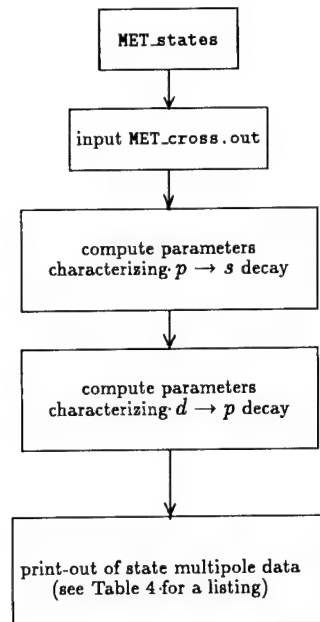


Fig. 4. Logical flowchart detailing computational tasks in program MET_states.

$$I_2(\rho, \gamma(\theta)) = \int_{-\infty}^{\infty} dZ \left(\kappa_n(\rho, Z) [\kappa_n(\rho, Z) - k_n] + \frac{\hbar^2}{\mu} V_{nn} \right) \times C_n(\rho, Z) \exp[i\gamma(\theta)Z], \quad (7b)$$

and the matrix elements (1) which appear in (2) and (5) are factored into radial and azimuthal parts as [16]

$$V_{nj}(\mathbf{R}) = V_{nj}(R, \Theta) \exp(i\Delta\Phi). \quad (8)$$

It proves advantageous in performing the Z -integration needed in evaluating I_1 and I_2 in (7), to choose the Z -grid in solving (2) to be the pivot points to be used in performing the quadratures in (7). Once the integrals I_1 and I_2 have been evaluated, the ρ -integration in (5) and the θ -integration in (6) are done using the Gauss–Legendre quadrature [17]. With the assumption of straight-line trajectories, the coupled equations (2) are independent of the electron scattering angle θ . The scattering angle dependence arises in (5) in the term $\gamma(\theta)$ and in the argument q' of the Bessel function $J_\Delta(x)$, of integer order Δ , which itself arises due to the factorization (6) of the azimuthal angle Φ dependence of the matrix elements (1). Finally, once the complex scattering amplitudes $f_{i \rightarrow n}(\theta)$ for each of the states in the basis set have been obtained from (5), the subsequent determination of the state multipoles, Stokes parameters and the orientation and alignment parameters are obtained without further quadrature in MET_states. In the appendix we collect together for completeness the expressions used in MET_states to determine the orientation and alignment parameters, state multipoles and Stokes parameters (hereafter denoted collectively as state multipole data).

An important feature of the coupled equations (2) is that the impact-parameter dependence only appears parametrically. As discussed in more detail elsewhere [13], the majority of the time in the MET is spent in solving (2) and then evaluating the quadratures (7). Hence the heart of the code MET_cross is the loop in which (2) is solved and (7) evaluated and is illustrated schematically in Fig. 5. A judicious

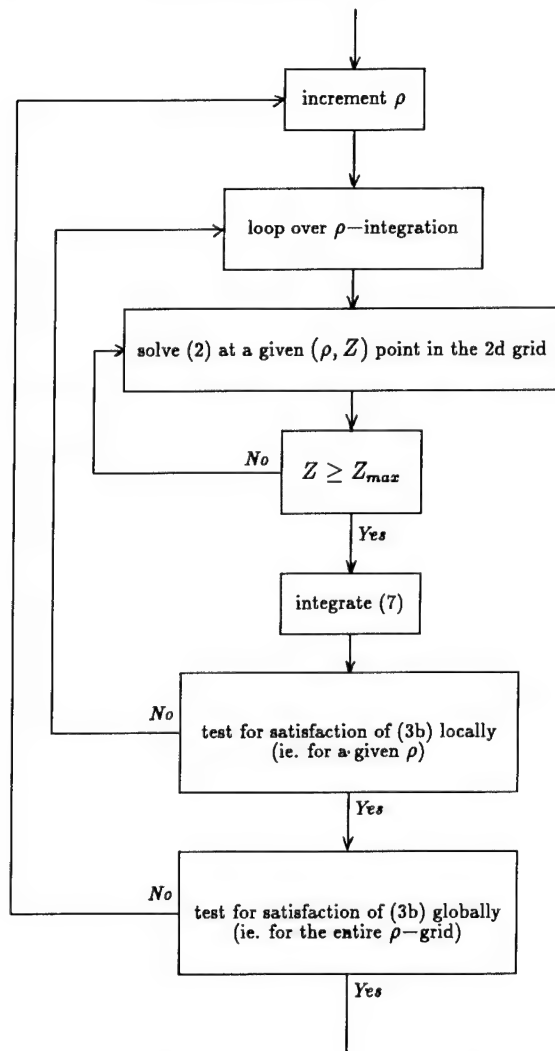


Fig. 5. General logical ordering of the solution of the coupled equations (2).

choice of the Z -grid therefore will eliminate the need for interpolation in the quadrature (7) and save a considerable amount of time in the execution of the code. In addition, by placing the quadrature (7) *inside* the loop over the impact parameter (see Fig. 5), the need to index the arrays storing the integrand of (5) with respect to Z is eliminated, thereby reducing the memory requirements of the code (since indexing the integrand of (5) with respect to the state (n), scattering angle (θ) and impact parameter (ρ) must already be done).

After extensive testing [13] of a variety of rectangular grids and solution methods for the coupled first-order partial differential equations (2), a robust integration scheme has been developed and incorporated into `MET_cross` which should require only minimal user intervention and which makes use of the loop structure shown in Fig. 5. A nonlinear grid in Z (chosen to cluster points near the origin at $Z = 0$) is used with the extrapolation method of Bulirsch and Stoer [18] to solve the coupled equations (2). The subsequent quadrature (7) over the nonlinear Z -grid used to solve (2) is performed with the

NAG routine `D01GAF` [19] which uses a third-order finite difference formula due to Gill and Miller [20]. The outer loop over the impact parameter (see Fig. 5) is executed until the constraint (3b) is satisfied for *all* states in the basis set. The evaluation of (7a, b) over the nonlinear Z -grid used to solve (2) must necessarily be done for all states in the basis set and all electron scattering angles θ at each stage of the ρ -loop. The real and imaginary parts of the term in square brackets in (5) is then assembled from (7) and stored in the arrays `FRR` and `FIR` indexed by scattering angle, state and impact parameter (see Table 1 in Section 3). Upon exiting the outer ρ -loop, the subsequent integration of (5) over the impact parameter is achieved by an 80-point Gauss–Legendre quadrature [17] over the entire extent of the impact parameter grid: $0 \leq \rho \leq \rho_{\max}$.

When dealing with transitions $i \rightarrow n$ among metastable states, the long-range dipole interactions present in optically allowed transitions influence dramatically [15] the distant, large-impact-parameter region. The long-range dipole interaction yields complex amplitudes $C_n(\rho, Z)$ with substantial long-range tails at large impact parameters, which in turn results in non-negligible contributions to (5) in the range $\rho_{\max} \leq \rho < \infty$. The contribution from the range $\rho_{\max} \leq \rho < \infty$ to small-angle scattering is especially important, and hence cannot be neglected in the calculation of the scattering amplitudes. Labeling the scattering amplitude obtained from the 80-point Gauss–Legendre quadrature over the range $0 \leq \rho \leq \rho_{\max}$ by $f_{i \rightarrow n}^{(\text{MET})}(\theta)$ and the remainder by $f_{i \rightarrow n}^{(\text{dipole})}(\theta)$ we have the expression [14]

$$f_{i \rightarrow n}^{(\text{DMET})}(\theta) = \begin{cases} f_{i \rightarrow n}^{(\text{MET})}(\theta) + f_{i \rightarrow n}^{(\text{dipole})}(\theta), & \Delta l = \pm 1, \\ f_{i \rightarrow n}^{(\text{MET})}(\theta), & \Delta l = 0, \end{cases} \quad (9a)$$

$$(9b)$$

where the contribution to the scattering amplitude from the long-range dipole interaction in the limit of large impact parameter is [14]

$$f_{i \rightarrow n}^{(\text{dipole})}(\theta) = \Gamma(i)^{\Delta} \frac{2\mu d'_{ni}}{\hbar^2} \frac{\alpha'}{q'^2 + \alpha'^2} [\chi_1 J_{\Delta+1}(\chi_1) K_{\Delta}(\chi_2) - \chi_2 J_{\Delta}(\chi_1) K_{\Delta+1}(\chi_2)], \quad (10)$$

with $\alpha' = \gamma(\theta) - \alpha$, $\chi_1 = q'\rho_{\max}$, $\chi_2 = \alpha'\rho_{\max}$ and $\Gamma = -(i)^{\Delta+1}$. The dipole moment d_{ni} for the transition $i \rightarrow n$ appears in the term d'_{ni} as $d'_{ni} = (3\pi/4)^{1/2} d_{ni}$.

Therefore, for optically allowed dipole-coupled transitions, once $f_{i \rightarrow n}^{(\text{MET})}(\theta)$ has been stored, Eq. (10) is evaluated and, using the prescription (9), the contribution the long-range tails of the amplitude functions $C_n(\rho, Z)$ make to the scattering amplitude is accounted for.

Finally, the differential cross section is determined from (6a) and the integral cross section from (6b). The integration over scattering angle θ in (6b) is done using 64- and 80-point Gauss–Legendre quadrature [17].

We should note that the use of a succession of 1-, 2-, 4- and 10-point Gauss–Legendre quadratures in the outer ρ -loop in solving (2) to estimate (4) results in the storage of the integrand of (5) with respect to the impact-parameter index *not* in an ascending order. A simple sort is then performed to allow the subsequent integration over ρ to proceed. The Gauss–Legendre quadratures over ρ in (5) and θ in (6b) are performed via a cubic spline interpolation [21] of the appropriate integrand. Other choices for the ρ -quadrature (5) are possible (e.g. Gauss–Kronrod) and necessarily involve trade-offs between execution time and storage requirements. Further details on the results of testing a number of different quadrature methods for the ρ -integration in (4) and (5) are given in [13].

The method used in `MET_cross` to generate the ρ -grid used to solve (2) has been automated as much as possible to require minimal user intervention. Once the user inputs the ρ -grid spacing $\Delta\rho$ and the impact-parameter cross section tolerance ϵ , the code will continue to increase the ρ -grid (in increments of $\Delta\rho$) until the constraint (3b) is satisfied. The unitarity constraint (3a) is evaluated and output but is

Table 1
Major variables in program MET_cross

Mathematical symbol	Variable name in code	Comments
\mathcal{N}_r	NST	no. of states in basis set
$2\mathcal{N}_r$	NEQ	no. of real amplitude equations to solve
	NANG	no. of scattering angles at which $f_j^{(\text{DMET})}(\theta)$ are computed
	NRO	maximum number of impact parameters allowed in calculation
	NROW	actual number of impact parameters used
	NGP	no. of non-zero L states in basis set
	NCOL	NST + NGP
	NZ	initial no. of points in Z -grid in the range $-Z_{\text{max}} \leq Z \leq 0$
	MZ	total no. of points allowed in Z -grid
	NPT	maximum no. of points in GL-quadrature (4)
	NPTGL	no. of different GL-quadratures used in a given iteration of the ρ -loop
$\mathcal{N}_j^{(\text{GL})}$	NG(NPTGL)	no. of points in current GL-quadrature
i	INT	initial state label
$\Delta L, \Delta$	DL, DM	change in orbital and magnetic quantum nos.
$\kappa_r(\rho, Z), k_n$	KAPPA(NST), K(NST)	local and asymptotic channel wavenumbers, resp.
k'	KP	$k_n \sin \theta$
μ	REMASS	reduced mass
α	ALPHA	$(\epsilon_n - \epsilon_i) / v$
$\gamma(\theta)$	GAMMA	$k_n(1 - \cos \theta)$
d_{ni}	DIPOLE	dipole moment of transition
ϵ_n	E(NST)	energies of atomic states in the basis set
L, M_L	L(NST), ML(NST)	orbital and magnetic quantum nos. of states in the basis set
ρ	RHO	current impact parameter
ρ	RO(NRO)	impact parameters used to solve (2)
$\rho_{\text{lower}}, \rho_{\text{upper}}$	LOW, UP	initial limits used in (4)
ρ_{min}	ROMIN	minimum impact parameter the ρ -grid will include
ρ_{max}	ROMAX	maximum impact parameter the ρ -grid can be extended to include
$\Delta \rho$	DELTA	amount the ρ -grid is increased in loop
	WG(NPTGL, NPT)	array of all GL-quadrature weights needed
φ_j	XXG(NPTGL, NPT)	array of all GL-quadrature pivots needed
ρ_j	WG(NPT)	current GL-quadrature weights
	XG(NPT)	current GL-quadrature pivots
Z_{max}	F(NRO, NST)	ρ -integrand of (4)
Z	ZMAX	maximum extent of Z -grid
	ZPIVOT(NZ), ZZ(LN2NZ)	initial and final Z -grid points used to solve (2), resp.
	Z, ZEND	initial and final Z -grid points at which (2) is solved, resp.
	CA(NWK), CB(NWK)	spline coefficients of ρ -integrand of (5)
$V_{ni}(\mathbf{R})$	VON(NST), VOFF(NST, NST)	arrays of integration matrix elements (1)
θ	THETA(NANG), PSI(NANG)	scattering angles in degrees and radians, resp.
	X(NANG)	θ -integrand of (6b)
	C(NWK2)	spline coefficients of θ -integrand of (6b)

$d\sigma^{(\text{DMET})}/d\Omega$	DDXN(NANG, NCOL)	DMET differential cross sections (in $a_0^2/\text{sr.}$)
$d\sigma^{(\text{MET})}/d\Omega$	DDXN2(NANG, NCOL)	MET differential cross sections (in $a_0^2/\text{sr.}$)
E	ENER	energy of incident electron
ϵ	TOL	tolerance criterion for satisfaction of (3b)
$Q_n(\rho_{\text{max}})$	QIP(NCOL, 3)	integral cross sections from (4)
$\sigma_n^{(\text{DMET})}$	QDMET(NCOL, 3)	DMET integral cross sections from (6b)
$\sigma_n^{(\text{MET})}$	QMET(NCOL, 3)	MET integral cross sections from (6b)
	LAB(NCOL)	spectroscopic labels of states in the basis set
	NNG(NGP)	no. of states in the basis set with $L = 1, 2, \dots$
	NSTS(NGP, NST)	integer label of each of the NNG states in the basis set
	NS, NLCP, NLCD	no. of S, P and D states in the basis set, resp.
	NPFRAC	no. of polarization fractions
	IS(NGP), IPO(NGP), IP1(NGP)	integer label of the s, $np_{0, \pm 1}$ states in the basis set, resp.
	ID0(NGP), ID1(NGP), ID2(NGP)	integer label of the d _m ($m = 0, \pm 1, \pm 2$) states in the basis set, resp.
$C_n(\rho, Z)$	Y(NEQ)	real and imaginary parts of the solution of (2) at the current (ρ, Z)-grid point
$ C_n(\rho, Z) ^2$	PROB(NRO, NST), PROBB(NRO, NST)	probabilities un-ordered and ordered w.r.t. ρ , resp.
	SUM(NRO), SSUM(NRO)	sum (3a) un-ordered and ordered (w.r.t. ρ), resp.
	IRO(NRO)	permutation matrix of impact parameters
	PREV(NST), PRES(NST)	two evaluations of (3b) for adjacent impact parameters
	FRR(NANG, NST, NRO)	real part of ρ -integrand of (5)
	FIR(NANG, NST, NRO)	imaginary part of ρ -integrand of (5)
	FRRZ(NST, LNZ: NZ), FIRZ(NST, LNZ: NZ)	real and imaginary parts of Z-integrand of (7) with exp term
	ZREAL(NST), ZIMAG(NST)	current values of real and imaginary parts of Z-integrand of (7) without exp term inside Z-loop
	RRZ(NST, LNZ: NZ), IRZ(NST, LNZ: NZ)	real and imaginary parts of Z-integrand of (7) without exp term
	H	current step size in Z-grid
	EPS	error tolerance used in solving (2)
	II, JJ	integer counters used in the ρ - and Z-loops, resp.
	ERR, ERROR	current and final values of (3b), resp.
	FJ(10), FK(10)	Bessel functions used in (10)
	FFR(NANG, NST)	real part of DMET scattering amplitude (9)
	FFI(NANG, NST)	imaginary part of DMET scattering amplitude (9)
	LAMP(NANG, 2), CHIP(NANG, 2)	collision frame parameters (A.5a) for p states
λ, X	LAMB, CHID, MUD, PSID	collision frame parameter set (A.8) for d states
$\{\lambda, X, \psi, \mu\}$	P(2, 3)	polarization fractions
$\sigma^{(\text{total})}$	QTOT(3)	total cross section obtained from optical theorem
	DXND0(NANG, NCOL)	integrand of (6b) for the DMET DCS
$ f_s , \beta_s$	FS, BETAS	modulus and phase angle of $f_i^{(\text{DMET})}(\theta)$ for the s states in the basis set
$ f_{p_m} , \beta_{p_m}$ ($m = 0, 1$)	FPO, FP1, BETAP0, BETAP1	moduli and phase angles of $f_{i \rightarrow n}^{(\text{DMET})}(\theta)$ for the p states in the basis set
$ f_{d_m} $ ($m = 0, 1, 2$)	FDO, FD1, FD2	moduli of $f_{i \rightarrow n}^{(\text{DMET})}(\theta)$ for the d states in the basis set
β_{d_m} ($m = 0, 1, 2$)	BETAD0, BETAD1, BETAD2	phase angles of $f_{i \rightarrow n}^{(\text{DMET})}(\theta)$ for the d states in the basis sets

Table 2
Major variables in program MET-states

Mathematical symbol	Variable name in code	Comments
N_p, N_d	NP, ND	number of p and d states in basis set
R_p, I_p	RP, IP	Fano–Macek parameters given by (A.5b,c)
$A_0^{(col.)}, A_{1+}^{(col.)}, A_{2+}^{(col.)}$	AOP, A1PP, A2PP	alignment tensor (A.1a) for p → s decay
$\mathcal{O}_{1-}^{(col.)}$	O1MP	orientation vector (A.1b) for p → s decay
$A_0^{(col.)}, A_{1+}^{(col.)}, A_{2+}^{(col.)}$	AOD, A1PD, A2PD	alignment tensor (A.7a,b) for d → p decay
$\mathcal{O}_{1-}^{(col.)}$	O1MD	orientation vector (A.7c) for d → p decay
γ	ANGMIN	orientation angle of charge cloud (A.6b)
$\langle L_{\perp} \rangle$	LPS, LDP	angular momentum transferred in p → s (A.2) and d → p (A.13) decays
μ, η	MU, ETA	natural frame parameters (A.2)
L_p, W_p	LP, WP	length and width of p state charge clouds
$\{\xi, \nu, \zeta, \omega\}$	XI, NU, ZETA, OMEGA	natural frame parameter set (A.12)
$P_i^{(col.)} (i=1-4)$	PC1, PC2, PC3, PC4	collision frame Stokes parameters (A.1c) and (A.7d,e)
$P_{lin.}^{(col.)}, P^{(col.)} $	PCL, PC	collision frame linear and total polarizations
$P_i^{(nat.)}$	PN1, PN2, PN3, PN4	natural frame Stokes parameters (A.9a,b)
$P_{lin.}^{(nat.)}, P^{(nat.)} $	PNL, PN	natural frame linear and total polarization
$\langle T(00)_{00}^+ \rangle$	T0000	p → s state multipole (A.3a)
$\langle T(10)_{1m}^+ (m=0, 1) \rangle$	T1010, T1011	p → s state multipole (A.3b): complex quantity written as arrays of length 2
$\langle T(11)_{00}^+ \rangle$	T1100	p → s state multipole (A.3c)
$\langle T(11)_{11}^+ \rangle$	T1111	p → s state multipole (A.3d)
$\langle T(11)_{20}^+ \rangle$	T1120	p → s state multipole (A.3e)
$\langle T(11)_{21}^+ \rangle$	T1121	p → s state multipole (A.3f)
$\langle T(11)_{22}^+ \rangle$	T1122	p → s state multipole (A.3g)
$\langle T(20)_{00}^+ \rangle$	T2200	d → p state multipole (A.14a)
$\langle T(20)_{2m}^+ (m=0, 1, 2) \rangle$	T2020, T2021, T2022	d → p state multipole (A.14b–d): complex quantity written as arrays of length 2
$\langle T(22)_{00}^+ \rangle$	T2200	d → p state multipole (A.14e)
$\langle T(22)_{11}^+ \rangle$	T2211	d → p state multipole (A.14f)
$\langle T(22)_{2m}^+ (m=0, 1, 2) \rangle$	T2220, T2221, T2222	d → p state multipole (A.14g–i)

not used to guide the code in grid generation as (3b) is used. The primary purpose of (3a) is that it provides a check on unitarity of the amplitude functions $C_n(\rho, Z)$, thereby allowing the user to gauge the choices of $\Delta\rho$, ρ_{\max} and Z_{\max} used.

3. Description of output data produced

In this section a summary of each module in the programs MET_cross and MET_states is given. Table 1 provides a list of the major variables used in the code MET_cross, while Table 2 provides a similar list of variables used in MET_states. In both Tables 1 and 2 the mathematical symbol used in this paper to identify a particular quantity is given along with the *label* used to identify it inside the code.

All calculations in both MET_cross and MET_states are done using 64-bit word lengths (double precision on 32-bit machines) and are written using standard ANSI FORTRAN 77 syntax. An earlier version of part of MET_cross, involving the numerical solution of coupled semiclassical equations, dates from 1969 in work published [32] by the second author. This early work on impact-parameter equations made extensive use of a module written by R.H.G. Reid for the solution of coupled differential equations. The semiclassical code which was developed by the second author then was used as a template

for the development, with K.J. McCann during the period 1972–74, of the original version of `MET_cross` to solve the coupled semiclassical equations (2) using at that time FORTRAN 66 syntax. Limitations on machine architecture at the time the MET code was originally developed required the solution of (2) and the evaluation of (5) to be done in two stages. In 1980 considerable changes in the original code developed by K.J. McCann and the second author were made by the first author and involved the evolution of `MET_cross` to FORTRAN 77 syntax, increasing by a factor of ten the accuracy of the solutions of (2) and evaluation of (5), and incorporating modifications to handle larger basis sets and the new procedure to solve the coupled equations (see Fig. 5 for details). The code `MET_states` dates from 1983 and was designed by the first author to be an adjunct to `MET_cross` to allow for the easy generation of additional state multipole data. Both codes have been in continual use and have been tested on a variety of mainframes since 1974 and (starting in 1990) on workstations and should be portable with little code modification required. Any questions regarding code usage and portability issues can be sent to the e-mail address of the first author.

3.1. Program `MET_cross`

`MET_cross`. The main routine first initializes all global and local constants, begins the loop over impact parameter, solves (2) over the range $-Z_{\max} \leq Z \leq Z_{\max}$, performs the quadratures in (7), and then tests for satisfaction of the constraint (3b) at both the current stage of the ρ -loop and then globally over the entire ρ -grid. Once (3b) is satisfied both locally and globally, then the ρ -loop is exited and the impact parameters used to solve (2) are sorted into ascending order, the scattering amplitudes $f_{i \rightarrow n}^{(\text{MET})}(\theta)$ and $f_{i \rightarrow n}^{(\text{dipole})}(\theta)$ (when needed) are computed and then $f_{i \rightarrow n}^{(\text{DMET})}(\theta)$ is assembled via the prescription (9). If (3b) is not satisfied locally, the next Gauss–Legendre quadrature is performed in succession until it is satisfied. The resultant errors associated with the ρ -quadrature (4) are then printed out in `MET_cross.out` (see test run output below). The relative magnitudes of the errors associated with the constraint (3a) give an indication of the accuracy of the semiclassical amplitudes $C_n(\rho, Z)$. A detailed analysis of the absolute error associated with different algorithms used to solve the coupled equations (2), and a comparison of the error associated with different quadrature schemes used in Eq. (4), (5) and (7) is given in [13]. As an example of the relative errors associated with the DMET cross sections of the different states in the basis set, we note that the sum of the probabilities for excitation of the 3d states of H, by an electron of energy 54.40 eV and impact parameter $\rho = 1.133 a_0$, is 0.119%, which is only about one-third the deviation of the sum of all the probabilities at that impact parameter from unity. The fact that the probability associated with the excitation of the 3d states is one-third the total deviation of the sum of the probabilities (3a) from unity is an indication of the increasing difficulty in computing cross sections for states in the basis set which have only a weak direct coupling mechanism to the initial state. For further details and for a discussion of the relative merits of different quadrature schemes and methods of solving the coupled equations (2) see [13].

Finally, the probabilities $|C_n(\rho, Z = Z_{\max})|^2$ are computed and printed out along with the cross sections from the impact-parameter expression (4), and the differential cross sections from $f_{i \rightarrow n}^{(\text{MET})}(\theta)$ and $f_{i \rightarrow n}^{(\text{DMET})}(\theta)$ are stored for later use in `DCS`. The subroutine `DCS` is then called, and once control is passed back to `MET_cross`, the integral cross sections σ_{ni} determined by (6b) are printed out.

The overall portability of `MET_cross` is only limited by the choice of integration routine used to solve (2), and the quadrature method invoked for (7). The results of extensive testing of a variety of algorithms for the initial value problem (2) and quadrature schemes for (7) are reported in [13]. The present version of `MET_cross` makes use of the Bulirsch–Stoer extrapolation algorithm [18] in the IMSL software library [22] and the integration routine `D01GAF` [19,20] for unequally spaced data from the NAG software library. Other choices are possible and are detailed in [13].

Besides the array sizes appearing in the `PARAMETER` statements, and the use of formatted `WRITE`

statements, the main parts of **MET_cross** which are dependent upon choice of target atom are the subroutines **CONST** and **DFN**. The program **Vij** (see accompanying paper [16]) can be used to generate subroutines **CONST** and **DFN** for target atoms H and He. To modify **MET_cross** to deal with other target atoms requires the user to supply the energy levels and matrix elements (1) as well as various arrays used to store labeling and basis set information. See the discussion under the **DFN** and **CONST** subroutines for details.

As an example of the adaptation of **MET_cross** to handle specific basis sets and target atoms, we provide three copies of the parts of the code dependent upon basis set and target atom data in the collection of programs distributed with this issue. The three copies, labeled **MET_cross.eh**, **MET_cross.ehe1** and **MET_cross.ehe3** are for the cases of electron scattering by H and He. The latter two routines for the scattering of electrons by helium are for the cases where the basis set is composed solely of singlet or triplet states.

CONST. This subroutine initializes the main arrays used to characterize the basis set. First, the energies of the atomic states in the basis set are set up in array **E**, the orbital and magnetic quantum numbers of the atomic states in arrays **L** and **ML**, respectively. The character array **LAB** contains the standard spectroscopic notation for each of the states in the basis set. Finally, the constants in the expressions for the spherical harmonics are given. The spherical harmonics are used in subroutine **DFN** in the evaluation of the matrix elements (1). This entire module may be generated by **Vij** [16] or supplied by the user.

DFN. In this subroutine the user supplies the algorithm used to solve the coupled equations (2) for the value of the derivatives $dC_n(\rho, Z)/dZ$ at each point in the 2D grid. The three copies of this module (**DFN.eh**, **DFN.ehe1**, **DFN.ehe3**), supplied with the collection of programs distributed with this issue, provide an example of the use of **Vij** [16] for generating entire sets of matrix elements for H and He.

The present version of **DFN** is designed to be called from **DIVPBS** [22] to compute the first derivatives of the amplitude functions, $dC_n(\rho, Z)/dZ$, given the spherical harmonics, matrix elements (1) and local wavenumbers $\kappa_n(\rho, Z)$. To complete the determination of the necessary spherical harmonics, the polar angle θ that **R** has with respect to the direction of the incident beam of electrons is computed from analytic geometry. This then allows for the complete determination of the spherical harmonics required in a given basis set.

The next segment of **DFN** is generally the longest and consists of an enumeration of all the matrix elements (1) required in the basis set. We have chosen to represent the matrix elements $V_{nj}(R, \theta)$ as explicit analytical functions rather than interpolate over an array of numerical data due to the number of times **DFN** is entered ($\sim 10^5$) and the total number of distinct matrix elements required (see Table 1 of [16]). Once all the matrix elements have been computed, the diagonal and off-diagonal elements are stored in arrays **VON** and **VOFF**, respectively. Next, the local wavenumbers $\kappa_n(\rho, Z)$ are computed, and the derivatives $dC_n(\rho, Z)/dZ$ are determined and stored. Note that the coupled equations (2) are written as \mathcal{N} complex equations whereas what is needed in **DFN** are *real* equations. The required algebra to convert the \mathcal{N} complex equations (2) into $2\mathcal{N}$ real equations is straightforward and is not repeated here, but is incorporated into the code.

Finally, in view of the need to perform the quadrature (5) after the integration of (2) over a given Z-grid has been completed, the real and imaginary components of the term in square brackets in (5) (without the $\exp[i\gamma(\theta)Z]$ term) are computed and stored in arrays **ZREAL** and **ZIMAG**, respectively, for later use in **MET_cross**.

As with **CONST**, the user can generate the code required in **DFN** for targets H and He by application of **Vij** or, using **DFN.eh**, **DFN.ehe1** and **DFN.ehe3** as templates, provide his own version of **DFN**. When modifying **DFN** to handle targets other than H or He, the same basic structure as Eq. (2) will be retained

if a single-configuration quasi one-electron representation of the target atom wavefunction is appropriate.

DCS. The principal purpose of this module is to compute, and return to **MET_cross**, the integral cross sections σ_{ni} , obtained from (6b), by direct numerical integration of the differential cross sections. The computation of σ_{ni} by direct quadrature in fact is quite rapid [16] and is broken up into 3 basic parts: (a) For all states with non-zero L a sum over magnetic substates is done for the differential cross sections $d\sigma^{(\text{DMET})}/d\Omega$ and $d\sigma^{(\text{MET})}/d\Omega$, which are computed, respectively, from the scattering amplitudes $f_{i \rightarrow n}^{(\text{DMET})}(\theta)$ and $f_{i \rightarrow n}^{(\text{MET})}(\theta)$ (see Section 2 for details); (b) Then, after forming the respective two integrands for $\sigma_{ni}^{(\text{DMET})}$ and $\sigma_{ni}^{(\text{MET})}$ by multiplying $d\sigma^{(\text{DMET})}/d\Omega$ and $d\sigma^{(\text{MET})}/d\Omega$ by $\sin \theta$, cubic spline interpolating polynomials [21] are computed and stored; and (c) The actual integration in (6b) over θ is accomplished using 64- and 80-point Gauss–Legendre quadratures over the respective cubic spline interpolating polynomials. The Gauss–Legendre quadrature of (6b) is done in stages,

$$\int_0^{\theta_{\max}} \frac{d\sigma_{ni}}{d\Omega} \sin \theta d\theta = \int_0^1 (80) + \int_1^{10} (80) + \int_{10}^{40} (64) + \int_{40}^{\theta_{\max}} (64), \quad (11)$$

to insure an accurate representation of the contribution the differential cross section in the forward direction makes to the integral cross section. Such a fine quadrature mesh is especially important when i is an excited state [15]. In (11) above, the angular limits are in degrees and the numbers in parentheses on the right-hand-side are the number of points in the respective Gauss–Legendre quadrature. In the present version of **MET_cross** the upper limit θ_{\max} is generally taken to be 50° . Differential cross sections are computed beyond $(\theta \sim 40^\circ)$ the region of validity of the eikonal approximation to provide a basis against which the results of Paper II of this series can be compared.

The remainder of the code in **DCS** is concerned with the generation of the coherence and alignment parameters and the moduli and phase angles of the complex scattering amplitudes $f_{i \rightarrow n}^{(\text{DMET})}(\theta)$. The familiar λ and χ parameters [23] for the P ($L = 1$) states and the $\{\lambda, \chi, \psi, \mu\}$ parameters [24] for the D ($L = 2$) states are also computed. Next, the moduli and phase angles of the complex scattering amplitudes $f_{i \rightarrow n}^{(\text{DMET})}(\theta)$ for all states in the basis set are determined and stored for future use in **MET_states**.

Lastly, the optical theorem is used to provide an estimate of the total integral cross section $\sigma^{(\text{total})}$, while the polarization fractions [25,26] for the P and D states are calculated. The module **DCS** then ends by printing out the two differential cross sections $d\sigma^{(\text{DMET})}/d\Omega$ and $d\sigma^{(\text{MET})}/d\Omega$, the moduli and phase angles of $f_{i \rightarrow n}^{(\text{DMET})}(\theta)$, the state multipole data mentioned above and the total cross section and polarization fraction data. See Table 3 for the specific variables that are output to **MET_cross.out**.

FR. Compute the real part of the integrand of (5), $J_\Delta(q\rho) \mathcal{R}(\rho) \rho$ for pivot point ρ , where the ordinary Bessel function of the first kind $J_n(x)$ is computed by standard methods (see below), and $\mathcal{R}(\rho)$ is the interpolated value, at the Gauss–Legendre pivot point ρ , of the cubic spline polynomial fitted to the real part of the complex quantity in square brackets in (5). See Section 2 and Table 1 for details.

FI. Compute the imaginary part of the integrand of (5), $J_\Delta(q\rho) \mathcal{I}(\rho) \rho$ for pivot point ρ , where again the Bessel function is straightforward to compute and $\mathcal{I}(\rho)$ is the interpolated value at ρ of the imaginary part of the complex quantity in square brackets in (5). See Section 2 and Table 1 for details.

FDXN. Compute the integrand (6b) at pivot point θ . The module makes use of routine **SPLN2** (see below) to evaluate the stored integrand $(k_n/k_i) |f_{i \rightarrow n}(\theta)|^2 \sin \theta$ at the Gauss–Legendre pivot point θ .

Block Data ANGLES. This module initializes the array **THETA** which contains the values of the electron scattering angles (in degrees) for which the complex scattering amplitudes are desired. The user

Table 3
Order of print-out of variables in program MET_cross

Variables output in module MET_cross:

NST, NROW, NANG, LOW, UP, ENER, TOL, VEL, ROMIN, ROMAX, ZINF, REMASS, NZAVG,
MZ, LAM(INT)

Repeated NROW times:

RO, (PROBB(I, J), J=1, 5)
ERROR(J), J=1, 5
RO, (PROBB(I, J), J=1, 6), NST, SSUM(I)
(ERROR(J), J=1, 6), NST

Repeated NST+NGP times:

LAB(I), (QIP(I, J), J=1, 3), QDMET(I, J), J=1, 3
LAB(I), (QMET(I, J), J=1, 3)

Variables output in module DCS:

Repeated NANG times:

THETA, (DDXN(I, J), J=1, 6)
THETA, (DDXN(I, J), J=7, NST)
THETA, (DDXN(I, J), J=NST+1, NCOL)
if INT=1: THETA, DDXN2(I, 3), DDXN2(I, 4), DDXN2(I, 6), DDXN2(I, 7),
DDXN2(I, 11), DDXN2(I, 12)
if 2 ≤ INT ≤ 4: THETA, DDXN2(I, 1), DDXN2(I, 5), DDXN2(I, 8), DDXN2(I, 9),
DDXN2(I, 10), DDXN2(I, 13)
THETA, (DCSDO(I, J), J=1, 6)
THETA, (DCSDO(I, J), J=7, 10)
THETA, (DCSDO(I, J), J=11, 13)
THETA, BETAP0(I, 1), BETAP1(I, 1), BETAP0(I, 2), BETAP1(I, 2)
THETA, BETAD0(I, 1), BETAD1(I, 1), BETAD2(I, 1)
THETA, FP0(I, 1), FP1(I, 1), FP0(I, 2), FP1(I, 2)
THETA, FD0(I, 1), FD1(I, 1), FD2(I, 1)
THETA, (FS(I, J), J=1, 3), (BETAS(I, J), J=1, 3)
THETA, (LAMP(I, J), CHIP(I, J), J=1, NLCP)
THETA, (LAMD(I, J), MUD(I, J), CHID(I, J), PSID(I, J), J=1, NLCD)
(P(1, J), J=1, 3)
QTOT(1), QTOT(2), QTOT(3)

may change the grid of scattering angles if needed and then simply update the length of the array THETA in the appropriate PARAMETER statements in MET_cross and MET_states.

The following six routines are provided with the program MET_cross for the execution of basic numerical tasks required in the calculation of the MET cross sections. The user may keep these routines and use them together with MET_cross, or place them in a separate user-defined software library.

3.2. Library routines

QG64, QG80. Functions used to perform a Gauss–Legendre 64- and 80-point quadrature over a specified (arbitrary) interval of a user-defined integrand. The user-defined integrand is computed in a FUNCTION subprogram and must be declared in an EXTERNAL statement from the calling routine. Examples of such integrands are the modules **FR**, **FI** and **FDXN**.

SPLN1. Module used to generate a cubic spline polynomial fit to N data points given arbitrary and conditions on the spline. The output is the $3N$ array of coefficients defining the cubic spline polynomials.

SPLN2. Module used to evaluate a cubic spline polynomial at a given point. Requires as input the $3N$ array of coefficients output by **SPLN1**. The output of **SPLN2** yields the desired function value, as well as the first three derivatives of the function at the interpolated abscissa. For a given set of N data points to be fitted, one call to **SPLN1** suffices to define the cubic spline polynomial. Then a separate call to **SPLN2** must be executed each time an interpolated value of the fitted function is required.

BESJ, BESK. Modules used to compute ordinary Bessel functions of the first kind $J_n(x)$ and modified Bessel functions of the first kind $K_n(x)$, respectively, for integer order n and real argument x . The modules compute, for a given argument x , the Bessel functions $J_n(x)$ and $K_n(x)$ for a range of indices $0 \leq n \leq n_{\max}$ by applying the standard three-term recurrence relationships for Bessel functions [27]. Module **BESJ** makes use of the IMSL functions [28] **DBSJ0** and **DBSJ1** in the recurrence relationship, while **BESK** makes use of IMSL functions **DBSK0** and **DBSK1**. The linkage of modules **BESJ** and **BESK** to the IMSL software library can be eliminated by calls to routines of the user's preference which perform the same tasks if necessary.

3.3. Program **MET_states**

MET_states. The program **MET_states** consists of a single module which first inputs the results of **MET_cross** from the file **MET_cross.out** (see Fig. 1), and then computes the remainder of the state multipole data. The calculation of the state multipole data is done in two parts. First, the orientation vector **O**, alignment tensor **A** and Fano–Macek parameters [29] R , I characterizing the polarization properties of the radiation emitted in the decay of the 2p state of H and the $2^{1,3}P$ states of He are computed. Also computed at this stage in **MET_states** are the Stokes parameters P_i ($i = 1-4$) [30] and the complete set of (spin-averaged) state multipoles [31] $\langle T(lm)_{LM}^+ \rangle$ in the collision frame which characterize the coherence and correlation of the $n = 2, 3$ S and P states of the target (currently limited to H and He).

At the second stage in **MET_states**, the alignment tensor in the collision frame [30], the $\{\lambda, \chi, \psi, \mu\}$ parameters [24] and the Stokes parameters in the collision and natural frames are all computed for the decay of the 3d state of H and the $3^{1,3}D$ states of He. In addition, the entire set of (spin-averaged) state multipoles $\langle T(lm)_{LM}^+ \rangle$ in the collision frame, characterizing the degree of coherence and correlation among the S and D states of the $n = 3$ manifold of the target are computed.

In the appendix we enumerate the definitions of the above state multipole data in terms of the underlying complex scattering amplitudes to make our discussion here relatively self-contained. Table 2 provides a list of the major variables in **MET_states** and their corresponding mathematical symbols. Therefore, cross-referencing between Table 2 and the appendix will allow the user of **MET_states** to identify a particular quantity or parameter of interest.

The remainder of **MET_states** contains the formatted WRITE statements needed to output the state multipole data generated. Table 4 lists the variables output by **MET_states** in the sequence printed using the same terminology as Table 2.

4. Description of input data and test runs

The amount of data to be input into **MET_cross** is quite small; however, the extent of the typical execution time is generally too long for interactive use of the code at present. Therefore, we recommend running **MET_cross** in the background or through the use of a batch queue system. Once **MET_cross** has completed execution, and **MET_cross.out** has been produced, the second program **MET_states** may be run interactively with no further user input required.

Table 4
Order of print-out of variables in program MET_states

Repeated for each p state in the basis set:

THETA, A0P, A1PP, A2PP, 01MP
 THETA, PC1, PC2, PC3, PC4, PCL, PC
 THETA, MU, ETA, GAMMA, THETA-MIN, LPS
 THETA, R0, R1, R, IO, I1, I
 THETA, T0000, T1010(1), T1010(2), T1011(1), T1011(2), T1100
 THETA, T1111/i, T1120, T1121, T1122, LP, WP

Repeated for each d state in the basis set:

THETA, A0D, A1PD, A2PD, 01MD
 THETA, PC1, PC2, PC3, PC4, PCL, PC
 THETA, PN1, PN2, PN3, PN4, PNL, PN
 THETA, XI, NU, ZETA, OMEGA, GAMMA, THETA-MIN
 THETA, R000, LDP, LD, WD
 THETA, R0, R1, R2, IO, I1, I2
 THETA, T0000, T2200, T2211/i, T2220, T2221, T2222
 THETA, T2020(1), T2020(2), T2021(1), T2021(2), T2022(1), T2022(2)

The specific order of variables to be input into MET_cross are given below. See Table 1 for definitions of the symbols.

Line 1: int
 Line 2: ATOM
 Line 3: if (ATOM = He) SPIN
 Line 4: ρ_{lower} , ρ_{upper} , ϵ
 Line 5: E

The sample test run provided, illustrating the use of MET_cross and MET_states, is for $e^- + \text{H}(1s)$ scattering at an incident energy of 54.40 eV. Only a sample of the output contained in MET_cross.out and MET_states.out is provided in this paper due to the length of the output. A full listing appears with the code in the tape provided with this issue.

4.1. Test run

example. $e^- + \text{H}(1s)$ scattering at $E = 54.40$ eV:

Line 1: 1
 Line 2: H
 Line 3: 0.0, 4.0, 0.005
 Line 4: 54.40

Acknowledgements

This research is supported by the US Air Force Office of Scientific Research under Grant no. F49620-94-1-0379.

Appendix

• Parameters characterizing the $p \rightarrow s$ decay in H and the $^1,3P \rightarrow ^1,3S$ decay in He. The orientation vector, alignment tensor components and Stokes parameters are given by [29,30]

$$A_0^{(\text{col.})} = \frac{1}{2}(1 - 3\lambda), \quad A_{1+}^{(\text{col.})} = \sqrt{\lambda(1 - \lambda)} \cos \chi, \quad A_{2+}^{(\text{col.})} = \frac{1}{2}(\lambda - 1), \quad (\text{A.1a})$$

$$\mathcal{O}_{1-}^{(\text{col.})} = -\sqrt{\lambda(1 - \lambda)} \sin \chi, \quad (\text{A.1b})$$

$$P_1 = 2\lambda - 1, \quad P_2 = -2\sqrt{\lambda(1 - \lambda)} \cos \chi, \quad P_3 = 2\sqrt{\lambda(1 - \lambda)} \sin \chi, \quad P_l = \sqrt{P_1^2 + P_2^2} \quad (\text{A.1c})$$

in the collision frame, while in the natural frame the parameters

$$\mu = -2\sqrt{\lambda(1 - \lambda)} \sin \chi, \quad \eta = \tan^{-1} \left(\frac{2\sqrt{\lambda(1 - \lambda)}}{1 - 2\lambda} \cos \chi \right), \quad \langle L_{\perp} \rangle = -P_3 \quad (\text{A.2})$$

completely characterize the decay of the p state.

• State multipoles for the $n = 2$ s and p states (collision frame) [31]:

$$\langle T(00)_{00}^+ \rangle = \sigma_{2s}(\theta), \quad (\text{A.3a})$$

$$\langle T(10)_{1m}^+ \rangle = [\sigma_{2s}(\theta) \sigma_{2p_m}(\theta)]^{1/2} [R_m(p_m s^*) + iI_m(p_m s^*)], \quad (\text{A.3b})$$

$$\langle T(11)_{00}^+ \rangle = \frac{1}{\sqrt{3}} \sigma_{2p}(\theta), \quad (\text{A.3c})$$

$$\langle T(11)_{1m}^+ \rangle = -i\sqrt{2} \sigma_{2p}(\theta) I \delta_{m1}, \quad (\text{A.3d})$$

$$\langle T(11)_{20}^+ \rangle = \sqrt{\frac{2}{3}} [\sigma_{2p+1}(\theta) - \sigma_{2p0}(\theta)], \quad (\text{A.3e})$$

$$\langle T(11)_{21}^+ \rangle = -\sqrt{2} \sigma_{2p}(\theta) R, \quad (\text{A.3f})$$

$$\langle T(11)_{22}^+ \rangle = -\frac{1}{2}(1 - \lambda) \sigma_{2p}(\theta), \quad (\text{A.3g})$$

where the complex amplitudes are written as

$$f_{2s}(\theta) = |f_{2s}(\theta)| \exp[i\beta_s(\theta)], \quad f_{2p_m}(\theta) = |f_{2p_m}(\theta)| \exp[i\beta_m(\theta)], \quad (\text{A.4})$$

and where the λ , χ , R_m , I_m , R and I parameters used in (A.1)–(A.3) are defined by

$$\lambda = \frac{\sigma_{2p0}(\theta)}{\sigma_{2p}(\theta)}, \quad \chi = \beta_1 - \beta_0, \quad R = \sqrt{\frac{\lambda(1 - \lambda)}{2}} \cos \chi, \quad I = \sqrt{\frac{\lambda(1 - \lambda)}{2}} \sin \chi, \quad (\text{A.5a})$$

$$R_m = \frac{\text{Re} \langle f_{2p_m}(\theta) f_{2s}(\theta)^* \rangle}{[\sigma_{2s}(\theta) \sigma_{2p_m}(\theta)]^{1/2}} = \frac{|f_{2s}(\theta)| |f_{2p_m}(\theta)| \cos(\beta_m - \beta_s)}{[\sigma_{2s}(\theta) \sigma_{2p_m}(\theta)]^{1/2}}, \quad (\text{A.5b})$$

$$I_m = \frac{\text{Im} \langle f_{2p_m}(\theta) f_{2s}(\theta)^* \rangle}{[\sigma_{2s}(\theta) \sigma_{2p_m}(\theta)]^{1/2}} = \frac{|f_{2s}(\theta)| |f_{2p_m}(\theta)| \sin(\beta_m - \beta_s)}{[\sigma_{2s}(\theta) \sigma_{2p_m}(\theta)]^{1/2}}, \quad (\text{A.5c})$$

with $\text{Re}(\mathcal{Z})$, $\text{Im}(\mathcal{Z})$ indicating the real and imaginary parts of the complex quantity \mathcal{Z} .

In terms of the collision frame Stokes parameters, the length (L) and width (W) of the charge cloud of the excited p state are given by [30]

$$L_p = \frac{1}{2}(1 + P_l), \quad W_p = \frac{1}{2}(1 - P_l), \quad (\text{A.6a})$$

while the angle the charge cloud makes with the direction of the incident beam is

$$\gamma = \frac{1}{2} \tan^{-1}(P_2/P_1). \quad (\text{A.6b})$$

• Parameters characterizing the $d \rightarrow p$ decay in H and the $^1,3D \rightarrow ^1,3P$ decays in He. The components of the alignment tensor and the Stokes parameters in the collision frame are [30]

$$A_0^{(\text{col.})} = 1 - 2\lambda - \frac{3}{2}\mu, \quad A_{1+}^{(\text{col.})} = \sqrt{\frac{1}{3}}\lambda\mu \cos \chi + \sqrt{\mu(1-\lambda-\mu)} \cos \psi, \quad (\text{A.7a})$$

$$A_{2+}^{(\text{col.})} = -\frac{1}{2}\mu + 2\sqrt{\frac{1}{3}}\lambda(1-\lambda-\mu) \cos(\chi + \psi), \quad (\text{A.7b})$$

$$\mathcal{O}_{1-}^{(\text{col.})} = -\sqrt{\frac{1}{3}}\lambda\mu \sin \chi - \frac{1}{3}\sqrt{\mu(1-\lambda-\mu)} \sin \psi, \quad (\text{A.7c})$$

$$P_1^{(\text{col.})} = \frac{-3(A_0^{(\text{col.})} - 3A_{2+}^{(\text{col.})})}{I^x}, \quad P_2^{(\text{col.})} = \frac{-6A_{1+}^{(\text{col.})}}{I^y}, \quad (\text{A.7d})$$

$$P_3^{(\text{col.})} = \frac{-18\mathcal{O}_{1-}^{(\text{col.})}}{I^y}, \quad P_4^{(\text{col.})} = \frac{-3(A_0^{(\text{col.})} + A_{2+}^{(\text{col.})})}{I^x}. \quad (\text{A.7e})$$

The $\{\lambda, \chi, \psi, \mu\}$ parameters in the collision frame are given by [24]

$$\lambda = \frac{\sigma_{3d_0}(\theta)}{\sigma_{3d}(\theta)}, \quad \chi = \beta_1 - \beta_0, \quad (\text{A.8a})$$

$$\mu = \frac{2\sigma_{3d_1}(\theta)}{\sigma_{3d}(\theta)}, \quad \psi = \beta_2 - \beta_1, \quad (\text{A.8b})$$

while in the natural frame the Stokes parameters are

$$P_1^{(\text{nat.})} = \frac{-6\nu \cos \xi}{3 - 2\xi}, \quad P_2^{(\text{nat.})} = \frac{-\sqrt{6} \nu \sin \xi}{3 - 2\xi}, \quad (\text{A.9a})$$

$$P_3^{(\text{nat.})} = \frac{-3\omega}{3 - 2\xi}, \quad P_4^{(\text{nat.})} = \frac{3 - 6\xi - \sqrt{6} \nu \cos \xi}{3 + 2\xi - \sqrt{6} \nu \cos \xi}, \quad (\text{A.9b})$$

$$I^x = 4 - (A_0^{(\text{col.})} - 3A_{2+}^{(\text{col.})}), \quad I^y = 4 - (A_0^{(\text{col.})} + 3A_{2+}^{(\text{col.})}). \quad (\text{A.10})$$

The $\{\xi, \nu, \zeta, \omega\}$ parameters in the natural frame are defined [24] by

$$\xi = \frac{|f_0^{(\text{nat.})}(\theta)|^2}{\sigma_d(\theta)}, \quad \nu = \frac{|f_0^{(\text{nat.})}(\theta) f_2^{(\text{nat.})*} + f_{-2}^{(\text{nat.})}(\theta) f_0^{(\text{nat.})*}|}{\sigma(\theta)}, \quad (\text{A.11a})$$

$$\zeta = \arg(f_0^{(\text{nat.})}(\theta) f_2^{(\text{nat.})*} + f_{-2}^{(\text{nat.})}(\theta) f_0^{(\text{nat.})*}), \quad \omega = \frac{||f_2^{(\text{nat.})}(\theta)|^2 - |f_{-2}^{(\text{nat.})}(\theta)|^2|}{\sigma(\theta)}. \quad (\text{A.11b})$$

The $\{\xi, \nu, \zeta, \omega\}$ set of parameters in the natural frame can be expressed in terms of the $\{\lambda, \chi, \psi, \mu\}$ parameter set in the collision frame as [24,35]

$$\xi = \frac{1}{4} [3 - 2\lambda - 3\mu + 2\sqrt{3}\lambda(1-\lambda-\mu) \cos(\chi + \psi)], \quad (\text{A.12a})$$

$$\begin{aligned} \nu^2 = & \frac{3}{8} (1 - 2\lambda - \mu)^2 + \frac{1}{2} [\lambda(1-\lambda-\mu) \cos^2(\chi + \psi) + \lambda\mu \cos^2 \chi + 3\mu(1-\lambda-\mu) \cos^2 \psi] \\ & + \sqrt{3}\lambda(1-\lambda-\mu) [\mu \cos \psi \cos \chi - \frac{1}{2}(1-\lambda-\mu) \cos(\chi + \psi)], \end{aligned} \quad (\text{A.12b})$$

$$\zeta = \tan^{-1} \left(\frac{\sqrt{\lambda\mu} \cos \chi + \sqrt{3\mu(1-\lambda-\mu)} \cos \psi}{\frac{1}{2}\sqrt{3}(1-2\lambda-\mu) - \sqrt{\lambda(1-\lambda-\mu)} \cos(\chi+\psi)} \right) - \tan^{-1} \left(\frac{\sqrt{3(1-\lambda-\mu)} \sin(\chi+\psi)}{\sqrt{\lambda} + \sqrt{3(1-\lambda-\mu)} \cos(\chi+\psi)} \right), \quad (\text{A.12c})$$

$$\omega = - \left[\sqrt{\mu(1-\lambda-\mu)} \sin \psi + \sqrt{3\lambda\mu} \sin \chi \right]. \quad (\text{A.12d})$$

The orientation vector and orbital angular momentum transferred are given by

$$\mathcal{O}_{1-}^{(\text{col.})} = \frac{1}{3}\omega, \quad \langle L_{\perp} \rangle = 2\omega. \quad (\text{A.13})$$

- State multipoles for the $n = 3$ s and d states (collision frame) [31]:

$$\langle T(20)_{00}^+ \rangle = \sigma_{3s}(\theta), \quad (\text{A.14a})$$

$$\begin{aligned} \langle T(20)_{20}^+ \rangle &= \langle f_{3d_0}(\theta) f_{3s}(\theta)^* \rangle \\ &= |f_{3s}(\theta)| |f_{3d_0}(\theta)| [\cos(\beta_0 - \beta_s) + i \sin(\beta_0 - \beta_s)], \end{aligned} \quad (\text{A.14b})$$

$$\begin{aligned} \langle T(20)_{21}^+ \rangle &= \langle f_{3d_1}(\theta) f_{3s}(\theta)^* \rangle \\ &= |f_{3s}(\theta)| |f_{3d_1}(\theta)| [\cos(\beta_1 - \beta_s) + i \sin(\beta_1 - \beta_s)], \end{aligned} \quad (\text{A.14c})$$

$$\begin{aligned} \langle T(20)_{22}^+ \rangle &= \langle f_{3d_2}(\theta) f_{3s}(\theta)^* \rangle \\ &= |f_{3s}(\theta)| |f_{3d_2}(\theta)| [\cos(\beta_2 - \beta_s) + i \sin(\beta_2 - \beta_s)], \end{aligned} \quad (\text{A.14d})$$

$$\langle T(22)_{00}^+ \rangle = \sqrt{\frac{1}{5}} \sigma_{3d}(\theta), \quad (\text{A.14e})$$

$$\begin{aligned} \langle T(22)_{11}^+ \rangle &= i\sqrt{\frac{4}{5}} \text{Im} \langle f_{3d_1}(\theta) f_{3d_2}(\theta)^* \rangle + i\sqrt{\frac{5}{6}} \text{Im} \langle f_{3d_0}(\theta) f_{3d_1}(\theta)^* \rangle \\ &= i \left[\sqrt{\frac{4}{5}} |f_{3d_1}(\theta)| |f_{3d_2}(\theta)| \sin(\beta_1 - \beta_2) \right. \\ &\quad \left. + \sqrt{\frac{5}{6}} |f_{3d_1}(\theta)| |f_{3d_0}(\theta)| \sin(\beta_0 - \beta_1) \right], \end{aligned} \quad (\text{A.14f'})$$

$$\begin{aligned} \langle T(22)_{20}^+ \rangle &= \sqrt{\frac{8}{7}} \langle |f_{3d_2}(\theta)|^2 \rangle - \sqrt{\frac{2}{7}} \langle |f_{3d_1}(\theta)|^2 \rangle - \sqrt{\frac{2}{7}} \langle |f_{3d_0}(\theta)|^2 \rangle \\ &= \sqrt{\frac{2}{7}} [2\sigma_{3d_2}(\theta) - \sigma_{3d_1}(\theta) - \sigma_{3d_0}(\theta)], \end{aligned} \quad (\text{A.14g})$$

$$\begin{aligned} \langle T(22)_{21}^+ \rangle &= -\sqrt{\frac{12}{7}} \text{Re} \langle f_{3d_1}(\theta) | f_{3d_2}(\theta)^* \rangle - \sqrt{\frac{2}{7}} \langle f_{3d_0}(\theta) f_{3d_1}(\theta)^* \rangle \\ &= -\sqrt{\frac{2}{7}} \left[\sqrt{6} |f_{3d_1}(\theta)| |f_{3d_2}(\theta)| \cos(\beta_1 - \beta_2) \right. \\ &\quad \left. + |f_{3d_0}(\theta)| |f_{3d_1}(\theta)| \cos(\beta_0 - \beta_1) \right], \end{aligned} \quad (\text{A.14h'})$$

$$\langle T(22)_{22}^+ \rangle = \sqrt{\frac{8}{7}} \text{Re} \langle f_{3d_0}(\theta) f_{3d_2}(\theta)^* \rangle - \sqrt{\frac{3}{7}} \langle |f_{3d_1}(\theta)|^2 \rangle \quad (\text{A.14i})$$

$$= \sqrt{\frac{1}{7}} [2 |f_{3d_0}(\theta)| |f_{3d_2}(\theta)| \cos(\beta_0 - \beta_2) - \sqrt{3} \sigma_{3d_1}(\theta)], \quad (\text{A.14i'})$$

and where the complex amplitudes for the $3l_m$ states are written in terms of moduli and phase angles as

$$f_{3s}(\theta) = |f_{3s}(\theta)| \exp[i\beta_s(\theta)], \quad f_{3d_0}(\theta) = |f_{3d_0}(\theta)| \exp[i\beta_0(\theta)], \quad (\text{A.15a})$$

$$f_{3d_1}(\theta) = |f_{3d_1}(\theta)| \exp[i\beta_1(\theta)], \quad f_{3d_2}(\theta) = |f_{3d_2}(\theta)| \exp[i\beta_2(\theta)]. \quad (\text{A.15b})$$

The real and imaginary components of the complex scattering amplitudes, $f_{2lm}(\theta)$ and $f_{3lm}(\theta)$, for the $2l_m$ and $3s, 3d_m$ states needed to compute the state multipole data are denoted, respectively, with an R or I superscript:

$$f_{2s}(\theta) = f_{2s}^{(R)}(\theta) + i f_{2s}^{(I)}(\theta), \quad f_{np_m}(\theta) = f_{np_m}^{(R)}(\theta) + i f_{np_m}^{(I)}(\theta) \quad (n = 2, 3), \quad (\text{A.16a})$$

$$f_{3s}(\theta) = f_{3s}^{(R)}(\theta) + i f_{3s}^{(I)}(\theta), \quad f_{3d_m}(\theta) = f_{3d_m}^{(R)}(\theta) + i f_{3d_m}^{(I)}(\theta), \quad (\text{A.16b})$$

where these real and imaginary components are determined from (5),

$$f_{i \rightarrow n}(\theta) = -(i)^{\Delta+1} \int_0^\infty J_\Delta(q'\rho) [I_1^{(R)}(\rho, \gamma(\theta)) + I_2^{(I)}(\rho, \gamma(\theta))] \rho \, d\rho, \quad (\text{A.17a})$$

$$f_{i \rightarrow n}(\theta) = (i)^\Delta \int_0^\infty J_\Delta(q'\rho) [I_1^{(I)}(\rho, \gamma(\theta)) - I_2^{(R)}(\rho, \gamma(\theta))] \rho \, d\rho, \quad (\text{A.17b})$$

where the real and imaginary components of integrals I_1 and I_2 , given by (6), are denoted by superscripts R and I, respectively. Expressions (A.17a,b) are alternately real or imaginary depending on whether Δ is an even or odd integer, respectively.

The moduli $|f_{nlm}(\theta)|$ and phase angles $\beta_m(\theta)$ for the np_m and $3s, 3d_m$ states are then simply given by

$$|f_{nlm}(\theta)| = \left\{ [f_{nlm}^{(R)}(\theta)]^2 + [f_{nlm}^{(I)}(\theta)]^2 \right\}^{1/2}, \quad \beta_m = \tan^{-1} \left(\frac{f_{nlm}^{(I)}(\theta)}{f_{nlm}^{(R)}(\theta)} \right),$$

where the phase angles β_m are computed (modulo π) using the FORTRAN intrinsic function ATAN2.

In the above expressions the differential cross sections for excitation of the $2p$ and $3d$ states are given by

$$\sigma_{2p}(\theta) = \sigma_{2p_0}(\theta) + 2\sigma_{2p_{+1}}(\theta), \quad \sigma_{3d}(\theta) = \sigma_{3d_0}(\theta) + 2\sigma_{3d_{+1}}(\theta) + 2\sigma_{3d_{+2}}(\theta),$$

wherein the differential cross sections for excitation of the $2p_m$ and $3d_m$ magnetic substates are denoted by $\sigma_{2p_m}(\theta)$ and $\sigma_{3d_m}(\theta)$, respectively.

References

- [1] D.W. Norcross, *Comput. Phys. Commun.* 1 (1969) 88.
K.A. Berrington et al., *Comput. Phys. Commun.* 8 (1974) 149.
K.A. Berrington et al., *Comput. Phys. Commun.* 14 (1978) 367.
N.S. Scott and K.T. Taylor, *Comput. Phys. Commun.* 25 (1982) 347.
V.M. Burke, P.G. Burke and N.S. Scott, *Comput. Phys. Commun.* 69 (1992) 76.
K. Bartachat, *Comput. Phys. Commun.* 75 (1993) 219.
- [2] R.J.W. Henry, S.P. Rountree and E.R. Smith, *Comput. Phys. Commun.* 23 (1981) 233.
- [3] W. Eissner and M.J. Seaton, *J. Phys. B* 5 (1972) 2187.
M.J. Seaton, *J. Phys. B: At. Mol. Phys.* 7 (1974) 1817.
M.A. Crees, M.J. Seaton and P.M.H. Wilson, *Comput. Phys. Commun.* 15 (1978) 23.
- [4] J.D. Lyons, R.K. Nesbet, C.C. Rankin and A.C. Yates, *J. Comput. Phys.* 13 (1973) 229.
C.J. Noble and R.K. Nesbet, *Comput. Phys. Commun.* 33 (1984) 399.
J. Callaway, *Phys. Rep.* 45 (1978) 89; *Adv. Phys.* 29 (1980) 771.
- [5] I.E. McCarthy and E. Weigold, *Adv. At. Mol. Opt. Phys.* 27 (1991) 165.
- [6] E.C. Sullivan and A. Temkin, *Comput. Phys. Commun.* 25 (1982) 97; 71 (1992) 319.
- [7] P.M.J. Sawey, K.A. Berrington, P.G. Burke and A.E. Kingston, *J. Phys. B* 23 (1990) 4321.
- [8] J.H. Wilkinson, *The Algebraic Eigenvalue Problem* (Oxford Univ. Press, Oxford, 1965).
D.M. Young, *Iterative Solution of Large Linear Systems*, (Academic, New York, 1971).
G.H. Golub and C.F. van Loan, *Matrix Computations*, 2nd Ed. (Johns Hopkins Univ. Press, Baltimore, MD, 1989).

- [9] H.R.J. Walters, *Phys. Rep.* 116 (1984) 1.
Y. Itikawa, *Phys. Rep.* 143 (1986) 69.
A. Burgess and C.T. Whelan, *Comput. Phys. Commun.* 47 (1987) 295.
G. Csanak, H.S. Taylor and R. Yaris, *Adv. At. Mol. Phys.* 7 (1971) 287.
- [10] C. Gaussorgues, R.D. Piacentini and A. Salin, *Comput. Phys. Commun.* 10 (1975) 223.
R.D. Piacentini and A. Salin, *Comput. Phys. Commun.* 13 (1977) 57.
A. Salin, *Comput. Phys. Commun.* 12 (1976) 199; 62 (1991) 58.
- [11] F.W. Byron and C.J. Joachain, *Phys. Rep.* 34 (1977) 233.
T.T. Gien, *Phys. Rep.* 160 (1988) 123.
E. Gerjuoy and B.K. Thomas, *Rep. Prog. Phys.* 37 (1974) 1345.
- [12] M.R. Flannery and K.J. McCann, *J. Phys. B* 7 (1974) 2518; 8 (1975) 1716; *Phys. Rev. A* 12 (1975) 846.
- [13] E.J. Mansky, *J. Comput. Phys.*, in preparation.
- [14] E.J. Mansky and M.R. Flannery, *J. Phys. B* 23 (1990) 4549, 4573.
- [15] E.J. Mansky and M.R. Flannery, *J. Phys. B* in preparation.
- [16] E.J. Mansky and M.R. Flannery, *Comput. Phys. Commun.* 88 (1995) 278, this issue.
- [17] M. Abramowitz and I.A. Stegun, eds., *Handbook of Mathematical Functions* (NBS, Washington, 1964).
- [18] J. Stoer and R. Bulirsch, *Introduction to Numerical Analysis*, 2nd Ed. (Springer, Berlin, 1993) chap. 7.
- [19] NAG Fortran Manual (Mark 15), Vol. 1, Chap. D01 (1991), NAG Inc., 1400 Opus Place, Suite 200, Downers Grove, IL 60515-5702.
- [20] P.E. Gill and G.F. Miller, *Comput. J.* 15 (1972) 80.
- [21] C. de Boor, *A Practical Guide to Splines* (Springer, Berlin, 1978).
- [22] IMSL User's Manual MATH/Library, Vol. 2, version 1.1 (1989) p. 653.
- [23] L.A. Morgan and M.R.C. McDowell, *J. Phys. B* 8 (1975) 1073.
- [24] G. Nienhuis, in: *Coherence and Correlation in Atomic Collisions* eds. H. Kleinpoppen and J.F. Williams (Plenum, New York, 1980) pp. 121–32.
E.J. Mansky and M.R. Flannery, *J. Phys. B* 20 (1987) L235.
- [25] I.C. Percival and M.J. Seaton, *Philos. Trans. R. Soc. London, Ser. A* 251 (1958) 113.
- [26] E.J. Mansky and M.R. Flannery, *J. Phys. B* 23 (1990) 3987.
- [27] I.S. Gradshteyn and I.M. Ryzhik, *Tables of Integrals, Series and Products* (Academic, New York, 1965) p. 967.
- [28] IMSL User's Manual SFUN/library, version 2.1 (1989) p. 32.
- [29] U. Fano and J.H. Macek, *Rev. Mod. Phys.* 45 (1973) 553.
J.H. Macek and D.H. Jaecks, *Phys. Rev. A* 4 (1971) 2288.
- [30] N. Andersen and S.E. Nielsen, *Adv. At. Mol. Phys.* 18 (1982) 265.
N. Andersen, J.W. Gallagher and I.V. Hertel, *Phys. Rep.* 165 (1988) 1.
- [31] H.W. Hermann and I.V. Hertel, *Comments At. Mol. Phys.* 12 (1982) 61, 127.
- [32] M.R. Flannery, *J. Phys. B* 3 (1970) 1083.
C. Bottcher and M.R. Flannery, *J. Phys. B* 3 (1970) 1600.
- [33] S. Vučić, S.R.M. Potvliege and C.J. Joachain, *J. Phys. B* 20 (1987) 3157.
- [34] P.G. Burke, C.J. Noble and P. Scott, *Proc. R. Soc. London, Ser. A* 410 (1987) 289.
- [35] E.J. Mansky, PhD thesis, Georgia Institute of Technology (1985) chap. 4, Appendix A.

TEST RUN OUTPUT

Test Run Output:

MULTICHANNEL EIKONAL CALCULATION OF E- + H(1S)

INPUT PARAMETERS : NST = 10 WRHO = 71 WANG = 126 LOW = .00 UP = 4.00 ENER = 5.440000E+01 EV. TOL = .00500
 VEL = 1.999632E+00 AU. ROMIN = 5.00000 ROMAX = 250.00000 ZINF = 120.00000 REMASS = 1.00000
 NZ-AVG = 1600.0000 NZ = 1601

RO	PROB(1S)	PROB(2S)	PROB(2P0)	PROB(2P1)	PROB(3S)
5.2186920000E-02	9.2027563598E-01	3.3982271517E-02	2.9995633077E-02	8.1627887151E-05	7.1541948197E-03
2.6987324000E-01	9.1489597289E-01	3.5624877055E-02	3.0322304182E-02	2.2616072033E-03	7.5583581486E-03
2.7772738000E-01	9.1474657640E-01	3.5606394510E-02	3.0325404032E-02	2.3958833476E-03	7.5517760781E-03
6.4118084000E-01	9.1160925587E-01	2.9698740545E-02	2.9676823100E-02	1.1982734611E-02	5.9310321438E-03
8.4529946000E-01	9.1200440280E-01	2.4071636421E-02	2.8621764507E-02	1.8962919768E-02	4.4904303479E-03
1.1332092000E+00	9.1394593445E-01	1.6370992989E-02	2.6423210659E-02	2.8249171987E-02	2.6630631463E-03
:	:	:	:	:	:
1.9154700540E+01	9.9998870368E-01	3.5922460322E-08	5.2458131403E-06	6.4923502006E-06	8.1098972939E-09

ERROR = 0.000000E+00 1.331835E-04 3.633493E-03 2.412475E-03 1.848415E-04

RO	PROB(3P0)	PROB(3P1)	PROB(3D0)	PROB(3D1)	PROB(3D2)	SUM
5.2186920000E-02	7.7383387999E-03	2.3306581211E-05	1.6506832062E-03	6.5914068384E-07	3.4408574419E-10	1.00090235
2.6987324000E-01	7.7662082755E-03	6.4757661171E-04	1.6310170419E-03	1.7843980580E-05	2.6848964752E-07	1.00072803
2.7772738000E-01	7.7648967582E-03	6.8599846243E-04	1.6285286195E-03	1.8896121575E-05	3.0121550863E-07	1.00072466
6.4118084000E-01	7.4958334334E-03	3.3952500517E-03	1.3943698236E-03	9.5140359579E-05	7.9725160041E-06	1.00128715
8.4529946000E-01	7.1543763232E-03	5.3107195941E-03	1.1950755005E-03	1.5322601187E-04	2.1683545878E-05	1.00198623
1.1332092000E+00	6.4713146014E-03	7.7445297896E-03	8.9725144219E-04	2.3548828427E-04	5.6685586179E-05	1.00305764
:	:	:	:	:	:	:
1.9154700540E+01	3.3920642320E-07	3.0065612449E-07	3.7342727977E-08	5.6773600372E-08	3.4093726245E-08	1.00000125

ERROR = 1.286331E-03 6.191309E-04 1.533987E-03 2.062938E-03 1.498004E-03

DIFFERENTIAL CROSS SECTIONS(A0**2)

THETA	DCS-DMET(1S)	DCS-DMET(2S)	DCS-DMET(2P0)	DCS-DMET(2P1)	DCS-DMET(3S)	DCS-DMET(3P0)
.0000	3.3070188313E+00	2.9291160352E+00	3.8473253274E+01	0.0000000000E+00	4.9921912577E-01	4.7801914362E+00
.0200	3.3069972125E+00	2.9290830845E+00	3.8472293722E+01	4.4168935440E-04	4.9921213202E-01	4.7801124334E+00
.0400	3.3069323576E+00	2.9289842353E+00	3.8469415273E+01	1.7665288569E-03	4.9919115136E-01	4.7798754358E+00
.0600	3.3068242710E+00	2.9288194959E+00	3.8464618539E+01	3.9744328927E-03	4.9915618554E-01	4.7794804760E+00
.0800	3.3066729600E+00	2.9285888803E+00	3.8457904539E+01	7.0644589956E-03	4.9910723745E-01	4.7789276080E+00
.1000	3.3064784352E+00	2.9282924083E+00	3.8449274705E+01	1.1035808185E-02	4.9904431118E-01	4.7782169075E+00
:	:	:	:	:	:	:

THETA	DCS-DMET(3P1)	DCS-DMET(3D0)	DCS-DMET(3D1)	DCS-DMET(3D2)
.0000	0.0000000000E+00	4.9164863223E-01	0.0000000000E+00	0.0000000000E+00
.0200	4.0545203776E-05	4.9164124841E-01	3.8127827279E-06	5.6384054389E-12
.0400	1.6217307436E-04	4.9161909761E-01	1.5250574924E-05	9.0211488757E-11
.0600	3.6486039219E-04	4.9158218179E-01	3.4311708722E-05	4.5667036512E-10
.0800	6.4856846680E-04	4.9153050419E-01	6.0993404659E-05	1.4431919476E-09
.1000	1.0132431501E-03	4.9146406939E-01	9.5291772150E-05	3.5230665543E-09
:	:	:	:	:

THETA DCS-DMET(2P) DCS-DMET(3P) DCS-DMET(3D)

.0000 3.8473253274E+01 4.7801914362E+00 4.9164863223E-01
 .0200 3.8472735412E+01 4.7801529786E+00 4.9164506120E-01
 .0400 3.8471181902E+01 4.7800376089E+00 4.9163434828E-01
 .0600 3.8468592971E+01 4.7798453364E+00 4.9161649395E-01
 .0800 3.8464968998E+01 4.7795761764E+00 4.9159149904E-01
 .1000 3.8460310513E+01 4.7792301506E+00 4.9155936469E-01

: : :

THETA DCS-MET(2P0) DCS-MET(2P1) DCS-MET(3P0) DCS-MET(3P1) DCS-MET(2P) DCS-MET(3P)

.0000 3.3273050862E+01 0.0000000000E+00 4.4767327247E+00 0.0000000000E+00 3.3273050862E+01 4.4767327247E+00
 .0200 3.3272489537E+01 2.9893385535E-04 4.4766736159E+00 3.3554870189E-05 3.3272788471E+01 4.4767071708E+00
 .0400 3.3270805627E+01 1.1956879815E-03 4.4764962949E+00 1.3421503431E-04 3.3272001315E+01 4.4766305099E+00
 .0600 3.3267999321E+01 2.6901200689E-03 4.4762007769E+00 3.0196715388E-04 3.3270689441E+01 4.4765027440E+00
 .0800 3.3264070934E+01 4.7819929698E-03 4.4757870877E+00 5.3678900086E-04 3.3268852927E+01 4.4763238767E+00
 .1000 3.3259020910E+01 7.4709747503E-03 4.4752552631E+00 8.3864946189E-04 3.3266491885E+01 4.4760939126E+00

: : : : :

ANGULAR DISTRIBUTIONS: SIN(THETA)*DXN(THETA)

THETA DXND0(1S) DXND0(2S) DXND0(2P0) DXND0(2P1) DXND0(3S) DXND0(3P0)

.0200 1.1543597708E-03 1.0224428570E-03 1.3429363652E-02 1.5417866698E-07 1.7425790386E-04 1.6665739777E-03
 .0400 2.3086741237E-03 2.0448165797E-03 2.6856716132E-02 1.2333395083E-06 3.4850113922E-04 3.3369822966E-03
 .0600 3.4628976459E-03 3.0670520434E-03 4.0280046979E-02 4.1620156319E-06 5.2271503962E-04 5.0050593357E-03
 .0800 4.6169849350E-03 4.0890801433E-03 5.3697347163E-02 9.8638423426E-06 6.9688494269E-04 6.6726395498E-03
 .1000 5.7708906043E-03 5.1108318038E-03 6.7106609790E-02 1.9261109066E-05 8.7099619214E-04 8.3395575070E-03

: : : : :

THETA DXND0(3P1) DXND0(3D0) DXND0(3D1) DXND0(3D2)

.0200 1.4152945748E-08 1.7161516698E-04 1.3309122183E-09 1.9681747495E-15
 .0400 1.1321815503E-07 3.4321484888E-04 1.0646908945E-08 6.2979494962E-14
 .0600 3.8208083939E-07 5.1478356289E-04 3.5931130784E-08 4.7822400065E-13
 .0800 9.0557211938E-07 6.8630583077E-04 8.5162830992E-08 2.0150754432E-12
 .1000 1.7684420115E-06 8.5776618113E-04 1.6631543297E-07 6.1489079921E-12

: : : :

THETA DXND0(2P) DXND0(3P) DXND0(3D)

.0200 1.3429517831E-02 1.6685881306E-03 1.7161649790E-04
 .0400 2.6857949471E-02 3.3370955147E-03 3.4322549585E-04
 .0600 4.0284208995E-02 5.0054441465E-03 5.1481949450E-04
 .0800 5.3707211005E-02 6.6735451219E-03 6.8639099562E-04
 .1000 6.7125870899E-02 8.3413259490E-03 8.5793250271E-04

: : :

ABSOLUTE PHASE ANGLES BETA (IN RADIANS)

THETA BETA(2P0) BETA(2P1) BETA(3P0) BETA(3P1)

.0200 -1.4835492148E+00 -1.5724402708E+00 -1.2736692641E+00 -1.3801947286E+00
 .0400 -1.4835463942E+00 -1.5724401170E+00 -1.2736651578E+00 -1.3801919347E+00
 .0600 -1.4835416932E+00 -1.5724398607E+00 -1.2736583142E+00 -1.3801872782E+00
 .0800 -1.4835351117E+00 -1.5724395018E+00 -1.2736487335E+00 -1.3801807594E+00
 .1000 -1.4835266498E+00 -1.5724390403E+00 -1.2736364160E+00 -1.3801723786E+00

: : : :

ABSOLUTE PHASE ANGLES BETA (IN RADIANS)

THETA	BETA(3D0)	BETA(3D1)	BETA(3D2)
.0200	-9.7380763076E-01	-6.3797165983E-01	-7.4569734361E-02
.0400	-9.7380671595E-01	-6.3796801219E-01	-7.4568195015E-02
.0600	-9.7380519157E-01	-6.3796193289E-01	-7.4565629487E-02
.0800	-9.7380305806E-01	-6.3795342211E-01	-7.4562037846E-02
.1000	-9.7380031607E-01	-6.3794248009E-01	-7.4557420191E-02
:	:	:	:

ABSOLUTE MAGNITUDE OF THE SCATTERING AMPLITUDE F(THETA) FOR THE 2P, 3P AND 3D STATES

THETA	ABS(F(2P0))	ABS(F(2P1))	ABS(F(3P0))	ABS(F(3P1))
.0200	6.5332219034E+00	2.2136646789E-02	2.3281801313E+00	6.7805865914E-03
.0400	6.5329774951E+00	4.4271682743E-02	2.3281224151E+00	1.3560849548E-02
.0600	6.5325701853E+00	6.6403497395E-02	2.3280262271E+00	2.0340465282E-02
.0800	6.5320000304E+00	8.8530481014E-02	2.3278915756E+00	2.7119110304E-02
.1000	6.5312671090E+00	1.1065102498E-01	2.3277184724E+00	3.3896461268E-02
:	:	:	:	:

THETA	ABS(F(3D0))	ABS(F(3D1))	ABS(F(3D2))
.0200	7.4665792518E-01	2.0793066933E-03	2.5285740315E-06
.0400	7.4664110472E-01	4.1585375838E-03	1.0114128051E-05
.0600	7.4661307144E-01	6.2376168726E-03	2.2756157848E-05
.0800	7.4657382655E-01	8.3164687691E-03	4.0453823123E-05
.1000	7.4652337174E-01	1.0395017494E-02	6.3205947562E-05
:	:	:	:

SCATTERING AMPLITUDES F(THETA) FOR THE 1S, 2S AND 3S STATES

THETA	ABS(F(1S))	ABS(F(2S))	ABS(F(3S))	BETA(1S)	BETA(2S)	BETA(3S)
.0000	1.8185210561E+00	1.8026925242E+00	7.5239020051E-01	5.2514739814E-01	-1.8125828499E+00	-1.2714859286E+00
.0200	1.8185151120E+00	1.8026823846E+00	7.5238493023E-01	5.2514826683E-01	-1.8125835417E+00	-1.2714850013E+00
.0400	1.8184972801E+00	1.8026519663E+00	7.5236911962E-01	5.2515087285E-01	-1.8125856170E+00	-1.2714822196E+00
.0600	1.8184675611E+00	1.8026012710E+00	7.5234276932E-01	5.2515521610E-01	-1.8125890761E+00	-1.2714775838E+00
.0800	1.8184259567E+00	1.8025303011E+00	7.5230588043E-01	5.2516129638E-01	-1.8125939196E+00	-1.2714710949E+00
.1000	1.8183724688E+00	1.8024390603E+00	7.5225845445E-01	5.2516911345E-01	-1.8126001479E+00	-1.2714627536E+00
:	:	:	:	:	:	:

COHERENCE AND ALIGNMENT PARAMETERS FOR THE 2P,3P STATES

THETA	LAMDA(2P)	CHI(2P)	LAMDA(3P)	CHI(3P)
.0200	9.9998851942E-01	-8.8891056023E-02	9.9999151801E-01	-1.0652546454E-01
.0400	9.9995407916E-01	-8.8893722849E-02	9.9996607285E-01	-1.0652677687E-01
.0600	9.9989668369E-01	-8.8898167548E-02	9.9992366690E-01	-1.0652896404E-01
.0800	9.9981634045E-01	-8.8904390099E-02	9.9986430419E-01	-1.0653202598E-01
.1000	9.9971305983E-01	-8.8912390476E-02	9.9978799030E-01	-1.0653596261E-01
:	:	:	:	:

COHERENCE AND ALIGNMENT PARAMETERS FOR THE 3D STATE

THETA	LAMDA(3D)	MU(3D)	CHI(3D)	PSI(3D)
.0200	9.9999224484E-01	7.7551531151E-06	3.3583597093E-01	5.6340192547E-01
.0400	9.9996897966E-01	3.1020157517E-05	3.3583870376E-01	5.6339981717E-01
.0600	9.9993020542E-01	6.9793648391E-05	3.3584325868E-01	5.6339630340E-01
.0800	9.9987592371E-01	1.2407335110E-04	3.3584963595E-01	5.6339138427E-01
.1000	9.9980613675E-01	1.9385608127E-04	3.3585783598E-01	5.6338505990E-01
:	:	:	:	:

POLARIZATION FRACTIONS FOR THE 2P,3P,3D STATES

REPRESENTATION	P(2P-1S)	P(3P-2S)	P(3D-2P)
W/O FS.	1.3204031211E-01	1.4375623883E-01	2.1861550773E-01
W/O HFS.	4.5343932250E-02	4.9500067044E-02	1.6910530932E-01

TOTAL CROSS SECTION (FROM OPTICAL THEOREM)

Q-TOTAL(A0**2)	Q-TOTAL(PI*A0**2)	Q-TOTAL(ANGST**2)
5.7294225258E+00	1.8237318321E+00	1.6044186259E+00

IMPACT PARAMETER AND DMET INTEGRAL CROSS SECTIONS

STATE	QIP(A0**2)	QIP(PI*A0**2)	QIP(ANGST**2)	QDMET(A0**2)	QDMET(PI*A0**2)	QDMET(ANGST**2)
1S	1.2927259437E+00	4.1148744801E-01	3.6200394942E-01	1.2907779571E+00	4.1086738462E-01	3.6145845188E-01
2S	2.7763643898E-01	8.8374423293E-02	7.7746940800E-02	2.5975816013E-01	8.2683590386E-02	7.2740460049E-02
2P0	1.2024740793E+00	3.8275938733E-01	3.3673058695E-01	1.0475809070E+00	3.3345535928E-01	2.9335562385E-01
2P1	2.3110194118E+00	7.3562032594E-01	6.4715816863E-01	1.6064056861E+00	5.1133481110E-01	4.4984414954E-01
3S	4.8231975429E-02	1.5352714609E-02	1.3506471096E-02	3.9599028148E-02	1.2604762143E-02	1.1088974158E-02
3P0	2.2518971996E-01	7.1680114130E-02	6.3060208850E-02	1.7915025782E-01	5.7025298175E-02	5.0167710477E-02
3P1	4.7969157816E-01	1.5269057165E-01	1.3432873893E-01	2.6823248759E-01	8.5381052596E-02	7.5113538445E-02
3D0	2.3630174621E-02	7.5217181942E-03	6.6171925923E-03	1.6532901963E-02	5.2625861420E-03	4.6297328797E-03
3D1	2.7824607484E-02	8.8568476413E-03	7.7917658027E-03	1.9067764242E-02	6.0694578656E-03	5.3395740961E-03
3D2	2.2949389327E-02	7.3050175048E-03	6.4265512840E-03	1.1316207581E-02	3.6020607473E-03	3.1688942710E-03
2P	3.5134934911E+00	1.1183797133E+00	9.8388875559E-01	2.6539865931E+00	8.4479017038E-01	7.4319977339E-01
3P	7.0488129812E-01	2.2437068578E-01	1.9738894778E-01	4.4738274541E-01	1.4240635077E-01	1.2528124892E-01
3D	7.4404171433E-02	2.3683583340E-02	2.0835509679E-02	4.8916873786E-02	1.4934104755E-02	1.3138201247E-02

MET INTEGRAL CROSS SECTIONS

STATE	QMET(A0**2)	QMET(PI*A0**2)	QMET(ANGST**2)
2P0	1.0443922192E+00	3.3244036842E-01	2.9246269090E-01
2P1	1.6025882409E+00	5.1011999888E-01	4.4877542479E-01
3P0	1.7898198430E-01	5.6971735050E-02	5.0120588595E-02
3P1	2.6805015711E-01	8.5323015000E-02	7.5062480172E-02
2P	2.6469814601E+00	8.4256036730E-01	7.4123811569E-01
3P	4.4703214140E-01	1.4229475005E-01	1.2518306877E-01

COMPUTER PHYSICS COMMUNICATIONS

Instructions to Authors (short version)

(A more detailed version of these instructions has been published in the preliminary pages of volume 83.)

Submission of papers

Manuscripts (one original + two copies), accompanied by a covering letter, should be sent to one of the Editors indicated on page 2 of the cover.

Original material. By submitting a paper for publication in Computer Physics Communications the authors imply that the material has not been published previously nor has been submitted for publication elsewhere and that the authors have obtained the necessary authority for publication.

Refereeing. Submitted papers will be refereed and, if necessary, authors may be invited to revise their manuscript. If a submitted paper relies heavily on published material, it would be helpful to have a copy of that material for the use of the referee.

Type of contributions

Two classes of papers are published by Computer Physics Communications:

- (i) Papers in the general area of computational physics and physical chemistry including research papers, notes conference proceedings, review papers and feature articles.
- (ii) Write-ups describing programs to be held in the CPC Program Library together with descriptions of new versions of existing programs and erratum notices. (A description of the CPC Program Library is given in Comput. Phys. Commun. 42 (1986) xxv-xxvii.)

Manuscript preparation

All manuscripts should be written in good English. The paper copies of the text should be prepared with double line spacing and wide margins, on numbered sheets. See notes opposite on electronic version of manuscripts.

Structure. Please adhere to the following order of presentation: Article title, Author(s), Affiliation(s), Abstract, PACS codes and keywords, Program summary*, Main text, Acknowledgements, Appendices, References, Test Run Input* and Output*, Figure captions, Tables. (Items marked with * are only requested for program descriptions; see more detailed Instructions to Authors.)

Corresponding author. The name, complete postal address, telephone and fax numbers and the e-mail address of the corresponding author should be given on the first page of the manuscript.

PACS codes/keywords. Please supply one or more relevant PACS-1995 classification codes and 6-8 keywords of your own choice for indexing purposes.

References. References to other work should be consecutively numbered in the text using square brackets and listed by number in the Reference list. Please refer to the more detailed instructions for examples.

Illustrations

Illustrations should also be submitted in triplicate: one master set and two sets of copies. The *line drawings* in the master set should be original laser printer or plotter output or drawn in black india ink, with careful lettering, large enough (3-5 mm) to remain legible after reduction for printing. The *photographs* should be originals, with somewhat more contrast than is required in the printed version. They should be unmounted unless part of a composite figure. Any scale markers should be inserted on the photograph, not drawn below it.

Colour plates. Figures may be published in colour, if this is judged essential by the Editor. The Publisher and the author will each bear part of the extra costs involved. Further information is available from the Publisher.

After acceptance

Notification. You will be notified by the Editor of the journal of the acceptance of your article and invited to supply an electronic version of the accepted text, if this is not already available.

Copyright transfer. You will be asked to transfer the copyright of the article to the Publisher. This transfer will ensure the widest possible dissemination of information.

Computer programs. After acceptance of the description of a computer program, you will be asked to send the program file to the CPC Program Library.

Electronic manuscripts

The Publisher welcomes the receipt of an electronic version of your accepted manuscript (*encode in LaTeX*). If you have not already supplied the final, revised version of your article (on diskette) to the Journal Editor, you are requested herewith to send a file with the text of the accepted manuscript directly to the Publisher by e-mail or on diskette (allowed formats 3.5" or 5.25" MS-DOS, or 3.5" Macintosh) to the address given below. Please note that no deviations from the version accepted by the Editor of the journal are permissible without the prior and explicit approval by the Editor. Such changes should be clearly indicated on an accompanying printout of the file.

LaTeX papers

If the electronic file is suitable for processing by the publisher, the article will be published without rekeying the full text. The article should be encoded in LaTeX, preferably using the Elsevier document style 'elsart' or alternatively the standard document style 'article' or the document style 'revtex'.

The Elsevier LaTeX package (including detailed instructions to authors) can be obtained using anonymous FTP from the Comprehensive TeX Archive Network (CTAN) from the directory: /tex-archive/macros/latex/contrib/supported/elsevier.

The participating hosts in the Comprehensive TeX Archive Network are: ftp.shsu.edu (TX, USA), ftp.dante.de (Germany), ftp.tex.ac.uk (UK). Questions concerning the LaTeX author-prepared article project and requests for the booklet with instructions to authors should be directed to the address below.

Author benefits

No page charges. Publishing in Computer Physics Communications is free.

Free offprints. The corresponding Author will receive 50 offprints free of charge. An offprint order form will be supplied by the Publisher for ordering any additional paid offprints.

Discount. Contributors to Elsevier Science journals are entitled to a 30% discount on all Elsevier Science books.

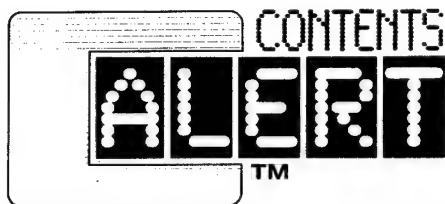
Contents Alert. Theoretical and High-Energy Physics papers scheduled for publication in Computer Physics Communications are included in Elsevier's pre-publication service Contents Alert.

Further information (after acceptance)

Elsevier Science B.V., Computer Physics Communication
Desk Editorial Department
P.O. Box 103, 1000 AC Amsterdam
The Netherlands
Tel.: +31 20 4852517
Fax: +31 20 4852319
E-mail: physdesk@elsevier.nl



North-Holland, an imprint of Elsevier Science



**A CURRENT AWARENESS SERVICE
FREE OF CHARGE
VIA ELECTRONIC MAIL**

FOR SCIENTISTS WORKING IN THE FIELD OF SURFACES, INTERFACES AND THIN FILMS

**FOR SCIENTISTS WORKING IN THE FIELD OF MATHEMATICAL & THEORETICAL
METHODS IN PHYSICS**

As the number of scientific publications grows daily it becomes increasingly important to trace the most interesting publications in a way that costs as little time as possible.

Elsevier Science Publishers now provides CONTENTS-Alert, **a free electronic service** that can assist you in carrying out time-saving searches on a regular, two-weekly basis.

CONTENTS-Alert is a current awareness service which delivers, through e-mail, the tables of contents of a selected group of journals. Not only will you receive these tables of contents **before or upon publication** of the journals but you can also browse through these tables of contents **at your own terminal**, in your own time. A survey carried out among researchers using CONTENTS-Alert has shown that this free service is very convenient and time-effective.

We offer two versions of CONTENTS-Alert each covering a specific field. One version of CONTENTS-Alert includes journals on Surfaces, Interfaces and Thin Films, and one includes journals on Mathematical and Theoretical Methods in Physics.

Journals covering the field of Surfaces, Interfaces and Thin Films

Applied Surface Science
Chemical Physics Letters
Materials Science and Engineering: R: Reports
Nuclear Instruments and Methods in Physics Research: Section B
Surface Science (including Surface Science Letters)
Surface Science Reports
Thin Solid Films
Vacuum

Our e-mail for this version is:
RFC-822: C-ALERT@ELSEVIER.NL
X.400: C=NL;A=400NET;P=SURF;O=ELSEVIER;S=C-ALERT

Journals covering the field of Mathematical and Theoretical Methods in Physics

Computer Physics Communications
Journal of Geometry and Physics
Nuclear Physics B
Physica A
Physica D
Physics Letters A
Physics Letters B
Physics Reports
Wave Motion

Our e-mail for this version is:
RFC-822: C-ALERT.MATHPHYS@ELSEVIER.NL
X.400: C=NL;A=400NET;P=SURF;O=ELSEVIER;
S=MATHPHYS; G=C-ALERT

Subscribe now to this **free pre-publication service** and find out how useful CONTENTS-Alert really is. Just send your full address to the e-mail number quoted above that corresponds with the CONTENTS-Alert version you wish to receive, or send it by post and we will make sure you will receive CONTENTS-Alert every two weeks.

Please allow three weeks processing time for your free subscription.

Yes, please add my name to the circulation list of

CONTENTS-Alert.

Version: ☐ Surfaces, Interfaces and Thin Films
☐ Mathematical and Theoretical Methods in Physics

Return to:

ELSEVIER SCIENCE PUBLISHERS B.V.,
Att: Mr. M. Stavenga,
P.O. BOX 103, 1000 AC Amsterdam, The Netherlands
Fax 31 20 5862580

Name _____
Initials _____ Title _____ ☐ Male ☐ Female
Institute _____
Department _____
Street/ PO Box _____
City _____
Country _____
Tel: _____ Fax: _____
E-mail _____

Principal Investigator Annual Data Collection (PIADC) Survey Form

Please submit the requested data for the period **1 October 1994 through 30 September 1995**. Request you follow the data requirements and format instructions below. This data is due to your AFOSR program manager *NLT 30 September 1995*.

NOTE: If there is insufficient space on this survey to meet your data submissions, please submit additional data in the same format as identified below.

PI DATA

Name (Last, First, MI): Flannery, M. Raymond

Institution Georgia Institute of Technology

Contract/Grant No. F 49620-94-1-0379

NUMBER OF CONTRACT/GRANT CO-INVESTIGATORS

Faculty _____ Post Doctorates 1 Graduate Students _____ Other _____

PUBLICATIONS RELATED TO AFOREMENTIONED CONTRACT/GRANT

NOTE: List names in the following format: Last Name, First Name, MI

Include: Articles in peer reviewed publications: journals, book chapters, conference papers.

Do Not Include: Unreviewed proceedings and reports, abstracts, "Scientific American" type articles, or articles that are not primary reports of new data, and articles submitted or accepted for publication, but with a publication date outside the stated time frame.

1. Name of Journal, Book, etc.: Physical Review A

Title of Article: Angular Momentum Transfer

Author(s): M. R. Flannery and M. R. Flannery

Publisher (if applicable): APS

Volume: 50 Page(s): 429-434 Month Published: July Year Published: 1994

2. Name of Journal, Book, etc.: Advances In Atomic, Molecular and Optical Physics

Title of Article: Electron-Ion and Ion-Ion Recombination Processes

Author(s): M. R. Flannery

Publisher (if applicable): Academic Press, N.Y.

Volume: 32 Page(s): 117-147 Month Published: _____ Year Published: 1994

3. Name of Journal, Book, etc.: Atomic Collisions:

Title of Article: Semiclassical Theory of Direct Dissociative Recombination

Author(s): M. R. Flannery

Publisher (if applicable): American Institute of Physics AIP

Volume: _____ Page(s): 53-76 Month Published: _____ Year Published: 1995

4. Name of Journal, Book, etc.: Computer Physics Communications

Title of Article: The Multichannel Eikonal Theory Program for Electron-Atom Scattering

Author(s): E. J. Mansky and M. R. Flannery

Publisher (if applicable): Elsevier

Volume: 88 Page(s): 249-277 Month Published: _____ Year Published: 1995

5. Name of Journal, Book, etc.: Computer Physics Communications

Title of Article: Automatic Generation of Analytical Matrix Elements for Electron-Atom Scattering

Author(s): E.J. Mansky and M.R. Flannery

Publisher (if applicable): Elsevier

Volume: 88 Page(s): 278-292 Month Published: _____ Year Published: 1995

HONORS/AWARDS RECEIVED DURING CONTRACT/GRANT LIFETIME

Include: All honors and awards received during the lifetime of the contract or grant, and any life achievement honors such as (Nobel prize, honorary doctorates, and society fellowships) prior to this contract or grant.

Do Not Include: Honors and awards unrelated to the scientific field covered by the contract/grant.

Honor/Award: 1995 Distinguished Professor Award Year Received: 1995

Honor/Award Recipient(s): M. Raymond Flannery

Awarding Organization: Georgia Institute of Technology

Honor/Award: _____ Year Received: _____

Honor/Award Recipient(s): _____

Awarding Organization: _____

VII. Appendix A:

Semiclassical Theory of Direct Dissociative Recombination

by

M. R. Flannery

School of Physics

Georgia Institute of Technology

Atlanta, Georgia 30332

Semiclassical Theory of Direct Dissociative Recombination

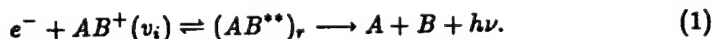
M. R. Flannery

*School of Physics
Georgia Institute of Technology
Atlanta, Georgia 30332-0430*

A generalized semiclassical theory of direct dissociative recombination is developed. It covers the possibility that two or more regions of stationary phase can contribute to the Franck-Condon overlap with and without autoionization. The analysis uniformly connects the stationary phase regions of large separation with the caustic region where these regions coalesce. The turning point divergence is also treated. It is shown how various interference effects from stationary phase regions can be exhibited in the cross section for the direct process even if left uncoupled from the indirect mechanism.

I. INTRODUCTION

Dissociative recombination (DR) for diatomic ions can occur (1) via a crossing at R_X between the bound and repulsive potential energy curves $V^+(R)$ and $V_d(R)$ for AB^+ and AB^{**} , respectively. This direct process involves the two-stage sequence



The first stage is dielectronic capture whereby the free electron of energy $\epsilon = V_d(R) - V^+(R)$ excites an electron of the diatomic ion AB^+ with internal separation R and is then resonantly captured by the ion at rate k_c to form a repulsive state d of the doubly excited molecule AB^{**} , which in turn can either autoionize at probability frequency ν_a , or else in the second stage predissociate into various channels at probability frequency ν_d . This competition continues until the (electronically excited) neutral fragments accelerate past the crossing at R_X . Beyond R_X the increasing energy of relative separation has reduced the total electronic energy to such an extent that autoionization is essentially precluded and the neutralization is then rendered permanent past the stabilization point R_X . This interpretation of Bates (1) has remained intact and robust in the current light of *ab initio* quantum chemistry and quantal scattering calculations for the simple diatomics (O_2^+ , N_2^+ , Ne_2^+ , etc.) where there are accessible curve crossings.

Based on a first-order treatment of Eq. (1), Bates (1,2) and Bardsley (3) provided simple expressions for the rate and cross section for this direct dissociative recombination. Bottcher (4) has provided a first-order semiclassical treatment of DR. Miller (5) has examined a semiclassical framework of associative and Penning ionization — the inverses of Eq. (1) where AB^+ is either vibrationally bound or dissociated, respectively. The local approximation for the survival probability has been invoked in previous studies (3-5).

In a tribute to Chris, the spirit of his approach will be used to develop a generalized semiclassical treatment to cover the possibility that two or more regions of stationary phase generally contribute to the Franck-Condon overlap between the bound and continuum vibrational wavefunctions. In so doing, a uniform Airy approximation will be provided which naturally remedies the divergence in the cross section at the "caustic" energy, where the two regions of stationary phase coalesce. The divergence in the cross section associated with a stationary phase at the classical turning point R_c of $A - B$ relative motion will also be addressed. New results will emerge.

The analysis will also show that various interference effects not in the first-order treatment (1-4) will be exhibited. These arise from the differences in the classical action between two separations $R_{1,2}$ of stationary phase on either the incoming and/or the outgoing legs of the trajectory and between the incoming and outgoing classical paths at a given $A - B$ relative separation R . Interferences at the caustic energies are also to be expected.

II. QUANTAL CROSS SECTIONS

The quantal expression for the autoionization frequency, with electron energy ϵ in the range $\epsilon, \epsilon + d\epsilon$ and with the ion left in state (v, J) , is

$$\frac{d\nu_a}{d\epsilon} d\epsilon = \frac{2\pi}{h} \sum_{M=-J}^J \left| \left\langle \phi_e(\vec{r}, R) \psi_v^+(\vec{R}) \mid \mathcal{H}_{el}(\vec{r}, R) \mid \Psi(\vec{r}, \vec{R}) \right\rangle \right|^2 \rho(\epsilon) d\epsilon \quad (2)$$

where the system wavefunction for $A - B^*$ collisions at energy E is

$$\Psi(\vec{r}, \vec{R}) = \frac{1}{R} \psi_d(E, R) Y_{JM}(\hat{R}) \phi_d(\vec{r}, R) \quad (3)$$

the product of the Born-Oppenheimer electronic wavefunction ϕ_d , the actual continuum (radial) vibrational wavefunction ψ_d in the presence of autoionization, and the rotational wavefunction $Y_{JM}(\hat{R})$. The rovibrational wavefunction for $AB^+(v, J)$ is

$$\psi_v^+(\vec{R}) = \frac{1}{R} \psi_v^+(R) Y_{JM}(\hat{R}). \quad (4)$$

Since the electronic angular momentum is relatively small, the molecular rotational energy remains conserved. The continuum vibrational wavefunction

$\psi_d(E, R)$ and the continuum electronic wavefunction ϕ_e^+ for the $(e^- - AB^+)$ system are both energy-normalized with unit densities $\rho(E)$, $\rho(\epsilon)$ of states, respectively. The incident current $(dj/dE)dE$ integrated for all directions of \vec{E} is therefore $(8\pi ME/h^3)dE = (k_{AB}^2/2\pi^2\hbar)dE$. The associative ionization cross section $(d\nu_a/dj)$ is then

$$\sigma_{AI}(E) = \frac{\pi}{k_{AB}^2} (2J+1) |a_Q(v)|^2 \quad (5)$$

where the quantal autoionization amplitude a_Q or transition matrix element T_Q is

$$a_Q(v) = 2\pi \int_0^\infty V_{de}^*(R) [\psi_e^{+*}(R) \psi_d(R)] dR \quad (6)$$

in terms of the bound-continuum electronic coupling matrix elements

$$V_{de}(R) = \langle \phi_d | \mathcal{H}_{el}(\vec{r}, R(t)) | \phi_e(\vec{r}, \mathbf{R}) \rangle_{\vec{r}, t} = V_{ed}^*(R) \quad (7)$$

where the integration is over the electronic coordinates \vec{r} and the direction \hat{e} of the ejected electron. The energy width for autoionization at a given R is

$$\Gamma(R) = 2\pi |V_{de}^*(R)|^2. \quad (8)$$

From detailed balance

$$\omega_{AB}^* k_{AB}^2 \sigma_{AI}(E; v, J) = (2\omega^+) (2J+1) k_e^2 \sigma_{DR}(\epsilon; v, J) \quad (9)$$

where ω_{AB}^* and ω^+ are the electronic statistical weights of AB^* and AB^+ and 2 is the spin-statistical weight of the incident electron, the cross section for $e^- - AB^+(v, J)$ dissociative recombination is

$$\sigma_{DR}(\epsilon) = \frac{\pi}{k_e^2} \left(\frac{\omega_{AB}^*}{2\omega^+} \right) |a_Q|^2 = \left(\frac{\hbar^2}{8\pi m\epsilon} \right) \left(\frac{\omega_{AB}^*}{2\omega^+} \right) |a_Q|^2 \quad (10)$$

where the amplitude (Eq. (6)) for a_Q is dimensionless.

A. Quantal Approximations

On ignoring the effect of autoionization on the continuum vibrational wavefunction $\psi_d(R)$, then a "Born" approximation to the T-matrix element (Eq. (6)) is

$$T_B = 2\pi \int_0^\infty V_{de}^*(R) [\psi_e^{+*}(R) \psi_d^{(0)}(R)] dR \quad (11)$$

where $\psi_d^{(0)}$ denotes ψ_d in the absence of the back reaction of autoionization. In this situation Eq. (10) reduces to the cross section

$$\sigma_c(\epsilon) = \frac{\pi}{k_e^2} \left(\frac{\omega_{AB}^*}{2\omega^+} \right) |T_B|^2 \quad (12)$$

for initial capture of the electron of energy ϵ by $AB^+(v_i)$. The effect of autoionization is now introduced by setting the DR cross section as

$$\sigma_{DR}(\epsilon) = \sigma_c(\epsilon) P_S \quad (13)$$

where P_S is the probability of survival against autoionization on the V_d curve until stabilization takes place. Since $|T_Q|^2 \leq 1$, the maximum capture cross section from Eq. (10) is

$$\sigma_c^{max} = \frac{\pi}{k_e^2} \left(\frac{\omega_{AB}^*}{2\omega^+} \right) = \left(\frac{h^2}{8\pi m \epsilon} \right) \left(\frac{\omega_{AB}^*}{2\omega^+} \right). \quad (14)$$

The Born matrix element T_B violates unitarity so that Eq. (12) can exceed Eq. (13). But any approximate Hermitian reactance K-matrix yields a T-matrix which satisfies unitarity. The Born K-matrix element is $K_B = T_B/2\pi$. The various scattering (S), transition (T), and reactance (R or K) matrices are interrelated by

$$S = \frac{I + iR}{I - iR} = \frac{I + i\pi K}{I - i\pi K} = 1 - iT. \quad (15)$$

On solving the Heitler-London damping equation,

$$\hat{T} = -2\hat{R} + i\pi\hat{R}\delta(E - H_0)\hat{T} \quad (16)$$

where the \hat{O} symbols denote operators, the corresponding unitarized T-matrix element for a two-(vibrational) state system $[AB^+(v_i), A - B]$ is

$$T = \frac{2R_B}{1 + |R_B|^2} = \frac{T_B}{1 + \frac{1}{4}|T_B|^2} \quad (17)$$

where T_B is given by Eq. (11). The cross section (Eq. (10)) is therefore given by Eq. (13) where

$$P_S = \left[1 + \frac{1}{4}|T_B|^2 \right]^{-1} = \left\{ 1 + \pi^2 \left| \int_0^\infty V_{de}^*(R) [\psi_v^{+*}(R) \psi_d^{(0)}(R)] dR \right|^2 \right\}^{-2} \quad (18)$$

is the survival probability. This derivation provides an alternate route to the weak-coupling expression of Giusti (6) for one open vibrational channel v_+ and pertains to recombination at low energies ϵ . As ϵ is increased, the number of accessible vibrational levels v_+ of the ion AB^+ increases and as a further approximation to P_S , $|T_B|^2$ in Eq. (18) is then summed (6,7) over all

accessible v_+ . In the higher-energy ϵ -limit where a large number of v_+ -levels can be populated following autoionization, then with the aid of closure,

$$\sum_{v_+} \psi_{v_+}^{+\ast}(R) \psi_{v_+}^+(R') = \delta(R - R')$$

the survival probability is

$$P_S = \left[1 + \pi^2 \int_{R_c}^{R_X} |V_{d\epsilon}^{\ast}(R)|^2 |\psi_d^{(0)}(R)|^2 dR \right]^{-2}. \quad (19)$$

Upon use of a semiclassical JWKB function for ψ_d (cf. §III, Eq. (25)), this reduces to

$$P_S = \left[1 + \frac{1}{2\hbar} \int_{R_c}^{R_X} \frac{\Gamma(R)}{v(R)} dR \right]^{-2} \sim \left(1 + \frac{1}{2} \langle \nu_a \rangle \tau_d \right)^{-2} \quad (20)$$

where $v(R)$ is the local radial speed of A-B relative motion, $\langle \nu_a \rangle$ is the frequency of autoionization averaged over time τ_d for the A-B to dissociate from their distance R_c of closest approach to the crossing point R_X . The survival probability is also given by a local approximation (3) as

$$P_S(R_c, R_X) = \exp \left[-\frac{1}{\hbar} \int_{R_c}^{R_X} \frac{\Gamma(R) dR}{v(R)} \right] = \exp \left[-\int_0^{\tau_d} \nu_a(t) dt \right] \quad (21)$$

where R_c and R_X are the initial capture and stabilization radii, respectively. On recognizing that AB^{**} formed in the first stage of Eq. (1) decays either by autoionization at frequency ν_a , or by dissociation at frequency $\nu_d \sim 1/\tau_d$, the stabilization probability is also

$$P_S = \frac{\nu_d}{(\nu_a + \nu_d)} = (1 + \nu_a \tau_d)^{-1} \quad (22)$$

as in Bates (1). Expressions (20)–(23) for P_S all agree in the weak coupling limit $\nu_a \ll \nu_d$. By adopting in Eq. (18) the Winans-Stueckelberg wavefunction,

$$\psi_d(R) = |V_d'(R)|^{-1/2} \delta(R - R_c), \quad (23)$$

the simplest continuum vibrational (energy-normalized) wavefunction, wherein R_c is the classical turning point for (A-B) relative motion (and the capture radius for a vertical transition from $V^+(R)$ to $V_d(R)$), then the capture cross section (Eq. (12)) reduces to

$$\sigma_c(\epsilon) = \frac{\pi}{k_\epsilon^2} \left(\frac{\omega_{AB}^{\ast}}{2\omega^+} \right) [2\pi\Gamma(R_c)] \left\{ |V_d'(R_c)|^{-1} |\psi_v^+(R_c)|^2 \right\} \quad (24)$$

where the term in braces is the effective Franck-Condon factor. This is the result (3) used so effectively by Bates in his explanation of super-dissociative recombination (2).

A further semiclassical connection of the high-energy result (Eq. (21)) with the low-energy weak-coupling limit (Eq. (18)) is provided in §V B. Further developments in applications of the quantal theory of configuration mixing and multichannel quantum defect theory have been well reviewed recently (8).

III. SEMICLASSICAL CROSS SECTIONS: JWKB FRANCK-CONDON OVERLAP WITHOUT AUTOIONIZATION

The JWKB normalized semiclassical wavefunctions for the bound vibrational level ($v = n, J = \ell$)¹ of AB^+ with vibrational frequency $\nu_{n\ell}$ is

$$\psi_v^+(R) \equiv 2 \left[\frac{\nu_{n\ell}}{v_+(R)} \right]^{1/2} \sin \left[\int_{R_0}^R k_+(R) dR + \frac{\pi}{4} \right], \quad R \gg R_0 \quad (25)$$

where $h\nu_{n\ell} = d\epsilon_{v,J}/dv$ is the level spacing, and R_0 is the classical turning point given by the innermost zero of

$$\frac{1}{2} M v_+^2(R) = \frac{\hbar^2 k_+^2(R)}{2M} = E - [V^+(R) + \epsilon] - \frac{J^2}{2MR^2} \quad (26)$$

the radial speed $v_+(R)$ of relative motion of energy ($E - \epsilon$) in potential $V^+(R)$. The JWKB wavefunction energy normalized to $\delta(E - E')$ for the vibrational continuum of AB^+ without autoionization is

$$\psi_d(R) = \frac{2}{[h\nu_d(R)]^{1/2}} \sin \left[\int_{R_c}^R k_d(R) dR + \frac{\pi}{4} \right], \quad R \gg R_c \quad (27)$$

where R_c is determined by the innermost zero of

$$\frac{1}{2} M v_d^2(R) = \frac{\hbar^2 k_d^2(R)}{2M} = E - V_d(R) - \frac{L^2}{2MR^2} \quad (28)$$

for the radial speed $v_d(R)$ of relative motion in the dissociative potential $V_d(R)$. Angular momentum of relative nuclear motion is conserved ($J = L$). The quantal amplitude (Eq. (6)) with the semiclassical product

$$\psi_v^{+*}(R) \psi_d(R) = (\nu_{n\ell}/h)^{1/2} (v_+ v_d)^{-1/2} [\exp +i\Delta(R) + \exp -i\Delta(R)] \quad (29)$$

is then

¹The quantum sets (n, ℓ) and (v, J) are used interchangeably whenever there is a need to distinguish the vibrational quantum number v from the radial speed $v(R)$.

$$a_Q(n) = 2\pi \left(\frac{\nu_n \ell}{h} \right)^{1/2} \int_0^\infty \{v_+(R)v_d(R)\}^{1/2} V_{de}^*(R) [\exp +i\Delta(R) + \exp -i\Delta(R)] dR \quad (30)$$

where the phase difference is

$$\Delta(R) = \int_{R_0}^R k_+(R) dR - \int_{R_0}^R k_d(R) dR \quad (31)$$

and where the (highly oscillatory) phase sums have been neglected. The (\pm) terms $\exp(\pm i\Delta)$ in Eq. (30) provide the contributions to S from the incoming $(-)$ and outgoing $(+)$ components of ψ_d . The phase Δ has a stationary point where $\Delta'(R) = d\Delta/dR = 0$, i.e., where

$$k_+(R_e) = k_d(R_e) \quad (32)$$

so that the kinetic energy of relative nuclear motion under each interaction V_d and V^+ is conserved at the point R_e of stationary phase. Let $W(R)$ be the potential energy difference $V_d(R) - V^+(R)$ so that

$$W(R) - \epsilon = V_d(R) - [V^+(R) + \epsilon] \quad (33a)$$

$$= (\hbar^2/2M) [k_+^2(R) - k_d^2(R)] \quad (33b)$$

$$= \frac{1}{2} \hbar [v_+(R) + v_d(R)] \Delta'(R). \quad (33c)$$

Hence Eq. (32) with Eq. (33b) implies that the condition

$$V_d(R_e) = V^+(R_e) + \epsilon \quad (34)$$

for a vertical transition at R_e is also satisfied. These two conditions (Eq. (32) and Eq. (34)) are illustrated in Fig. 1. On expanding

$$\Delta(R) = \Delta(R_e) + \Delta'(R_e)(R - R_e) + \frac{1}{2} \Delta''(R_e)(R - R_e)^2 \quad (35)$$

and on changing the integration variable to $x = R - R_e$ with limits $(\pm\infty)$, then Eq. (30) can be evaluated with the aid of

$$\int_{-\infty}^{\infty} \exp(\pm i|\alpha|x^2) d\alpha = \left[\frac{\pi}{|\alpha|} \right]^{1/2} \exp\left(\pm i\frac{\pi}{4}\right). \quad (36)$$

The quantal amplitude is therefore

$$a_Q = 2\pi V_{de}^*(R) \left[\left(\frac{\nu_n \ell}{h} \right)^{1/2} \frac{1}{v(R_e)} \left[\frac{2\pi}{|\Delta''(R_e)|} \right]^{1/2} \left\{ \exp +i \left[\Delta(R_e) \pm \frac{\pi}{4} \right] + \exp -i \left[\Delta(R_e) \pm \frac{\pi}{4} \right] \right\} \right] \quad (37)$$

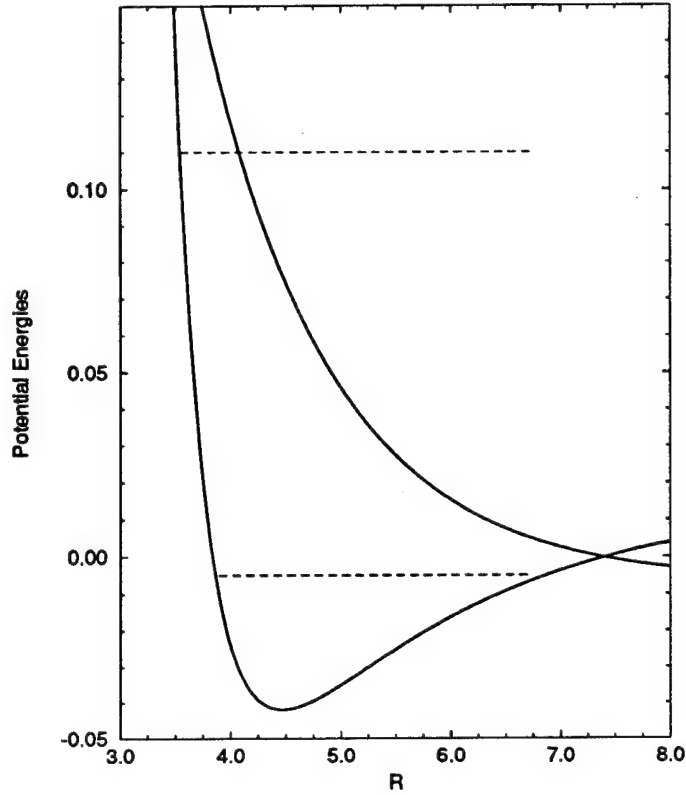


FIG. 1. Potential energy PE curves and energetics for dissociative recombination and associative ionization. $V_d(R), V^+(R)$: diabatic PE's for $AB^*(R)$ and $AB^+(R)$ which cross at R_X . ϵ : ejected electron energy with ion left in $AB^+(v)$. R_1, R_2 : location of stationary phase where $k_d(R) = k_+(R)$ which results in $\epsilon = V_d(R_1) - V_+(R_1)$. R_c : classical turning point of (A-B) motion with relative energy E .

where the constant phases ($\pm\pi/4$) pertain to positive or negative values of $\Delta''(R_\epsilon) = k'_+(R_\epsilon) - k'_d(R_\epsilon)$, respectively; i.e., to either minima or maxima in the phase difference Δ at R_ϵ . From Eq. (33c) and Eq. (32)

$$\Delta''(R_\epsilon) = \frac{1}{\hbar v(R_\epsilon)} \frac{d}{dR} (V_d - V^+)_{R_\epsilon} \equiv \frac{1}{\hbar v(R_\epsilon)} W'(R_\epsilon). \quad (38)$$

The cross section (Eq. (10)) for dissociative recombination for one point of stationary phase is then

$$\sigma_{DR}(\epsilon) = \left[\frac{\hbar^3}{8\pi m \epsilon_\epsilon} \left(\frac{\omega_{AB}^*}{2\omega^+} \right) \frac{\Gamma(R_\epsilon)}{\hbar} \right] |S(R_\epsilon)|^2 \equiv \sigma(R_\epsilon) \Gamma(R_\epsilon) |S(R_\epsilon)|^2 \quad (39)$$

where the semiclassical Franck-Condon (FC) bound-free factor $|S|^2$ has dimensions of $[E]^{-1}$ and is

$$|S^\pm(R_\epsilon)|^2 = \left[\frac{4\nu_{n\ell}}{v(R_\epsilon)} \right] |W'(R_\epsilon)|^{-1} \cos^2 \left[\Delta(R_\epsilon) \pm \frac{\pi}{4} \right] \quad (40)$$

which oscillates (rapidly for Δ large) about its average value

$$\langle |S|^2 \rangle = \left[\frac{2\nu_{n\ell}}{v(R_\epsilon)} \right] |W'(R_\epsilon)|^{-1} \quad (41)$$

which, when integrated over all ϵ , yields unity. For one root R_ϵ , S^+ pertains to phase minima when $W'(R) = dW/dR > 0$, and S^- to phase maxima when $W'(R) < 0$. For two widely separated regions of stationary phase at R_1 and R_2 , $W(R) = \epsilon$ has two roots specified by $R_1 < R_2$, $W'(R_1) > 0$, and $W'(R_2) < 0$, which then correspond to phase minima and maxima at R_1 and R_2 , respectively. In this situation

$$\sigma_{DR}(\epsilon) = \left| \sigma^{1/2}(R_1) S^+(R_1) + \sigma^{1/2}(R_2) S^-(R_2) \right|^2. \quad (42)$$

When the bound vibrational JWKB wavefunction ψ_+^+ of Eq. (25) is taken with respect to its right-hand turning point R'_0 , rather than the left-hand turning point R_0 , then the analysis is as above except with Δ replaced by

$$\tilde{\Delta}(R) = \int_R^{R'_0} k_+(R) dR - \int_{R_c}^R k_d(R) dR. \quad (43)$$

With the aid of the quantization condition

$$\hbar \oint_{R_0}^{R'_0} k_+(R) dR = \left(v + \frac{1}{2} \right) h \quad (44)$$

this reduces to

$$\tilde{\Delta}(R) = \left(v + \frac{1}{2} \right) \pi - \left[\int_{R_0}^R k_+(R) dR + \int_{R_c}^R k_d(R) dR \right]. \quad (45)$$

The smaller of Δ and $\tilde{\Delta}$ in practice is adopted in Eq. (37) for a_Q or Eq. (40) for $|S^\pm|^2$.

A. Special Cases: Turning Point and Caustic

Two cases of special interest now arise. One is when R_1 is the turning point R_c where the radial speed $v(R)$ vanishes and the Franck-Condon factor (Eq. (40)) diverges. The other case is when the two points R_1 and R_2 of stationary phase coalesce at the caustic where $\epsilon^* = W(R_{1,2})$ is maximum (as indicated in Fig. 2) so that $W'(R_{1,2})$ vanishes and Eq. (40) again diverges.

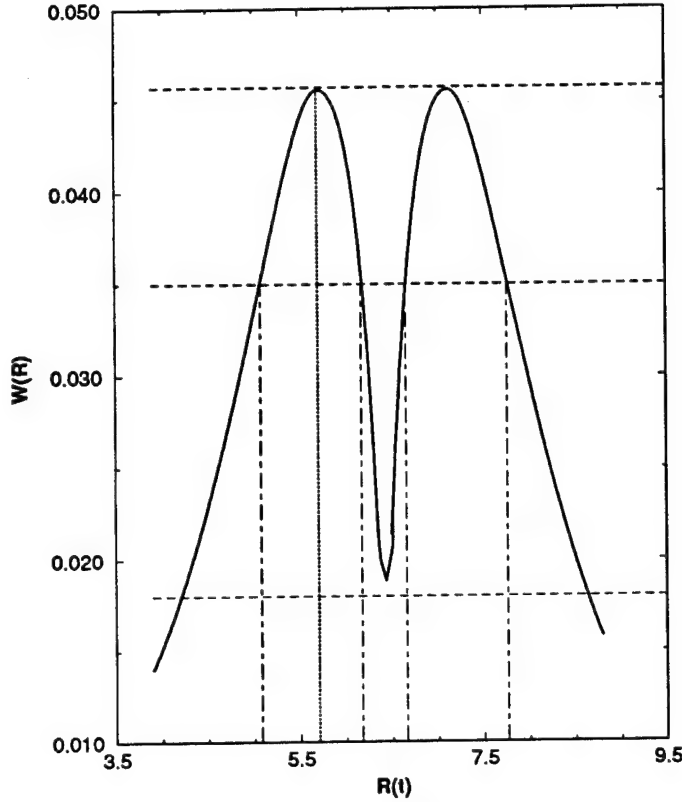


FIG. 2. Energy separation $W(R) = V_d(R) - V^+(R)$ for classical path $R(t)$. Stationary phase locations $\epsilon = W(R_{1,2})$. Caustic (Rainbow) at $\epsilon^* = W_{\max}(R^*)$. The three horizontal dashed lines represent the energies ϵ^* , ϵ_1 , ϵ_2 of the Caustic, 4 crossing point and 2 crossing point cases, respectively. The vertical dotted line represents t^* , while the four vertical dashed lines (from left to right) represent t_1 –4, respectively.

1. Turning Point Divergence

(a) In classical mechanics the quantal probability

$$|\psi_{n\ell}^+(R)|^2 dR = \frac{2dt}{T} = 2\nu_{n\ell}dt \quad (46)$$

is replaced by the corresponding classical average over the period T for vibrational motion, the factor of 2 arising from inward and outward radial motion, i.e., $|\psi_{n\ell}^+(R)|^2 = 2\nu_{n\ell}/v(R)$. This also follows from averaging the JWKB function (Eq. (25)). Use of this correspondence in Eq. (40) therefore yields the Franck-Condon factor

$$|S^\pm(R_\epsilon)|^2 = 2 |\psi_{n\ell}^+(R_\epsilon)|^2 \left| \frac{d}{dR}(V_d - V^+) \right|_{R_\epsilon}^{-1} \cos^2 \left[\Delta(R_\epsilon) \pm \frac{\pi}{4} \right]. \quad (47)$$

This form is advantageous in that it circumvents the divergence in the overlap (Eq. (40)) at the classical turning point R_c common to all JWKB-based approximations. The averaged FC factor is

$$\langle |S^\pm(R_c)|^2 \rangle = |\psi_\pm^+(R_c)|^2 \left| \frac{d}{dR} (V_d - V^+) \right|_{R_c}^{-1} \quad (48)$$

which is finite. The FC factor with the simplest continuum function (Eq. (23)) is

$$|S|^2 = |\psi_\pm^+(R_c)|^2 \left| \frac{dV_d}{dR} \right|_{R_c}^{-1} \quad (49)$$

to be compared with the more accurate expressions (Eq. (47) or Eq. (48)). It is therefore valid when $\left| \frac{dV_d}{dR} \right| \gg \left| \frac{dV^+}{dR} \right|$, i.e., the potential V_d is so steep and strongly repulsive relative to $V^+(R)$. The above Franck-Condon overlap (Eq. (49)) is that used by Bardsley to provide the cross section (Eq. (24)) for dissociative recombination.

(b) Airy Function Remedy:

In order to remedy the well-known breakdown of the JWKB functions (Eqs. (25) and (27)) close to the classical turning points, the JWKB functions can be replaced by their Airy function counterparts

$$\sin \left(\int_{R_c}^R k \, dR + \frac{\pi}{4} \right) \Rightarrow \pi^{1/2} z^{1/4} Ai(-z), \quad \frac{2}{3} z^{3/2} = \int_{R_c}^R k \, dR \quad (50)$$

in Eq. (6). The stationary phase result is (Eq. (39)) with

$$|\bar{S}|^2 = \left[\frac{4\nu}{v(R_c)} \right] |W'(R_c)|^{-1} \left[\pi^{1/2} \eta^{1/4} Ai(-\eta) \right]^2 \quad (51)$$

for the resulting overlap, where the argument of the Airy function Ai in terms of the phase difference (Eq. (31)) is

$$\eta(R_c) = \left[\frac{3}{2} \Delta(R_c) \right]^{2/3}. \quad (52)$$

For large arguments η , i.e., for R_c well removed from the classical turning points R_c and R_0 , then

$$\pi^{1/2} \eta^{1/4} Ai(-\eta) \xrightarrow{\eta \gg 1} \sin \left(\Delta + \frac{\pi}{4} \right) \quad R_c \gg R_c \quad (53)$$

so that Eq. (47) is recovered (for the case $W'(R_c) < 0$). The overlap (Eq. (51)) uniformly connects the classical accessible and inaccessible regions and does not diverge when R_c is located at the classical turning point R_c .

2. Caustic Region: $W'(R^*) = 0$

The caustic occurs at the maximum energy $\epsilon^* = W(R)$ where $W'(R^*) = 0$ so that both Δ' and Δ'' vanish at R^* and hence the FC overlap within Eq. (37) for a_Q diverges. In the vicinity of the caustic

$$\Delta'(R, \epsilon) = (\epsilon - \epsilon^*) \left(\frac{d\Delta'}{d\epsilon} \right)_{\epsilon^*} = (\epsilon^* - \epsilon)/\hbar v_*, \quad (54)$$

where $v^* = v(R^*)$. The amplitude (Eq. (37)) under the expansion

$$\Delta(R, \epsilon) = \Delta(R^*) + \left[\frac{(\epsilon^* - \epsilon)}{\hbar v_*} \right] (R - R^*) + \frac{1}{6} \Delta'''(R^*) (R - R^*)^3 \quad (55)$$

is then

$$a_Q(n) = 2\pi V_{de}^*(R^*) \left[2 \left(\frac{\nu_{nl}}{\hbar} \right)^{1/2} \frac{2\pi}{v_*} \left(\frac{2}{|\Delta'''(R_0)|} \right)^{1/3} Ai(-z) \right] \quad (56)$$

where Ai is the Airy function with argument

$$z = \Delta'(R^*, \epsilon) \left[\frac{2}{\Delta'''(R^*)} \right]^{1/3} = \left[\frac{2\hbar v_*}{|W'''(R^*)|} \right]^{1/3} \frac{(\epsilon^* - \epsilon)}{\hbar v_*}. \quad (57)$$

The amplitude (Eq. (56)) and the cross section (Eq. (10)) are now finite at the caustic ($z=0$). The divergent term $[2\pi/|\Delta'''(R)|]^{1/2}$ in Eq. (37) is, in effect, replaced by $2\pi[2/\Delta'''(R)]^{1/3} Ai(-z)$. The cross section is given by Eq. (39) where the Franck-Condon factor, appropriate to one stationary phase point located at the caustic, is

$$|S(R^*)|^2 = \frac{2\pi}{\hbar} \left(\frac{4\nu_{nl}}{v_*^2} \right) \left[\frac{2\hbar v_*}{|W'''(R^*)|} \right]^{2/3} Ai^2(-z) \quad (58)$$

which is finite. Although this procedure has eliminated the divergence of Eq. (37) at the caustic, the result (Eq. (56)) does not uniformly connect with Eq. (37) for well-separated regions of stationary phase. A uniform result will now be presented in the following section, together with generalization of the JWKB wavefunctions so as to include autoionization.

IV. FRANCK-CONDON OVERLAP WITH AUTOIONIZATION

Autoionization is, in effect, within the reaction zone between the crossing point R_X , where $V_d = V^+$, and the distance R_c of closest approach on $V_d(R)$ at energy E . To account for this, the JWKB vibrational wavefunction (Eq. (27)) decaying in the continuum is generalized to

$$\psi_d(R) \equiv \frac{i}{[h v_d(R)]^{1/2}} \left[c(R) \exp -i \left(\int_{R_c}^R k_d dR + \frac{\pi}{4} \right) - s(R) \exp i \left(\int_{R_c}^R k_d dR + \frac{\pi}{4} \right) \right] \quad (59)$$

where $c(R)$ is the amplitude for survival on $V_d(R)$ from R_X to R on the incoming leg, and $s(R)$ is the survival amplitude from $R_X \xrightarrow{\text{in}} R_c \xrightarrow{\text{out}} R$ on the outgoing leg. These amplitudes can be obtained from a recent classical path formulation (9) of DR. The Franck-Condon amplitude

$$S = \int_0^\infty \psi_+^*(R) \psi_d(R) dR \quad (60)$$

in terms of Eq. (31) for the phase difference Δ is

$$S = \left(\frac{\nu_{n\ell}}{h} \right)^{1/2} \int_0^\infty \{v_+(R) v_d(R)\}^{1/2} [c(R) \exp +i\Delta(R) + s(R) \exp -i\Delta(R)] dR. \quad (61)$$

Evaluation of S by a stationary phase method to yield a result which uniformly connects the caustic region ($\Delta'' = 0$) with the regions of well-separated phase is formally identical to the well-established analysis of classical rainbow scattering (10). Here $\Delta(R)$, $W(R)$, R , and ϵ above are analogous to the phase shift $\eta(\ell)$, deflection function $\chi(\ell) = d\eta/d\ell$, angular momentum ℓ , and scattering angle θ , respectively, in semiclassical elastic scattering. By mapping the phase $\Delta(\epsilon; R)$ onto the integrand of the Airy function, a uniform Airy approximation which uniformly connects Eq. (51) for two points $R_{1,2}$ of stationary phase with the caustic region can therefore be constructed. The uniform Airy approximation (10) to the integrals

$$A^\pm(\epsilon) = \int g(\epsilon; R) \exp [\pm i\Delta(\epsilon; R)] dR \quad (62)$$

is written here in compact form as

$$A^+(\epsilon) = a_1(\epsilon) \exp \left[i(\Delta_1 + \frac{\pi}{4}) \right] F^*(\Delta_{21}) + a_2(\epsilon) \exp \left[i(\Delta_2 - \frac{\pi}{4}) \right] F(\Delta_{21}) \quad (63a)$$

$$\equiv [a_1(\epsilon) F^*(\Delta_{21}) - i a_2(\epsilon) \exp(i\Delta_{21}) F(\Delta_{21})] \exp \left[i(\Delta_1 + \frac{\pi}{4}) \right] \quad (63b)$$

and

$$A^-(\epsilon) = a_1(\epsilon) \exp \left[-i(\Delta_1 + \frac{\pi}{4}) \right] F(\Delta_{21}) + a_2(\epsilon) \exp \left[-i(\Delta_2 - \frac{\pi}{4}) \right] F^*(\Delta_{21}) \quad (63c)$$

$$\equiv [a_1(\epsilon) F(\Delta_{21}) + i a_2(\epsilon) \exp(-i\Delta_{21}) F^*(\Delta_{21})] \times \exp \left[-i(\Delta_1 + \frac{\pi}{4}) \right]. \quad (63d)$$

The amplitudes

$$a_i(\epsilon) = [2\pi / |\Delta_i''|]^{1/2} g(\epsilon, R_i) \quad (64)$$

are assumed real, and

$$\Delta_i = \Delta(R_i) \quad ; \quad \Delta_{21} = \Delta_2 - \Delta_1 > 0. \quad (65)$$

The complex function F is defined in terms of the Airy function $Ai(z)$ and its z -derivative $Ai'(z)$ by

$$F[\Delta_{21}(\epsilon)] = \left[\pi^{1/2} z^{1/4} Ai(-z) + i\pi^{1/2} z^{-1/4} Ai'(-z) \right] \exp -i \left(\frac{\Delta_{21}}{2} - \frac{\pi}{4} \right),$$

$$\frac{4}{3} |z|^{3/2} = \Delta_{21} > 0. \quad (66)$$

The points $R_{1,2}$ are such that $W'(R_1) > 0$, i.e., $\Delta''(R_1) > 0$ where the phase Δ is minimum, and $W'(R_2) < 0$, i.e., $\Delta''(R_2) < 0$ where the phase is maximum. Since Δ_{21} is the area enclosed by the $W(R)$ curve and the straight line $W = \epsilon$ (cf. Fig. 2), it is always positive, except when it is zero at $\epsilon = \epsilon^* = W(R^*)$. It is shown below (§IV A) that the divergence in the constructive interference term ($a_1 + a_2$) at the caustic ($\Delta_i'' = 0$) is exactly balanced by the vanishing of the coefficient $z^{1/4}$ of Ai ; also the divergence in the coefficient $z^{-1/4}$ of $Ai'(-z)$ at the caustic is offset by the destructive interference term ($a_1 - a_2$) which vanishes more rapidly. In the limit of high $z \gg 1$, or for well-separated regions $\Delta_{21} \gg 1$, $F(\Delta_{21}) \rightarrow 1$, with unit amplitude and zero phase such that Eq. (63) tends to the primitive form (Eq. (37)). The uniform Airy result (Eq. (63)) is general in that it continuously connects the caustic ($\Delta_{12} = 0, \Delta_i'' = 0$) result (Eq. (56)) at ϵ^* with the result (Eq. (37)) for well-separated regions.

Application of Eq. (63) to Eq. (61) therefore yields

$$S = \{S_1 c_1 F_{21}^* - i S_2 c_2 F_{21} \exp i \Delta_{21}\} \exp \left[+i \left(\Delta_1 + \frac{\pi}{4} \right) \right]$$

$$+ \{S_1 s_1 F_{21} + i S_2 s_2 F_{21}^* \exp -i \Delta_{21}\} \exp \left[-i \left(\Delta_1 + \frac{\pi}{4} \right) \right] \quad (67a)$$

$$\equiv S_{in} \exp \left[+i \left(\Delta_1 + \frac{\pi}{4} \right) \right] + S_{out} \exp \left[-i \left(\Delta_1 + \frac{\pi}{4} \right) \right] \quad (67b)$$

where

$$S_i = \left[\frac{\nu_{nl}}{v(R_i)} |W'(R_i)|^{-1} \right]^{1/2} \quad (68)$$

and where the in-out contributions S_{in} and S_{out} are associated with $c_i = c(R_i)$ and $s_i = s(R_i)$, respectively. Alternatively, the Franck-Condon overlap is

$$S = [S_1 \{c_1 F_{21}^* - s_1 F_{21} \exp(-2i\Delta_1)\} - s_2 \exp(i\Delta_{21}) \{c_2 F_{21} + s_2 F_{21}^* \exp(-2i\Delta_2)\}] \exp[i(\Delta_1 + \frac{\pi}{4})]. \quad (69)$$

For widely separated phase regions $F \rightarrow 1$ the primitive form

$$S = S_1 \{c_1 - s_1 \exp(-2i\Delta_1)\} \exp\left[i(\Delta_1 + \frac{\pi}{4})\right] + S_2 \{c_2 + s_2 \exp(-2i\Delta_2)\} \exp\left[i(\Delta_2 - \frac{\pi}{4})\right] \quad (70)$$

for S is obtained. The above results (Eqs. (67)–(70)) provide the generalization of Eq. (40) to include autoionization. For one region of stationary phase, the Franck-Condon factor reads

$$|S|^2 = S_1^2 (c_1^2 + s_1^2 - 2c_1 s_1 \sin 2\Delta_1). \quad (71)$$

When autoionization in Eq. (70) is ignored, $c_i = 1 = s_i$. Then

$$S = 2 \left[S_1 \cos(\Delta_1 + \frac{\pi}{4}) + S_2 \cos(\Delta_2 - \frac{\pi}{4}) \right] \quad (72)$$

and each amplitude is in agreement with Eq. (40).

A. Caustic

The divergence in S_i due to the vanishing of $W'(R)$ at the caustic $R^* = R_{1,2}$ is exactly balanced by the behavior of the function $F(\Delta)$ of Eq. (66) as $\Delta \rightarrow 0$. This becomes apparent by rewriting the in-out contributions (Eq. (67b)) to S as

$$S_{in} = (S_1 c_1 + S_2 c_2) A(\Delta_{21}) - i [S_1 c_1 - S_2 c_2] A'(\Delta_{21}) \quad (73a)$$

$$S_{out} = (S_1 s_1 + S_2 s_2) A(\Delta_{21}) + i [S_1 s_1 - S_2 s_2] A'(\Delta_{21}) \quad (73b)$$

where

$$A(\Delta_{21}) = \pi^{1/2} z^{1/4} Ai(-z); \quad A'(\Delta_{21}) = \pi^{1/2} z^{-1/4} Ai'(-z) \quad (74)$$

with argument

$$z = [3\Delta_{21}/4]^{2/3}. \quad (75)$$

The form (Eq. (67a)) for S is useful for probing the limit $\Delta_{21} \gg 1$ for well-separated regions when $F_{21} \rightarrow 1$, while the form (Eq. (73)) in Eq. (67b) for S is useful in the neighborhood of the caustic region when $\Delta_{21} \rightarrow 0$. Since $\epsilon = \epsilon^* = W(R^*)$ and $W'(R^*) = 0$ at the caustic R^* , then

$$W(R) = \epsilon^* - \frac{1}{2} |W''(R^*)| (R - R^*)^2 \quad (76)$$

so that $\epsilon = W(R)$ at the two separations

$$R_{2,1} = R^* \pm [2(\epsilon^* - \epsilon) |W''(R^*)|]^{1/2}. \quad (77)$$

The derivative $W'(R)$ therefore tends to zero on each side of the caustic at R^* as

$$W'(R, \epsilon) = \pm [2(\epsilon^* - \epsilon) |W''(R^*)|]^{1/2}. \quad (78)$$

The phase Δ is expanded consistently with Eq. (76) as

$$\Delta(R) = \Delta(R^*) + \Delta'(R^*)(R - R^*) + \frac{1}{6} \left(\frac{d^3 \Delta}{dR^3} \right)_{R^*} (R - R^*)^3 \quad (79a)$$

$$= \Delta(R^*) + \frac{1}{\hbar v_*} (\epsilon^* - \epsilon)(R - R^*) - \frac{1}{6\hbar v_*} |W''(R^*)| (R - R^*)^3 \quad (79b)$$

since $\Delta''(R^*)$ vanishes and $\Delta'(R) = [W(R) - \epsilon]/\hbar v_*$. The phase difference is therefore

$$\Delta_{21}(\epsilon) = \Delta(R_2) - \Delta(R_1) = \frac{2^{5/2}}{3\hbar v_*} \frac{(\epsilon^* - \epsilon)^{3/2}}{|W''(R^*)|^{1/2}}. \quad (80)$$

The dimensionless argument z of the Airy functions in Eq. (74) is

$$z(\epsilon) = \left| \frac{2\hbar v_*}{W''(R^*)} \right|^{1/3} \frac{(\epsilon^* - \epsilon)}{\hbar v_*}. \quad (81)$$

As $R_1 \rightarrow R_2 \rightarrow R^*$,

$$S_i = \left[\frac{\nu_{nl}}{v_* |W'|} \right] \rightarrow \left(\frac{\nu_{nl}}{v_*} \right)^{1/2} [2(\epsilon^* - \epsilon) |W''(R^*)|]^{-1/4} \quad (82)$$

the $(\epsilon \rightarrow \epsilon^*)$ divergence of which is exactly balanced by the $(\epsilon^* - \epsilon)^{-1/4}$ variation of $z^{1/4}$ in $A(\Delta_{21})$ of Eq. (73a). Also $S_1(\epsilon)c_1 - S_2(\epsilon)c_2 \rightarrow 0$ as $\epsilon \rightarrow \epsilon^*$ faster than the divergence of $z^{-1/4}$ in $A'(\Delta_{21})$ of Eq. (74). The Franck-Condon factor in the caustic region is then

$$|S(\epsilon)|^2 = |2S_1c_1A(\Delta_{21}) + 2S_1s_1A(\Delta_{21})\exp(-2i\Delta_1)|^2 \quad (83a)$$

$$= |S_C(\epsilon)|^2 [c^2(R) + s^2(R) + 2c(R)s(R)\cos 2\Delta(R)] \quad (83b)$$

where

$$|S_C(\epsilon)|^2 = \frac{2\pi\nu_{nl}}{\hbar v_*^2} \left| \frac{2\hbar v_*}{W''(R)} \right|^{2/3} \text{Ai}^2(-z) \quad (84)$$

is finite. When the effect of autoionization in the continuum vibrational wavefunction is neglected, then $c = s = 1$ and Eq. (83b) reduces to the previous result (Eq. (58)) so that, for $\epsilon \sim \epsilon^*$,

$$\sigma(\epsilon) = \frac{\hbar^3}{8\pi m \epsilon} \left(\frac{\omega_{AB}^*}{2\omega^+} \right) \left[\frac{\Gamma(R)}{\hbar} \right] \left\{ \frac{2\pi}{\hbar} \frac{4\nu_{nl}}{v_*^2} \left| \frac{2\hbar v_*}{W''(\epsilon^*)} \right|^{2/3} \text{Ai}^2(-z) \right\}. \quad (85)$$

V. DECAY AMPLITUDES AND STABILIZATION PROBABILITIES

A recent classical path $R = R(t)$ theory (9) of dissociative recombination has shown that the amplitude $c(t)$ is determined by the following integral equation:

$$-2\pi\hbar^2 c(t) = \int_{t_X}^t dt' \int_0^\infty d\epsilon \Gamma(\epsilon, t; t') c(t') \exp i[\gamma(\epsilon; t) - \gamma(\epsilon; t')] \quad (86)$$

at time t . This depends on the previous history of the system between t_X and t via the non-local interaction

$$\Gamma(\epsilon, t; t') = 2\pi V_{d\epsilon}(t) V_{d\epsilon}^*(t') \quad (87)$$

and on the phase difference

$$\gamma(\epsilon; t) - \gamma(\epsilon; t') = \frac{1}{\hbar} \int_{t'}^t [V_d - (V^+ + \epsilon)] dt \quad (88)$$

at different times. Once this equation is solved by numerical procedures, the amplitude $s(t) = c(t + t_c)$, where t_c is the time for nuclear motion from separation R_X to the distance of closest approach R_c , can be determined.

A. High-Energy Local Approximation

A local approximation to Eq. (86) yields (8)

$$c(t) = \exp \left(-\frac{1}{2\hbar} \int_0^t \Gamma(t) dt \right) \quad (89)$$

for the amplitude for survival of travel from R_X to $R(t)$ on the inward leg ($t < t_c$), and

$$s(t) = c(\tau_X - t) = \exp \left[-\frac{1}{2\hbar} \int_0^{\tau_X} \Gamma(t) dt \right] \exp \left(+\frac{1}{2\hbar} \int_0^t \Gamma(t) dt \right) \quad (90)$$

for the amplitude for survival during the sequence $R_X \xrightarrow{\text{in}} R_c \xrightarrow{\text{out}} R(\tau_X - t) = R(t)$ on the outward leg.

In terms of R , these amplitudes are

$$c(R) = \exp \left(-\frac{\pi}{\hbar} \int_R^{R_x} \frac{|V_{d\epsilon}(R)|^2 dR}{v(R)} \right) = \exp \left(-\frac{1}{2\hbar} \int_R^{R_x} \frac{\Gamma(R) dR}{v(R)} \right) \quad (91)$$

and

$$s(R) = \exp \left[-\frac{1}{2\hbar} \oint_{R_c}^{R_x} \frac{\Gamma(R)}{v(R)} dR \right] \exp \left[+\frac{1}{2\hbar} \int_R^{R_x} \frac{\Gamma(R)}{v(R)} dR \right]. \quad (92)$$

In this (high-energy) local approximation the averaged FC factor (Eq. (69)), which involves autoionization to many vibrational levels n of the ion, reduces for one point R_i of stationary phase to

$$\begin{aligned} \langle |S|^2 \rangle = & \left[\frac{2\nu_{nt}}{v(R)} |W'(R)|^{-1} \right] \left\{ \exp \left[-\frac{1}{\hbar} \int_{R_c}^{R_x} \frac{\Gamma(R)}{v(R)} dR \right] \right. \\ & \left. \times \cosh \left[\frac{1}{\hbar} \int_{R_c}^{R_i} \frac{\Gamma(R)}{v(R)} dR \right] \right\}. \end{aligned} \quad (93)$$

When R_i coincides with the classical turning point R_c , then

$$\langle |S|^2 \rangle = |\psi_{\star}^+(R_c)|^2 |W'(R_c)|^{-1} P_S(R_x) \quad (94)$$

where the probability P_S against autoionization is given by Eq. (21).

B. Low- and High-Energy Semiclassical Correspondance of P_S

In $e^- - AB^+(v_i)$ recombination at low energies ϵ , AB^+ decays by autoionization only into a limited number of open vibrational levels $n = 0, 1, 2, \dots$ of AB^+ . The DR cross section is (Eq. (13)) where the probability P_S against autoionization is

$$P_S^B = \left[1 + \frac{1}{4} \sum_n |T_B(v_i; n)|^2 \right]^{-2}. \quad (95)$$

Stationary phase evaluation of the weak-coupling (Born) T_B of Eq. (11) yields

$$|T_B|^2 = 2\pi\Gamma(R) |S_0(R)|^2 = \frac{\Gamma(R)}{\hbar} \frac{2\hbar\nu_{nt}}{v(R)} \frac{dR}{d\epsilon} \quad (96)$$

where $\epsilon = W(R)$ and where S_0 is the overlap S without autoionization. Hence,

$$\frac{1}{4} \sum_n |T_B|^2 = \frac{1}{4} \int_0^{\epsilon_m} |T_B|^2 \left(\frac{dn}{d\epsilon} \right) d\epsilon = \frac{1}{2\hbar} \int_{R_c}^{R_x} \frac{\Gamma(R)}{v(R)} dR \equiv \frac{1}{2} x \quad (97)$$

since the level spacing ($d\epsilon/dn$) is $h\nu_{nl}$. The maximum energy of electron ejection is ϵ_m . Expanding Eq. (95) yields

$$P_S^B \sim 1 - x + \frac{3}{4}x^2 - \frac{1}{2}x^3 + \dots \quad (98)$$

which agrees only in the weak-coupling limit ($x \ll 1$) with the expansion

$$P_S^L \sim 1 - x + \frac{1}{2}x^2 - \frac{1}{6}x^3 \quad (99)$$

for the local probability (Eq. (21)). Since

$$x \sim \langle \Gamma/\hbar \rangle \tau = \langle \nu_a \rangle / \nu_d = \langle \nu_a \rangle \tau_d$$

where $\langle \nu_a \rangle$ is the frequency of autoionization averaged over the time $\tau = \nu_d^{-1}$ for dissociation from R_c to R_X , then expansion of the probability (Eq. (22)) yields

$$P_S = \nu_d / (\nu_a + \nu_d) = (1 + \nu_a \tau_d)^{-1} \sim 1 - x + x^2 - x^3 + \dots \quad (100)$$

in agreement with Eq. (21) and Eq. (95) in the weak-coupling limit. This establishes the semiclassical correspondence between the various low- and high-energy survival probabilities.

VI. SEMICLASSICAL CROSS SECTIONS

The quantal amplitude (Eq. (6)) with the semiclassical product

$$a_Q(\epsilon) = 2\pi(\nu_{nl}/h)^{1/2} \int_0^\infty (v_+ v_d)^{-1/2} V_{de}^*(R) [c(R) \exp + i\Delta(R) + s(R) \exp - i\Delta(R)] dR \quad (101)$$

can be similarly evaluated by the stationary phase technique of §IV. The semiclassical cross section (Eq. (10)) for dissociative recombination is then

$$\sigma_{DR}(\epsilon; n) = \left| \sigma_1^{1/2} [c_1 F_{21}^* - i s_1 F_{21} \exp(-2i\Delta_1)] - i \sigma_2^{1/2} \exp\left[-i(\Delta_{21} + \frac{\pi}{4})\right] \times [c_2 F_{21} + i s_2 F_{21}^* \exp(-2i\Delta_{21})] \right|^2 \quad (102)$$

where the magnitudes $\sigma_i = \sigma(R_i)$ are

$$\sigma(R) = \frac{\hbar^3}{8\pi m \epsilon_e} \left(\frac{\omega_{AB}^*}{2\omega^+} \right) \left[\frac{\Gamma(R)}{\hbar} \right] \left\{ |W'(R)|^{-1} \left(\frac{\nu_{nl}}{v(R)} \right) \right\} \quad (103)$$

and where the decay amplitudes $c_i = c(R_i)$ and hence $s_i = s(R)$ are determined in general from Eq. (86). This is the basic expression for the cross section for dissociative recombination in the present semiclassical theory with

all the phase interference information included in Δ_{21} and F . For one point of stationary phase, then $F_{21} = 1$ and $\sigma_2 = 0$ in Eq. (102) which reduces to

$$\sigma_{DR}(\epsilon; n) = \sigma(R) [c^2(R) + s^2(R) - 2c(R)s(R) \sin 2\Delta_1] \quad (104)$$

which exhibits a pattern of rapid oscillations of frequency $\pi/\Delta(R)$ which varies with ϵ and impact parameter b . It oscillates with ϵ about the classical mean

$$\langle \sigma(\epsilon) \rangle = \sigma(R) [c^2(R) + s^2(R)] \quad (105)$$

between the envelopes $|c \pm s|^2 \sigma(R)$. These oscillations are due to the action difference Δ at R between the incoming and outgoing legs. This in-out interference effect is present also in the more general result (Eq. (85)) which, in addition, exhibits broader oscillations due to the Airy function within F . When the one region of stationary phase coincides with the distance of closest approach R_c , then, on replacing $2\nu_{nl}/v(R)$ in Eq. (103) by $|\psi_\nu^+(R)|^2$,

$$\sigma_{DR}(\epsilon_s) = 2\sigma_1(R_c) c^2(R_c) = \left[\frac{\hbar^3}{8\pi m \epsilon_s} \left(\frac{\omega_{AB}^*}{2\omega^+} \right) \frac{\Gamma(R_c)}{\hbar} \right] \left\{ |W'(R_c)|^{-1} \cdot |\psi_\nu^+(R_c)|^2 P_S(R_X) \right\} \quad (106)$$

where $P_S = |c(R_c)|^2$ is the survival probability between R_X and R_c against autoionization. This simple result then represents a first improvement over the result of Bardsley (cf. Eq. (24) and Eq. (21) in Eq. (13)) in that it includes $W'(R) = \frac{d}{dR} [V_d - V^+]$ rather than V_d' alone. The simple result of Bardsley (Eq. (24)) is therefore valid (a) when one region of stationary phase at R_c is assumed, (b) when V^+ is so shallow that $k_+(R_c) = 0$, and (c) when V_d is so steep that the Winans-Stueckelberg wavefunction $|V_d'(R_c)|^{-1/2} \delta(R - R_c)$ can be used for the continuum vibrational state.

The cross section (Eq. (103)) reduces in the neighborhood of the caustic energy $\epsilon^* = W(R^*)$ where $W'(R^*) = 0$ to

$$\sigma(\epsilon) = \frac{\hbar^3}{8\pi m \epsilon_s} \left(\frac{\omega_{AB}^*}{2\omega^+} \right) \left[\frac{\Gamma(R^*)}{\hbar} \right] \left\{ \frac{2\pi}{\hbar} \frac{4\nu_{nl}}{v_*^2} \left| \frac{2\hbar v_*}{W''(R^*)} \right|^{2/3} Ai^2(-z) \right\} \quad (107)$$

which remains finite at the caustic.

VII. RATE OF DIRECT DISSOCIATIVE RECOMBINATION

For a Maxwellian distribution of electron energies $\epsilon = \epsilon'(kT)$ at temperature T , the DR rate is

$$\alpha(T) = \bar{v} \int_{\epsilon_0}^{\infty} \sigma_{DR}(\epsilon) \epsilon' \exp(-\epsilon') d\epsilon' \equiv \bar{v} \langle \sigma_{DR}(T) \rangle \quad (108)$$

where \bar{v} is the mean electron speed $(8kT/\pi m)^{1/2}$ and $\langle \sigma_{DR} \rangle$ is a mean cross section at temperature T . An energy threshold $\epsilon_0 = V_d(R'_0) - V_+(R'_0) \geq 0$ is appropriate for the case when the energy $V_d(R_X)$ at the crossing exceeds the original vibrational energy of $AB^+(v)$. In terms of the probability $|a(\epsilon)|^2$ for dissociative recombination, the cross section can also be written as

$$\sigma_{DR}(\epsilon) = \left(\frac{h^2}{8\pi m \epsilon} \right) \left(\frac{\omega_{AB}^*}{2\omega^+} \right) |a(\epsilon)|^2 \quad (109)$$

where the semiclassical probability for dissociative recombination is

$$|a(\epsilon)|^2 = \left| P_1^{1/2}(n) [c_1 F_{21}^* - i s_1 F_{21} \exp(-2i\Delta_1)] - i P_2^{1/2}(n) \right. \\ \left. \times \exp \left[-i \left(\Delta_{21} + \frac{\pi}{4} \right) \right] [c_2 F_{21} + i s_2 F_{21}^* \exp(-2i\Delta_2)] \right|^2 \quad (110)$$

in terms of

$$P_i(n) = 2\pi\Gamma(R_i) \left\{ |W'(R_i)|^{-1} \left(\frac{\nu_{nl}}{v(R_i)} \right) \right\} \quad (111)$$

which is dimensionless. Thus,

$$\alpha(T) = \frac{h^2}{(2\pi m k T)^{3/2}} \left(\frac{\omega_{AB}^*}{2\omega^+} \right) \int_{\epsilon_0}^{\infty} |a(n; \epsilon)|^2 \exp(-\epsilon/kT) d\epsilon \quad (112)$$

is the basic expression for the rate which includes all the interference effects present in Eq. (110).

A. Approximate Rates

In order to obtain a simplified analytical rate, assume that there is only one region of stationary phase at R_ϵ so that $\epsilon = V_d(R_\epsilon) - V_+(R_\epsilon)$ and that the in-out interference effect is averaged out. The probability is then

$$|a(n; \epsilon)|^2 = \left[\frac{\Gamma(R)}{\hbar v(R)} |W'(R)|^{-1} \right]_{R_\epsilon} h\nu_{nl} [c^2(R_\epsilon) + s^2(R_\epsilon)] \quad (113)$$

which, with Eqs. (91) and (92), is

$$|a(n; \epsilon)|^2 = \left[\frac{\Gamma(R)}{\hbar v(R)} |W'(R)|^{-1} \right]_{R_\epsilon} 2h\nu_{nl} \left\{ \exp \left[-\frac{1}{\hbar} \int_{R_\epsilon}^{R_X} \frac{\Gamma(R)}{v(R)} dR \right] \right. \\ \left. \times \cosh \left[\frac{1}{\hbar} \int_{R_\epsilon}^{R_\epsilon} \frac{\Gamma(R)}{v(R)} dR \right] \right\} \quad (114)$$

where the term in braces, appropriate at high ϵ , is the average probability for survival from $R_\epsilon \xrightarrow{\text{out}} R_X$ and $R_\epsilon \xrightarrow{\text{in}} R_\epsilon \xrightarrow{\text{out}} R_X$ on $V_d(R)$. Adoption of Eq.

(114) in Eq. (112) therefore demands the location R_c which depends in turn on the energy

$$E = \frac{\hbar^2 k_d^2(R)}{2M} + V_d(R) + \frac{L^2}{2MR^2} \quad (115)$$

of relative motion under V_d . From $\epsilon = V_d(R_c) - V_+(R_c)$ and the vibrational-rotational level (v, L) of AB^+ , $k_+(R_c) \sim k_d(R_c)$ and E can then be determined to provide R_c as a function of ϵ . Further reduction of Eq. (112) with Eq. (114) is therefore not possible without additional assumptions.

(a) In the low-energy limit $\epsilon \rightarrow 0$, the capture and stabilization separations are close so that $P_S \rightarrow 1$. Hence,

$$|a(n; \epsilon \rightarrow 0)|^2 = 2\pi\Gamma(R_X) |W'(R_X)|^{-1} \left\{ \left[\frac{2\nu_{nl}}{v(R_X)} \right] \equiv |\psi_+^+(R_X)|^2 \right\} \quad (116)$$

such that Eq. (112) reduces at low T to

$$\alpha(T) = \frac{\hbar^3}{(2\pi mkT)^{3/2}} \left(\frac{\omega_{AB}^*}{2\omega^+} \right) \frac{\Gamma(R_X)}{\hbar} \left\{ |\psi_+^+(R_X)|^2 kT |W'(R_X)|^{-1} \right\}. \quad (117)$$

The term in braces is an effective thermal Franck-Condon factor for bound-free transitions. This analytical result is a generalized version of the result of Bates (2) in that it includes $W'(R) = \frac{d}{dR}(V_d - V_+)$ rather than V_d' alone. It therefore allows for a distinction to be made between crossings on either side of the potential minimum. For crossings at the potential minimum, the results are identical.

(b) Assume either that V^+ is so shallow that $k_+(R_c) \sim 0$ or that V_d is so steep. Then $R_c = R_e$ which is given universally by $\epsilon = V_d(R_c) - V_+(R_c)$. The recombination of electrons of energy ϵ originates at the distance of closest approach so that the cross section (Eq. (106)) can be used directly in Eq. (108) to give

$$\alpha(T) = \frac{\hbar^3}{(2\pi mkT)^{3/2}} \left(\frac{\omega_{AB}^*}{2\omega^+} \right) (2\nu_{nl}kT) \int_0^\infty P(\epsilon) \exp(-\epsilon') d\epsilon' \quad (118)$$

where $P(\epsilon)$ is the probability density (Eq. (113)) given in the local approximation by

$$P(\epsilon) = \frac{dP_d}{d\epsilon} = \frac{\Gamma(R)}{\hbar v(R)} |W'(R)|^{-1} \exp \left(-\frac{1}{\hbar} \int_R^{R_x} \frac{\Gamma(R)}{v(R)} dR \right) \quad (119)$$

where $\epsilon = W(R)$. For constant drainage $dP_d/d\epsilon$ is constant and Eq. (117) is recovered from Eq. (119).

VIII. SUMMARY

A detailed semiclassical theory of direct dissociative recombination (DR) has been developed in the spirit of Bottcher (4). Semiclassical expressions (Eqs. (67) and (69)) for the Franck-Condon bound-free vibrational overlap S , with and without autoionization, have been presented here (to the author's knowledge) for the first time. These results are uniform in that they continuously connect the primitive forms (Eqs. (40) and (72)), valid for well-separated regions of stationary phase, with the caustic result (Eq. (58)) appropriate to the instance when the vertical separation energy ϵ between $V_d(R)$ and $V_+(R)$ is maximum at R^* ie. $V_d'(R^*) = V_+'(R^*)$.

New semiclassical expressions (Eq. (102) and Eqs. (110)–(112)) for DR cross sections σ_{DR} and rates α_{DR} are also derived. They represent considerable improvement and generality over previous simpler results (2,3). The present theory is applicable to DR which may or may not involve curve crossings. The present developments for S and σ_{DR} represent required generalization of the important semiclassical analysis of both Miller (5) for the reverse process of associative ionization and of Bottcher (4) for dissociative recombination.

The decaying amplitudes, $c(R)$ and $s(R)$ integral to this analysis, are determined from a recent classical path theory (9) of DR. This yields, in the high-energy limit, a local approximation for the survival probability adopted previously (3–5). The classical path theory, represented by Eqs. (86)–(88), removes the need for using the local approximation to $c(R)$ and $s(R)$ within expressions for S and $\sigma_{DR}(\epsilon)$ at lower energies ϵ . It also removes the need for using continuum vibrational wavefunctions $\psi_d(R)$ without the effect of autoionization within the quantal result (Eq. (10) with Eq. (6)).

ACKNOWLEDGEMENTS

This research is supported by the U. S. Air Force Office of Scientific Research under Grant No. F49620-94-1-0379.

REFERENCES

1. D. R. Bates, Phys. Rev. **78**, 492 (1950).
2. D. R. Bates, J. Phys. B: At. Mol. Opt. Phys. **24**, 703 (1991).
3. J. N. Bardsley, J. Phys. B: Proc. Phys. Soc. **1**, 365 (1968).
4. C. Bottcher, J. Phys. B: At. Mol. Phys. **9**, 2899 (1976).
5. W. H. Miller, J. Chem. Phys. **52**, 3563 (1970).
6. A. Giusti, J. Phys. B: At. Mol. Phys. **13**, 3867 (1980).
7. S. L. Guberman, this volume (1995).
8. A. Giusti-Suzor, I. F. Schneider, and O. Dulieu, in *Dissociative Recombination: Theory, Experiment and Applications*, B. R. Rowe, J. B. A. Mitchell, and A. Canosa (eds.) (Plenum Press, NY, 1993).
9. M. R. Flannery, Phys. Rev. A, *submitted* (1995).

10. M. S. Child, *Semiclassical Mechanics with Molecular Applications*, Oxford Univ. Press, 1991, Appendix B, p 334.

VIII. Appendix B:

The Semiclassical-Classical Path Theory of Direct Electron-Ion
Dissociative Recombination and $e^- + H_3^+$ Recombination

by

M. R. Flannery

School of Physics

Georgia Institute of Technology

Atlanta, Georgia 30332

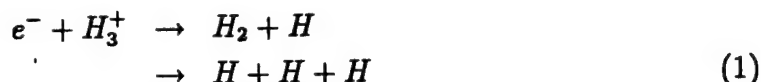
The Semiclassical-Classical Path Theory of Direct Electron-Ion Dissociative Recombination and $e^- + H_3^+$ Recombination

M. R. Flannery

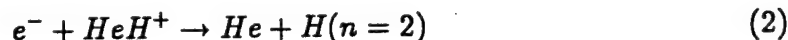
School of Physics
Georgia Institute of Technology
Atlanta, Georgia 30332-0430

1. Introduction

The dissociative recombination (DR) processes,

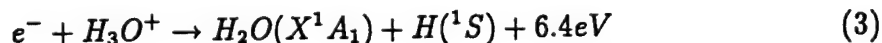


at low electron energy ϵ and,

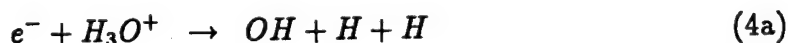


have spurred renewed theoretical interest because they both proceed¹⁻⁵ at respective rates of $(2 \cdot 10^{-7} - 2 \cdot 10^{-8}) \text{ cm}^3 \text{ s}^{-1}$ and $10^{-8} \text{ cm}^3 \text{ s}^{-1}$ at 300 K. Such rates are generally associated with the direct DR which involves favorable curve crossings between the potential energy surfaces (PES), $V^+(R)$ and $V_d(R)$ for the ion AB^+ and neutral dissociative AB^{**} states. The difficulty with (1) and (2) is that there are no such curve crossings, except⁶ at $\epsilon \geq 8 \text{ eV}$ for (1). In this instance, standard theory would support only extremely small rates when electronic resonant conditions do not prevail at thermal energies.

Seminal investigations^{7,8} of David Smith and his colleagues (N. G. Adams and C. R. Herd) in 1989-91 had already established that the non-crossing recombination channel



where the products are in their ground states is just as rapid as the channels



which involve favorable curve crossings. As is now realized, this observation provides an important signal (to theorists) that non-crossing DR can be rapid and that ground states can be populated.

Bates⁹ and Bates *et al*¹⁰ reasoned that DR for (1) could proceed via intermediate Rydberg levels of H_3^{**} which then connect, via quantum tunneling of the various vibrational wavefunctions, with the non-crossing dissociative product state whose PES lies to left and falls below all the Rydberg states. Although the tunneling probabilities are small, the final step involves only a single electron transition, rather than the much smaller dielectronic transition rate involved with the direct process. The overall rate may therefore be quite large. In a different interpretation, Guberman⁴ has proposed that DR for (2) is driven by the action of the nuclear kinetic energy operator on the adiabatic potential curves.

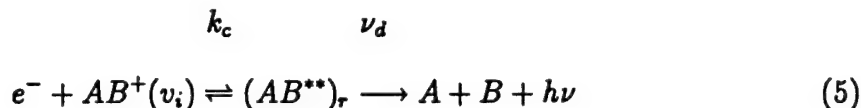
It is now time to re-examine the whole basis of dissociative recombination with a view towards providing a new mechanism and a more tractable theory capable of implementation on a level more accurate than currently being performed. We shall see that current calculations are based upon a first-order theory in the sense that the vibrational wavefunctions associated with $V_d(R)$ do not include autoionization. This effect is subsequently acknowledged by introducing, after the fact, a probability P_S for stabilization against autoionization.

In this paper a new mechanism for DR in the absence of curve crossing will be proposed in § 3, and a semiclassical-classical path theory of direct DR will be presented in § 5. Some background and standard theory are reviewed in § 2 and § 4.

2. Past and Recent Background

2.1. Direct Process

Bates¹¹ postulated that, dissociative recombination (DR) for diatomic ions can occur via a crossing at R_X between the bound and repulsive potential energy curves $V^+(R)$ and $V_d(R)$ for AB^+ and AB^{**} , respectively. Here, DR involves the two-stage sequence,

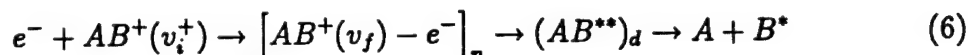


The first stage is dielectronic capture whereby the free electron of energy $\epsilon = V_d(R) - V^+(R)$ excites an electron of the diatomic ion AB^+ with internal separation R and is then resonantly captured by the ion, at rate k_c , to form a repulsive state d of the doubly excited molecule AB^{**} , which in turn can either autoionize at probability frequency ν_a , or else in the second stage predissociate into various channels at probability frequency ν_d . This competition continues until the (electronically excited)

neutral fragments accelerate past the crossing at R_X . Beyond R_X the increasing energy of relative separation has reduced the total electronic energy to such an extent that autoionization is essentially precluded and the neutralization is then rendered permanent past the stabilization point R_X . Bates' interpretation has remained intact and robust in the current light of *ab-initio* quantum chemistry and quantal scattering calculations for the simple diatomics (O_2^+ , N_2^+ , Ne_2^+ , etc.). Observation of emitted radiation $h\nu$ yields information on the excited products. Mechanism (5) is termed the direct process.

2.2. Indirect Process

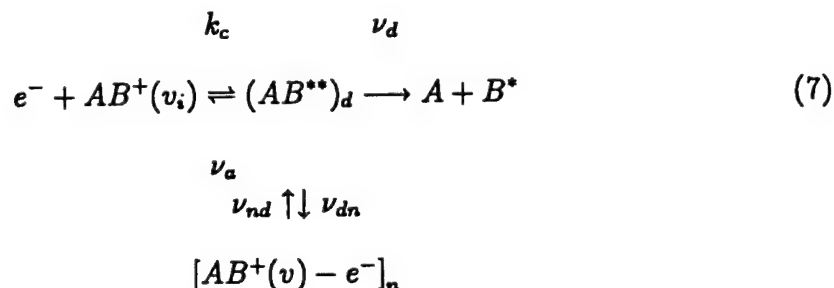
Bardsley ¹² pointed out the possibility that a three-stage sequence,



the so-called *indirect* process, might contribute. Here the accelerating electron loses energy by vibrational excitation ($v_i^+ \rightarrow v_f$) of the ion and is then resonantly captured into a Rydberg orbital of the bound molecule AB^* in vibrational level v_f which then interacts one way (via configuration mixing) with the doubly excited repulsive molecule AB^{**} . The capture initially proceeds via a small effect - vibronic coupling (the matrix element of the nuclear kinetic energy) induced by the breakdown of the Born-Oppenheimer approximation - at certain resonance energies $\epsilon_n = E(v_f) - E(v_i^+)$ and, in the absence of the direct channel (5), would therefore be manifest by a series of characteristic very narrow Lorentz profiles in the cross section. Uncoupled from (5) the indirect process would augment the rate. Vibronic capture proceeds more easily when $v_f = v_i^+ + 1$ so that Rydberg states with $n \approx 7 - 9$ would be involved (for $H_2^+(v_i^+ = 0)$) so that the resulting longer periods of the Rydberg electron would permit changes in nuclear motion to compete with the electronic dissociation. Recombination then proceeds as in the second stage of (5) ie. by electronic coupling to the dissociative state d at the crossing point. Giusti ¹³ has provided a unified account of the direct and indirect processes.

2.3. Interrupted Recombination

O'Malley ¹⁴ noted that the process,



proceeds via the first (dielectronic capture) stage of (5) followed by a two-way electronic transitions with frequency ν_{dn} and ν_{nd} between the d and n states. All (n, v) Rydberg states can be populated, particularly those in low n and high v since the electronic $d-n$ interaction varies as $n^{-1.5}$ with broad structure. Although the dissociation process proceeds here via a second order effect (ν_{dn} and ν_{nd}) the electronic coupling may dominate the indirect vibronic capture and will interrupt the recombination in contrast to (6) which as written in the one-way direction feeds the recombination. Such dip-structure has been observed. Guberman and Giusti-Suzor¹⁵ have assessed the effect of each contribution of (5), (6) and (7) to the resonance shape and integral cross section.

2.4. Multistep Indirect Model

For DR cases as $e^- - H_3^+, HeH^+$ which do *not* involve curve crossings between the ion and neutral potential energy surfaces (PES), Bates⁹ postulated a multistep model wherein the electron is first captured into a Rydberg state n with the vibrational quantum number v increasing from 0 to 1, as in the first stage of the indirect process (6). Quantal tunnelling to the other neutral levels (n', v') then proceeds via A-B nuclear motion until recombination becomes stabilized by predissociation to the repulsive potential of the ground state via a single electron radiationless transition. These intermediate multisteps violate the Born-Oppenheimer (BO) approximation at each step, are generally restricted to vibrational increases $\Delta v \approx 1$, and are associated with many-order perturbation theory (e.g. third-order for three steps). Although the multisteps can also proceed in the reverse manner $(n', v' \rightarrow n, v - 1)$, it may be rationalized that intramolecular vibrational rearrangement of multiatomic species may inhibit or close these reverse channels. The key idea with this model is that the small multistep probabilities are augmented by the large rate for the single-electron transition in the final step, in contrast to the smaller rate of the dielectronic transition involved in the direct process (5) when PES cross.

2.5. Nuclear Driven Operator Method

Guberman⁴ proposed that the non-crossing DR is driven by action of the nuclear kinetic-energy operator on *adiabatic* potential curves. The kinetic-energy derivative operator allows for capture into repulsive curves that are outside of the classical turning points for the nuclear motion.

3. New Mechanism for $e^- + H_3^+$ Recombination

The previous two mechanisms critically depend on quantum tunneling in the nuclear motion of the Rydberg neutral molecule. Another mechanism can be based on the fact that interaction of the Rydberg electron with the core produces energy and angular momentum changes in the Rydberg electron which therefore cascades down to

lower Rydberg levels. The key idea here is that the nuclear motion readjusts itself to the (slower) electronic motion, rather than the (faster) electronic motion readjusting itself to the (slower) nuclear motion as in §2.4 and §2.5.

The direct mechanism (5) is only operative for $(e^- + H_3^+)$ recombination at high electron energies $\epsilon \geq 8\text{eV}$ for access to the resonance state (2A_1 configuration $1a_1, 2a_1^2$) which crosses the potential for the ground 1A_1 of the H_3^+ state and which dissociates to $H_2^+(X^2\Sigma_g^+) + H^-(1s^2)$. At low ϵ , neither the direct or indirect mechanisms (5) and (6) are operative. The first stage of (6),

$$e^-(\epsilon, \ell = 0, 1) + H_3^+(v = 0; J) \rightarrow [e^- - H_3^+(v'; J')]_{\epsilon', \ell'} \quad (8)$$

is however feasible. Here a low energy electron in a core-penetrating hyperbolic orbit with low angular momentum and therefore high eccentricity, vibrationally excites H_3^+ and is itself captured into a highly eccentric elliptic orbit with energy $\epsilon' < 0$ corresponding to a Rydberg orbit with principal quantum number $n \sim 6 - 8$. Energy resonance, for example, occurs for $\epsilon = 0.03\text{eV} \sim 1.2kT$ at 300 K when $v' = 1, n = 7$. At the pericenter of the $(n\ell')$ -orbit is energy and angular momentum mainly transferred to the core ion by,

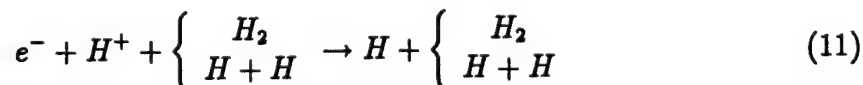
$$[e^- - H_3^+(v', J')]_{\epsilon', \ell'} \rightarrow [e^- - H_3^+(v'', J'')]_{\epsilon'', \ell''} \quad (9)$$

where ro-vibrational transitions occur and the Rydberg electron is left in a smaller Rydberg orbit ($\epsilon'' < \epsilon', \ell''$). Every time the electron (periodically) returns to the pericenter further ro-vibrational excitation can occur. Energy is transferred periodically as in the winding up of a watch. Resonance conditions can occur when the electron period T_e is a multiple of $\frac{1}{2}$ times the rotational period T_R . In the outer part of the *elliptic* orbit far from the pericenter the electron moves only under the isotropic Coulomb part of the ion potentials. Close to the pericenter the electron interacts with the molecular ion via an orientation-dependent potential producing rotational and vibrational excitation and possibly de-excitation.

This process continues until dissociation (fragmentation),



occurs via centrifugal explosion and stretching forces at which time a single electron capture transition,

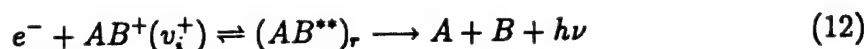


simultaneously occurs thereby completing the recombination. Theoretical description of this overall mechanism is currently being developed from both classical and quantal viewpoints.

The mechanisms in §2.4 and §2.5 depend on the (fast) bound electron readjusting itself to the (slower) nuclear motion — a breakdown of BO. The mechanism proposed here originates from the interaction of the (slow) Rydberg electron with the core, thereby increasing the nuclear motion via rotational and vibrational excitation of the molecular ion i.e. the nuclear motion readjusts itself to the electronic motion, rather than vice versa as in §2.4 and §2.5.

4. Quantal Cross Section

The cross section for direct dissociative recombination (DR),



of electrons of energy ϵ , wavenumber k_e and spin statistical weight 2, for a molecular ion $AB^+(v_i^+)$ of electronic statistical weight ω_{AB}^+ in vibrational level v_i^+ is,

$$\sigma_{DR}(\epsilon) = \frac{\pi}{k_e^2} \left(\frac{\omega_{AB}^*}{2\omega^+} \right) |a_Q|^2 = \left(\frac{h^2}{8\pi m \epsilon} \right) \left(\frac{\omega_{AB}^*}{2\omega^+} \right) |a_Q|^2 \quad (13)$$

Here ω_{AB}^* is the electronic statistical weight of the dissociative neutral state of AB^* whose potential energy curve V_d may or may not cross the corresponding potential energy curve V^+ of the ionic state. The transition T-matrix element for autoionization of AB^* embedded in the (moving) electronic continuum of $AB^+ + e^-$ is the quantal amplitude,

$$a_Q(v) = 2\pi \int_0^\infty V_{de}^*(R) [\psi_v^{+*}(R) \psi_d(R)] dR \quad (14)$$

for autoionization. Here ψ_v^+ and ψ_d are the nuclear bound and continuum vibrational wavefunctions for AB^+ and AB^* , respectively, while,

$$V_{de}(R) = \langle \phi_d | \mathcal{H}_{el}(\vec{r}, R(t)) | \phi_e(\vec{r}, R) \rangle_{\vec{r}, \epsilon} = V_{ed}^*(R) \quad (15)$$

are the bound-continuum electronic matrix elements coupling the diabatic electronic bound state wavefunctions $\psi_d(\vec{r}, R)$ for AB^* with the electronic continuum state wavefunctions $\phi_e(\vec{r}, R)$ for $(AB^+ + e^-)$. Both continuum electronic and vibrational wavefunctions are energy normalized and,

$$\Gamma(R) = 2\pi |V_{de}^*(R)|^2 \quad (16)$$

is the energy width for autoionization at a given internuclear separation R . Given $\Gamma(R)$ from quantum chemistry codes, the problem reduces to evaluation of continuum vibrational wavefunctions in the presence of autoionization.

4.1. Maximum Cross Section and Rate

Since the probability for recombination must remain less than unity, $|a_Q|^2 \leq 1$ and (13) yields the maximum cross section

$$\sigma_{DR}^{max}(\epsilon) = \frac{\pi}{k_e^2} \left(\frac{\omega_{AB}^*}{2\omega^+} \right) = \left(\frac{h^2}{8\pi m \epsilon} \right) (2l+1) \quad (17)$$

where ω_{AB}^* has been replaced by $2(2l+1)\omega^+$ under the assumption that the captured electron is bound in a high level Rydberg state of angular momentum l . The maximum rate associated with a Maxwellian distribution of electrons at temperature T and mean speed $\bar{v}_e = 1.05 \cdot 10^7 (T/300)^{3/2}$ is therefore

$$\alpha_{max} = \left[\frac{8kT}{\pi m} \right]^{1/2} \int \epsilon \sigma_{DR}^{max}(\epsilon) \exp(-\epsilon/kT) d\epsilon / (kT)^2 \quad (18)$$

$$(19)$$

which reduces to

$$\alpha_{max} = \bar{v}_e \frac{h^2}{(8\pi m kT)} (2l+1) = \bar{v}_e \sigma_{DR}^{max}(\epsilon = kT) \quad (20)$$

$$(21)$$

such that

$$\alpha_{max} \approx 5 \cdot 10^{-7} (300/T)^{1/2} (2l+1) cm^3 s^{-1} \quad (22)$$

Cross section maxima $5(2l+1)(300/T) \cdot 10^{-14} cm^2$ are therefore possible being consistent with the rate (22).

4.2. First-Order Quantal Approximation

When the effect of autoionization on the continuum vibrational wavefunction $\psi_d(R)$ for AB^* is ignored, then a first-order undistorted approximation to the quantal amplitude (14) is,

$$T_B(v^+) = 2\pi \int_0^\infty V_{de}^*(R) [\psi_v^{+*}(R) \psi_d^{(0)}(R)] dR \quad (23)$$

where $\psi_d^{(0)}$ is ψ_d in the absence of the back reaction of autoionization. Under this assumption then (13) reduces to,

$$\sigma_c(\epsilon, v^+) = \frac{\pi}{k_e^2} \left(\frac{\omega_{AB}^*}{2\omega^+} \right) |T_B(v^+)|^2 \quad (24)$$

which is then the cross section for initial electron capture since autoionization has been precluded. Although the Born T-matrix (23) violates unitarity, the capture cross section (24) must remain less than the maximum value,

$$\sigma_c^{max} = \frac{\pi}{k_e^2} \left(\frac{\omega_{AB}^*}{2\omega^+} \right) = \left(\frac{h^2}{8\pi m \epsilon} \right) \left(\frac{\omega_{AB}^*}{2\omega^+} \right) \quad (25)$$

since $|a_Q|^2 \leq 1$. So as to acknowledge after the fact the effect of autoionization, assumed small, and neglected by (23), the DR cross section can be approximated as,

$$\sigma_{DR}(\epsilon, v^+) = \sigma_c(\epsilon, v^+) P_S \quad (26)$$

where P_S is the probability of survival against autoionization on the V_d curve until stabilization takes place at some crossing point R_X .

By utilizing the reactance K-matrix, Flannery¹⁶ has shown that a unitarized T-matrix can be written as,

$$T = \frac{2R_B}{1 + |R_B|^2} = \frac{T_B}{1 + \left| \frac{1}{2} T_B \right|^2} \quad (27)$$

(a) The DR cross section is then given by (26) with,

$$P_S(\text{low } \epsilon) = \left[1 + \frac{1}{4} |T_B|^2 \right]^{-1} = \left\{ 1 + \pi^2 \left| \int_0^\infty V_{de}^*(R) [\psi_v^{+*}(R) \psi_d^{(0)}(R)] dR \right|^2 \right\}^{-2} \quad (28a)$$

which is valid at low ϵ when only one vibrational level v^+ ie. the initial level of the ion is re-populated by autoionization.

(b) At higher ϵ when population of many other ionic levels v_f^+ occurs then,

$$P_S(\epsilon) = \left[1 + \frac{1}{4} \sum_f |T_B(v_f^+)|^2 \right]^{-1} \quad (28b)$$

where the summation is over all the open vibrational levels v_f^+ of the ion.

When no intermediate Rydberg $AB^*(v)$ states are energy resonant with the initial $e^- + AB^+(v^+)$ state ie. coupling with the indirect mechanism is neglected, then (26) with (28b) is the direct DR cross section normally calculated^{4,11}.

These survival probabilities (28a) and (28b) agree with the weak-coupling results of Giusti¹³. The result (26) is therefore valid within the framework of the Born approximation (23).

(c) In the high ϵ -limit when an infinite number of v_f^+ levels are populated following autoionization the survival probability, with the aid of closure, is then,

$$P_S = \left[1 + \pi^2 \int_{R_c}^{R_X} |V_{de}^*(R)|^2 |\psi_d(R)|^2 dR \right]^{-2} \quad (29)$$

(d) On adopting in (29) the semiclassical wavefunction,

$$\psi_v^+(R) \equiv 2 \left[\frac{\nu_{nl}}{v_+(R)} \right]^{1/2} \sin \left[\int_{R_0}^R k_+(R) dR + \frac{\pi}{4} \right], \quad R \gg R_0 \quad (30a)$$

where $\hbar\nu_{nl} = d\epsilon_{vJ}/dv$ is the level spacing, and R_0 is the classical turning point given by the innermost zero of

$$\frac{1}{2} M v_+^2(R) = \frac{\hbar^2 k_+^2(R)}{2M} = E - [V^+(R) + \epsilon] - \frac{J^2}{2MR^2} \quad (30b)$$

The survival probability (29) then reduces to,

$$P_S(\text{high } \epsilon) = \left[1 + \frac{1}{2\hbar} \int_{R_c}^{R_x} \frac{\Gamma(R)}{v(R)} dR \right]^{-2} = \left[1 + \frac{1}{2} \int_{t_c}^{t_x} \nu_a(t) dt \right]^{-2} \quad (31)$$

where $v(R)$ is the local radial speed of A-B relative motion, and where $\langle \nu_a \rangle$ is the frequency $\nu_a(t)$ of autoionization averaged over time τ_d for the A-B to dissociate from their distance R_c of closest approach at time t_c to the crossing point R_x at time t_x .

(e) A classical path local approximation for P_S yields ^{12,17},

$$P_S = \exp \left(- \int_{t_c}^{t_x} \nu_a(t) dt \right) \quad (32)$$

which agrees to first-order for small ν , with the expansion of (31).

(f) A partitioning of (5) yields,

$$P_S = \nu_d / (\nu_a + \nu_d) = (\tau_a^{-1} + \tau_d^{-1}) \tau_a \quad (33)$$

on adopting macroscopic averaged frequencies ν_i and associated lifetimes $\tau_i = \nu_i^{-1}$. The stabilization probabilities in (a)–(f) above are all suitable for use in the DR cross section (26).

4.3. Further Approximation

The Franck-Condon Approximation to (23) provides,

$$|T_B(v_i^+)|^2 = 4\pi^2 |V_{de}^*(R)|^2 F(v^+, \epsilon) \quad (34a)$$

$$\equiv 2\pi \Gamma_a F(\epsilon) \equiv \hbar \bar{\nu}_a(\epsilon) F(\epsilon) \quad (34b)$$

where F is the Franck-Condon (FC) factor and $\bar{\nu}_a = \Gamma_a/\hbar$ is the R -averaged autoionization frequency. Hence the DR cross section (24) in (26) is,

$$\sigma_{DR}(\epsilon, v^+) = \frac{\hbar^3}{8\pi m \epsilon} \left(\frac{\omega_{AB}^*}{2\omega^+} \right) F(\epsilon) \bar{\nu}_a(\epsilon) P_S(\epsilon) \quad (35)$$

where P_S is given by any of the expressions (28a) - (33), (28b) being the most accurate.

The recombination rate is,

$$\begin{aligned}\alpha(T) &= \bar{v} \int_0^\infty \epsilon' \sigma_{DR}(\epsilon') \exp(-\epsilon') d\epsilon' \\ &= \bar{v} \langle \sigma_{DR} \rangle; \quad \epsilon' = \epsilon/kT\end{aligned}\quad (36)$$

where \bar{v} is the mean electron speed $(8kT/\pi m)^{1/2}$ appropriate to a Maxwellian velocity distribution at temperature T . With (35),

$$\alpha(T) = \left[\frac{h^3}{(2\pi m kT)^{3/2}} \right] \left(\frac{\omega_{AB}^*}{2\omega^+} \right) \int_0^\infty F(\epsilon, v_i^+) \bar{\nu}_a(\epsilon) P_S(\epsilon) \exp(-\epsilon/kT) d\epsilon \quad (37a)$$

$$\sim \left[\frac{h^3}{(2\pi m kT)^{3/2}} \right] \left(\frac{\omega_{AB}^*}{2\omega^+} \right) \langle \bar{\nu}_a P_S \rangle \int_0^\infty F(\epsilon, v_i^+) \exp(-\epsilon/kT) d\epsilon \quad (37b)$$

where $\langle \bar{\nu}_a P_S \rangle$ is the ϵ -averaged frequency. On adopting averaged frequencies and lifetimes, $\tau_a = \langle \bar{\nu}_a \rangle^{-1}$ and $\tau_d = \nu_d^{-1}$, by definition, then (31) and (32) are consistent with (33), and,

$$\bar{\nu}_a P_S = \bar{\nu}_a \nu_d / (\nu_a + \nu_d) = \tau_a^{-1} + \tau_d^{-1} \quad (38)$$

Adoption of the Winan-Stueckelberg wavefunction,

$$\psi_d(R) = |V_d'(R)|^{-1/2} \delta(R - R_c) \quad (39)$$

where R_c is the classical turning point for $A - B$ relative motion, then the FC factor is,

$$F(\epsilon) = \left[\left| \frac{dV_d}{dR} \right|^{-1} |\psi_v^+|^2 \right]_{R_c} \quad (40)$$

This FC factor (40), when inserted in (37b), with (38), is the original DR rate of Bates¹¹. The DR cross section of Bardsley¹² is recovered by inserting both (32) and (40) into (35). Flannery¹⁶ has shown in a semiclassical analysis that an improved FC factor is given by,

$$F(\epsilon) = |\psi_v^+(R_c)|^2 \left| \frac{d}{dR} (V_d - V^+) \right|_{R_c}^{-1} \quad (41)$$

where $\epsilon(R) = V_d(R) - V^+(R)$ is the energy for a vertical transition. Hence (37b) yields,

$$\alpha(T) = \left[\frac{h^3}{(2\pi m kT)^{3/2}} \right] \left(\frac{\omega_{AB}^*}{2\omega^+} \right) \langle \bar{\nu}_a P_S \rangle \int_{R_c}^{R_x} |\psi_v^+(R)|^2 \exp[-\epsilon(R)/kT] dR \quad (42)$$

The physical significance of this rate becomes apparent upon comparison with the following macroscopic rate.

4.4. Macroscopic Treatment

A steady-state macroscopic (kinetic rate) analysis of the two-stage sequence (12) provides the overall two-body rate $\alpha(\text{cm}^3\text{s}^{-1})$ at electron temperature T as,

$$\alpha(T) = k_c P_S = K(T) \nu_a P_S \quad (43)$$

where the reaction volume,

$$K(T) = \tilde{n}_{AB}^* / \tilde{n}_e \tilde{n}_+ = k_c / \nu_a \quad (44)$$

expresses detailed balance between the rate k_c for dielectronic capture and the frequency ν_a for autoionization ie. for the first forward-reverse stage of (12). The thermodynamic equilibrium number densities are denoted by \tilde{n}_i of species i . For DR at low ϵ then K , which is not an equilibrium constant in the usual sense since \tilde{n}_{AB}^* includes only those states which satisfy energy and angular momentum conservation above the dissociation limit, on comparison with (42) is

$$K(T) = \left[\frac{h^3}{(2\pi m k T)^{3/2}} \right] \left(\frac{\omega_{AB}^*}{2\omega^+} \right) \int_{R_c}^{R_x} |\psi_v^+(R)|^2 \exp[-\epsilon(R)/kT] dR \quad (45)$$

5. Present Semiclassical-Classical Path Theory

5.1. Full Theory

The strategy¹⁶⁻¹⁸ here is to insert within the original T-matrix (14) or probability amplitude a_Q the semiclassical JWKB wavefunctions (30a) for $\psi_v^+(R)$ and,

$$\begin{aligned} \psi_d(R) \equiv \frac{i}{[h v_d(R)]^{1/2}} & \left[c(R) \exp -i \left(\int_{R_c}^R k_d dR + \frac{\pi}{4} \right) \right. \\ & \left. - s(R) \exp i \left(\int_{R_c}^R k_d dR + \frac{\pi}{4} \right) \right] \end{aligned} \quad (46)$$

which is the JWKB wavefunction for nuclear motion under interaction $V_d(R)$ in the presence of autoionization. The turning point R_c is determined by the innermost zero of,

$$\frac{1}{2} M v_d^2(R) = \frac{\hbar^2 k_d^2(R)}{2M} = E - V_d(R) - \frac{L^2}{2MR^2} \quad (47)$$

for the radial speed $v_d(R)$ of relative motion in the dissociative potential $V_d(R)$. Angular momentum of relative nuclear motion is assumed conserved ($J = L$, large) since the angular momentum ℓ of the autoionizing electron is small.

The amplitudes for survival of $A - B$ motion under $V_d(R)$ against autoionization from the crossing point R_X to R , on the incoming leg of the classical trajectory $R = R(t)$, and from R_X to R_c and back to R on the outgoing leg, are $c(R)$ and $s(R)$, respectively. No crossing between V_d and V^+ implies infinite R_X and is covered by the present theory. Since the nuclear motion is now considered to follow the classical orbit $R = R(t)$, these amplitudes can be determined from a recent classical path theory¹⁷ of associative ionization and recombination. The classical path $R = R(t)$ theory¹⁷ of dissociative recombination shows that the amplitude $c(t)$ is determined by the following integral equation,

$$-2\pi\hbar^2 c(t) = \int_{t_X}^t dt' \int_0^\infty d\epsilon \Gamma(\epsilon, t; t') c(t') \exp i[\gamma(\epsilon; t) - \gamma(\epsilon; t')] \quad (48)$$

at time t . This depends on the previous history of the system between t_X and t via the non-local interaction,

$$\Gamma(\epsilon, t; t') = 2\pi V_{de}(t) V_{de}^*(t') \quad (49)$$

and on the phase difference,

$$\gamma(\epsilon; t) - \gamma(\epsilon; t') = \frac{1}{\hbar} \int_{t'}^t [V_d - (V^+ + \epsilon)] dt \quad (50)$$

at different times. Once this equation is solved by numerical procedures, the other amplitude $s(t) = c(t + t_c)$ where t_c is the time for nuclear motion from separation R_X to the distance of closest approach R_c can be determined.

The full theory involves inserting the classical path solutions of (48) for the amplitudes of $A - B$ survival against autoionization into the semiclassical JWKB function (46) for $A - B$ nuclear motion for use in the basic amplitude (14). It is therefore a hybrid semiclassical-classical path theory¹⁶⁻¹⁸. The full quantal numerical wavefunction or the JWKB wavefunction (30a) can be used for $\psi_v^+(R)$.

5.2. Stationary Phase Amplitudes

The quantal amplitude (14) with the semiclassical product for $\psi_v^+(R)\psi_d(R)$ is^{16,17},

$$a_Q(\epsilon) = 2\pi(\nu_{nl}/h)^{1/2} \int_0^\infty (v_+ v_d)^{-1/2} V_{de}^*(R) [c(R) \exp i\Delta(R) + s(R) \exp -i\Delta(R)] dR \quad (51)$$

The method of stationary phase can be used to provide analytical expressions^{16,17} for the transition amplitude (51) in terms of $c(R_i)$ and $s(R_i)$ evaluated at the points R_i where the difference,

$$\Delta(R) = \int_{R_0}^R k_+(R) dR - \int_{R_c}^R k_d(R) dR \quad (52)$$

is stationary. Various interference oscillatory patterns can then be exhibited in the cross section $\sigma_{DR}(\epsilon)$ of (13) even when coupling with the indirect mechanism is ignored. These oscillations arise from the different phases of the various stationary phase contributions to the amplitude (51).

Moreover, the integral equation (48) for $c(t)$ can also be solved approximately in analytical form by the method of stationary phase when there is a crossing between $V^+(R)$ and $V_d(R)$ at R_X . When there is no crossing, other techniques can be implemented. A hierarchy of the various levels of approximation and analytical results for $c(R(t))$ and $a_Q(\epsilon)$ are provided in reference 17.

Acknowledgements

It is a pleasure for me to acknowledge the pioneering and seminal work of David Smith and his co-workers to the whole subject area of electron-ion and ion-ion recombination and to wish David congratulations on the occasion of his sixtieth birthday.

This research is supported by the U. S. Air Force Office of Scientific Research under grant no. F49620-94-1-0379.

References

1. D. Smith and P. Španěl, *Int. J. Mass Spectrom. Ion Phys.*, **129** (1993) 163
2. M. Larsson, H. Danared, J. R. Mowat, P. Sigraý, G. Sundström, L. Broström, A. Filevich, A. Källberg, S. Mannervik, K. G. Rensfelt and S. Datz, *Phys. Rev. Letts.* **70** (1993) 430.
3. T. Gougousi, R. Johnsen, and M. F. Golde *J. Mass Spectrom. Ion Phys.*, (this issue).
4. S. L. Guberman, *Phys. Rev. A* **49** (1994) R4277.
5. G. Sundström, S. Batz, J. R. Mowat, S. Mannervik, L. Broström, M. Carlson, H. Danared and M. Larsson, *Phys. Rev. A* **50** (1994) R2806.
6. A. E. Orel and K. C. Kulander, *Phys. Rev. Letts.* **71** (1993) 4315.
7. N. G. Adams and D. Smith, *Chem. Phys. Lett.* **144** (1988) 11.
8. N. G. Adams, C. R. Herd and D. Smith, *J. Chem. Phys.* **91** (1989) 963.
9. D. R. Bates, *J. Phys. B: At. Mol. Opt. Phys.* **25** (1992) 5479; *Comments At. Mol. Phys.* **29** (1993) 53.
10. D. R. Bates, Guest M. F. and Kendall R. A., *Planet. Space Sci.* **41** (1003) 9.
11. D. R. Bates, *Phys. Rev.* **78** (1950) 492.
12. J. N. Bardsley, *J. Phys. B: At. Mol. Phys.* **1** (1968) 365.
13. A. Giusti, *J. Phys. B: At. Mol. Phys.* **13** (1980) 3867.
14. T. F. O' Malley, *J. Phys. B: At. Mol. Phys.* **14** (1981) 1229; *Recombination - Analytic Theory in Dissociative Recombination: Theory, Experiment and Applications* (J. B. A. Mitchell and S. L. Guberman eds.), World Scientific, Singapore (1989).

15. S. L. Guberman and A. Giusti-Suzor, *J. Chem. Phys.* **95** (1991) 2602.
16. M. R. Flannery, in Proceedings of the Bottcher Memorial Symposium (D. R. Schultz and J. H. Macek Eds.), AIP Press *in press* (1995).
17. M. R. Flannery, *Phys. Rev. A* (1995) in preparation.
18. M. R. Flannery, in *Atomic and Molecular Physics: Fourth US/Mexico Symposium* (C. Cisneros and T. J. Morgan, Eds.), World Scientific Publishing Co., Singapore (1995).

IX. Appendix C:

Electron-Ion and Ion-Ion Recombination

by

M. R. Flannery

School of Physics

Georgia Institute of Technology

Atlanta, Georgia 30332

Electron-Ion and Ion-Ion Recombination

M. R. Flannery

School of Physics, Georgia Institute of Technology, Atlanta, Georgia 30332-0430

44.1	RECOMBINATION PROCESSES	2
44.1.1	Electron-Ion Recombination	2
44.1.2	Positive-Ion Negative-Ion Recombination	2
44.1.3	Balances	2
44.2	COLLISIONAL-RADIATIVE RECOMBINATION	3
44.2.1	Saha and Boltzmann Distributions	3
44.2.2	Quasi-Steady State Distributions	4
44.2.3	Ionization and Recombination Coefficients	4
44.3	MACROSCOPIC METHODS	5
44.3.1	Resonant Capture-Stabilization Model: Dissociative and Dielectronic Recombination	5
44.3.2	Reactive Sphere Model: Three-Body Electron-Ion and Ion-Ion Recombination	5
44.3.3	Working Formulae for Three-Body Collisional Recombination at Low Density	6
44.3.4	Recombination Influenced by Diffusional Drift At High Gas Densities	7
44.4	DISSOCIATIVE RECOMBINATION	8
44.4.1	Curve-Crossing Mechanisms	8
44.4.2	Quantal Cross Section	9
44.4.3	Noncrossing Mechanism	11
44.5	MUTUAL NEUTRALIZATION	11
44.5.1	Landau-Zener Probability for Single Crossing at R_X	11
44.5.2	Cross Section and Rate Coefficient for Mutual Neutralization	11
44.6	ONE-WAY MICROSCOPIC EQUILIBRIUM CURRENT, FLUX, AND PAIR-DISTRIBUTIONS	12
44.7	MICROSCOPIC METHODS FOR TERMOLECULAR ION-ION RECOMBINATION	13
44.7.1	Time Dependent Method: Low Gas Density	13
44.7.2	Time Independent Methods: Low Gas Density	14
44.7.3	Recombination at Higher Gas Densities	15
44.7.4	Master Equations	15
44.7.5	Recombination Rate	16
44.8	RADIATIVE RECOMBINATION	16
44.8.1	Detailed Balance and Recombination-Ionization Cross Sections	17
44.8.2	Kramers Cross Sections, Rates, Electron Energy-Loss Rates and Radiated Power for Hydrogenic Systems	17
44.8.3	Basic Formulae for Quantal Cross Sections	19

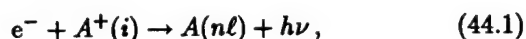
44.8.4	Bound-Free Oscillator Strengths	21
44.8.5	Radiative Recombination Rate	21
44.8.6	Gaunt Factor, Cross Sections and Rates for Hydrogenic Systems	22
44.8.7	Exact Universal Rate Scaling Law and Results for Hydrogenic Systems	22
44.9	USEFUL QUANTITIES	23
44.10	GENERAL REFERENCES	23

44.1 RECOMBINATION PROCESSES

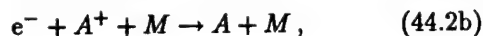
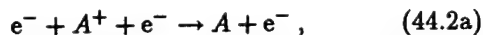
44.1.1 Electron-Ion Recombination

This proceeds via the following four processes:

(a) radiative recombination (RR)

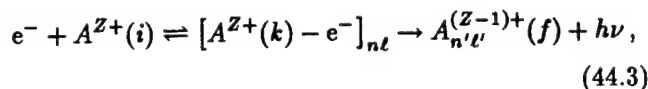


(b) three-body collisional-radiative recombination

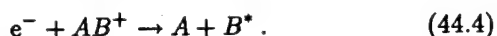


where the third body can be an electron or a neutral gas.

(c) dielectronic recombination (DLR)



(d) dissociative recombination (DR)

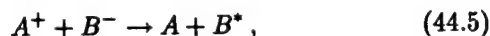


Electron recombination with bare ions can proceed only via (a) and (b), while (c) and (d) provide additional pathways for ions with at least one electron initially or for molecular ions AB^+ . *Electron radiative capture* denotes the combined effect of RR and DLR.

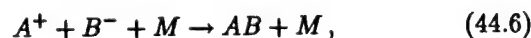
44.1.2 Positive-Ion Negative-Ion Recombination

This proceeds via the following three processes:

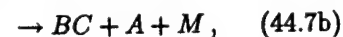
(e) mutual neutralization



(f) three-body (termolecular) recombination



(g) tidal recombination

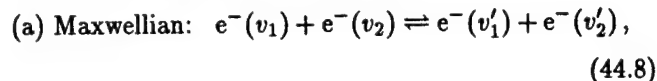


where M is some third species (atomic, molecular or ionic). Although (e) always occurs when no gas M is present, it is greatly enhanced by coupling to (f). The dependance of the rate $\hat{\alpha}$ on density N of background gas M is different for all three cases, (e)–(g).

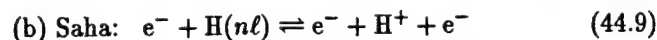
Processes (a), (c), (d) and (e) are elementary processes in that microscopic detailed balance (proper balance) exists with their true inverses, i.e., with photoionization (both with and without autoionization) as in (c) and (a), associative ionization and ion-pair formation as in (d) and (e), respectively. Processes (b), (f) and (g) in general involve a complex sequence of elementary energy-changing mechanisms as collisional and radiative cascade and their overall rates are determined by an input-output continuity equation involving microscopic continuum-bound and bound-bound collisional and radiative rates.

44.1.3 Balances

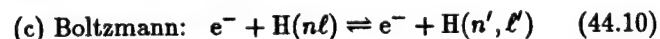
Proper balances are detailed microscopic balances between forward and reverse mechanisms that are direct inverses of one another, as in



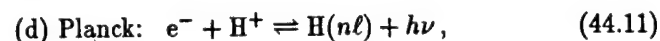
where the kinetic energy of the particles is redistributed;



between direct ionization from and direct recombination into a given level $n\ell$;



between excitation and de-excitation among bound levels;



which involves interaction between radiation and atoms in photoionization/recombination to a given level $n\ell$.

Improper balances maintain constant densities via production and destruction mechanisms that are *not* pure inverses of each other. They are associated with flux activity on a macroscopic level as in the transport of particles into the system for recombination and net production and transport of particles (i.e. e^- , A^+) for ionization. Improper balances can then exist between dissimilar elementary production-depletion processes as in (a) *coronal balance* between electron-excitation into and radiative decay out of level n . (b) *radiative balance* between radiative capture into and radiative cascade out of level n . (c) *excitation saturation balance* between upward collisional excitations $n-1 \rightarrow n \rightarrow n+1$ between adjacent levels. (d) *de-excitation saturation balance* between downward collisional de-excitations $n+1 \rightarrow n \rightarrow n-1$ into and out of level n .

44.2 COLLISIONAL-RADIATIVE RECOMBINATION

Radiative recombination. Process (44.1) involves a free-bound electronic transition with radiation spread over the recombination continuum. It is the inverse of photoionization without autoionization and favors high energy gaps with transitions to low $n \sim 1, 2, 3$ and low angular momentum states $\ell \sim 0, 1, 2$ at higher electron energies.

Three-body electron-ion recombination. Processes (44.2a,b) favor free-bound collisional transitions to high levels n , within a few $k_B T$ of the ionization limit of $A(n)$ and collisional transitions across small energy gaps. Recombination becomes stabilized by *collisional-radiative cascade* through the lower bound levels of A . Collisions of the $e^- - A^+$ pair with third bodies becomes more important for higher levels n and radiative emission is important down to and among the lower levels n . In optically thin plasmas this radiation is lost, while in optically thick plasmas it may be re-absorbed. At low electron densities radiative recombination dominates with predominant transitions taking place to the ground level. For process (44.2a) at high electron densities, three-body collisions into high Rydberg levels dominate, followed by cascade which is collision dominated at low electron temperatures T_e and radiation dominated at high T_e . For process (44.2b) at low gas densities N , the recombination is collisionally-radiatively controlled while, at high N , it eventually becomes controlled by the rate of diffusional drift (44.61) through the gas M .

Collisional-radiative recombination. Here the cascade collisions and radiation are coupled via the continuity equation. The population n_i of an individual excited level i of energy E_i is determined by the rate equations

$$\frac{dn_i}{dt} = \frac{\partial n_i}{\partial t} + \nabla \cdot (n_i \mathbf{v}_i) \quad (44.12)$$

$$= \sum_{i \neq f} [n_f \nu_{fi} - n_i \nu_{if}] = P_i - n_i D_i, \quad (44.13)$$

which involve temporal and spatial relaxation in (44.12) and collisional-radiative production rates P_i and destruction frequencies D_i of the elementary processes included in (44.13). The total collisional and radiative transition frequency between levels i and f is ν_{if} and the f -sum is taken over all discrete and continuous (c) states of the recombining species. The transition frequency ν_{if} includes all contributing elementary processes that directly link states i and f , eg., collisional excitation and de-excitation, ionization ($i \rightarrow c$) and recombination ($c \rightarrow i$) by electrons and heavy particles, radiative recombination ($c \rightarrow i$), radiative decay ($i \rightarrow f$), possibly radiative absorption for optically thick plasmas, autoionization and dielectronic recombination.

Production rates and processes. The production rate for a level i is

$$P_i = \sum_{f \neq i} n_e n_f K_{fi}^c + n_e^2 N^+ k_{ci}^R + \sum_{f > i} n_f [A_{fi} + B_{fi} \rho_\nu] + n_e N^+ [\alpha_i^{RR} + \beta_i \rho_\nu], \quad (44.14)$$

where the terms in the above order represent (1) collisional excitation and de-excitation by $e^- - A(f)$ collisions, (2) three-body $e^- - A^+$ collisional recombination into level i , (3) spontaneous and stimulated radiative cascade, and (4) spontaneous and stimulated radiative recombination.

Destruction rates and processes. The destruction rate for a level i is

$$n_i D_i = n_e n_i \sum_{f \neq i} K_{if}^c + n_e n_i S_i + n_i \sum_{f < i} [A_{if} + B_{if} \rho_\nu] + n_i \sum_{f > i} B_{if} \rho_\nu + n_i B_{ic} \rho_\nu, \quad (44.15)$$

where the terms in the above order represent (1) collisional destruction, (2) collisional ionization, (3) spontaneous and stimulated emission, (4) photo-excitation, and (5) photoionization.

44.2.1 Saha and Boltzmann Distributions

Collisions of $A(n)$ with third bodies such as e^- and M are more rapid than radiative decay above a certain excited level n^* . Since each collision process is accompanied by its exact inverse the principle of detailed balance determines the population of levels $i > n^*$.

Saha distribution. This connects equilibrium densities \tilde{n}_i , \tilde{n}_e and \tilde{N}^+ of bound levels i , of free electrons at temperature T_e and of ions by

$$\frac{\tilde{n}_i}{\tilde{n}_e \tilde{N}^+} = \left[\frac{g(i)}{g_e g_A^+} \right] \frac{h^3}{(2\pi m_e k T_e)^{3/2}} \exp(I_i / k_B T_e), \quad (44.16)$$

where the electronic statistical weights of the free electron, the ion of charge $Z + 1$ and the recombined $e^- - A^+$ species of net charge Z and ionization potential I_i are $g_e = 2$, g_A^+ and $g(i)$, respectively. Since $n_i \leq \tilde{n}_i$ for all i , then the Saha-Boltzmann distributions imply that $n_1 \gg n_i$ and $n_e \gg n_i$ for $i \neq 1, 2$, where $i = 1$ is the ground state.

Boltzmann Distribution. This connects the equilibrium populations of bound levels i of energy E_i by

$$\tilde{n}_i/\tilde{n}_j = [g(i)/g(j)] \exp [-(E_i - E_j)/k_B T_e]. \quad (44.17)$$

44.2.2 Quasi-Steady State Distributions

The reciprocal lifetime of level i is the sum of radiative and collisional components and is therefore shorter than the pure radiative lifetime $\tau_R \sim 10^{-7} Z^{-4}$ s. The lifetime τ_1 for the ground level is collisionally controlled, is dependent upon n_e , and generally is within the range of 10^2 and 10^4 s for most laboratory plasmas and the solar atmosphere. The excited level lifetimes τ_i are then much shorter than τ_1 . The (spatial) diffusion or plasma decay (recombination) time is then much longer than τ_i and the total number of recombined species is much smaller than the ground-state population n_1 . The recombination proceeds on a timescale much longer than the time for population/destruction of the excited levels. The condition for quasi-steady state, or QSS-condition, $dn_i/dt = 0$ for the bound levels $i \neq 1$, therefore holds. The QSS distributions n_i therefore satisfy $P_i = n_i D_i$.

44.2.3 Ionization and Recombination Coefficients

Under QSS, the continuity equation (44.13) then reduces to a finite set of simultaneous equations $P_i = n_i D_i$. This gives a matrix equation which is solved numerically for $n_i (i \neq 1) \leq \tilde{n}_i$ in terms of n_1 and n_e . The net ground-state population frequency per unit volume ($\text{cm}^{-3} \text{s}^{-1}$) can then be expressed as

$$\frac{dn_1}{dt} = n_e N^+ \hat{\alpha}_{CR} - n_e n_1 S_{CR}, \quad (44.18)$$

where $\hat{\alpha}_{CR}$ and S_{CR} , respectively, are the overall rate coefficients for recombination and ionization via the collisional-radiative sequence. The determined $\hat{\alpha}_{CR}$ equals the direct ($c \rightarrow 1$) recombination to the ground level supplemented by the net collisional-radiative cascade from that portion of bound-state population which originated from the continuum. The determined S_{CR} equals direct depletion (excitation and ionization) of the ground state reduced by the de-excitation collisional radiative cascade from that portion of the bound levels accessed originally from the ground level. At low n_e , $\hat{\alpha}_{CR}$

and S_{CR} reduce, respectively, to the radiative recombination coefficient summed over all levels and to the collisional ionization coefficient for the ground level.

C , \mathcal{E} and S Blocks of Energy Levels

For the recombination processes (44.2a), (44.2b) and (44.6) which involve a sequence of elementary reactions, the $e^- - A^+$ or $A^+ - B^-$ continuum levels and the ground $A(n = 1)$ or the lowest vibrational levels of AB are therefore treated as two large particle reservoirs of reactants and products. These two reservoirs act as reactant and as sink blocks C and S which are, respectively, drained and filled at the same rate via a conduit of highly excited levels which comprise an intermediate block of levels \mathcal{E} . This C draining and S filling proceeds, via block \mathcal{E} , on a timescale large compared with the short time for a small amount from the reservoirs to be re-distributed within block \mathcal{E} . This forms the basis of QSS.

Working Formulae

For electron-atomic-ion collisional-radiative recombination (44.2a), detailed QSS calculations can be fitted by the rate [1]

$$\hat{\alpha}_{CR} = [3.8 \times 10^{-9} T_e^{-4.5} n_e + 1.55 \times 10^{-10} T_e^{-0.63} + 6 \times 10^{-9} T_e^{-2.18} n_e^{0.37}] \text{ cm}^3 \text{ s}^{-1} \quad (44.19)$$

agrees with experiment for a Lyman α optically thick plasma with n_e and T_e in the range: $10^9 \text{ cm}^{-3} \leq n_e \leq 10^{13} \text{ cm}^{-3}$ and $2.5 \text{ K} \leq T_e \leq 4000 \text{ K}$. The first term is the pure collisional rate (44.49), the second term is the radiative cascade contribution, and the third term arises from collisional-radiative coupling.

For ($e^- - He_2^+$) recombination in a high (5–100 Torr) pressure helium afterglow the rate for (44.2b) is [2]

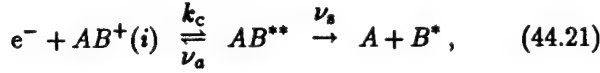
$$\hat{\alpha}_{CR} = [(4 \pm 0.5) \times 10^{-20} n_e] \left(\frac{T_e}{293} \right)^{-(4 \pm 0.5)} + \{(5 \pm 1) \times 10^{-27} n(He) + (2.5 \pm 2.5) \times 10^{-10}\} \times \left(\frac{T_e}{293} \right)^{-(1 \pm 1)} \text{ cm}^3/\text{s}. \quad (44.20)$$

The first two terms are in accord with the purely collisional rates (44.49) and (44.52b), respectively.

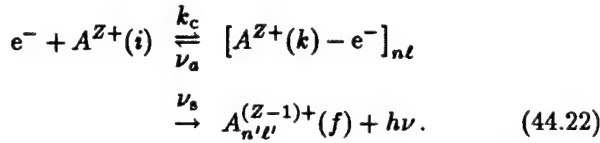
44.3 MACROSCOPIC METHODS

44.3.1 Resonant Capture-Stabilization Model: Dissociative and Dielectronic Recombination

The electron is captured dielectronically (cf. (44.41)) into an energy-resonant long-lived intermediate collision complex of super-excited states d which can autoionize or be stabilized irreversibly into the final product channel f either by molecular fragmentation



as in direct dissociative recombination (DR), or by emission of radiation as in dielectronic recombination (DLR)



Production Rate of Super-Excited States d .

$$\frac{dn_d^*}{dt} = n_e N^+ k_c(d) - n_d^* [\nu_A(d) + \nu_S(d)]; \quad (44.23)$$

$$\nu_A(d) = \sum_{i'} \nu_a(d \rightarrow i'), \quad (44.24a)$$

$$\nu_S(d) = \sum_{f'} \nu_s(d \rightarrow f'). \quad (44.24b)$$

Steady-State Distribution. For a steady-state distribution, the capture volume is

$$\frac{n_d^*}{n_e N^+} = \frac{k_c(d)}{\nu_A(d) + \nu_S(d)}. \quad (44.25)$$

Recombination Rate and Stabilization Probability. The recombination rate to channel f is

$$\hat{\alpha}_f = \sum_d \left[\frac{k_c(d) \nu_s(d \rightarrow f)}{\nu_A(d) + \nu_S(d)} \right], \quad (44.26a)$$

and the rate to all product channels is

$$\hat{\alpha} = \sum_d \frac{k_c(d) \nu_S(d)}{\nu_A(d) + \nu_S(d)}. \quad (44.26b)$$

In the above, the quantities

$$P_f^S(d) = \nu_s(d \rightarrow f) / [\nu_A(d) + \nu_S(d)], \quad (44.27)$$

$$P^S(d) = \nu_S(d) / [\nu_A(d) + \nu_S(d)], \quad (44.28)$$

represent the corresponding stabilization probabilities.

Macroscopic Detailed Balance and Saha Distribution.

$$K_{di}(T) = \frac{\tilde{n}_d^*}{\tilde{n}_e \tilde{N}^+} = \frac{k_c(d)}{\nu_a(d \rightarrow i)} = k_c(d) \tau_a(d \rightarrow i) \quad (44.29a)$$

$$= \frac{h^3}{(2\pi m_e k_B T)^{3/2}} \left[\frac{\omega(d)}{2\omega^+} \right] \exp[-E_{di}^*/k_B T], \quad (44.29b)$$

where E_{di}^* is the energy of super-excited neutral levels AB^{**} above that for ion level $AB^+(i)$, and ω are the corresponding statistical weights.

Alternative Rate Formula.

$$\hat{\alpha}_f = \sum_d K_{di} \left[\frac{\nu_a(d \rightarrow i) \nu_s(d \rightarrow f)}{\nu_A(d) + \nu_S(d)} \right]. \quad (44.30)$$

Normalized Excited State Distributions.

$$\rho_d = n_d^*/\tilde{n}_d^* = \frac{\nu_a(d \rightarrow i)}{[\nu_A(d) + \nu_S(d)]}. \quad (44.31)$$

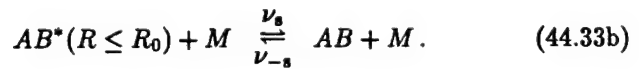
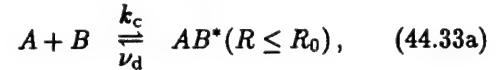
$$\hat{\alpha} = \sum_d k_c(d) P^S(d) = \sum_d K_{di} \rho_d \nu_S(d) \quad (44.32a)$$

$$= \sum_d k_c(d) [\rho_d \nu_S(d) \tau_a(d \rightarrow i)]. \quad (44.32b)$$

Although equivalent, Eqs. (44.26a) and (44.30) are normally invoked for (44.21) and (44.22), respectively, since $P^S \leq 1$ for DR so that $\hat{\alpha}_{DR} \rightarrow k_c$; and $\nu_A \gg \nu_S$ for DLR with $n \ll 50$ so that $\hat{\alpha} \rightarrow K_{di} \nu_s$. For $n \gg 50$, $\nu_S \gg \nu_A$ and $\hat{\alpha} \rightarrow k_c$. The above results (44.26a) and (44.30) can also be derived from microscopic Breit-Wigner scattering theory for isolated (nonoverlapping) resonances.

44.3.2 Reactive Sphere Model: Three-Body Electron-Ion and Ion-Ion Recombination

Since the Coulomb attraction cannot support quasi-bound levels, three body electron-ion and ion-ion recombination do not in general proceed via time-delayed resonances, but rather by reactive (energy-reducing) collisions with the third body M . This is particularly effective for A - B separations $R \leq R_0$, as in the sequence



In contrast to (44.21) and (44.22) where the stabilization is irreversible, the forward step in (44.33b) is reversible. The sequence (44.33a) and (44.33b) represents a closed system where thermodynamic equilibrium is eventually established.

Steady State Distribution of AB^* Complex.

$$n^* = \left(\frac{k_c}{\nu_s + \nu_d} \right) n_A(t)n_B(t) + \left(\frac{\nu_{-s}}{\nu_s + \nu_d} \right) n_s(t). \quad (44.34)$$

Saha and Boltzmann balances:

$$\begin{aligned} \text{Saha:} \quad & \tilde{n}_A \tilde{n}_B k_c = \tilde{n}^* \nu_d, \\ \text{Boltzmann:} \quad & \tilde{n}_s \nu_{-s} = \tilde{n}^* \nu_s. \end{aligned} \quad (44.35)$$

\tilde{n}^* is in Saha balance with reactant block C and in Boltzmann balance with product block S .

Normalized Distributions.

$$\rho^* = \frac{n^*}{\tilde{n}^*} = P^D \gamma_c(t) + P^S \gamma_s(t), \quad (44.36a)$$

$$\gamma_c(t) = \frac{n_A(t)n_B(t)}{\tilde{n}_A \tilde{n}_B}, \quad \gamma_s(t) = \frac{n_s(t)}{\tilde{n}_s}. \quad (44.36b)$$

Stabilization and Dissociation Probabilities.

$$P^S = \frac{\nu_s}{(\nu_s + \nu_d)}, \quad P^D = \frac{\nu_d}{(\nu_s + \nu_d)}. \quad (44.37)$$

Time Dependent Equations.

$$\frac{dn_c}{dt} = -k_c P^S \tilde{n}_A \tilde{n}_B [\gamma_c(t) - \gamma_s(t)], \quad (44.38a)$$

$$\frac{dn_s}{dt} = -\nu_{-s} P^D \tilde{n}_s [\gamma_s(t) - \gamma_c(t)], \quad (44.38b)$$

$$\frac{dn_c}{dt} = -\hat{\alpha}_3 n_A(t)n_B(t) + k_d n_s(t). \quad (44.39)$$

where the recombination rate coefficient (cm^3/s) and dissociation frequency are, respectively,

$$\hat{\alpha}_3 = k_c P^S = \frac{k_c \nu_s}{(\nu_s + \nu_d)}, \quad (44.40)$$

$$k_d = \nu_{-s} P^D = \frac{\nu_{-s} \nu_d}{(\nu_s + \nu_d)}, \quad (44.41)$$

which also satisfy the macroscopic detailed balance relation

$$\hat{\alpha}_3 \tilde{n}_A \tilde{n}_B = k_d \tilde{n}_s. \quad (44.42)$$

Time Independent Treatment. The rate $\hat{\alpha}_3$ given by the time dependent treatment can also be deduced by viewing the recombination process as a source block C kept fully filled with dissociated species A and B maintained at equilibrium concentrations \tilde{n}_A , \tilde{n}_B (i.e. $\gamma_c = 1$) and draining at the rate $\hat{\alpha}_3 \tilde{n}_A \tilde{n}_B$ through a steady-state intermediate block \mathcal{E} of excited levels into a fully absorbing sink block S of fully associated species AB kept fully depleted with $\gamma_s = 0$ so that there is no backward re-dissociation from block S . The frequency k_d is deduced as if the reverse scenario, $\gamma_s = 1$ and $\gamma_c = 0$, holds. This picture uncouples $\hat{\alpha}$ and k_d , and allows each coefficient to be calculated

independently. Both dissociation (or ionization) and association (recombination) occur within block \mathcal{E} .

If $\gamma_c = 1$ and $\gamma_s = 0$, then

$$\rho^* = n^*/\tilde{n}^* = \nu_d/(\nu_s + \nu_d), \quad (44.43a)$$

$$K = \tilde{n}^*/\tilde{n}_A \tilde{n}_B = k_c/\nu_d = k_c \tau_d, \quad (44.43b)$$

$$P^S = \nu_s/(\nu_s + \nu_d) = \rho^* \nu_s \tau_s, \quad (44.43c)$$

and the recombination coefficient is

$$\hat{\alpha} = k_c P^S = k_c [\rho^* \nu_s \tau_d] = K \rho^* \nu_s. \quad (44.44)$$

Microscopic Generalization. From (44.167), the microscopic generalizations of rate (44.40) and probability (44.43c) are, respectively,

$$\hat{\alpha} = \bar{\nu} \int_0^\infty \epsilon e^{-\epsilon} d\epsilon \int_0^{R_0} 2\pi b db P^S(\epsilon, b; R_0), \quad (44.45a)$$

$$P^S(\epsilon, b; R_0) = \oint_{R_i}^{R_0} \rho_i(R) \nu_i^b(R) dt \equiv \langle \nu_s \rangle \tau_d, \quad (44.45b)$$

where $\rho_i(R) = n(\epsilon, b; R)/\tilde{n}(\epsilon, b; R)$; ν_i^b is the frequency (44.164a) of $(A-B)-M$ continuum-bound collisional transitions at fixed $A-B$ separation R , R_i is the pericenter of the orbit, $|i\rangle \equiv |\epsilon, b\rangle$, and

$$b_0^2 = R_0^2 [1 - V(R)/E], \quad \epsilon = E/k_B T, \quad (44.45c)$$

$$\hat{\alpha} \equiv k_c \langle P^S \rangle_{\epsilon, b}, \quad \bar{\nu} = (8k_B T/\pi M_{AB})^{1/2}, \quad (44.45d)$$

$$k_c = \{ \pi R_0^2 [1 - V(R_0)/k_B T] \bar{\nu} \}. \quad (44.45e)$$

where M_{AB} is the reduced mass of A and B .

Low Gas Densities. Here $\rho_i(R) = 1$ for $E > 0$,

$$P^S(\epsilon, b; R_0) = \oint_{R_i}^{R_0} \nu(t) dt = \int_{R_i}^{R_0} ds/\lambda_i. \quad (44.46)$$

$\lambda_i = (N\sigma)^{-1}$ is the microscopic path length towards the $(A-B)-M$ reactive collision with frequency $\nu = N\nu\sigma$. For λ_i constant, the rate (44.45a) reduces at low N to

$$\hat{\alpha} = (\nu\sigma_0 N) \int_0^{R_0} \left[1 - \frac{V(R)}{k_B T} \right] 4\pi R^2 dR \quad (44.47)$$

which is linear in the gas density N .

44.3.3 Working Formulae for Three-Body Collisional Recombination at Low Density

For three-body ion-ion collisional recombination of the form $A^+ + B^- + M$ in a gas at low density N , set $V(R) = -e^2/R$. Then (44.47) yields

$$\hat{\alpha}^c(T) = \left(\frac{8k_B T}{\pi M_{AB}} \right)^{1/2} \frac{4}{3} \pi R_0^3 \left[1 + \frac{3}{2} \frac{R_e}{R_0} \right] (\sigma_0 N), \quad (44.48)$$

where $R_e = e^2/k_B T$, and the trapping radius R_0 , determined by the classical variational method, is $0.41R_e$, in agreement with detailed calculation. The special cases are:

(a) $e^- + A^+ + e^-$. Here, $\sigma_0 = \frac{1}{9}\pi R_e^2$ for $(e^- - e^-)$ collisions for scattering angles $\theta \geq \pi/2$ so that

$$\hat{\alpha}_{ee}^c(T) = 2.7 \times 10^{-20} \left(\frac{300}{T}\right)^{4.5} n_e \text{ cm}^3 \text{ s}^{-1} \quad (44.49)$$

in agreement with Mansbach and Keck [3].

(b) $A^+ + B^- + M$. Here, $\sigma_0 \bar{v} \sim 10^{-9} \text{ cm}^3 \text{ s}^{-1}$, which is independent of T for polarization attraction. Then

$$\hat{\alpha}_3(T) = 2 \times 10^{-25} \left(\frac{300}{T}\right)^{2.5} N \text{ cm}^3 \text{ s}^{-1}. \quad (44.50)$$

(c) $e^- + A^+ + M$. Only a small fraction $\delta = 2m/M$ of the electron's energy is lost upon $(e^- - M)$ collision so that (44.45a) for constant λ is modified to

$$\hat{\alpha}_{eM} = \sigma_0 N \int_0^{R_0} 4\pi R^2 dR \int_0^{E_m} \bar{n}(R, E) v dE \quad (44.51a)$$

$$= \bar{v}_e \sigma_0 N \int_0^{R_0} 4\pi R^2 dR \int_0^{\epsilon_m} \left[1 - \frac{V(R)}{E}\right] \epsilon e^{-\epsilon} d\epsilon \quad (44.51b)$$

where $\epsilon = E/k_B T$, and $E_m = \delta e^2/R = \epsilon_m k_B T$ is the maximum energy for collisional trapping. Hence,

$$\hat{\alpha}_{eM}(T_e) = 4\pi\delta \left(\frac{8k_B T_e}{\pi m_e}\right)^{1/2} R_e^2 R_0 [\sigma_0 N] \quad (44.52a)$$

$$\sim \frac{10^{-26}}{M} \left(\frac{300}{T}\right)^{2.5} N \text{ cm}^3 \text{ s}^{-1}, \quad (44.52b)$$

where the mass M of the gas atom is now in amu. This result agrees with the energy diffusion result of Pitaevskii [4] when R_0 is taken as the Thomson radius $R_T = \frac{2}{3}R_e$.

44.3.4 Recombination Influenced by Diffusional Drift At High Gas Densities

Diffusional-Drift Current. The drift current of A^+ towards B^- in a gas under an $A^+ - B^-$ attractive potential $V(R)$ is

$$\mathbf{J}(R) = -D\nabla n(R) - \left[\frac{K}{e}\nabla V(R)\right] n(R) \quad (44.53a)$$

$$= -\left[D\tilde{N}_A\tilde{N}_B e^{-V(R)/k_B T} \frac{\partial \rho}{\partial R}\right] \hat{\mathbf{R}}. \quad (44.53b)$$

Relative Diffusion and Mobility Coefficients.

$$\begin{aligned} D &= D_A + D_B, \\ K &= K_A + K_B, \quad De = K(k_B T), \end{aligned} \quad (44.54)$$

where the D_i and K_i are, respectively, the diffusion and mobility coefficients of species i in gas M .

Normalized Ion-Pair R -Distribution.

$$\rho(R) = \frac{n(R)}{\tilde{N}_A \tilde{N}_B \exp[-V(R)/k_B T]}. \quad (44.55)$$

Continuity Equations for Currents and Rates.

$$\frac{\partial n}{\partial t} + \nabla \cdot \mathbf{J} = 0, \quad R \geq R_0 \quad (44.56a)$$

$$\hat{\alpha}_{RN}(R_0)\rho(R_0) = \hat{\alpha}\rho(\infty) \quad (44.56b)$$

The rate of reaction for ion-pairs with separations $R \leq R_0$ is $\alpha_{RN}(R_0)$. This is the recombination rate that would be obtained for a thermodynamic equilibrium distribution of ion pairs with $R \geq R_0$, i.e. for $\rho(R \geq R_0) = 1$.

Steady-State Rate of Recombination.

$$\hat{\alpha}\tilde{N}_A\tilde{N}_B = \int_{R_0}^{\infty} \left(\frac{\partial n}{\partial t}\right) d\mathbf{R} = -4\pi R_0^2 J(R_0). \quad (44.57)$$

Steady-State Solution.

$$\rho(R) = \rho(\infty) \left[1 - \frac{\hat{\alpha}}{\hat{\alpha}_{TR}(R_0)}\right], \quad R \geq R_0 \quad (44.58a)$$

$$\rho(R_0) = \rho(\infty) [\hat{\alpha}/\hat{\alpha}_{RN}(R_0)]. \quad (44.58b)$$

Recombination Rate.

$$\hat{\alpha} = \frac{\hat{\alpha}_{RN}(R_0)\hat{\alpha}_{TR}(R_0)}{\hat{\alpha}_{RN}(R_0) + \hat{\alpha}_{TR}(R_0)} \quad (44.59a)$$

$$\rightarrow \begin{cases} \hat{\alpha}_{RN}, & N \rightarrow 0 \\ \hat{\alpha}_{TR}, & N \rightarrow \infty. \end{cases} \quad (44.59b)$$

Diffusional-Drift Transport Rate.

$$\hat{\alpha}_{TR}(R_0) = 4\pi D \left[\int_{R_0}^{\infty} \frac{e^{V(R)/k_B T}}{R^2} dR \right]^{-1}. \quad (44.60)$$

With $V(R) = -e^2/R$,

$$\hat{\alpha}_{TR}(R_0) = 4\pi K e [1 - \exp(-R_e/R_0)]^{-1}, \quad (44.61)$$

where $R_e = e^2/k_B T$ provides a natural unit of length.

Langevin Rate. For $R_0 \ll R_e$, the transport rate

$$\hat{\alpha}_{TR} \rightarrow \hat{\alpha}_L = 4\pi K e, \quad (44.62)$$

tends to the Langevin rate which varies as N^{-1} .

Reaction Rate. When R_0 is large enough that R_0 -pairs are in (E, L^2) equilibrium (cf. (44.167)),

$$\begin{aligned}\hat{\alpha}_{\text{RN}}(R_0) &= \bar{v} \int_0^\infty \epsilon e^{-\epsilon} d\epsilon \int_0^{b_0} 2\pi b db P^S(\epsilon, b; R_0) \\ &\equiv \bar{v} \int_0^\infty \epsilon e^{-\epsilon} d\epsilon [\pi b_0^2 P^S(\epsilon; R_0)] \quad (44.63a) \\ &\equiv \bar{v} \pi b_{\text{max}}^2 P^S(R_0), \quad (44.63b)\end{aligned}$$

where

$$b_0^2 = R_0^2 [1 - V(R_0)/E], \quad \epsilon = E/k_B T, \quad (44.64a)$$

$$\bar{v} = (8kT/\pi M_{AB})^{1/2}, \quad (44.64b)$$

$$b_{\text{max}}^2 = R_0^2 \left[1 - \frac{V(R_0)}{k_B T} \right]. \quad (44.64c)$$

The probability P^S and its averages over b and (b, E) for reaction between pairs with $R \leq R_0$ is determined in (44.63a)–(44.63b) from solutions of coupled master equations. P^S increases linearly with N initially and tends to unity at high N . The recombination rate (44.59a) with (44.63a) and (44.61) therefore increases linearly with N initially, reaches a maximum when $\hat{\alpha}_{\text{TR}} \sim \hat{\alpha}_{\text{RN}}$ and then decreases eventually as N^{-1} , in accord with (44.3.4).

Reaction Probability. The classical absorption solution of (44.157) is

$$P^S(E, b; R_0) = 1 - \exp \left[- \oint_{R_i}^{R_0} \frac{ds_i}{\lambda_i} \right]. \quad (44.65)$$

With the binary decomposition $\lambda_i^{-1} = \lambda_{iA}^{-1} + \lambda_{iB}^{-1}$,

$$P^S = P_A + P_B - P_A P_B. \quad (44.66)$$

Exact b^2 -Averaged Probability. With $V_c = -e^2/R$ for the A^+B^- interaction in (44.63a), and at low gas densities N ,

$$P_{A,B}(E, R_0) = \frac{4R_0}{3\lambda_{A,B}} \left[1 - \frac{3V_c(R_0)}{2E_i} \right] \quad (44.67)$$

appropriate for constant mean free path λ_i .

(E, b^2) -Averaged Probability. $P^S(R_0)$ in (44.63b) at low gas density is

$$P_{A,B}(R_0) = P_{A,B}(E = k_B T, R_0). \quad (44.68)$$

Thomson Trapping Distance. When the kinetic energy gained from Coulomb attraction is assumed lost upon collision with third bodies, then bound $A-B$ pairs are formed with $R \leq R_T$. Since $E = \frac{3}{2}k_B T - e^2/R$, then

$$R_T = \frac{2}{3} \left(\frac{e^2}{k_B T} \right) = \frac{2}{3} R_e. \quad (44.69)$$

Thomson Straight-Line Probability. The $E \rightarrow \infty$ limit of (44.65) is

$$P_{A,B}^T(b; R_T) = 1 - \exp [-2(R_T^2 - b^2)/\lambda_{A,B}]. \quad (44.70)$$

The b^2 -average is the Thomson probability

$$P_{A,B}^T(R_T) = 1 - \frac{1}{2X^2} [1 - e^{-2X}(1 + 2X)] \quad (44.71a)$$

for reaction of $(A-B)$ pairs with $R \leq R_T$. As $N \rightarrow 0$

$$P_{A,B}^T(R_T) \rightarrow \frac{4}{3}X \left[1 - \frac{3}{4}X + \frac{2}{5}X^2 - \frac{1}{6}X^3 + \dots \right] \quad (44.71b)$$

and tends to unity at high N . $X = R_T/\lambda_{A,B} = N(\sigma_0 R_T)$. These probabilities have been generalized [13] to include hyperbolic and general trajectories.

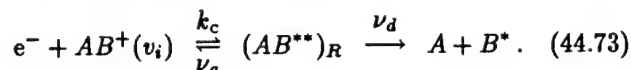
Thomson Reaction Rate.

$$\begin{aligned}\hat{\alpha}_T &= \pi R_T^2 \bar{v} [P_A^T + P_B^T - P_A^T P_B^T] \quad (44.72) \\ &\rightarrow \begin{cases} \frac{4}{3} \pi R_T^3 (\lambda_A^{-1} + \lambda_B^{-1}), & N \rightarrow 0 \\ \pi R_T^2 \bar{v}, & N \rightarrow \infty. \end{cases}\end{aligned}$$

44.4 DISSOCIATIVE RECOMBINATION

44.4.1 Curve-Crossing Mechanisms

Direct Process. Dissociative recombination (DR) for diatomic ions can occur via a crossing at R_X between the bound and repulsive potential energy curves $V^+(R)$ and $V_d(R)$ for AB^+ and AB^{**} , respectively. Here, DR involves the two-stage sequence



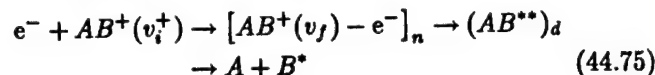
The first stage is dielectronic capture whereby the free electron of energy $\epsilon = V_d(R) - V^+(R)$ excites an electron of the diatomic ion AB^+ with internal separation R and is then resonantly captured by the ion, at rate k_c , to form a repulsive state d of the doubly excited molecule AB^{**} , which in turn can either autoionize at probability frequency ν_a , or else in the second stage predissociate into various channels at probability frequency ν_d . This competition continues until the (electronically excited) neutral fragments accelerate past the crossing at R_X . Beyond R_X the increasing energy of relative separation reduces the total electronic energy to such an extent that autoionization is essentially precluded and the neutralization is then rendered permanent past the stabilization point R_X . This interpretation [5] has remained intact and robust in the current light of *ab initio* quantum chemistry and quantal scattering calculations for the simple diatomics (O_2^+ , N_2^+ , Ne_2^+ , etc.). Mechanism (44.73) is termed the direct process which, in terms

of the macroscopic frequencies in (44.73), proceeds at the rate

$$\hat{\alpha} = k_c P_S = k_c [\nu_d / (\nu_a + \nu_d)], \quad (44.74)$$

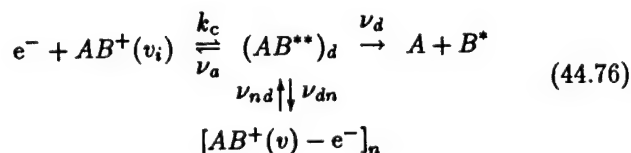
where P_S is probability for $A - B^*$ survival against autoionization from the initial capture at R_c to the crossing point R_X . Configuration mixing theories of this direct process are available in the quantal [6] and semiclassical-classical path formulations [7].

Indirect Process. In the three-stage sequence



the so-called *indirect* process might contribute. Here the accelerating electron loses energy by vibrational excitation ($v_i^+ \rightarrow v_f$) of the ion and is then resonantly captured into a Rydberg orbital of the bound molecule AB^* in vibrational level v_f , which then interacts one way (via configuration mixing) with the doubly excited repulsive molecule AB^{**} . The capture initially proceeds via a small effect — vibronic coupling (the matrix element of the nuclear kinetic energy) induced by the breakdown of the Born-Oppenheimer approximation — at certain resonance energies $\varepsilon_n = E(v_f) - E(v_i^+)$ and, in the absence of the direct channel (44.73), would therefore be manifest by a series of characteristic very narrow Lorentz profiles in the cross section. Uncoupled from (44.73) the indirect process would augment the rate. Vibronic capture proceeds more easily when $v_f = v_i^+ + 1$ so that Rydberg states with $n \approx 7 - 9$ would be involved [for $H_2^+(v_i^+ = 0)$] so that the resulting longer periods of the Rydberg electron would permit changes in nuclear motion to compete with the electronic dissociation. Recombination then proceeds as in the second stage of (44.73), i.e., by electronic coupling to the dissociative state d at the crossing point. A multichannel quantum defect theory [8] has combined the direct and indirect mechanisms

Interrupted Recombination. The process

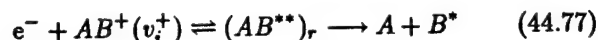


proceeds via the first (dielectronic capture) stage of (44.73) followed by a two-way electronic transition with frequency ν_{dn} and ν_{nd} between the d and n states. All (n, v) Rydberg states can be populated, particularly those in low n and high v since the electronic $d - n$ interaction varies as $n^{-1.5}$ with broad structure. Although the dissociation process proceeds here via a second order effect (ν_{dn} and ν_{nd}), the electronic coupling may dominate the indirect vibronic capture and interrupt the recombination, in contrast to (44.75) which, as written in

the one-way direction, feeds the recombination. Such dip structure has been observed [9].

44.4.2 Quantal Cross Section

The cross section for direct dissociative recombination



of electrons of energy ε , wavenumber k_e and spin statistical weight 2, for a molecular ion $AB^+(v_i^+)$ of electronic statistical weight ω_{AB}^+ in vibrational level v_i^+ is

$$\sigma_{DR}(\varepsilon) = \frac{\pi}{k_e^2} \left(\frac{\omega_{AB}^*}{2\omega^+} \right) |a_Q|^2 = \left(\frac{\hbar^2}{8\pi m_e \varepsilon} \right) \left(\frac{\omega_{AB}^*}{2\omega^+} \right) |a_Q|^2. \quad (44.78)$$

Here ω_{AB}^* is the electronic statistical weight of the dissociative neutral state of AB^* whose potential energy curve V_d crosses the corresponding potential energy curve V^+ of the ionic state. The transition T-matrix element for autoionization of AB^* embedded in the (moving) electronic continuum of $AB^+ + e^-$ is the quantal probability amplitude

$$a_Q(v) = 2\pi \int_0^\infty V_{de}^*(R) [\psi_v^{+*}(R) \psi_d(R)] dR \quad (44.79)$$

for autoionization. Here ψ_v^+ and ψ_d are the nuclear bound and continuum vibrational wavefunctions for AB^+ and AB^* , respectively, while

$$V_{de}(R) = \langle \phi_d | \mathcal{H}_{el}(\mathbf{r}, R(t)) | \phi_e(\mathbf{r}, \mathbf{R}) \rangle_{\mathbf{r}, \hat{\epsilon}} = V_{ed}^*(R) \quad (44.80)$$

are the bound-continuum electronic matrix elements coupling the diabatic electronic bound state wavefunctions $\psi_d(\mathbf{r}, \mathbf{R})$ for AB^* with the electronic continuum state wavefunctions $\phi_e(\mathbf{r}, \mathbf{R})$ for $AB^+ + e^-$. The matrix element is an average over electronic coordinates \mathbf{r} and all directions $\hat{\epsilon}$ of the continuum electron. Both continuum electronic and vibrational wavefunctions are energy normalized (see Sect. 44.8.3), and

$$\Gamma(R) = 2\pi |V_{de}^*(R)|^2 \quad (44.81)$$

is the energy width for autoionization at a given nuclear separation R . Given $\Gamma(R)$ from quantum chemistry codes, the problem reduces to evaluation of continuum vibrational wavefunctions in the presence of autoionization. The rate associated with a Maxwellian distribution of electrons at temperature T is

$$\hat{\alpha} = \bar{v}_e \int \varepsilon \sigma_{DR}(\varepsilon) e^{-\varepsilon/k_B T} d\varepsilon / (k_B T)^2 \quad (44.82)$$

where \bar{v}_e is the mean speed (see Sect. 44.9).

Maximum Cross Section and Rate. Since the probability for recombination must remain less than unity, $|a_Q|^2 \leq 1$ so that the maximum cross section and rates are

$$\sigma_{DR}^{\max}(\epsilon) = \frac{\pi}{k_e^2} \left(\frac{\omega_{AB}^*}{2\omega^+} \right) = \left(\frac{h^2}{8\pi m_e \epsilon} \right) (2\ell + 1), \quad (44.83)$$

where ω_{AB}^* has been replaced by $2(2\ell + 1)\omega^+$ under the assumption that the captured electron is bound in a high level Rydberg state of angular momentum ℓ , and

$$\hat{\alpha}_{\max}(T) = \bar{v}_e \sigma_{DR}^{\max}(\epsilon = k_B T) \quad (44.84a)$$

$$\approx 5 \times 10^{-7} (300/T)^{1/2} (2\ell + 1) \text{ cm}^3/\text{s}. \quad (44.84b)$$

Cross section maxima of $5(2\ell + 1)(300/T) \times 10^{-14} \text{ cm}^2$ are therefore possible, being consistent with the rate (44.84b).

First-Order Quantal Approximation. When the effect of autoionization on the continuum vibrational wavefunction $\psi_d(R)$ for AB^* is ignored, then a first-order undistorted approximation to the quantal amplitude (44.79) is

$$T_B(v^+) = 2\pi \int_0^\infty V_{de}^*(R) [\psi_v^{+*}(R) \psi_d^{(0)}(R)] dR \quad (44.85)$$

where $\psi_d^{(0)}$ is ψ_d in the absence of the back reaction of autoionization. Under this assumption, (44.78) reduces to

$$\sigma_c(\epsilon, v^+) = \frac{\pi}{k_e^2} \left(\frac{\omega_{AB}^*}{2\omega^+} \right) |T_B(v^+)|^2, \quad (44.86)$$

which is then the cross section for initial electron capture since autoionization has been precluded. Although the Born T-matrix (44.85) violates unitarity, the capture cross section (44.86) must remain less than the maximum value

$$\sigma_c^{\max} = \frac{\pi}{k_e^2} \left(\frac{\omega_{AB}^*}{2\omega^+} \right) = \left(\frac{h^2}{8\pi m_e \epsilon} \right) \left(\frac{\omega_{AB}^*}{2\omega^+} \right), \quad (44.87)$$

since $|a_Q|^2 \leq 1$. So as to acknowledge after the fact the effect of autoionization, assumed small, and neglected by (44.85), the DR cross section can be approximated as

$$\sigma_{DR}(\epsilon, v^+) = \sigma_c(\epsilon, v^+) P_S, \quad (44.88)$$

where P_S is the probability of survival against autoionization on the V_d curve until stabilization takes place at some crossing point R_X .

Approximate Capture Cross Section. With the energy-normalized Winans-Stückelberg vibrational wavefunction

$$\psi_d^{(0)}(R) = |V_d'(R)|^{-1/2} \delta(R - R_c), \quad (44.89)$$

where R_c is the classical turning point for $(A - B^*)$ relative motion, (44.86) reduces to

$$\sigma_c(\epsilon, v^+) = \frac{\pi}{k_e^2} \left(\frac{\omega_{AB}^*}{2\omega^+} \right) [2\pi\Gamma(R_c)] \left\{ \frac{|\psi_v^+(R_c)|^2}{|V_d'(R_c)|} \right\} \quad (44.90)$$

where the term inside the braces in (44.90) is the effective Franck-Condon factor.

Six Approximate Stabilization Probabilities.

(1) A unitarized T -matrix is

$$T = \frac{T_B}{1 + \frac{1}{2}|T_B|^2}, \quad (44.91)$$

so that $P_S = |T|^2 / |T_B|^2$ to give

$$\begin{aligned} P_S(\text{low } \epsilon) &= \left[1 + \frac{1}{4}|T_B|^2 \right]^{-2} \\ &= \left\{ 1 + \pi^2 \left| \int_0^\infty V_{de}^*(R) [\psi_v^{+*}(R) \psi_d^{(0)}(R)] dR \right|^2 \right\}^{-2} \end{aligned} \quad (44.92a)$$

which is valid at low ϵ when only one vibrational level v^+ , i.e., the initial level of the ion is repopulated by autoionization.

(2) At higher ϵ , when population of many other ionic levels v_j^+ occurs, then

$$P_S(\epsilon) = \left[1 + \frac{1}{4} \sum_j |T_B(v_j^+)|^2 \right]^{-2}, \quad (44.92b)$$

where the summation is over all the open vibrational levels v_j^+ of the ion. When no intermediate Rydberg $AB^*(v)$ states are energy resonant with the initial $e^- + AB^+(v^+)$ state, i.e., coupling with the indirect mechanism is neglected, then (44.88) with (44.92b) is the direct DR cross section normally calculated.

(3) In the high- ϵ limit when an infinite number of v_j^+ levels are populated following autoionization, the survival probability, with the aid of closure, is then

$$P_S = \left[1 + \pi^2 \int_{R_c}^{R_X} |V_{de}^*(R)|^2 |\psi_d^{(0)}(R)|^2 dR \right]^{-2}. \quad (44.93)$$

(4) On adopting in (44.93) the JWKB semiclassical wavefunction for $\psi_d^{(0)}$, then

$$\begin{aligned} P_S(\text{high } \epsilon) &= \left[1 + \frac{1}{2\hbar} \int_{R_c}^{R_X} \frac{\Gamma(R)}{v(R)} dR \right]^{-2} \\ &= \left[1 + \frac{1}{2} \int_{t_c}^{t_X} \nu_a(t) dt \right]^{-2}, \end{aligned} \quad (44.94)$$

where $v(R)$ is the local radial speed of $A - B$ relative motion, and where the frequency $\nu_a(t)$ of autoionization is Γ/\hbar .

(5) A classical path local approximation for P_S yields

$$P_S = \exp \left(- \int_{t_c}^{t_x} \nu_a(t) dt \right), \quad (44.95)$$

which agrees to first-order for small ν with the expansion of (44.94).

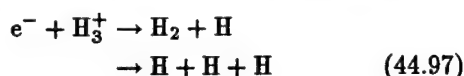
(6) A partitioning of (44.73) yields

$$P_S = \nu_d / (\nu_a + \nu_d) = (1 + \nu_a \tau_d)^{-1}, \quad (44.96)$$

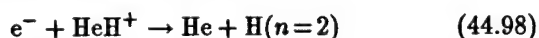
on adopting macroscopic averaged frequencies ν_i and associated lifetimes $\tau_i = \nu_i^{-1}$. The six survival probabilities in (44.92a), (44.92b), (44.93)–(44.96) are all suitable for use in the DR cross section (44.88).

44.4.3 Noncrossing Mechanism

The dissociative recombination (DR) processes



at low electron energy ϵ , and



have spurred renewed theoretical interest because they both proceed at respective rates of $(2 \times 10^{-7} \text{ to } 2 \times 10^{-8}) \text{ cm}^3 \text{ s}^{-1}$ and $10^{-8} \text{ cm}^3 \text{ s}^{-1}$ at 300 K. Such rates are generally associated with the direct DR, which involves favorable curve crossings between the potential energy surfaces, $V^+(R)$ and $V_d(R)$ for the ion AB^+ and neutral dissociative AB^{**} states. The difficulty with (44.97) and (44.98) is that there are no such curve crossings, except at $\epsilon \geq 8 \text{ eV}$ for (44.97). In this instance, the previous standard theories would support only extremely small rates when electronic resonant conditions do not prevail at thermal energies. Theories [10, 11] are currently being developed for application to processes such as (44.97).

44.5 MUTUAL NEUTRALIZATION



Diabatic Potentials. $V_i^{(0)}(R)$ and $V_f^{(0)}(R)$ for initial (ionic) and final (covalent) states are diagonal elements of

$$V_{if}(R) = \langle \Psi_i(\mathbf{r}, R) | \mathcal{H}_{el}(\mathbf{r}, R) | \Psi_f(\mathbf{r}, R) \rangle_r, \quad (44.100)$$

where $\Psi_{i,f}$ are diabatic states and \mathcal{H}_{el} is the electronic Hamiltonian at fixed internuclear distance R .

Adiabatic Potentials for a Two-State System.

$$V^\pm(R) = V_0(R) \pm [\Delta^2(R) + |V_{if}(R)|^2]^{1/2} \quad (44.101a)$$

$$V_0(R) = \frac{1}{2} [V_i^{(0)}(R) + V_f^{(0)}(R)] \quad (44.101b)$$

$$\Delta(R) = [V_i^{(0)}(R) - V_f^{(0)}(R)] \quad (44.101c)$$

For a single crossing of diabatic potentials at R_X then $V_i^{(0)}(R_X) = V_f^{(0)}(R_X)$ and the adiabatic potentials at R_X are,

$$V^\pm(R_X) = V_i^{(0)}(R_X) \pm V_{if}(R_X) \quad (44.102)$$

with energy separation $2V_{if}(R_X)$.

44.5.1 Landau-Zener Probability for Single Crossing at R_X

On assuming $\Delta(R) = (R - R_X)\Delta'(R_X)$, where $\Delta'(R) = d\Delta(R)/dR$, the probability for single crossing is

$$P_{if}(R_X) = \exp [\eta(R_X)/v_X(b)] \quad (44.103a)$$

$$\eta(R_X) = \left(\frac{2\pi}{\hbar} \right) \frac{|V_{if}(R_X)|^2}{\Delta'(R_X)} \quad (44.103b)$$

$$v_X(b) = \left[1 - V_i^{(0)}(R_X)/E - b^2/R_X^2 \right]^{1/2}. \quad (44.103c)$$

Overall Charge-Transfer Probability. From the incoming and outgoing legs of the trajectory,

$$P^X(E) = 2P_{if}(1 - P_{if}). \quad (44.104)$$

44.5.2 Cross Section and Rate Coefficient for Mutual Neutralization

$$\sigma_M(E) = 4\pi \int_0^{b_X} P_{if}(1 - P_{if})b db = \pi b_X^2 P_M, \quad (44.105a)$$

$$\begin{aligned} \pi b_X^2 &= \pi \left[1 - \frac{V_i^{(0)}(R_X)}{E} \right] R_X^2 \\ &= \pi \left[1 + \frac{14.4}{R_X(\text{\AA})E(\text{eV})} \right] R_X^2. \end{aligned} \quad (44.105b)$$

P_M is the b^2 -averaged probability (44.104) for charge-transfer reaction within a sphere of radius R_X .

The rate is

$$\hat{\alpha}_M = (8k_B T / \pi M_{AB})^{1/2} \int_0^\infty \epsilon \sigma_M(\epsilon) e^{-\epsilon} d\epsilon \quad (44.106)$$

where $\epsilon = E/k_B T$.

44.6 ONE-WAY MICROSCOPIC EQUILIBRIUM CURRENT, FLUX, AND PAIR-DISTRIBUTIONS

Notation:

- M reduced mass $M_A M_B / (M_A + M_B)$
 R internal separation of $A - B$
 E orbital energy $\frac{1}{2} M v^2 + V(R)$
 L orbital angular momentum
 L^2 $2MEb^2$ for $E > 0$
 v_R radial speed $|\dot{R}|$
 \bar{v} mean relative speed $(8kT/\pi M_{AB})^{1/2}$
 ϵ normalized energy $E/k_B T$
 n_i pair distribution function $n_i^+ + n_i^-$
 n_i^\pm component of n_i with $\dot{R} > 0$ (+) and $\dot{R} < 0$ (-).

All quantities on the RHS in the expressions (a)–(e) below are to be multiplied by $\tilde{N}_A \tilde{N}_B [\omega_{AB}/\omega_A \omega_B]$ where the ω_i denote the statistical weights of species i which are *not* included by the density of states associated with the E, L^2 orbital degrees of freedom.

Case (a): $|i\rangle \equiv |R, E, L^2\rangle$.

$$\text{Current: } j_i^\pm(R) = n^\pm(R, E, L^2) v_R \equiv n_i^\pm v_R$$

$$\text{Flux: } 4\pi R^2 j_i^\pm(R) dE dL^2 = \frac{4\pi^2 e^{-E/k_B T}}{(2\pi M k_B T)^{3/2}} dE dL^2. \quad (44.107)$$

This flux is independent of R . For dissociated pairs $E > 0$,

$$4\pi R^2 j_i^\pm(R) dE dL^2 = [\bar{v} \epsilon e^{-\epsilon} d\epsilon] [2\pi b db]. \quad (44.108)$$

$$\begin{aligned} (R, E, L^2) - \text{Distribution: } n(R, E, L^2) dR dE dL^2 \\ = \frac{(8\pi^2/v_R) e^{-E/k_B T}}{(2\pi M k_B T)^{3/2}} \left(\frac{dR}{4\pi R^2} \right) dE dL^2. \end{aligned} \quad (44.109)$$

Case (b): $|i\rangle \equiv |R, E\rangle$; L^2 -integrated quantities.

$$\text{Current: } j_i^\pm(R) = \frac{1}{2} v n^\pm(R, E) \equiv \frac{1}{2} v n_i^\pm, \quad (44.110)$$

$$\text{Flux: } 4\pi R^2 j_i^\pm(R) dE = [\bar{v} \epsilon e^{-\epsilon} d\epsilon] \pi b_0^2, \quad (44.111a)$$

$$\pi b_0^2 = \pi R^2 [1 - V(R)/E], \quad (44.111b)$$

(R, E)-Distribution:

$$\begin{aligned} n(R, E) dR dE &= \frac{2}{\sqrt{\pi}} \left[\frac{E - V(R)}{k_B T} \right]^{1/2} e^{-\epsilon} d\epsilon dR \\ &\equiv G_{MB}(E, R) dR, \end{aligned} \quad (44.112)$$

which defines the *Maxwell-Boltzmann velocity distribution* G_{MB} in the presence of the field $V(R)$.

Case (c): (E, L^2)-integrated quantities.

$$\text{Current: } j^\pm(R) = \frac{1}{4} \bar{v} e^{-V(R)/k_B T}, \quad (44.113)$$

$$\text{Flux: } 4\pi R^2 j^\pm(R) = \pi R^2 \bar{v} e^{-V(R)/k_B T}, \quad (44.114)$$

$$\text{Distribution: } n(R) = e^{-V(R)/k_B T}. \quad (44.115)$$

When E -integration is only over dissociated states ($E > 0$), the above quantities are

$$j_d^\pm(R) = \frac{1}{4} \bar{v} [1 - V(R)/k_B T], \quad (44.116)$$

$$4\pi R^2 j_d^\pm(R) = \pi R^2 \left[1 - \frac{V(R)}{k_B T} \right] \bar{v} \equiv \pi b_{\max}^2 \bar{v}, \quad (44.117)$$

$$n(R) = [1 - V(R)/k_B T]. \quad (44.118)$$

Case (d): (E, L^2)-Distribution. For Bound Levels

$$n(E, L^2) dE dL^2 = \frac{4\pi^2 \tau_R(E, L)}{(2\pi M k_B T)^{3/2}} e^{-E/k_B T} dE dL^2, \quad (44.119)$$

where $\tau_R = \oint dt = (\partial J_R / \partial E)$ is the period for bounded radial motion of energy E and radial action $J_R(E, L) = M \oint v_R dR$.

Case (e): E -Distribution. For bound levels

$$n(E) dE = \frac{2e^{-\epsilon}}{\sqrt{\pi}} d\epsilon \int_0^{R_A} \left(\frac{E - V}{k_B T} \right)^{1/2} dR, \quad (44.120)$$

where R_A is the turning point $E = V(R_A)$.

Example: For electron-ion bounded motion, $V(R) = -Ze^2/R$, $R_A = Ze^2/|E|$, $R_e = Ze^2/k_B T$, $\epsilon = E/k_B T$. Then $\tau_R = 2\pi(m/Ze^2)^{1/2} (R_A/2)^{3/2}$,

$$\int_0^{R_A} \left[\frac{R_e}{R} - |\epsilon| \right]^{1/2} dR = \frac{\pi^2}{4} R_A^{5/2} R_e^{1/2}, \quad (44.121)$$

and

$$n^*(E) dE = \left[\frac{2e^{-\epsilon}}{\sqrt{\pi}} d\epsilon \right] \frac{\pi^2}{4} R_A^{5/2} R_e^{1/2} \quad (44.122)$$

$$= \left[\frac{2e^{-\epsilon}}{\sqrt{\pi}} d\epsilon \right] \left(\frac{\pi^2 R_e^3}{4 |\epsilon|^{5/2}} \right). \quad (44.123)$$

For closely spaced levels in a hydrogenic $e^- - A^{Z+}$ system,

$$n^*(p, \ell) = n(E, L^2) \left(\frac{dE}{dp} \right) \left(\frac{dL^2}{d\ell} \right) \quad (44.124a)$$

$$n^*(p) = n(E) \left(\frac{dE}{dp} \right). \quad (44.124b)$$

Using $E = -(2p^2)^{-1} (Z^2 e^2 / a_0)$ and $L^2 = (\ell + 1/2)^2 \hbar^2$ for level (p, ℓ) then

$$\tau_R(E, L) \frac{dE}{dp} \left[\frac{dL^2}{d\ell} \right] = \left[\frac{dJ_R}{dp} \right] \left[\frac{dL^2}{d\ell} \right] \quad (44.125)$$

$$= h [(2\ell + 1) \hbar^2] \quad (44.126)$$

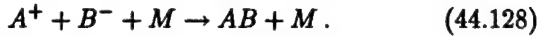
$$\frac{n^*(p, \ell)}{n_e N^+} = \frac{2(2\ell + 1)}{2\omega_A^+} \frac{h^3}{(2\pi m_e k_B T)^{3/2}} e^{I_p/k_B T}, \quad (44.127a)$$

$$\frac{n^*(p)}{n_e N^+} = \frac{2p^2}{2\omega_A^+} \frac{h^3}{(2\pi m_e k_B T)^{3/2}} e^{I_p/k_B T}, \quad (44.127b)$$

in agreement with the Saha ionization formula (44.16) where N^+ is the equilibrium concentration of A^{Z+} ions in their ground electronic states. The spin statistical weights are $\omega_{eA} = \omega_e = 2$.

44.7 MICROSCOPIC METHODS FOR TERMOLECULAR ION-ION RECOMBINATION

At low gas density, the basic process



is characterized by nonequilibrium with respect to E . Dissociated and bound A^+-B^- ion pairs are in equilibrium with respect to their separation R , but bound pairs are *not* in E -equilibrium with each other. L^2 -equilibrium can be assumed for ion-ion recombination but *not* for ion-atom association reactions.

At higher gas densities N , there is non-equilibrium in the ion-pair distributions with respect to R , E and L^2 . In the limit of high N , there is only non-equilibrium with respect to R . See the appropriate reference list for full details of theory.

44.7.1 Time Dependent Method: Low Gas Density

Energy levels E_i of A^+-B^- pairs are so close that they form a quasi-continuum with a nonequilibrium distribution over E_i determined by the *master equation*

$$\frac{dn_i(t)}{dt} = \int_{-D}^{\infty} (n_i \nu_{if} - n_f \nu_{fi}) dE_f, \quad (44.129)$$

where $n_i dE_i$ is the number density of pairs in the interval dE_i about E_i , and $\nu_{if} dE_f$ is the frequency of i -pair collisions with M that change the i -pair orbital energy from E_i to between E_f and $E_f + dE_f$. The greatest binding energy of the A^+-B^- pair is D .

Association Rate.

$$R^A(t) = \int_{-D}^{\infty} P_i^S \left(\frac{dn_i}{dt} \right) dE_i \quad (44.130a)$$

$$= \hat{\alpha} N_A(t) N_B(t) - k n_s(t), \quad (44.130b)$$

where P_i^S is the probability for collisional stabilization (recombination) of i -pairs via a sequence of energy changing collisions with M . The coefficients for $C \rightarrow S$ recombination out of the C -block with ion concentrations

$N_A(t)$, $N_B(t)$ (in cm^{-3}) into the S block of total ion-pair concentrations $n_s(t)$ and for $S \rightarrow C$ dissociation are $\hat{\alpha}$ ($\text{cm}^3 \text{s}^{-1}$) and k (s^{-1}), respectively.

One-Way Equilibrium Collisional Rate and Detailed Balance.

$$C_{if} = \tilde{n}_i \nu_{if} = \tilde{n}_f \nu_{fi} = C_{fi}, \quad (44.131)$$

where the tilde denotes equilibrium (Saha) distributions.

Normalized Distribution Functions.

$$\gamma_i(t) = n_i(t)/\tilde{n}_i^S, \quad \gamma_s(t) = n_s(t)/\tilde{n}_s^B(t), \quad (44.132)$$

$$\gamma_c(t) = N_A(t) N_B(t) / \tilde{N}_A \tilde{N}_B, \quad (44.133)$$

where \tilde{n}_i^S and \tilde{n}^B are the Saha and Boltzmann distributions.

Master Equation for $\gamma_i(t)$.

$$\frac{d\gamma_i(t)}{dt} = - \int_{-D}^{\infty} [\gamma_i(t) - \gamma_f(t)] \nu_{if} dE_f. \quad (44.134)$$

Quasi-Steady State (QSS) Reduction. Set

$$\gamma_i(t) = P_i^D \gamma_c(t) + P_i^S \gamma_s(t) \xrightarrow{t \rightarrow \infty} 1 \quad (44.135)$$

where P_i^D and P_i^S are the respective time-independent portions of the normalized distribution γ_i which originate, respectively, from blocks C and S . The energy separation between the C and S blocks is so large that $P_i^S = 0$ ($E_i \geq 0$, C block), $P_i^S \leq 1$ ($0 > E_i \geq -S$, \mathcal{E} block), $P_i^S = 1$ ($-S \geq E_i \geq -D$, S block). Since $P_i^S + P_i^D = 1$, then

$$\frac{d\gamma_i(t)}{dt} = - [\gamma_c(t) - \gamma_s(t)] \int_{-D}^{\infty} (P_i^D - P_f^D) C_{if} dE_f. \quad (44.136)$$

Recombination and Dissociation Coefficients.

Equation (44.135) in (44.130a) enables the recombination rate in (44.130b) to be written as

$$\hat{\alpha} \tilde{N}_A \tilde{N}_B = \int_{-D}^{\infty} P_i^D dE_i \int_{-D}^{\infty} (P_i^D - P_f^D) C_{if} dE_f. \quad (44.137)$$

The QSS condition ($dn_i/dt = 0$ in block \mathcal{E}) is then

$$P_i^D \int_{-D}^{\infty} \nu_{if} dE_f = \int_{-D}^E \nu_{if} P_f^D dE_f, \quad (44.138)$$

which involves only *time independent* quantities. Under QSS, (44.137) reduces to the net downward current across bound level $-E$,

$$\hat{\alpha} \tilde{N}_A \tilde{N}_B = \int_{-E}^{\infty} dE_i \int_{-D}^{-E} (P_i^D - P_f^D) C_{if} dE_f, \quad (44.139)$$

which is independent of the energy level ($-E$) in the range $0 \geq -E \geq -S$ of block \mathcal{E} .

The dissociation frequency k in (44.130b) is

$$k\tilde{n}_s = \int_{-D}^{-E} dE_i \int_{-E}^{\infty} (P_i^S - P_f^S) C_{if} dE_f, \quad (44.140)$$

and macroscopic detailed balance $\hat{\alpha}\tilde{N}_A\tilde{N}_B = k\tilde{n}_s$ is automatically satisfied. $\hat{\alpha}$ is the direct ($\mathcal{C} \rightarrow \mathcal{S}$) collisional contribution (small) plus the (much larger) net collisional cascade downward contribution from that fraction of bound levels which originated in the continuum \mathcal{C} . k_d is the direct dissociation frequency (small) plus the net collisional cascade upward contribution from that fraction of bound levels which originated in block \mathcal{S} .

44.7.2 Time Independent Methods: Low Gas Density

QSS-Rate. Since recombination and dissociation (ionization) involve only that fraction of the bound state population which originated from the \mathcal{C} and \mathcal{S} blocks, respectively, recombination can be viewed as time independent with

$$N_A N_B = \tilde{N}_A \tilde{N}_B, \quad n_s(t) = 0, \quad (44.141a)$$

$$\rho_i = n_i / \tilde{n}_i \equiv P_i^D \quad (44.141b)$$

$$\hat{\alpha}\tilde{N}_A\tilde{N}_B = \int_{-E}^{\infty} dE_i \int_{-D}^{-E} (\rho_i - \rho_f) C_{if} dE_f. \quad (44.141c)$$

QSS Integral Equation.

$$\rho_i \int_{-D}^{\infty} \nu_{if} dE_f = \int_{-S}^{\infty} \rho_f \nu_{if} dE_f \quad (44.142)$$

is solved subject to the boundary condition

$$\rho_i = 1 (E_i \geq 0), \quad \rho_i = 0 (-S \geq E_i \geq -D). \quad (44.143)$$

Collisional Energy-Change Moments.

$$D_i^{(m)}(E_i) = \frac{1}{m!} \int_{-D}^{\infty} (E_f - E_i)^m C_{if} dE_f, \quad (44.144)$$

$$D_i^{(m)} = \frac{1}{m!} \frac{d}{dt} \langle (\Delta E)^m \rangle. \quad (44.145)$$

Averaged Energy-Change Frequency. For an equilibrium distribution \tilde{n}_i of E_i -pairs per unit interval dE_i per second,

$$D_i^{(1)} = \frac{d}{dt} \langle \Delta E \rangle.$$

Averaged Energy-Change per Collision.

$$D_i^{(1)} = D_i^{(1)} / D_i^{(0)}.$$

Time Independent Dissociation. The time independent picture corresponds to

$$n_s(t) = \tilde{n}_s, \quad \gamma_c(t) = 0, \quad \rho_i = n_i / \tilde{n}_i \equiv P_i^S, \quad (44.146)$$

in analogy to the macroscopic reduction of (44.38ab).

Variational Principle

The QSS-condition (44.135) implies that the fraction P_i^D of bound levels i with precursor \mathcal{C} are so distributed over i that (44.137) for $\hat{\alpha}$ is a minimum. Hence P_i^D or ρ_i are obtained either from the solution of (44.142) or from minimizing the *variational functional*

$$\hat{\alpha}\tilde{N}_A\tilde{N}_B = \int_{-D}^{\infty} n_i dE_i \int_{-D}^{\infty} (\rho_i - \rho_f) \nu_{if} dE_f \quad (44.147a)$$

$$= \frac{1}{2} \int_{-D}^{\infty} dE_i \int_{-D}^{\infty} (\rho_i - \rho_f)^2 C_{if} dE_f \quad (44.147b)$$

with respect to variational parameters contained in a trial analytic expression for ρ_i . Minimization of the quadratic functional (44.147b) has an analogy with the *principle of least dissipation* in the theory of electrical networks.

Diffusion-in-Energy-Space Method

Integral Equation (44.142) can be expanded in terms of energy-change moments, via a Fokker-Planck analysis to yield the differential equation

$$\frac{\partial}{\partial E_i} \left[D_i^{(2)} \frac{\partial \rho_i}{\partial E_i} \right] = 0, \quad (44.148)$$

with the QSS analytical solution

$$\rho_i(E_i) = \left[\int_{E_i}^0 \frac{dE}{D^{(2)}(E)} \right] \left[\int_{-S}^0 \frac{dE}{D^{(2)}(E)} \right]^{-1} \quad (44.149)$$

of Pitaevskii [4] for ($e^- + A^+ + M$) recombination where collisional energy changes are small. This distribution does not satisfy the exact QSS condition (44.142). When inserted in the exact non-QSS rate (44.147b), highly accurate $\hat{\alpha}$ for heavy-particle recombination are obtained.

Bottleneck Method

The one-way equilibrium rate ($\text{cm}^{-3} \text{s}^{-1}$) across $-E$, i.e., Eq. (44.141c) with $\rho_i = 1$ and $\rho_f = 0$, is

$$\hat{\alpha}(-E)\tilde{N}_A\tilde{N}_B = \int_{-E}^{\infty} dE_i \int_{-D}^{-E} C_{if} dE_f. \quad (44.150)$$

This is an upper limit to (44.141c) and exhibits a minimum at $-E^*$, the *bottleneck location*. The least upper limit to $\hat{\alpha}$ is then $\hat{\alpha}(-E^*)$.

Trapping Radius Method

Assume that pairs with internal separation $R \leq R_T$ recombine with unit probability so that the one-way equilibrium rate across the dissociation limit at $E = 0$ for these pairs is

$$\hat{\alpha}(R_T) \tilde{N}_A \tilde{N}_B = \int_0^{R_T} dR \int_{V(R)}^0 C_{if}(R) dE_f, \quad (44.151)$$

where $V(R) = -e^2/R$, and $C_{if}(R) = \tilde{n}_i(R) \nu_{if}(R)$ is the rate per unit interval $(dR dE_i) dE_f$ for the $E_i \rightarrow E_f$ collisional transitions at fixed R in

$$(A^+ - B^-)_{E_i, R} + M \rightarrow (A^+ - B^-)_{E_f, R} + M. \quad (44.152)$$

The concentration (cm^{-3}) of pairs with internal separation R and orbital energy E_i in the interval $dR dE_i$ about (R, E_i) is $\tilde{n}_i(R) dR dE_i$. Agreement with the Exact treatment is found by assigning $R_T = (0.48 - 0.55)(e^2/k_B T)$ for the recombination of equal mass ions in an equal mass gas for various ion-neutral interactions. For further details on the above methods, see the appropriate references on termolecular recombination in Sect. 44.10.

44.7.3 Recombination at Higher Gas Densities

As the density N of the gas M is raised, the recombination rate $\hat{\alpha}$ increases initially as N to such an extent that there are increasingly more pairs $n_i^-(R, E)$ in a state of contraction in R than there are those $n_i^+(R, E)$ in a state of expansion; i.e., the ion-pair distribution densities $n_i^\pm(R, E)$ per unit interval $dE dR$ are not in equilibrium with respect to R in blocks \mathcal{C} and \mathcal{E} . Those in the highly excited block \mathcal{E} in addition are not in equilibrium with respect to energy E . Basic sets of coupled master equations have been developed [12] for the microscopic nonequilibrium distributions $n^\pm(R, E, L^2)$ and $n^\pm(R, E)$ of expanding (+) and contracting (-) pairs with respect to A - B separation R , orbital energy E and orbital angular momentum L^2 .

With $n(R, E_i, L_i^2) \equiv n_i(R)$, and using the notation defined at the beginning of Sect. 44.6, the distinct regimes for the master equations discussed in Sect. 44.7.4 are:

Low N	Equilibrium in R , but not in E, L^2 → master equation for $n(E, L^2)$.
For Pure Coul. attraction	Equilibrium in L^2 → master equation for $n(E)$.
High N	Nonequilibrium in R, E, L^2 → master equation for $n_i^\pm(R)$.
Highest N	Equilibrium in (E, L^2) but not in R → macroscopic transport equation (44.56a) in $n(R)$.

Normalized Distributions

For a state $|i\rangle \equiv |E, L^2\rangle$,

$$\rho_i(R) = \frac{n_i(R)}{\tilde{n}_i(R)}, \quad \rho_i^\pm(R) = \frac{n_i^\pm(R)}{\tilde{n}_i^\pm(R)}, \quad (44.153)$$

$$\rho_i(R) = \frac{1}{2}(\rho_i^+ + \rho_i^-).$$

Orbital Energy and Angular Momentum.

$$E_i = \frac{1}{2} M_{AB} v^2 + V(R) \quad (44.154a)$$

$$E_i = \frac{1}{2} M_{AB} v_R^2 + V_i(R) \quad (44.154b)$$

$$V_i(R) = V(R) + \frac{L_i^2}{2M_{AB}R^2} \quad (44.154c)$$

$$L_i = |\mathbf{R} \times M_{AB} \mathbf{v}|, \quad L_i^2 = (2M_{AB}E_i)b^2, \quad E_i > 0. \quad (44.154d)$$

Maximum Orbital Angular Momenta.

(1) A specified separation R can be accessed by all orbits of energy E_i with L_i^2 between 0 and

$$L_{im}^2(E_i, R) = 2M_{AB}R^2[E_i - V(R)]. \quad (44.155a)$$

(2) Bounded orbits of energy $E_i < 0$ can have L_i^2 between 0 and

$$L_{ic}^2(E_i) = 2M_{AB}R_c^2[E_i - V(R_c)], \quad (44.155b)$$

where R_c is the radius of the circular orbit determined by $\partial V_i / \partial R = 0$, i.e., by $E_i = V(R_c) + \frac{1}{2}R_c(\partial V / \partial R)_{R_c}$.

44.7.4 Master Equations

Master Equation for $n_i^\pm(R) \equiv n^\pm(R, E_i, L_i^2)$. [12]

$$\begin{aligned} & \pm \frac{1}{R^2} \frac{\partial}{\partial R} [R^2 n_i^\pm(R) |v_R|]_{E_i, L_i^2} \\ &= - \int_{V(R)}^\infty dE_f \int_0^{L_{jm}^2} dL_f^2 [n_i^\pm(R) \nu_{if}(R) \\ & \quad - n_f^\pm(R) \nu_{fi}(R)]. \end{aligned} \quad (44.156)$$

The set of master equations for n_i^+ is coupled to the n_i^- set by the boundary conditions $n_i^-(R_i^+) = n_i^+(R_i^+)$ at the pericenter R_i^- for all E_i and apocenter R_i^+ for $E_i < 0$ of the E_i, L_i^2 -orbit.

Master Equations for Normalized Distributions. [12]

$$\begin{aligned} \pm |v_R| \frac{\partial \rho_i^\pm}{\partial R} &= - \int_{V(R)}^\infty dE_f \int_0^{L_{jm}^2} dL_f^2 \\ & \quad \times [\rho_i^\pm(R) - \rho_f^\pm(R)] \nu_{if}(R). \end{aligned} \quad (44.157)$$

Corresponding Master equations for the L^2 integrated distributions $n^\pm(R, E)$ and $\rho^\pm(R, E)$ have been derived [12].

Continuity Equations.

$$J_i = [n_i^+(R) - n_i^-(R)] |v_R| = [\rho_i^+ - \rho_i^-] \tilde{j}_i^\pm \quad (44.158)$$

$$\begin{aligned} \frac{1}{R^2} \frac{\partial}{\partial R} (R^2 J_i) = & - \int_{V(R)}^\infty dE_f \int_0^{L_{jm}^2} dL_f^2 \\ & \times [n_i(R) \nu_{if}(R) - n_f(R) \nu_{fi}(R)], \end{aligned} \quad (44.159)$$

$$\begin{aligned} \frac{1}{2} |v_R| \frac{\partial [\rho_i^+(R) - \rho_i^-(R)]}{\partial R} = & - \int_{V(R)}^\infty dE_f \int_0^{L_{jm}^2} dL_f^2 \\ & \times [\rho_i(R) - \rho_f(R)] \nu_{if}(R). \end{aligned} \quad (44.160)$$

44.7.5 Recombination Rate

Flux Representation.

The $R_0 \rightarrow \infty$ limit of

$$\hat{\alpha} \tilde{N}_A \tilde{N}_B = -4\pi R_0^2 J(R_0) \quad (44.161)$$

has the microscopic generalization

$$\begin{aligned} \hat{\alpha} \tilde{N}_A \tilde{N}_B = & \int_{V(R_0)}^\infty dE_i \int_0^{L_{ic}^2} dL_i^2 [4\pi R_0^2 \tilde{j}_i^\pm(R_0)] \\ & \times [\rho_i^-(R_0) - \rho_i^+(R_0)], \end{aligned} \quad (44.162)$$

where L_{ic}^2 is given by (44.155b) with $R_c = R_0$ for bound states and is infinite for dissociated states, and where

$$\rho_i^-(R_0) - \rho_i^+(R_0) = \oint_{R_i}^{R_0} \rho_i(R) [\nu_i^b(R) + \nu_i^c(R)] dt, \quad (44.163)$$

with

$$\begin{aligned} \rho_i(R) \nu_i^b(R) = & \int_{V(R)}^{V(R_0)} dE_f \int_0^{L_{jm}^2} dL_f^2 [\rho_i(R) - \rho_f(R)] \\ & \times \nu_{if}(R), \end{aligned} \quad (44.164a)$$

$$\begin{aligned} \rho_i(R) \nu_i^c(R) = & \int_{V(R_0)}^\infty dE_f \int_0^{L_{jm}^2} dL_f^2 [\rho_i(R) - \rho_f(R)] \\ & \times \nu_{if}(R). \end{aligned} \quad (44.164b)$$

Collisional Representation.

$$\begin{aligned} \hat{\alpha} \tilde{N}_A \tilde{N}_B = & \int_{V(R_0)}^\infty dE_i \int_0^{L_{ic}^2} dL_i^2 \int_{R_i}^{R_0} \tilde{n}_i(R) dR \\ & \times [\rho_i(R) \nu_i^b(R)], \end{aligned} \quad (44.165)$$

which is the microscopic generalization of the macroscopic result $\hat{\alpha} = K \rho^* \nu_s = \alpha_{RN}(R_0) \rho(R_0)$.

The flux for dissociated pairs $E_i > 0$ is

$$4\pi R^2 |v_R| \tilde{n}_i^\pm(R) dE dL^2 = [\bar{v} \epsilon e^{-\epsilon} d\epsilon] [2\pi b db] \tilde{N}_A \tilde{N}_B, \quad (44.166)$$

so the rate (44.165) as $R_0 \rightarrow \infty$ is

$$\hat{\alpha} = \bar{v} \int_0^\infty \epsilon e^{-\epsilon} d\epsilon \int_0^{b_0} 2\pi b db \oint_{R_i}^{R_0} \rho_i(R) \nu_i^b(R) dt, \quad (44.167)$$

which is the microscopic generalization (44.45b) of the macroscopic result $\hat{\alpha} = k_c P^S$ of (44.44).

Reaction Rate $\alpha_{RN}(R_0)$: On solving (44.157) subject to $\rho(R_0) = 1$, then according to (44.56b), $\hat{\alpha}$ determined by (44.162) is the rate $\hat{\alpha}_{RN}$ of recombination within the $(A - B)$ sphere of radius R_0 . The overall rate of recombination $\hat{\alpha}$ is then given by the full diffusional-drift reaction rate (44.59b) where the rate of transport to R_0 is determined uniquely by (44.60).

For development of theory and computer simulations, see the appropriate reference list on Termolecular Ion-Ion Recombination: Theory and Simulations, respectively.

44.8 RADIATIVE RECOMBINATION

In the radiative recombination (RR) process

$$e^-(E, \ell') + A^{Z+}(c) \rightarrow A^{(Z-1)+}(c, n\ell) + h\nu, \quad (44.168)$$

the accelerating electron e^- with energy and angular momentum (E, ℓ') is captured, via coupling with the weak quantum electrodynamical interaction $(e/mc)\mathbf{A} \cdot \mathbf{p}$ associated with the electromagnetic field of the moving ion, into an excited state $n\ell$ with binding energy $I_{n\ell}$ about the parent ion A^{Z+} (initially in an electronic state c). The simultaneously emitted photon carries away the excess energy $h\nu = E + I_{n\ell}$ and angular momentum difference between the initial and final electronic states. The cross section $\sigma_R^{n\ell}(E)$ for RR is calculated (a) from the Einstein A coefficient for free-bound transitions or (b) from the cross section $\sigma_I^{n\ell}(h\nu)$ for photoionization (PI) via the detailed balance (DB) relationship appropriate to (44.168).

The rates $\langle v_e \sigma_R \rangle$ and averaged cross sections $\langle \sigma_R \rangle$ for a Maxwellian distribution of electron speeds v_e are then determined from either

$$\hat{\alpha}_R^{n\ell}(T_e) = \bar{v}_e \int_0^\infty \epsilon \sigma_R^{n\ell}(\epsilon) \exp(-\epsilon) d\epsilon = \bar{v}_e \langle \sigma_R^{n\ell}(T_e) \rangle, \quad (44.169)$$

where $\epsilon = E/k_B T_e$, or from the Milne DB relation (44.243) between the forward and reverse macroscopic rates of (44.168). Using the hydrogenic semiclassical

σ_I^n of Kramers [13], together with an asymptotic expansion [14] for the g -factor of Gaunt [15], the quantum/semiclassical cross section ratio in (44.249), Seaton [16] calculated $\hat{\alpha}_R^{n\ell}$.

The rate of electron energy loss in RR is

$$\left\langle \frac{dE}{dt} \right\rangle_{n\ell} = n_e \bar{v}_e (k_B T_e) \int_0^\infty \epsilon^2 \sigma_R^{n\ell}(\epsilon) e^{-\epsilon} d\epsilon, \quad (44.170)$$

and the radiated power produced in RR is

$$\left\langle \frac{d(h\nu)}{dt} \right\rangle_{n\ell} = n_e \bar{v}_e \int_0^\infty \epsilon h\nu \sigma_R^{n\ell}(\epsilon) e^{-\epsilon} d\epsilon \quad (44.171)$$

Standard Conversions

$$E = p_e^2/2m = \hbar^2 k_e^2/2m = k_e^2 a_0^2 (e^2/2a_0) \quad (44.172a)$$

$$= \kappa^2 (Z^2 e^2/2a_0) = \epsilon (Z^2 e^2/2a_0), \quad (44.172b)$$

$$E_\nu = h\nu = \hbar\omega = \hbar k_\nu c = (I_n + E) \quad (44.172c)$$

$$\equiv [1 + n^2 \epsilon] (Z^2 e^2/2n^2 a_0), \quad (44.172d)$$

$$h\nu/I_n = 1 + n^2 \epsilon, \quad k_e^2 a_0^2 = 2E/(e^2/a_0), \quad (44.172e)$$

$$k_\nu a_0 = (h\nu)\alpha/(e^2/a_0), \quad (44.172f)$$

$$k_\nu^2/k_e^2 = (h\nu)^2/(2Emc^2) \quad (44.172g)$$

$$= \alpha^2 (h\nu)^2 / [2E(e^2/a_0)], \quad (44.172h)$$

$$I_H = e^2/2a_0, \quad \alpha = e^2/\hbar c = 1/137.0359895$$

$$\alpha^{-2} = mc^2/(e^2/a_0), \quad I_n = (Z^2/n^2)I_H. \quad (44.172i)$$

The electron and photon wavenumbers are k_e and k_ν , respectively.

44.8.1 Detailed Balance and Recombination-Ionization Cross Sections

Cross sections $\sigma_R^{n\ell}(E)$ and $\sigma_I^{n\ell}(h\nu)$ for radiative recombination (RR) into and photoionization (PI) out of level $n\ell$ of atom A are interrelated by the *detailed balance* relation

$$g_e g_A^+ k_e^2 \sigma_R^{n\ell}(E) = g_\nu g_A k_\nu^2 \sigma_I^{n\ell}(h\nu), \quad (44.173)$$

where $g_e = g_\nu = 2$. Electronic Statistical weights of A and A^+ are g_A and g_A^+ , respectively. Thus, using Eq. (44.172g) for k_ν^2/k_e^2 ,

$$\sigma_R^{n\ell}(E) = \left(\frac{g_A}{2g_A^+} \right) \left[\frac{(h\nu)^2}{Emc^2} \right] \sigma_I^{n\ell}(h\nu). \quad (44.174)$$

The statistical factors are:

(a) For $(A^+ + e^-)$ state $c[S_c, L_c; \epsilon, \ell', m']$:

$$g_A^+ = (2S_c + 1)(2L_c + 1).$$

(b) For $A(n\ell)$ state $b[S_c, L_c; n, \ell]SL$:

$$g_A = (2S + 1)(2L + 1).$$

(c) For $n\ell$ electron outside a closed shell:

$$g_A^+ = 1, g_A = 2(2\ell + 1).$$

Cross sections are averaged over initial and summed over final degenerate states. For case (c),

$$\sigma_I^n = \frac{1}{n^2} \sum_{\ell=0}^{n-1} (2\ell + 1) \sigma_I^{n\ell}; \quad (44.175a)$$

$$\sigma_R^n = \sum_{\ell=0}^{n-1} 2(2\ell + 1) \sigma_R^{n\ell}. \quad (44.175b)$$

44.8.2 Kramers Cross Sections, Rates, Electron Energy-Loss Rates and Radiated Power for Hydrogenic Systems

These are all calculated from application of detailed balance (44.173) to the original $\sigma_I^n(h\nu)$ of Kramers [13].

Semiclassical (Kramers) Cross Sections

For hydrogenic systems,

$$I_n = \frac{Z^2 e^2}{2n^2 a_0}, \quad h\nu = I_n + E. \quad (44.176)$$

The results below are expressed in terms of the quantities

$$b_n = \frac{I_n}{k_B T_e} \quad (44.177)$$

$$\sigma_{I0}^n = \frac{64\pi a_0^2 \alpha}{3\sqrt{3}} \left(\frac{n}{Z^2} \right) = 7.907071 \times 10^{-18} (n/Z^2) \text{ cm}^2, \quad (44.178)$$

$$\sigma_{R0}(E) = \left(\frac{8\pi a_0^2 \alpha^3}{3\sqrt{3}} \right) \frac{(Z^2 e^2/a_0)}{E}, \quad (44.179)$$

$$\hat{\alpha}_0(T_e) = \bar{v}_e \left(\frac{8\pi a_0^2 \alpha^3}{3\sqrt{3}} \right) \frac{(Z^2 e^2/a_0)}{k_B T_e} \quad (44.180)$$

PI and RR Cross Sections for Level n . In the Kramer (K) semiclassical approximation,

$$\kappa \sigma_I^n(h\nu) = \left(\frac{I_n}{h\nu} \right)^3 \sigma_{I0}^n = \kappa \sigma_I^{n\ell}(h\nu) \quad (44.181)$$

$$\kappa \sigma_R^n(E) = \sigma_{R0}(E) \left(\frac{2}{n} \right) \left(\frac{I_n}{I_n + E} \right) = 3.897 \times 10^{-20} [n\epsilon(13.606 + n^2 \epsilon^2)]^{-1} \text{ cm}^2, \quad (44.182)$$

where ϵ is in units of eV and is given by

$$\epsilon = E/Z^2 \equiv (2.585 \times 10^{-2}/Z^2) (T_e/300). \quad (44.183)$$

Equation (44.182) illustrates that RR into low n at low E is favored.

Cross Section for RR into Level $n\ell$.

$$\kappa \sigma_R^{n\ell} = [(2\ell + 1)/n^2] \kappa \sigma_R^n. \quad (44.184)$$

Rate for RR into Level n .

$$\hat{\alpha}_R^n(T_e) = \hat{\alpha}_0(T_e) (2/n) b_n e^{b_n} E_1(b_n), \quad (44.185a)$$

which tends for large b_n (i.e. $k_B T_e \ll I_n$) to

$$\begin{aligned} \hat{\alpha}_R^n(T_e \rightarrow 0) &= \hat{\alpha}_0(T_e) (2/n) \\ &\times [1 - b_n^{-1} + 2b_n^{-2} - 6b_n^{-3} + \dots]. \end{aligned} \quad (44.185b)$$

The Kramers cross section for photoionization at threshold is σ_{R0}^n and

$$\sigma_{R0}^n = 2\sigma_{R0}/n; \quad \hat{\alpha}_0^n = 2\hat{\alpha}_0/n \quad (44.186)$$

provide the corresponding Kramers cross section and rate for recombination as $E \rightarrow 0$ and $T_e \rightarrow 0$, respectively.

RR Cross Sections and Rates into all Levels $n \geq n_f$.

$$\begin{aligned} \sigma_R^T(E) &= \int_{n_f}^{\infty} \sigma_R^n(E) dn \\ &= \sigma_{R0}(E) \ln(1 + I_f/E), \end{aligned} \quad (44.187a)$$

$$\hat{\alpha}_R^T(T_e) = \hat{\alpha}_0(T_e) [\gamma + \ln b_f + e^{b_f} E_1(b_f)] \quad (44.187b)$$

Useful Integrals.

$$\int_0^{\infty} e^{-x} \ln x dx = \gamma \quad (44.188a)$$

$$\int_b^{\infty} x^{-1} e^{-x} dx = E_1(b) \quad (44.188b)$$

$$\int_0^b e^x E_1(x) dx = \gamma + \ln b + e^b E_1(b) \quad (44.188c)$$

$$\int_0^b [1 - x e^x E_1(x)] dx = \gamma + \ln b + e^b (1 - b) E_1(b) \quad (44.188d)$$

where $\gamma = 0.5772157$ is Euler's constant, and $E_1(b)$ is the first exponential integral such that

$$b e^b E_1(b) \xrightarrow{b \gg 1} 1 - b^{-1} + 2b^{-2} - 6b^{-3} + 24b^{-4} + \dots \quad (44.188e)$$

Electron Energy Loss Rate

Energy Loss Rate for RR into Level n .

$$\left\langle \frac{dE}{dt} \right\rangle_n = n_e \hat{\alpha}_R^n(T_e) k_B T_e \left[\frac{1 - b_n e^{b_n} E_1(b_n)}{e^{b_n} E_1(b_n)} \right], \quad (44.189a)$$

which for large b_n (i.e. $(k_B T_e) \ll I_n$) tends to

$$n_e \hat{\alpha}_R^n(T_e) k_B T_e [1 - b_n^{-1} + 3b_n^{-2} - 13b_n^{-3} + \dots] \quad (44.189b)$$

with (44.185a) for $\hat{\alpha}_R^n$.

Energy Loss Rate for RR into all Levels $n \geq n_f$.

$$\begin{aligned} \left\langle \frac{dE}{dt} \right\rangle &= n_e k_B T_e \hat{\alpha}_0(T_e) [\gamma + \ln b_f + e^{b_f} E_1(b_f) (1 - b_f)] \\ &= n_e (k_B T_e) [\hat{\alpha}_R^T(T_e) - \hat{\alpha}_0(T_e) b_f e^{b_f} E_1(b_f)] \end{aligned} \quad (44.190a)$$

$$(44.190b)$$

with (44.187b) and (44.180) for $\hat{\alpha}_R^T$ and $\hat{\alpha}_0$.

Radiated Power

Radiated Power for RR into level n .

$$\left\langle \frac{d(h\nu)}{dt} \right\rangle_n = n_e \hat{\alpha}_R^n(T_e) I_n [b_n e^{b_n} E_1(b_n)]^{-1}, \quad (44.191a)$$

which for large b_n (i.e. $(k_B T_e) \ll I_n$) tends to

$$n_e \hat{\alpha}_R^n(T_e) I_n [1 + b_n^{-1} - b_n^{-2} + 3b_n^{-3} + \dots] \quad (44.191b)$$

Radiated Power for RR into all Levels $n \geq n_f$.

$$\left\langle \frac{d(h\nu)}{dt} \right\rangle = n_e \hat{\alpha}_0(T_e) I_f. \quad (44.192)$$

To allow n -summation, rather than integration as in (44.187a), to each of the above expressions is added $\frac{1}{2}\sigma_R^{n_f}$, $\frac{1}{2}\hat{\alpha}_R^{n_f}$, $\frac{1}{2}\langle \frac{dE}{dt} \rangle_{n_f}$ and $\frac{1}{2}\langle \frac{d(h\nu)}{dt} \rangle_{n_f}$, respectively. The expressions valid for bare nuclei of charge Z are also fairly accurate for recombination to a core of charge Z_c and atomic number Z_A , provided that Z is identified as $\frac{1}{2}(Z_A + Z_c)$.

Differential Cross Sections for Coulomb Elastic Scattering:

$$\sigma_c(E, \theta) = \frac{b_0^2}{4 \sin^4 \frac{1}{2}\theta}, \quad b_0^2 = (Ze^2/2E)^2. \quad (44.193)$$

The integral cross section for Coulomb scattering by $\theta \geq \pi/2$ at energy $E = (3/2)k_B T$ is

$$\sigma_c(E) = \pi b_0^2 = \frac{1}{9} \pi R_e^2, \quad R_e = e^2/k_B T. \quad (44.194)$$

Photon Emission Probability.

$$P_\nu = \sigma_R^n(E)/\sigma_c(E). \quad (44.195a)$$

This is small and increases with decreasing n as

$$P_\nu(E) = \left(\frac{8\alpha^3}{3\sqrt{3}} \right) \frac{8}{n} \frac{E}{(e^2/a_0)} \left(\frac{I_n}{h\nu} \right). \quad (44.195b)$$

44.8.3 Basic Formulae for Quantal Cross Sections

Radiative Recombination and Photoionization Cross Sections

The cross section σ_R^{nl} for recombination follows from the continuum-bound transition probability P_{if} per unit time. It is also provided by the detailed balance relation (44.173) in terms of σ_I^{nl} which follows from P_{fi} . The number of radiative transitions per second is

$$\begin{aligned} & [g_e g_A^+ \rho(E) dE d\hat{\mathbf{k}}_e] P_{if} [\rho(E_\nu) dE_\nu d\hat{\mathbf{k}}_\nu] \\ &= g_e g_A^+ v_e \frac{d\mathbf{p}_e}{(2\pi\hbar)^3} \sigma_R(\mathbf{k}_e) \\ &= g_\nu g_A c \frac{d\mathbf{k}_\nu}{(2\pi)^3} \sigma_I(\mathbf{k}_\nu), \end{aligned} \quad (44.196)$$

where the electron current ($\text{cm}^{-2} \text{s}^{-1}$) is

$$\frac{v_e d\mathbf{p}_e}{(2\pi\hbar)^3} = \left(\frac{2mE}{h^3} \right) dE d\hat{\mathbf{k}}_e, \quad (44.197)$$

and the photon current ($\text{cm}^{-2} \text{s}^{-1}$) is

$$c \frac{d\mathbf{k}_\nu}{(2\pi)^3} = c \frac{(h\nu)^2}{(2\pi\hbar c)^3} dE_\nu d\hat{\mathbf{k}}_\nu. \quad (44.198)$$

Time Dependent Quantum Electrodynamical Interaction.

$$\begin{aligned} V(\mathbf{r}, t) &= \frac{e}{mc} \mathbf{A} \cdot \mathbf{p} = ie \left(\frac{2\pi\hbar\nu}{V} \right)^{1/2} (\hat{\mathbf{e}} \cdot \mathbf{r}) e^{-i(\mathbf{k}_\nu \cdot \mathbf{r} - \omega t)} \\ &\equiv V(\mathbf{r}) e^{i\omega t}. \end{aligned} \quad (44.199)$$

In the dipole approximation, $e^{-i\mathbf{k}_\nu \cdot \mathbf{r}} \sim 1$.

Continuum-Bound State-to-State Probability.

$$\begin{aligned} P_{if} &= \frac{2\pi}{\hbar} |V_{fi}|^2 \delta[E_\nu - (E + I_n)] \\ V_{fi} &= \langle \Psi_{nlm}(\mathbf{r}) | V(\mathbf{r}) | \Psi_i(\mathbf{r}, \mathbf{k}_e) \rangle. \end{aligned} \quad (44.200)$$

Number of photon states in volume V .

$$\begin{aligned} \rho(E_\nu, \hat{\mathbf{k}}_\nu) dE_\nu d\hat{\mathbf{k}}_\nu &= V(h\nu)^2 / (2\pi\hbar c)^3 dE_\nu d\hat{\mathbf{k}}_\nu \quad (44.201a) \\ &= V [\omega^2 / (2\pi c)^3] d\omega d\hat{\mathbf{k}}_\nu. \end{aligned} \quad (44.201b)$$

Continuum-Bound Transition Rate.

On summing over the two directions ($g_\nu = 2$) of polarization, the rate for transitions into all final photon states is

$$\begin{aligned} A_{nlm}(E, \hat{\mathbf{k}}_e) &= \int P_{if} \rho(E_\nu) dE_\nu d\hat{\mathbf{k}}_\nu \\ &= \frac{4e^2 (h\nu)^3}{3\hbar (\hbar c)^3} |\langle \Psi_{nlm} | \mathbf{r} | \Psi_i(\mathbf{k}_e) \rangle|^2. \end{aligned} \quad (44.202)$$

Transition Frequency: Alternative Formula.

$$A_{nlm}(E, \hat{\mathbf{k}}_e) = (2\pi/\hbar) |D_{fi}|^2, \quad (44.203)$$

where the dipole atom-radiation interaction coupling is

$$D_{fi}(\mathbf{k}_e) = \left(\frac{2\omega^3}{3\pi c^3} \right)^{1/2} \langle \Psi_{nlm} | e\mathbf{r} | \Psi_i(\mathbf{k}_e) \rangle. \quad (44.204)$$

RR Cross Section into level (n, ℓ, m) .

$$\begin{aligned} \sigma_R^{nlm}(E) &= \frac{1}{4\pi} \int \sigma_R^{nlm}(\mathbf{k}_e) d\hat{\mathbf{k}}_e \\ &= \frac{h^3 \rho(E)}{8\pi m_e E} \int A_{nlm}(E, \hat{\mathbf{k}}_e) d\hat{\mathbf{k}}_e. \end{aligned} \quad (44.205)$$

RR Cross Section into level (n, ℓ) .

$$\begin{aligned} \sigma_R^{n\ell}(E) &= \frac{8\pi^2}{3} \left[\frac{(\alpha h\nu)^3}{2(e^2/a_0)E} \right] \rho(E) R_I^{n\ell}(E) \\ R_I^{n\ell}(E) &= \int d\hat{\mathbf{k}}_e \sum_m |\langle \Psi_{nlm} | \mathbf{r} | \Psi_i(\mathbf{k}_e) \rangle|^2. \end{aligned} \quad (44.206)$$

Transition T-matrix for RR.

$$\sigma_R^{n\ell}(E) = \frac{\pi a_0^2}{(ka_0)^2} |T_R|^2 \rho(E), \quad (44.207)$$

$$|T_R|^2 = 4\pi^2 \int \sum_m |D_{fi}|^2 d\hat{\mathbf{k}}_e. \quad (44.208)$$

Photoionization Cross Section. From detailed balance in Eq. (44.196), $\sigma_I^{n\ell}$ is

$$\sigma_I^{n\ell}(h\nu) = \left(\frac{8\pi^2}{3} \right) \alpha h\nu \left(\frac{g_A^+}{g_A} \right) \rho(E) R_I^{n\ell}(E). \quad (44.209)$$

Continuum Wavefunction Expansion.

$$\Psi_i(\mathbf{k}_e, \mathbf{r}) = \sum_{\ell'm'} i^{\ell'} e^{i\eta_{\ell'}} R_{E\ell'}(\mathbf{r}) Y_{\ell'm'}(\hat{\mathbf{k}}_e) Y_{\ell'm'}(\hat{\mathbf{r}}). \quad (44.210)$$

Energy Normalization. With $\rho(E) = 1$,

$$\int \Psi_i(\mathbf{k}_e; \mathbf{r}) \Psi_i^*(\mathbf{k}'_e; \mathbf{r}) d\mathbf{r} = \delta(E - E') \delta(\hat{\mathbf{k}}_e - \hat{\mathbf{k}}'_e). \quad (44.211)$$

Plane Wave Expansion.

$$e^{i\mathbf{k} \cdot \mathbf{r}} = 4\pi \sum_{\ell=0}^{\infty} i^{\ell} j_{\ell}(kr) Y_{\ell m}^*(\hat{\mathbf{k}}) Y_{\ell m}(\hat{\mathbf{r}}) \quad (44.212)$$

$$j_{\ell}(kr) \sim \sin(kr - \frac{1}{2}\ell\pi)/(kr). \quad (44.213)$$

For bound states,

$$\Psi_{nlm}(\mathbf{r}) = R_{nl}(\mathbf{r}) Y_{\ell m}(\hat{\mathbf{r}}). \quad (44.214)$$

RR and PI Cross Sections and Radial Integrals.

$$\sigma_R^{nl}(E) = \frac{8\pi^2}{3} \left[\frac{(\alpha h\nu)^3}{2(e^2/a_0)E} \right] \rho(E) R_I(E; n\ell). \quad (44.215)$$

For electron outside a closed core,

$$g_A^+ = 1, \quad g_A = 2(2\ell + 1)$$

$$\sigma_I^{nl}(h\nu) = \frac{4\pi^2 \alpha h\nu \rho(E)}{3(2\ell + 1)} R_I(E; n\ell), \quad (44.216a)$$

$$R_{nl}^{\epsilon, \ell'} = \int_0^\infty (R_{\epsilon \ell'} r R_{n\ell}) r^2 dr, \quad (44.216b)$$

$$R_I(E; n\ell) = \ell \left| R_{nl}^{\epsilon, \ell-1} \right|^2 + (\ell + 1) \left| R_{nl}^{\epsilon, \ell+1} \right|^2. \quad (44.216c)$$

For an electron outside an unfilled core (c) in the process $(A^+ + e^-) \rightarrow A(n\ell)$, the weights are

State i : $[S_c, L_c; \epsilon]$, $g_A^+ = (2S_c + 1)(2L_c + 1)$

State f : $[(S_c, L_c; n\ell)S, L]$, $g_A = (2S + 1)(2L + 1)$.

$$R_I(E; n\ell) = \frac{(2L + 1)}{(2L_c + 1)} \sum_{\ell'=\ell \pm 1} \sum_{L'} (2L' + 1) \left\{ \begin{matrix} \ell & L & L_c \\ L' & \ell' & 1 \end{matrix} \right\}^2 \times \ell_{\max} \left| \int_0^\infty (R_{\epsilon \ell'} r R_{n\ell}) r^2 dr \right|^2. \quad (44.217)$$

This reduces to (44.216c) when the radial functions $R_{i,f}$ do not depend on (S_c, L_c, S, L) .

Cross Section for Dielectronic Recombination

$$\sigma_{DLR}^{nl}(E) = \frac{\pi a_0^2}{(ka_0)^2} |T_{DLR}(E)|^2 \rho(E), \quad (44.218)$$

$$|T_{DLR}(E)|^2 = 4\pi^2 \int d\hat{k}_e \times \sum_j \left| \frac{\langle \Psi_f | D | \Psi_j \rangle \langle \Psi_j | V | \Psi_i(\mathbf{k}_e) \rangle}{(E - \epsilon_j + i\Gamma_j/2)} \right|^2, \quad (44.219)$$

which is the generalization of the T-matrix (44.208) to include the effect of intermediate doubly-excited autoionizing states $|\Psi_j\rangle$ in energy resonance to within width Γ_j of the initial continuum state Ψ_i . The electrostatic interaction $V = e^2 \sum_{i=1}^N (\mathbf{r}_i - \mathbf{r}_{N+1})^{-1}$ initially produces dielectronic capture by coupling the initial state i with the resonant states j which become stabilized by coupling via the dipole radiation field interaction $D = (2\omega^3/3\pi c^3)^{1/2} \sum_{i=1}^{N+1} (e\mathbf{r}_i)$ to the final stabilized state f . The above cross section for (44.3) is valid for isolated, non-overlapping resonances.

Continuum Wave Normalization and Density of States

The basic formulae (44.206) for σ_R^{nl} depends on the density of states $\rho(E)$ which in turn varies according to the particular normalization constant N adopted for the continuum radial wave,

$$R_{E\ell}(r) \sim N \sin(kr - \frac{1}{2}\ell\pi + \eta_\ell)/r, \quad (44.220)$$

in (44.210) where the phase is

$$\eta_\ell = \arg \Gamma(\ell + 1 + i\beta) - \beta \ln 2kr + \delta_\ell. \quad (44.221)$$

The phase corresponding to the Hartree-Fock short-range interaction is δ_ℓ . The Coulomb phase shift for electron motion under $(-Ze^2/r)$ is $(\eta_\ell - \delta_\ell)$ with $\beta = Z/(ka_0)$.

For a plane wave $\phi_{\mathbf{k}}(\mathbf{r}) = N' \exp(i\mathbf{k} \cdot \mathbf{r})$,

$$\begin{aligned} \langle \phi_{\mathbf{k}}(\mathbf{r}) | \phi_{\mathbf{k}'}(\mathbf{r}) \rangle d\mathbf{k} &= (2\pi)^3 |N'|^2 \rho(\mathbf{k}) d\mathbf{k} \delta(\mathbf{k} - \mathbf{k}') \\ &\equiv \left(\frac{h^3}{mp} \right) |N'|^2 \rho(E, \hat{\mathbf{k}}) dE d\hat{\mathbf{k}} \delta(E - E') \delta(\hat{\mathbf{k}} - \hat{\mathbf{k}'}). \end{aligned} \quad (44.222)$$

On integrating (44.222) over all E and $\hat{\mathbf{k}}$ for a single particle distributed over all $|E, \hat{\mathbf{k}}\rangle$ states, N' and ρ are then interrelated by

$$|N'|^2 \rho(E, \hat{\mathbf{k}}) = mp/h^3. \quad (44.223)$$

The incident current is

$$j dE d\hat{\mathbf{k}}_e = v |N'|^2 \rho(E, \hat{\mathbf{k}}) dE d\hat{\mathbf{k}}_e \quad (44.224a)$$

$$= (2mE/h^3) dE d\hat{\mathbf{k}}_e = v dp_e/h^3. \quad (44.224b)$$

Radial Wave Connection. From Eq. (44.210) and (44.212), $N = (4\pi N'/k)$, so that the connection between N of (44.220) and $\rho(E)$ is

$$|N|^2 \rho(E, \hat{\mathbf{k}}) = \frac{(2m/\hbar^2)}{\pi k} = \frac{(2/\pi)}{(ka_0)e^2}. \quad (44.225)$$

RR Cross Sections for Common Normalization Factors of Continuum Radial Functions

$$(a) \quad N = 1; \quad \rho(E) = \frac{(2m/\hbar^2)}{\pi k} = \frac{(2/\pi)}{(ka_0)e^2}, \quad (44.226)$$

$$\sigma_R^{nl}(E) = \frac{8\pi^2 a_0^2}{(ka_0)^3} \int \sum_m |D_{fi}|^2 d\hat{\mathbf{k}}_e, \quad (44.227)$$

where D_{fi} of (44.204) is dimensionless.

$$(b) \quad N = k^{-1}; \quad \rho(E) = (2m/\hbar^2)(k/\pi), \quad (44.228)$$

$$\sigma_R^{nl}(E) = \frac{16\pi a_0^2}{3\sqrt{2}} \left(\frac{\alpha h\nu}{e^2/a_0} \right)^3 \left(\frac{(e^2/a_0)}{E} \right)^{1/2} \left(\frac{R_I}{a_0^5} \right) \quad (44.229)$$

where (44.216b) and (44.216c) for R_I has dimension $[L^5]$.

$$(c) N = k^{-1/2}; \quad \rho(E) = \frac{(2m/\hbar^2)}{\pi}, \quad (44.230)$$

$$\sigma_R^{n\ell}(E) = \frac{8\pi a_0^2}{3} \left[\frac{\alpha^3 (h\nu)^3}{(e^2/a_0)^2 E} \right] \left(\frac{R_I}{a_0^4} \right), \quad (44.231)$$

where R_I has dimensions of $[L^4]$.

$$(d) N = (2m/\hbar^2 \pi^2 E)^{1/4}; \quad \rho(E) = 1, \quad (44.232)$$

$$\sigma_R^{n\ell}(E) = \frac{4(\pi a_0)^2}{3} \left[\frac{\alpha^3 (h\nu)^3}{(e^2/a_0)^2 E} \right] \left(\frac{R_I}{e^2 a_0} \right), \quad (44.233)$$

where R_I has dimensions of $[L^2 E^{-1}]$.

44.8.4 Bound-Free Oscillator Strengths

For a transition $n\ell \rightarrow E$ to $E + dE$,

$$\frac{df_{n\ell}}{dE} = \frac{2}{3} \frac{(h\nu)}{(e^2/a_0)} \frac{1}{(2\ell+1)} \sum_m \sum_{\ell'm'} \left| r_{n\ell m}^{\ell' m'} \right|^2, \quad (44.234)$$

$$\begin{aligned} R_I(\epsilon; n\ell) &= \int d\hat{k}_e \sum_m \left| \langle \Psi_{n\ell m} | \vec{r} | \Psi_i(E; \hat{k}_e; \ell' m') \rangle \right|^2 \\ &= \sum_{m, \ell', m'} \left| r_{n\ell m}^{\ell' m'} \right|^2, \end{aligned} \quad (44.235)$$

$$\sigma_R^{n\ell}(E) = 2\pi^2 \alpha a_0^2 g_A \left(\frac{k_\nu^2}{k_e^2} \right) \left(\frac{e^2}{a_0} \right) \frac{df_{n\ell}}{dE}, \quad (44.236a)$$

$$\sigma_I^{n\ell}(h\nu) = 2\pi^2 \alpha a_0^2 g_A^+ \left(\frac{e^2}{a_0} \right) \frac{df_{n\ell}}{dE}. \quad (44.236b)$$

Semiclassical Hydrogenic Systems

$$g_A = g_{n\ell} = 2(2\ell+1), \quad g_A^+ = 1,$$

$$\sigma_R^n(E) = \sum_{\ell=0}^{n-1} \sigma_R^{n\ell}(E) = 2\pi^2 \alpha a_0^2 \left(\frac{k_\nu^2}{k_e^2} \right) \frac{dF_n}{dE}, \quad (44.237)$$

$$\frac{dF_n}{dE} = \sum_{\ell=0}^{n-1} g_{n\ell} \frac{df_{n\ell}}{dE} = 2 \sum_{\ell, m} \frac{df_{n\ell m}}{dE}. \quad (44.238)$$

Bound-Bound absorption oscillator strength. For a transition $n \rightarrow n'$,

$$F_{nn'} = 2 \sum_{\ell m} \sum_{\ell' m'} f_{n\ell m}^{n' \ell' m'} \quad (44.239a)$$

$$= \frac{2^6}{3\sqrt{3}\pi} \left[\left(\frac{1}{n^2} - \frac{1}{n'^2} \right)^{-3} \right] \frac{1}{n^3} \frac{1}{n'^3}, \quad (44.239b)$$

$$\frac{dF_n}{dE} = \frac{2^5}{3\sqrt{3}\pi} n \frac{I_n^2}{(h\nu)^3} = 2n^2 \frac{df_{n\ell}}{dE}, \quad (44.239c)$$

$$\sigma_R^n(E) = \frac{2^5 \alpha^3}{3\sqrt{3}} \left[\frac{n I_n^2}{E(h\nu)} \right] \pi a_0^2, \quad (44.239d)$$

$$\sigma_I^{n\ell}(h\nu) = \frac{2^6 \alpha}{3\sqrt{3}} \frac{n}{Z^2} \left(\frac{I_n}{h\nu} \right)^3 \pi a_0^2, \quad (44.239e)$$

$$= 7.907071 \left(\frac{n}{Z^2} \right) \left(\frac{I_n}{h\nu} \right)^3 \text{ Mb}. \quad (44.239f)$$

This semiclassical analysis yields exactly Kramers PI and associated RR cross sections in Sect. 44.8.2.

44.8.5 Radiative Recombination Rate

$$\hat{\alpha}_R^{n\ell}(T_e) = \bar{v}_e \int_0^\infty \epsilon \sigma_R^{n\ell}(\epsilon) e^{-\epsilon} d\epsilon \quad (44.240a)$$

$$\equiv \bar{v}_e \langle \sigma_R^{n\ell}(T_e) \rangle, \quad (44.240b)$$

where $\epsilon = E/k_B T$ and $\langle \sigma_R^{n\ell}(T_e) \rangle$ is the Maxwellian-averaged cross section for radiative recombination.

In terms of the continuum-bound $A_{n\ell}(E)$,

$$\hat{\alpha}_R^{n\ell}(T_e) = \frac{h^3}{(2\pi m_e k_B T)^{3/2}} \int_0^\infty \left(\frac{dA_{n\ell}}{d\epsilon} \right) e^{-\epsilon} d\epsilon, \quad (44.241)$$

$$\frac{dA_{n\ell}}{dE} = \rho(E) \sum_m \int A_{n\ell m}(E, \hat{k}_e) d\hat{k}_e. \quad (44.242)$$

Milne Detailed Balance Relation.

In terms of $\sigma_I^{n\ell}(h\nu)$,

$$\hat{\alpha}_R^{n\ell}(T_e) = \bar{v}_e \left(\frac{g_A}{2g_A^+} \right) \left(\frac{k_B T_e}{mc^2} \right) \left(\frac{I_n}{k_B T_e} \right)^2 \langle \sigma_I^{n\ell}(T_e) \rangle, \quad (44.243)$$

where, in reduced units $\omega = h\nu/I_n$, $T = k_B T_e/I_n = b_n^{-1}$, the averaged PI cross section corresponding to (44.174) is

$$\langle \sigma_I^{n\ell}(T) \rangle = \frac{e^{1/T}}{T} \int_1^\infty \omega^2 \sigma_I^{n\ell}(\omega) e^{-\omega/T} d\omega. \quad (44.244)$$

When $\sigma_I^{n\ell}(\omega)$ is expressed in Mb (10^{-18} cm^2),

$$\begin{aligned} \hat{\alpha}_R^{n\ell}(T_e) &= 1.508 \times 10^{-13} \left(\frac{300}{T_e} \right)^{1/2} \left(\frac{I_n}{I_H} \right)^2 \left(\frac{g_A}{2g_A^+} \right) \\ &\times \langle \sigma_I^{n\ell}(T) \rangle \text{ cm}^3 \text{ s}^{-1}. \end{aligned} \quad (44.245)$$

When σ_I can be expressed in terms of the threshold cross section σ_0^n [Eq. (44.178)] as

$$\sigma_I^{n\ell}(h\nu) = (I_n/h\nu)^p \sigma_0(n); \quad (p = 0, 1, 2, 3), \quad (44.246)$$

then $\langle \sigma_I^{n\ell}(T) \rangle = S_p(T) \sigma_0(n)$, where

$$S_0(T) = 1 + 2T + 2T^2, \quad S_1(T) = 1 + T, \quad (44.247a)$$

$$S_2(T) = 1, \quad (44.247b)$$

$$S_3(T) = \left[e^{1/T}/T \right] E_1(1/T) \quad (44.247c)$$

$$T \lesssim 1 - T + 2T^2 - 6T^3. \quad (44.247d)$$

The case $p = 3$ corresponds to Kramers PI cross section (44.181) so that

$$\kappa \hat{\alpha}_R^{nl}(T_e) = \frac{(2\ell+1)}{n^2} \frac{2}{n} \hat{\alpha}_0(T_e) S_3(T) \quad (44.248a)$$

$$\equiv \kappa \hat{\alpha}_R^{nl}(T_e \rightarrow 0) S_3(T), \quad (44.248b)$$

such that $\kappa \hat{\alpha}_R^{nl} \sim Z^2/(n^3 T_e^{1/2})$ as $T = (k_B T_e / I_n) \rightarrow 0$.

44.8.6 Gaunt Factor, Cross Sections and Rates for Hydrogenic Systems

The Gaunt Factor G_{nl} is the ratio of the quantal to Kramers (K) semiclassical PI cross section such that

$$\sigma_I^{nl}(h\nu) = \kappa \sigma_I^n(h\nu) G_{nl}(\omega); \quad (44.249)$$

$$\omega = h\nu / I_n = 1 + E / I_n.$$

(a) Radiative Recombination Cross Section.

$$\sigma_R^{nl}(E) = \left(\frac{g_A}{g_A^+} \right) \left[\frac{\alpha^2 (h\nu)^2}{2E(\epsilon^2/a_0)} \right] G_{nl}(\omega) \kappa \sigma_I^n(h\nu) \quad (44.250a)$$

$$= G_{nl}(\omega) \kappa \sigma_R^{nl}(E) \quad (44.250b)$$

$$= \left[\frac{(2\ell+1)}{n^2} G_{nl}(\omega) \right] \kappa \sigma_R^n(E), \quad (44.250c)$$

$$\sigma_R^n(E) = G_n(\omega) \kappa \sigma_R^n(E) \quad (44.250d)$$

where the Gaunt Factor, or quantum mechanical correction to the semiclassical cross sections

$$G_{nl}(\omega) \rightarrow \begin{cases} 1, & \omega \rightarrow 1 \\ \omega^{-(\ell+1/2)}, & \omega \rightarrow \infty \end{cases} \quad (44.251)$$

favors low nl states. The ℓ -averaged Gaunt factor is

$$G_n(\omega) = (1/n^2) \sum_{\ell=0}^{n-1} (2\ell+1) G_{nl}(\omega). \quad (44.252)$$

Approximations for G_n : as ϵ increases from zero,

$$G_n(\epsilon) = \left[1 + \frac{4}{3}(a_n + b_n) + \frac{28}{18}a_n^2 \right]^{-3/4} \quad (44.253a)$$

$$\simeq 1 - (a_n + b_n) + \frac{7}{3}a_n b_n + \frac{7}{6}b_n^2 \quad (44.253b)$$

where $E = \epsilon(Z^2 e^2 / 2a_0)$, $\omega = 1 + n^2 \epsilon$, and

$$a_n(\epsilon) = 0.172825(1 - n^2 \epsilon) c_n(\epsilon) \quad (44.254a)$$

$$b_n(\epsilon) = 0.04959 \left[1 + \frac{4}{3}n^2 \epsilon + n^4 \epsilon^2 \right] c_n^2(\epsilon) \quad (44.254b)$$

$$c_n(\epsilon) = n^{-2/3} (1 + n^2 \epsilon)^{-2/3}. \quad (44.254c)$$

Radiative Recombination Rate.

$$\hat{\alpha}_R^{nl}(T_e) = \kappa \hat{\alpha}_R^{nl}(T_e \rightarrow 0) F_{nl}(T), \quad (44.255)$$

$$\hat{\alpha}_R^{nl}(T_e \rightarrow 0) = \frac{(2\ell+1)}{n^2} \left(\frac{2}{n} \right) \hat{\alpha}_0(T_e), \quad (44.256)$$

in accordance with (44.185b).

$$F_{nl}(T) = \frac{e^{1/T}}{T} \int_1^\infty \frac{G_{nl}(\omega)}{\omega} e^{-\omega/T} d\omega. \quad (44.257)$$

The multiplicative factors F and G convert the semiclassical (Kramers) $T_e \rightarrow 0$ rate and cross section to their quantal values. Departures from the scaling rule ($Z^2/n^3 T_e^{1/2}$) for RR rates is measured by $F_{nl}(T)$.

44.8.7 Exact Universal Rate Scaling Law and Results for Hydrogenic Systems

$$\hat{\alpha}_R^{nl}(Z, T_e) = Z \hat{\alpha}_R^{nl}(1, T_e/Z^2) \quad (44.258)$$

as exhibited by (44.243) with (44.239e) and (44.244).

Recombination rates are greatest into low n levels and the $\omega^{-\ell-1/2}$ variation of G_{nl} preferentially populates states with low $\ell \sim 2-5$. Highly accurate analytical fits for $G_{nl}(\omega)$ have been obtained for $n \leq 20$ so that (44.249) can be expressed in terms of known functions of fit parameters [17]. This procedure (which does not violate the S_2 sum rule) has been extended to nonhydrogenic systems of neon-like Fe XVII, where $\sigma_I^{nl}(\omega)$ is a monotonically decreasing function of ω .

Variation of the ℓ -averaged values

$$n^{-2} \sum_{\ell=0}^{n-1} (2\ell+1) F_{nl}(T)$$

is close in both shape and magnitude to the corresponding semiclassical function $S_3(T)$, given by (44.257) with $G_{nl}(\omega) = 1$. Hence the ℓ -averaged recombination rate is

$$\hat{\alpha}_R^n(Z, T) = (300/T)^{1/2} (Z^2/n) F_n(T) \times 1.1932 \times 10^{-12} \text{ cm}^3 \text{ s}^{-1}, \quad (44.259)$$

where F_n can be calculated directly from (44.257) or be approximated as $G_n(1)S(T)$. A computer program based on a three-term expansion of G_n is also available [18]. From a three-term expansion for G , the rate of radiative recombination into all levels of a hydrogenic system is

$$\hat{\alpha}(Z, T) = 5.2 \times 10^{-14} Z \lambda^{1/2} \left[0.43 + \frac{1}{2} \ln \lambda + 0.47/\lambda^{1/2} \right], \quad (44.260)$$

where $\lambda = 1.58 \times 10^5 Z^2/T$ and $[\hat{\alpha}] = \text{cm}^3/\text{s}$. Tables [19] exist for the effective rate

$$\hat{\alpha}_E^{n\ell}(T) = \sum_{n'=n}^{\infty} \sum_{\ell'=0}^{n'-1} \hat{\alpha}_R^{n'\ell'} C_{n'\ell',n\ell} \quad (44.261)$$

of populating a given level $n\ell$ of H via radiative recombination into all levels $n' \geq n$ with subsequent radiative cascade ($i \rightarrow f$) with probability $C_{i,f}$ via all possible intermediate paths. Tables [19] also exist for the full rate

$$\hat{\alpha}_F^N(T) = \sum_{n=N}^{\infty} \sum_{\ell=0}^{n-1} \hat{\alpha}_R^{n\ell} \quad (44.262)$$

of recombination, into all levels above $N = 1, 2, 3, 4$, of hydrogen. They are useful in deducing time scales of radiative recombination and rates for complex ions.

44.9 USEFUL QUANTITIES

(a) Mean Speed.

$$\bar{v}_e = \left(\frac{8k_B T}{\pi m_e} \right)^{1/2} = 1.076042 \times 10^7 \left[\frac{T}{300} \right]^{1/2} \text{ cm/s}$$

$$= 6.69238 \times 10^7 T_{eV}^{1/2} \text{ cm/s}$$

$$\bar{v}_i = 2.51116 \times 10^5 \left[\frac{T}{300} \right]^{1/2} (m_p/m_i)^{1/2} \text{ cm/s}$$

where $(m_p/m_e)^{1/2} = 42.850352$, and $T = 11604.45 T_{eV}$ relates the temperature in K and in eV.

(b) Natural Radius: $|V(R_e)| = e^2/R_e = k_B T$.

$$R_e = \frac{e^2}{k_B T} = 557 \left(\frac{300}{T} \right) \text{ \AA} = \left(\frac{14.4}{T_{eV}} \right) \text{ \AA}.$$

(c) Boltzmann Average Momentum.

$$\langle p \rangle = \int_{-\infty}^{\infty} e^{-p^2/2mk_B T} dp = (2\pi m_e k_B T)^{1/2}.$$

(d) De Broglie Wavelength.

$$\lambda_{dB} = \frac{h}{\langle p \rangle} = \frac{h}{(2\pi m_e k_B T)^{1/2}} = \frac{7.453818 \times 10^{-6}}{T_e^{1/2}} \text{ cm}$$

$$= 43.035 \left(\frac{300}{T_e} \right)^{1/2} \text{ \AA} = \frac{6.9194}{T_{eV}^{1/2}} \text{ \AA}.$$

Acknowledgments

This research is supported by the U. S. Air Force Office of Scientific Research under Grant no. F49620-94-1-0379. I wish to thank Dr. E. J. Mansky for numerous discussions on the content and form of this chapter and without whose expertise in computer typesetting this chapter would not have been possible.

44.10 GENERAL REFERENCES

General Recombination:

M. R. Flannery, *Electron-Ion and Ion-Ion Recombination Processes* in Adv. At. Mol. Phys. **32**, 117 (1994).

M. R. Flannery, *Recombination Processes in Molecular Processes in Space*, edited by T. Watanabe, I. Shimamura, M. Shimiza, and Y. Itikawa (Plenum Press, New York, 1990), Ch. 7, p. 145.

D. R. Bates, *Recombination in Electronic and Atomic Collisions*, edited by H. B. Gilbody, W. R. Newell, F. H. Read and A. C. H. Smith (North-Holland, Amsterdam, 1988), p. 3.

D. R. Bates, *Recombination in Case Studies in Atomic Physics*, edited by E. W. McDaniel and M. R. C. McDowell, (North-Holland, Amsterdam 1974), vol. 4, p. 57.

D. R. Bates and A. Dalgarno, *Electronic Recombination in Atomic and Molecular Processes*, edited by D. R. Bates (Academic Press, New York 1962)

D. R. Bates, *Aspects of Recombination*, Adv. At. Mol. Phys. **15**, 235 (1979).

W. G. Graham (ed.), *Recombination of Atomic Ions*, (Plenum Press, New York, 1992).

J. N. Bardsley, *Recombination Processes in Atomic and Molecular Physics in Atomic and Molecular Collision Theory* edited by F. A. Gianturco (Plenum Press, New York, 1980), p. 123.

J. Dubau and S. Volonte, *Dielectronic Recombination and its applications in astronomy*, Rep. Prog. Phys. **43**, 199 (1980).

Y. Hahn, *Theory of Dielectronic Recombination*, Adv. At. Mol. Phys. **21** 123 (1985).

Y. Hahn and K. J. LaGattuta, *Dielectronic Recombination and Related Processes*, Phys. Rept. **116** 195 (1988).

E. W. McDaniel and E. J. Mansky, *Guide to Bibliographies, Books, Reviews and Compendia of Data on Atomic Collisions*, Adv. At. Mol. Opt. Phys. **33** 389 (1994).

Three-Body Electron-Ion Collisional-Radiative Recombination: Theory

D. R. Bates, A. E. Kingston, and R. W. P. McWhirter, *Recombination between electrons and atomic ions I. Optically thin plasmas, II. Optically thick plasmas*, Proc. R. Soc. London Ser. A **267**, 297 (1962); **270**, 155 (1962).

D. R. Bates and S. P. Khare, *Recombination of positive ions and electrons in a dense neutral gas*, Proc. Phys. Soc. **85**, 231 (1965).

D. R. Bates, V. Malaviya, and N. A. Young, *Electron-ion recombination in a dense molecular gas*, Proc. R. Soc.

(London) Ser. A 320, 437 (1971).

A. Burgess and H. P. Summers, *The Recombination and Level Populations of Ions I. Hydrogen and Hydrogenic Ions*, Mon. Not. R. Astron. Soc. 174, 345 (1976).

H. P. Summers, *The Recombination and level populations of ions II. Resolution of angular momentum states*, Mon. Not. R. Astron. Soc. 178, 101 (1977).

N. N. Ljepojevic, R. J. Hutcheon, and J. Payne, *COLRAD - A Program to calculate population densities of the excited atomic levels of Hydrogen-like ions in a plasma*, Comp. Phys. Commun. 44, 157 (1987).

Electron-Ion Recombination: Molecular Dynamics Simulations

W. L. Morgan, *Electron-Ion Recombination in Water Vapor*, J. Chem. Phys. 80, 4564 (1984).

W. L. Morgan, *Molecular Dynamics Simulation of Electron-Ion Recombination in a Nonequilibrium Weakly Ionized Plasma*, Phys. Rev. A 30, 979 (1984).

W. L. Morgan and J. N. Bardsley, *Monte-Carlo Simulation of Electron-Ion Recombination at High Pressure*, Chem. Phys. Lett. 96, 93 (1983).

W. L. Morgan, in *Recent Studies in Atomic and Molecular Processes*, edited by A. E. Kingston, (Plenum Press, New York, 1987), p. 149.

Ion-Ion Recombination: Review Articles

M. R. Flannery, *Three-Body Recombination between Positive and Negative Ions in Case Studies in Atomic Collision Physics*, edited by E. W. McDaniel and M. R. C. McDowell, (North-Holland, Amsterdam, 1972), Vol. 2, Ch. 1, p. 1.

M. R. Flannery, *Ionic Recombination in Atomic Processes and Applications*, edited by P. G. Burke and B. L. Moiseiwitsch, (North-Holland, Amsterdam, 1976), Ch. 12, p. 407.

M. R. Flannery, *Ion-Ion Recombination in High Pressure Plasmas in Applied Atomic Collision Physics*, edited by E. W. McDaniel and W. L. Nighan (Academic Press, New York, 1983), Vol. 3 *Gas Lasers*, Ch. 5, p. 393.

M. R. Flannery, *Microscopic and Macroscopic Perspectives of Termolecular Association of Atomic Reactants in a Gas in Recent Studies in Atomic and Molecular Processes*, edited by A. E. Kingston (Plenum Press, London, 1987), p. 167.

D. R. Bates, *Ion-Ion Recombination in an Ambient Gas*, Adv. At. Mol. Phys. 20, 1 (1985).

B. H. Mahan, *Recombination of Gaseous Ions*, Adv. Chem. Phys. 23, 1 (1973).

J. T. Moseley, R. E. Olson, and J. R. Peterson, in *Case Studies in Atomic Collision Physics*, edited by M. R. C. McDowell and E. W. McDaniel (North-Holland, Amsterdam, 1972), p. 1.

D. Smith and N. G. Adams, *Studies of Ion-Ion Re-*

combination using Flowing Afterglow Plasmas in Physics of Ion-Ion and Electron-Ion Collisions, edited by F. Brouillard and J. W. McGowan, (Plenum Press, New York, 1982), p. 501.

Termolecular Ion-Ion Recombination: Theory

(A) Low Gas Densities: Linear Region

M. R. Flannery and E. J. Mansky, *Termolecular Recombination at Low Gas Density: Strong Collision, Bottleneck, and Exact Treatments*, J. Chem. Phys. 88, 4228 (1988).

M. R. Flannery and E. J. Mansky, *Termolecular Recombination: Coupled Nearest-Neighbor Limit and Uncoupled Intermediate Levels Limit*, J. Chem. Phys. 89, 4086 (1988).

M. R. Flannery, *Variational Principle for Termolecular Recombination in a Gas*, J. Chem. Phys. 89, 214 (1988).

M. R. Flannery, *Diffusional Theory of Termolecular Recombination and Association of Atomic Species in a Gas*, J. Chem. Phys. 87, 6947 (1987).

M. R. Flannery, *Ion-Ion Recombination in $(X^+ + Y^- + Z)$ Systems at Low Gas Densities I. Symmetrical Resonance Charge-Transfer Contribution*, J. Phys. B 13, 3649 (1980).

M. R. Flannery, *Ion-Ion Recombination in $(X^+ + Y^- + Z)$ Systems at Low Gas Densities II. Elastic Ion-Neutral Collisions*, J. Phys. B 14, 915 (1981).

D. R. Bates and I. Mendaš, *Termolecular Ionic Recombination at Low Ambient Gas Density for the Case of a Polarization Interaction*, J. Phys. B 15, 1949 (1982).

D. R. Bates, P. B. Hays, and D. Sprevak, *Kinetic Energy of Ion Pairs in Three-Body Ionic Recombination*, J. Phys. B 4, 962 (1971).

D. R. Bates and M. R. Flannery, *Recombination of Positive and Negative Ions II. General Third Body*, Proc. R. Soc. London Ser. A 302, 367 (1968).

D. R. Bates and R. J. Moffett, *Recombination of Positive and Negative Ions I. Ions Recombining in Their Parent Gas*, Proc. R. Soc. London Ser. A 291, 1 (1966).

(B) All Gas Densities: Non-Linear Region

M. R. Flannery, *Microscopic and Macroscopic Theories of Termolecular Recombination between Atomic Ions*, pp. 205 in *Dissociative Recombination*, B. R. Rowe, J. B. A. Mitchell and A. Canosa (eds.), Plenum Press (1993).

M. R. Flannery, *Transport-Collisional Master Equations for Termolecular Recombination as a Function of Gas Density*, J. Chem. Phys. 95, 8205 (1991).

M. R. Flannery, *Theory of Ion-Ion Recombination*, Phil. Trans. R. Soc. London Ser. A 304, 447 (1982).

D. R. Bates and I. Mendaš, *Ionic Recombination*

in an Ambient Gas I. Extension of Quasi-Equilibrium Statistical Method into Nonlinear Region, Proc. R. Soc. London Ser. A **359**, 275 (1978).

J. J. Thomson, *Recombination of Gaseous Ions, the Chemical Combination of Gases and Monomolecular Reactions*, Phil. Mag. **47**, 337 (1924).

Ion-Ion Recombination: Monte-Carlo Simulations

P. J. Feibelman, *Numerical Study of the Three-Body Ion-Ion Recombination*, J. Chem. Phys. **42**, 2462 (1965).

A. Jones and J. L. J. Rosenfeld, *Monte-Carlo simulation of hydrogen-atom recombination*, Proc. R. Soc. London Ser. A **333**, 419 (1973).

D. R. Bates and I. Mendaš, *Ionic Recombination in an Ambient Gas II. Computer Experiment with Specific Allowance for Binary Recombination*, Proc. R. Soc. London Ser. A **359**, 287 (1978).

D. R. Bates, *Universal Curve for Termolecular Ionic Recombination Coefficients*, Chem. Phys. Lett. **75**, 409 (1980).

J. N. Bardsley and J. M. Wadehra, *Monte-Carlo Simulation of Three Body Ion-Ion Recombination*, Chem. Phys. Lett. **72**, 477 (1980).

D. R. Bates, *Mutual Neutralization Coefficient in an Ambient Gas*, J. Phys. B **14**, 4207 (1981).

D. R. Bates, *Effect of Inelastic Collisions on the Rate of Termolecular Ionic Recombination*, J. Phys. B **14**, 2853 (1981).

D. R. Bates and I. Mendaš, *Rate Coefficients for Termolecular Ionic Recombination*, Chem. Phys. Lett. **88**, 528 (1982).

W. L. Morgan, J. N. Bardsley, J. Lin, and B. L. Whitten, *Theory of Ion-Ion Recombination in Plasmas*, Phys. Rev. A **26**, 1696 (1982).

B. L. Whitten, W. L. Morgan, and J. N. Bardsley, *Monte-Carlo Calculations of Two- and Three-Body Ionic Recombination*, J. Phys. B **15**, 319 (1982).

Ion-Ion Tidal Recombination: Molecular Dynamics Simulations

D. R. Bates and W. L. Morgan, *New Recombination Mechanism: Tidal Termolecular Ionic Recombination*, Phys. Rev. Lett. **64**, 2258 (1990).

W. L. Morgan and D. R. Bates, *Tidal Termolecular Ionic Recombination*, J. Phys. B **25**, 5421 (1992).

Radiative Recombination: Theory

M. J. Seaton, *Radiative Recombination of Hydrogenic Ions*, Mon. Not. R. Astron. Soc. **119**, 81 (1959).

D. R. Flower and M. J. Seaton, *A Program to Calculate Radiative Recombination Coefficients of Hydrogenic*

Ions, Comp. Phys. Commun. **1**, 31 (1969).

A. Burgess and H. P. Summers, *Radiative Gaunt Factors*, Mon. Not. R. Astron. Soc. **226**, 257 (1987).

Y. S. Kim and R. H. Pratt, *Direct Radiative Recombination of Electrons with Atomic Ions: Cross Sections and Rate Coefficients*, Phys. Rev. A **27**, 2913 (1983).

F. D. Aaron, A. Costescu, and C. Dinu, *Direct Radiative Recombination and Photoeffect Cross Sections for Arbitrary Atomic Coulomb Bound States*, J. Phys. II (Paris) **3** 1227 (1993).

D. J. McLaughlin and Y. Hahn, *Scaling Behavior of Radiative Recombination Cross Sections and Rate Coefficients*, Phys. Rev. A **43**, 1313 (1991).

Dissociative Recombination: Theory and Experiment

D. Zajfman, J. B. A. Mitchell, B. R. Rowe and D. Schwalin (eds.), *Dissociative Recombination: Theory, Experiment and Applications III.*, World Scientific, Singapore (1996).

D. R. Bates, *Dissociative Recombination: Crossing and Tunnelling Modes*, Adv. At. Mol. Phys. **34**, 427 (1994).

B. R. Rowe, J. B. A. Mitchell and A. Canosa (eds.), *Dissociative Recombination: Theory, Experiment and Applications II.*, Plenum Press, New York (1993).

J. B. A. Mitchell and S. L. Guberman (eds.), *Dissociative Recombination: Theory, Experiment and Applications I.*, World Scientific, Singapore (1989).

J. B. A. Mitchell, *The Dissociative Recombination of Molecular Ions*, Phys. Rep. **186**, 215 (1990).

A. Giusti-Suzor, *Recent Developments in the Theory of Dissociative Recombination and Related Processes in Atomic Processes in Electron-Ion and Ion-Ion Collisions*, edited by F. Brouillard, (Plenum Press, New York 1986).

J. N. Bardsley and M. A. Biondi, *Dissociative Recombination*, Adv. At. Mol. Phys. **6**, 1 (1970).

REFERENCES

1. J. Stevfelt, J. Boulmer and J-F. Delpech, Phys. Rev. A **12** 1246 (1975).
2. R. Deloche, P. Monchicourt, M. Cheret and F. Lambert, Phys. Rev. A **13** 1140 (1976).
3. P. Mansbach and J. Keck, Phys. Rev. **181**, 275 (1965).
4. L. P. Pitaevskii, Sov. Phys. JETP **15**, 919 (1962).
5. D. R. Bates, *Dissociative Recombination*, Phys. Rev. **78**, 492 (1950).
6. J. N. Bardsley, *The Theory of Dissociative Recombination*, J. Phys. A: Proc. Phys. Soc. [2] **1**, 365 (1968).
7. M. R. Flannery, *Semiclassical Theory of Direct Dissociative Recombination in Atomic Collisions: A Symposium in Honor of Christopher Bottcher*, edited

by D. R. Schultz, M. R. Strayer and J. H. Macek (AIP Press 1995).

8. A. Giusti, *A Multichannel Quantum Defect Theory Approach to Dissociative Recombination*, J. Phys. B **13**, 3867 (1980).
9. P. van der Donk, F. B. Yousif, J. B. A. Mitchell and A. P. Hickman, Phys. Rev. Lett. **68** 2252 (1992).
10. S. L. Guberman, Phys. Rev. A **49** R4277 (1994).
11. M. R. Flannery, Int. J. Mass Spectrom. Ion Processes *in press* (1995).
12. M. R. Flannery, J. Chem. Phys. **95**, 8205 (1991).
13. H. A. Kramers, Phil. Mag. **46** 836 (1923).
14. A. Burgess, Mon. Not. R. Astron. Soc. **118** 477 (1958).
15. J. A. Gaunt, Phil. Trans. Roy. Soc. A **229** 163 (1930).
16. M. J. Seaton, Mon. Not. R. Astron. Soc. **119**, 81 (1959).
17. B. F. Rozsnyai and V. L. Jacobs, Astrophys. J. **327**, 485 (1988).
18. D. R. Flower and M. J. Seaton, Comp. Phys. Commun. **1**, 31 (1969).
19. P. G. Martin, Astrophys. J. Supp. Ser. **66**, 125 (1988).

X. Appendix D:

Rydberg Collisions: Binary Encounter, Born and Impulse Approximations

by

E. J. Mansky

School of Physics

Georgia Institute of Technology

Atlanta, Georgia 30332

Rydberg Collisions: Binary Encounter, Born and Impulse Approximations

E. J. Mansky

School of Physics, Georgia Institute of Technology, Atlanta, Georgia 30332-0430,

**Controlled Fusion Atomic Data Center, Oak Ridge National Laboratory, Oak Ridge, Tennessee 37831-6372.*

45.1	INTRODUCTION	2
45.1.1	Rydberg Collision Processes	2
45.2	GENERAL PROPERTIES OF RYDBERG STATES	2
45.2.1	Dipole Moments	2
45.2.2	Radial Integrals	3
45.2.3	Line Strengths	4
45.2.4	Form Factors	4
45.2.5	Impact Broadening	5
45.3	CORRESPONDENCE PRINCIPLES	5
45.3.1	Bohr-Sommerfeld Quantization	5
45.3.2	Bohr Correspondence Principle	5
45.3.3	Heisenberg Correspondence Principle	5
45.3.4	Strong Coupling Correspondence Principle	6
45.3.5	Equivalent Oscillator Theorem	6
45.4	DISTRIBUTION FUNCTIONS	6
45.4.1	Spatial Distributions	6
45.4.2	Momentum Distributions	6
45.5	CLASSICAL THEORY	7
45.6	WORKING FORMULAE FOR RYDBERG COLLISIONS	8
45.6.1	Inelastic n, ℓ -Changing Transitions	8
45.6.2	Inelastic $n \rightarrow n'$ Transitions	8
45.6.3	Quasi-elastic ℓ -Mixing Transitions	9
45.6.4	Elastic $n\ell \rightarrow n\ell'$ Transitions	9
45.6.5	Fine Structure $n\ell J \rightarrow n\ell' J'$ Transitions	10
45.7	IMPULSE APPROXIMATION	10
45.7.1	Quantal Impulse Approximation	10
45.7.2	Classical Impulse Approximation	14
45.7.3	Semiquantal Impulse Approximation	15
45.8	BINARY ENCOUNTER APPROXIMATION	16
45.8.1	Differential Cross Sections	16
45.8.2	Integral Cross Sections	17
45.8.3	Classical Ionization Cross Section	19
45.8.4	Classical Charge Transfer Cross Section	19
45.9	BORN APPROXIMATION	20
45.9.1	Form Factors	20
45.9.2	Hydrogenic Form Factors	20

45.9.3	Excitation Cross Sections	21
45.9.4	Ionization Cross Sections	22
45.9.5	Capture Cross Sections	22

45.1 INTRODUCTION

Rydberg collisions are collisions of electrons, ions and neutral particles with atomic or molecular targets which are in highly excited Rydberg states characterized by large principal quantum numbers ($n \gg 1$). Rydberg collisions of atoms and molecules with neutral and charged particles includes the study of collision-induced transitions both to and from Rydberg states and transitions among Rydberg levels. The basic quantum mechanical structural properties of Rydberg states are given in Chap. ???. This Chapter collects together many of the equations used to study theoretically the collisional properties of both charged and neutral particles with atoms and molecules in Rydberg states or orbitals. The primary theoretical scattering approximations enumerated in this Chapter are the *impulse approximation*, *binary encounter approximation* and the *Born approximation*. The theoretical techniques used to study Rydberg collisions complement and supplement the *eigenfunction expansion* approximations used for collisions with target atoms and molecules in their ground ($n = 1$) or first few excited states ($n > 1$), as discussed in Chap. ???.

Direct application of eigenfunction expansion techniques to Rydberg collisions, wherein the target particle can be in a Rydberg orbital with principal quantum number in the range $n \geq 100$, is prohibitively difficult due to the need to compute numerically and store wave functions with n^3 nodes. For $n = 100$ this amounts to $\sim 10^6$ nodes for each of the wave functions represented in the eigenfunction expansion. Therefore, a variety of approximate scattering theories have been developed to deal specifically with the peculiarities of Rydberg collisions.

45.1.1 Rydberg Collision Processes

(A) State-changing Collisions

Quasi-elastic ℓ -mixing collisions:

$$A^*(n\ell) + B \rightarrow A^*(n\ell') + B. \quad (45.1)$$

Quasi-elastic J -mixing collisions: Fine structure transitions with $J = |\ell \pm 1/2| \rightarrow J' = |\ell \pm 1/2|$ are

$$A^*(n\ell J) + B \rightarrow A^*(n\ell J') + B. \quad (45.2)$$

Energy transfer n -changing collisions:

*present address

$$A^*(n) + B(\beta) \rightarrow A^*(n') + B(\beta'), \quad (45.3)$$

where, if B is a molecule, the transition $\beta \rightarrow \beta'$ represents an inelastic energy transfer to the rotational-vibrational degrees of freedom of the molecule B from the Rydberg atom A^* .

Elastic scattering:

$$A^*(\gamma) + B \rightarrow A^*(\gamma) + B, \quad (45.4)$$

where the label γ denotes the set of quantum numbers n, ℓ or n, ℓ, J used.

Depolarization collisions:

$$A^*(n\ell m) + B \rightarrow A^*(n\ell m') + B, \quad (45.5a)$$

$$A^*(n\ell JM) + B \rightarrow A^*(n\ell JM') + B. \quad (45.5b)$$

(B) Ionizing Collisions

Direct and associative ionization:

$$A^*(\gamma) + B(\beta) \rightarrow \begin{cases} A^+ + B(\beta') + e^- \\ BA^+ + e^- \end{cases} \quad (45.6)$$

Penning ionization:

$$A^*(\gamma) + B \rightarrow A + B^+ + e^-. \quad (45.7)$$

Ion pair formation:

$$A^*(\gamma) + B \rightarrow A^+ + B^-. \quad (45.8)$$

Dissociative attachment:

$$A^*(\gamma) + BC \rightarrow A^+B^- + C. \quad (45.9)$$

45.2 GENERAL PROPERTIES OF RYDBERG STATES

Table 45.1 displays the general n -dependence of a number of key properties of Rydberg States and some specific representative values for hydrogen.

45.2.1 Dipole Moments

Definition: $D_{i \rightarrow f} = -eX_{i \rightarrow f}$ where

$$X_{i \rightarrow f} = \langle \phi_f | \sum_j e^{ik \cdot r_j} r_j | \phi_i \rangle. \quad (45.10)$$

Table 45.1. General n -dependence of characteristic properties of Rydberg states. Adapted from Ref. [1].

Property	n -Dependence	$n = 10$	$n = 100$	$n = 500$	$n = 1000$
Radius (cm)	$n^2 a_0 / Z$	5.3×10^{-7}	5.3×10^{-5}	1.3×10^{-3}	5.3×10^{-3}
Velocity (cm/s)	$v_B Z / n$	2.18×10^7	2.18×10^6	4.4×10^5	2.18×10^5
Area (cm ²)	$\pi a_0^2 n^4 / Z^2$	8.8×10^{-13}	8.8×10^{-9}	5.5×10^{-6}	8.8×10^{-5}
Ionization potential (eV)	$Z^2 R_\infty / n^2$	1.36×10^{-1}	1.36×10^{-3}	5.44×10^{-5}	1.36×10^{-6}
Radiative lifetime (s) ^a	$n^5 [3 \ln n - \frac{1}{4}] / (A_0 Z^4)$	8.4×10^{-5}	17	7.3×10^4	7.22 hours
Period of classical motion (s)	$2\pi / \omega_{n,n\pm 1} = \hbar n^3 / (2Z^2 R_\infty)$	1.5×10^{-13}	1.5×10^{-10}	1.9×10^{-8}	1.5×10^{-7}
Transition frequency (s ⁻¹)	$\omega_{n,n\pm 1} = 2Z^2 R_\infty / (\hbar n^3)$	4.1×10^{13}	4.1×10^{10}	3.3×10^8	4.1×10^7
Wavelength (cm)	$\lambda_{n,n\pm 1} = 2\pi c / \omega_{n,n\pm 1}$	4.6×10^{-3}	4.6	570	4560.9

$$^a A_0 = [8\alpha^3 / (3\sqrt{3}\pi)] (v_B / a_0)$$

Hydrogenic Dipole Moments: See Bethe and Salpeter [2] and the references by Khandelwal and co-workers [3–6] for details and tables.

Exact Expressions: In the limit $|k| \rightarrow 0$, the dipole allowed transitions summed over final states are

$$|X_{1s \rightarrow n}|^2 = \frac{2^8 n^7 (n-1)^{2n-5}}{3 (n+1)^{2n+5}}, \quad (45.11a)$$

$$|X_{2s \rightarrow n}|^2 = \frac{2^5 \left(\frac{1}{2} - \frac{1}{n}\right)^{2n-7}}{3n^3 \left(\frac{1}{2} + \frac{1}{n}\right)^{2n+7}} \left(\frac{1}{4} - \frac{1}{n^2}\right) \left(1 - \frac{1}{n^2}\right), \quad (45.11b)$$

$$|X_{2p \rightarrow n}|^2 = \frac{2^5}{144} \frac{1}{n^3} \left(\frac{1}{2} - \frac{1}{n}\right)^{2n-7} \left(11 - \frac{12}{n^2}\right). \quad (45.11c)$$

Asymptotic Expressions: For $n \gg 1$,

$$n^3 |X_{1s \rightarrow n}|^2 \sim 1.563 + \frac{5.731}{n^2} + \frac{13.163}{n^4} + \frac{24.295}{n^6} + \frac{39.426}{n^8} + \frac{58.808}{n^{10}}, \quad (45.12a)$$

$$n^3 |X_{2s \rightarrow n}|^2 \sim 14.658 + \frac{180.785}{n^2} + \frac{1435.854}{n^4} + \frac{9341.634}{n^6} + \frac{54208.306}{n^8} + \frac{292202.232}{n^{10}}, \quad (45.12b)$$

$$n^3 |X_{2p \rightarrow n}|^2 \sim 13.437 + \frac{218.245}{n^2} + \frac{2172.891}{n^4} + \frac{17118.786}{n^6} + \frac{117251.682}{n^8} + \frac{731427.003}{n^{10}}. \quad (45.12c)$$

45.2.2 Radial Integrals

Definition:

$$R_{n\ell}^{n'\ell'} \equiv \int_0^\infty R_{n\ell}(r) r R_{n'\ell'}(r) r^2 dr, \quad (45.13)$$

where $R_{n\ell}(r)$ are solutions to the radial Schrödinger equation. See Chap. ?? for specific representations of $R_{n\ell}$ for hydrogen.

Exact Results for Hydrogen: For $\ell' = \ell - 1$ and $n \neq n'$ [7],

$$R_{n\ell}^{n'\ell-1} = \frac{a_0}{Z} \frac{(-1)^{n'-\ell} (4nn')^{\ell+1} (n-n')^{n+n'-2\ell-2}}{4(2\ell-1)!(n+n')^{n+n'}} \times \left[\frac{(n+\ell)!(n'+\ell-1)!}{(n'+\ell')!(n-\ell-1)!} \right]^{1/2} \times \left\{ {}_2F_1(-n+\ell+1, -n'+\ell; 2\ell; Y) - \left(\frac{n-n'}{n+n'} \right)^2 {}_2F_1(-n+\ell-1, -n'+\ell; 2\ell; Y) \right\}, \quad (45.14)$$

where $Y = -4nn'/(n-n')^2$. For $n = n'$,

$$R_{n\ell}^{n\ell-1} = (a_0/Z) \frac{3}{2} n \sqrt{n^2 - \ell^2}. \quad (45.15)$$

Semiclassical Quantum Defect Representation: (see Ref. [8]).

$$|R_{n\ell}^{n'\ell'}|^2 = \left(\frac{a_0}{Z} \right)^2 \left| \frac{n_c^2}{2\Delta} \left[\left(1 - \frac{\Delta\ell\ell_{>}}{n_c} \right) J_{\Delta-1}(-x) - \left(1 + \frac{\Delta\ell\ell_{>}}{n_c} \right) J_{\Delta+1}(-x) + \frac{2}{\pi} \sin(\pi\Delta)(1-e) \right] \right|^2, \quad (45.16)$$

where

$$n_c = 2n^* n'^* / (n^* + n'^*), \quad (45.17a)$$

$$\Delta = n'^* - n^*, \quad (45.17b)$$

$$\Delta\ell = \ell' - \ell, \quad \ell_{>} = \max(\ell, \ell'), \quad (45.17c)$$

$$x = e\Delta, \quad e = \sqrt{1 - (\ell_{>}/n_c)^2}, \quad (45.17d)$$

and $J_n(y)$ is the Anger function.

The energies of the states $n\ell$ and $n'\ell'$ are given in terms of the quantum defects by

$$E_{n\ell} = -Z^2 R_{\infty} / n^{*2}, \quad n^* = n - \delta_{\ell}, \quad (45.18a)$$

$$E_{n'\ell'} = -Z^2 R_{\infty} / n'^{*2}, \quad n'^* = n' - \delta_{\ell'}. \quad (45.18b)$$

Sum Rule: For hydrogen

$$\sum_{n'} |R_{n\ell}^{n'\ell'-1}|^2 = \sum_{n'} |R_{n\ell}^{n'\ell'+1}|^2 \quad (45.19a)$$

$$= \frac{n^2 a_0^2}{2 Z^2} [5n^2 + 1 - 3\ell(\ell+1)]. \quad (45.19b)$$

See §61 of Ref. [2] for additional sum rules.

45.2.3 Line Strengths

Definition:

$$S(n'\ell', n\ell) = e^2 (2\ell+1) |r_{n'\ell', n\ell}|^2 \quad (45.20a)$$

$$= e^2 \max(\ell, \ell') |R_{n\ell}^{n'\ell'}|^2, \quad (45.20b)$$

where $\ell' = \ell \pm 1$. For hydrogen

$$S(n', n) = 32 \left(\frac{ea_0}{Z} \right)^2 (nn')^6 \frac{(n-n')^{2(n+n')-3}}{(n+n')^{2(n+n')+4}} \times \{ [{}_2F_1(-n', -n+1; 1; Y)]^2 - [{}_2F_1(-n'+1, -n; 1; Y)]^2 \}, \quad (45.21)$$

where $Y = -4nn'/(n-n')^2$.

Semiclassical Representation: [9]

$$S(n', n) = \frac{32}{\pi\sqrt{3}} \left(\frac{ea_0}{Z} \right)^2 \frac{(\varepsilon\varepsilon')^{3/2}}{(\varepsilon - \varepsilon')^4} G(\Delta n), \quad (45.22)$$

where $\varepsilon = 1/n^2$, $\varepsilon' = 1/n'^2$, and the *Gaunt factor* $G(\Delta n)$ is given by

$$G(\Delta n) = \pi\sqrt{3} |\Delta n| J_{\Delta n}(\Delta n) J'_{\Delta n}(\Delta n). \quad (45.23)$$

where the prime on the Anger function denotes differentiation with respect to the argument Δn . Equation (45.23) can be approximated to within 2% by the expression

$$1 - \frac{1}{4|\Delta n|}. \quad (45.24)$$

Relation to Oscillator Strength:

$$S(n', n) = \sum_{\ell, \ell'} S(n'\ell', n\ell) = 3e^2 a_0^2 \frac{R_{\infty}}{\hbar\omega} \sum_{\ell, \ell'} f_{n'\ell', n\ell}, \quad (45.25)$$

$$(45.26)$$

Connection with Radial Integral:

$$-f_{n'\ell', n\ell} = \frac{\hbar\omega}{3R_{\infty}} \frac{\max(\ell, \ell')}{(2\ell+1)} |R_{n\ell}^{n'\ell'}|^2. \quad (45.27)$$

Density of Line Strengths: For bound-free $n\ell \rightarrow E\ell'$ transitions in a Coulomb field, the semiclassical representation [1] is

$$\frac{d}{dE} S(n\ell, E) = 2n(2\ell+1) \left(\frac{R_{\infty}}{\hbar\omega} \right)^2 \left[J'_{\Delta}(e\Delta)^2 + \left(1 - \frac{1}{e^2} \right) J_{\Delta}(e\Delta)^2 \right] \frac{e^2 a_0^2}{R_{\infty}}, \quad (45.28)$$

where $\Delta = \hbar\omega n^3 / 2R_{\infty}$ and $e = \sqrt{1 - (\ell + \frac{1}{2})^2 / n^2}$.

Asymptotic Expression for $\Delta \gg 1$:

$$\frac{d}{dE} S(n\ell, E) = \frac{2(2\ell+1)}{3\pi^2} \left(\frac{R_{\infty}}{\hbar\omega} \right)^2 \frac{(\ell + \frac{1}{2})^4}{n^3} \times [K_{1/3}^2(\eta) + K_{2/3}^2(\eta)] \frac{e^2 a_0^2}{R_{\infty}}, \quad (45.29)$$

where $\eta = (E/R_{\infty})(\ell + 1/2)^3/6$ and the $K_{\nu}(x)$ are Bessel functions of the third kind.

Line Strength of Line n :

$$S_n \equiv S(n) = \sum_{k \neq 0} S(n+k, n) \frac{1}{k^3}. \quad (45.30)$$

Born Approximation to Line Strength S_n : [1]

$$S_n^B = \frac{Z^2 R_{\infty}}{E} \left\{ \frac{1}{2} \ln(1 + \varepsilon_e / \varepsilon) \sum_{k \neq 0} \left(1 - \frac{1}{4k} \right) \frac{1}{k^4} + \frac{4}{3} \frac{\varepsilon_e}{\varepsilon + \varepsilon_e} \sum_{k \neq 0} \left(1 - \frac{0.60}{k} \right) \frac{1}{k^3} \right\} = \frac{Z^2 R_{\infty}}{E} \left[0.82 \ln \left(1 + \frac{\varepsilon_e}{\varepsilon} \right) + \frac{1.47 \varepsilon_e}{\varepsilon + \varepsilon_e} \right], \quad (45.31)$$

where $\varepsilon = |E_n| Z^2 / R_{\infty}$ and $\varepsilon_e = \varepsilon / Z^2 R_{\infty}$.

45.2.4 Form Factors

$$F_{n'n}(Q) = \sum_{\ell, m} \sum_{\ell', m'} |\langle n\ell m | e^{i\mathbf{Q} \cdot \mathbf{r}} | n'\ell' m' \rangle|^2. \quad (45.32)$$

Connection with Generalized Oscillator Strengths:

$$f_{n'n}(Q) = \frac{Z^2 \Delta E}{n^2 Q^2 a_0^2} F_{n'n}(Q). \quad (45.33)$$

Semiclassical Limit:

$$\lim_{Q \rightarrow 0} f_{n'n}(Q) = \frac{32}{3n^2} \left[\frac{nn'}{\Delta n(n+n')} \right]^3 \Delta n J_{\Delta n}(\Delta n) J'_{\Delta n}(\Delta n) \quad (45.34)$$

where $J_m(y)$ denotes the Bessel function.

Representation as Microcanonical Distribution:

$$F_{n',n\ell}(Q) = (2\ell + 1) \frac{2Z^2 R_\infty}{n'^3} \int d\mathbf{p} |g_{n\ell}(p)|^2 \times \delta \left(\frac{(\mathbf{p} - \hbar \mathbf{Q})^2}{2m} - \frac{p^2}{2m} - E_{n'} - E_{n\ell} \right), \quad (45.35)$$

$$F_{n',n}(Q) = \frac{4Z^2 R_\infty^2}{(nn')^3} \int \frac{d\mathbf{p} d\mathbf{r}}{(2\pi\hbar)^3} \delta \left(\frac{p^2}{2m} - \frac{Ze^2}{r} - E_n \right) \times \delta \left[\frac{(\mathbf{p} - \hbar \mathbf{Q})^2}{2m} - \frac{Ze^2}{r} - E_{n'} \right], \quad (45.36)$$

$$= \frac{2^9}{3\pi(nn')^3} \frac{\kappa^5}{(\kappa^2 + \kappa_+^2)^3 (\kappa^2 + \kappa_-^2)^3}, \quad (45.37)$$

where $\kappa = Qa_0/Z$ and $\kappa_\pm = |1/n \pm 1/n'|$.

45.2.5 Impact Broadening

The total broadening cross section of a level n is

$$\sigma_n = (\pi a_0^2 / Z^4) n^4 S_n. \quad (45.38)$$

The width of a line $n \rightarrow n+k$ is [10]

$$\gamma_{n,n+k} = n_e [\langle v\sigma_n \rangle + \langle v\sigma_{n+k} \rangle], \quad (45.39)$$

where n_e is the number density of electrons, and

$$\langle v\sigma_n \rangle = \sum_{k \neq 0} \langle v\sigma_{n+k,n} \rangle = \frac{n^4}{Z^3} K_n \quad (45.40a)$$

$$= \frac{n^4 \pi a_0^2 v_B}{Z^3 \theta^{3/2}} \int_0^\infty e^{-E/k_B T} S_n \frac{E dE}{(Z^2 R_\infty)^2}, \quad (45.40b)$$

where $\theta = k_B T / Z^2 R_\infty$. See Chap. ?? for collisional line broadening.

45.3 CORRESPONDENCE PRINCIPLES

These are used to connect quantum mechanical observables with the corresponding classical quantities in the limit of large n . See Ref. [11] for details on the equations in this section.

45.3.1 Bohr-Sommerfeld Quantization

$$A_i = J_i \Delta w_i \oint p_i dq_i = 2\pi\hbar(n_i + \alpha_i), \quad (45.41)$$

where $n_i = 0, 1, 2, \dots$ and $\alpha_i = 0$ if the generalized coordinate q_i represents rotation, and $\alpha_i = 1/2$ if q_i represents a libration.

45.3.2 Bohr Correspondence Principle

$$E_{n+s} - E_n = h\nu_{n+s,n} \sim s\hbar\omega_n, \quad s = 1, 2, \dots \ll n, \quad (45.42)$$

where $\nu_{n+s,n}$ is the line emission frequency and ω_n is the angular frequency of classical orbital motion. The number of states with quantum numbers in the range Δn is

$$\Delta N = \prod_{i=1}^D \Delta n = \prod_{i=1}^D (\Delta J_i \Delta w_i) / (2\pi\hbar)^D \\ = \prod_{i=1}^D (\Delta p_i \Delta q_i) / (2\pi\hbar)^D, \quad (45.43)$$

for systems with D degrees of freedom, and the mean value \bar{F} of a physical quantity $F(q)$ in the quantum state Ψ is

$$\bar{F} = \langle \Psi | F(q) | \Psi \rangle = \sum_{n,m} a_m^* a_n F_{mn}^{(q)} e^{i\omega_{mn}t}, \quad (45.44)$$

where the $F_{mn}^{(q)}$ are the quantal matrix elements between time independent states.

The first order S-matrix is

$$S_{fi} = -\frac{i\omega}{2\pi\hbar} \int_{-\infty}^{\infty} dt \int_0^{2\pi/\omega} V[\mathbf{R}(t), \mathbf{r}(t_1)] e^{is\omega(t_1-t)} dt_1, \quad (45.45)$$

where \mathbf{R} denotes the classical path of the projectile and \mathbf{r} the orbital of the Rydberg electron.

45.3.3 Heisenberg Correspondence Principle

For one degree of freedom [11],

$$F_{mn}^{(q)}(\mathbf{R}) = \int_0^\infty \phi_m^*(\mathbf{r}) F(\mathbf{r}, \mathbf{R}) \phi_n(\mathbf{r}) d\mathbf{r} \quad (45.46)$$

$$= \frac{\omega}{2\pi} \int_0^{2\pi/\omega} F^{(c)}[\mathbf{r}(t)] e^{is\omega t} dt. \quad (45.47)$$

The three-dimensional generalization is [11]

$$F_{\mathbf{n},\mathbf{n}'}^{(q)} \sim F_{\mathbf{s}}^{(c)}(\mathbf{J}) = \frac{1}{8\pi^3} \int F^{(c)}[\mathbf{r}(\mathbf{J}, \mathbf{w})] e^{is \cdot \mathbf{w}} d\mathbf{w}, \quad (45.48)$$

where \mathbf{n} , \mathbf{n}' denotes the triple of quantum numbers (n, ℓ, m) , (n', ℓ', m') , respectively, and $\mathbf{s} = \mathbf{n} - \mathbf{n}'$.

The correspondence between the three dimensional quantal and classical matrix elements in (45.48) follows from the general Fourier expansion for any classical function $F^{(c)}(\mathbf{r})$ periodic in \mathbf{r} ,

$$F^{(c)}[\mathbf{r}(t)] = \sum_{\mathbf{s}} F_{\mathbf{s}}^{(c)}(\mathbf{J}) \exp(-i\mathbf{s} \cdot \mathbf{w}). \quad (45.49)$$

where \mathbf{J}, \mathbf{w} denotes the action-angle conjugate variables for the motion. For the three dimensional Coulomb problem, the action-angle variables are

$$\begin{aligned} J_n &= n\hbar, & w_n &= \left(\frac{\partial E}{\partial J_n}\right) t + \delta, \\ J_\ell &= (\ell + \frac{1}{2})\hbar, & w_\ell &= \psi_E, \\ J_m &= m\hbar, & w_m &= \phi_E, \end{aligned} \quad (45.50)$$

where ψ_E is the Euler angle between the line of nodes and a direction in the plane of the orbit (usually taken to be the direction of the perihelion or perigee), and is constant for a Coulomb potential. The Euler angle ϕ_E is the angle between the line of nodes and the fixed x -axis. See Ref. [11] for details.

The first order S-matrix is

$$S_{fi} = -\frac{i\omega}{2\pi\hbar} \int_0^{2\pi/\omega} dt_e \int_{-\infty}^{\infty} dt V[\mathbf{R}(t), \mathbf{r}(t+t_e)] e^{i s \omega t_e}, \quad (45.51)$$

with $s = i - f$, \mathbf{R} is the classical path of projectile, and $\mathbf{r}(t_e)$ is the classical internal motion of the Rydberg electron.

45.3.4 Strong Coupling Correspondence Principle

The S-matrix is

$$S_{fi} = \frac{\omega}{2\pi} \int_0^{2\pi/\omega} dt_e \exp \left\{ i(s\omega t_e) - \frac{i}{\hbar} \int_{-\infty}^{\infty} V[\mathbf{R}(t), \mathbf{r}(t+t_e)] dt \right\}. \quad (45.52)$$

See Refs. [11-14] for additional details.

45.3.5 Equivalent Oscillator Theorem

$$\sum_n a_n(t) V_{fn}(t) e^{i\omega_f t} = \sum_{d=-f}^f a_{d+f}(t) V_d(t) e^{-i d \omega t}. \quad (45.53)$$

The S-matrix is

$$\begin{aligned} S_{\mathbf{n}', \mathbf{n}} &= a_{\mathbf{n}'}(t \rightarrow \infty) \\ &= \int_0^{2\pi} \frac{d\mathbf{w}}{8\pi^3} \exp \left[i\mathbf{s} \cdot \mathbf{w} - \frac{i}{\hbar} \int_{-\infty}^{\infty} V(\mathbf{w} + \omega t, t) dt \right]. \end{aligned} \quad (45.54)$$

45.4 DISTRIBUTION FUNCTIONS

The function $W_\alpha(x)dx$ characterizes the probability (distribution) of finding an electron in a Rydberg orbital α within a volume dx centered at the point x in phase space. Integration of the distribution function W_α over all phase space volumes dx yields, depending upon the normalization chosen, either unity or the density of states appropriate to the orbital α .

45.4.1 Spatial Distributions

Distribution over n, ℓ, m [1]:

$$\begin{aligned} W_{n\ell m}(\mathbf{r}, \theta) r^2 \sin \theta dr d\theta \\ = \frac{r^2 \sin \theta dr d\theta}{\pi^2 a^2 r \{ [e^2 - (1 - r/a)^2] [\sin^2 \theta - (m/\ell)^2] \}^{1/2}}, \end{aligned} \quad (45.55)$$

where $a = Ze^2/2|E| = n^2\hbar^2/mZe^2\hbar^2$ is the semimajor axis, and $e^2 = 1 - (\ell/n)^2$ is the eccentricity.

Distribution over n, ℓ :

$$\begin{aligned} W_{n\ell}(\mathbf{r}, \theta) r^2 \sin \theta dr d\theta \\ = g(n\ell) \frac{r^2 \sin \theta dr d\theta}{2\pi a^2 r [e^2 - (1 - r/a)^2]^{1/2}}, \end{aligned} \quad (45.56)$$

where $g(n\ell) = 2\ell$.

Distribution over n :

$$W_n(\mathbf{r}) r^2 dr = g(n) \frac{2}{\pi} \left[1 - \left(1 - \frac{r}{a} \right)^2 \right]^{1/2} \frac{r dr}{a^2}, \quad (45.57)$$

with $g(n) = n^2$.

45.4.2 Momentum Distributions

Distribution over n, ℓ [1]:

$$W_{n\ell}(p) p^2 dp = g(n\ell) \frac{4}{\pi} \frac{dx}{(1+x^2)^2}, \quad (45.58)$$

where $x = p/p_n$ and $p_n^2 = 2m|E|$.

Distribution over n :

$$W_n(p) p^2 dp = g(n) \frac{32}{\pi} \frac{x^2 dx}{(1+x^2)^4}. \quad (45.59)$$

Sum Rules:

$$\frac{1}{n^2} \sum_{\ell, m} |G_{n\ell m}(\mathbf{k})|^2 = \left(\frac{na_0}{Z} \right)^3 \frac{8}{\pi^2 (x^2 + 1)^4}, \quad (45.60a)$$

$$\frac{1}{n^2} \sum_{\ell=0}^{n-1} (2\ell+1) |g_{n\ell}(k)|^2 k^2 = \frac{32na_0 x^2}{\pi Z (x^2 + 1)^4}, \quad (45.60b)$$

where $x = nka_0/Z$, and

$$G_{nlm}(\mathbf{k}) = g_{nl}(k) Y_{lm}(\hat{\mathbf{k}}), \quad (45.61a)$$

$$g_{nl}(k) = \left(\frac{2(n-\ell-1)!}{\pi(n+\ell)!} \right)^{1/2} \left(\frac{a_0}{Z} \right)^{3/2} 2^{2(\ell+1)} n^2 \ell! \\ \times \frac{(-ix)^\ell}{(x^2+1)^{\ell+2}} C_{n-\ell-1}^{(\ell+1)} \left(\frac{x^2-1}{x^2+1} \right), \quad (45.61b)$$

where $C_i^{(j)}(y)$ is the associated Gegenbauer polynomial. See Chap. ?? for additional details on hydrogenic wave functions.

Quantum Defect Representation: [15]

$$g_{nl}(k) = - \left[\frac{2}{\pi} \frac{\Gamma(n^*-1)}{\Gamma(n^*+\ell+1)} \right]^{1/2} n^* (a_0/Z)^{3/2} 2^{2(\ell+1)} \\ \times \frac{(\ell+1)!(-ix)^\ell}{(x^2+1)^{\ell+2}} \mathcal{J}(n^*, \ell+1; X), \quad (45.62)$$

where $n^* = n - \delta$, δ being the quantum defect, and $x = n^* k a_0 / Z$. The function \mathcal{J} is given by the recurrence relation

$$\mathcal{J}(n^*, \ell+1; X) = - \frac{1}{2(2\ell+2)} \frac{\partial}{\partial X} \mathcal{J}(n^*, \ell; X), \quad (45.63) \\ \mathcal{J}(n^*, 0; X) = - \frac{n^* \sin[n^*(\beta - \pi)]}{\sin(\beta - \pi)} \\ - \frac{\sin n^* \pi}{\pi} \int_0^1 \frac{(1-s^2)s^{n^*}}{(1-2Xs+s^2)} ds, \quad (45.64)$$

where $X = (x^2 - 1)/(x^2 + 1)$, and $\beta = \cos^{-1} X$. In the limit $\ell \ll n^*$, Eq. (45.62) becomes

$$|g_{nl}(k)|^2 = 4 \left(\frac{n^* a_0}{Z} \right)^3 \frac{1 - (-1)^\ell \cos[2n^*(\beta - \pi)]}{\pi x^2 (x^2 + 1)^2}. \quad (45.65)$$

Classical Density of States:

$$\rho(E) = \int \delta[E - H(\mathbf{p}, \mathbf{r})] \frac{d\mathbf{p} d\mathbf{r}}{(2\pi\hbar)^3} = \frac{n^5 \hbar^2}{m Z^2 e^4}. \quad (45.66)$$

45.5 CLASSICAL THEORY

The classical cross section for energy transfer ΔE between two particles, with arbitrary masses m_1, m_2 and charges Z_1, Z_2 , is given by [16]

$$\sigma_{\Delta E}(\mathbf{v}_1, \mathbf{v}_2) = \frac{2\pi(Z_1 Z_2 e^2 V)^2}{v^2 |\Delta E|^3} \left[1 + \cos^2 \bar{\theta} + \frac{\Delta E}{\mu v V} \cos \bar{\theta} \right] \quad (45.67)$$

valid for $-1 \leq \cos \bar{\theta} - \Delta E/(\mu v V) \leq 1$, and $\sigma_{\Delta E}(\mathbf{v}_1, \mathbf{v}_2) = 0$ otherwise, where

$$\mathbf{v} = \mathbf{v}_1 - \mathbf{v}_2, \quad (45.68a)$$

$$\mathbf{V} = (m_1 \mathbf{v}_1 + m_2 \mathbf{v}_2)/M, \quad (45.68b)$$

$$\cos \bar{\theta} = \frac{1}{vV} \mathbf{v} \cdot \mathbf{V}, \quad (45.68c)$$

and $\mu = m_1 m_2 / M$, $M = m_1 + m_2$. If particle 2 has an isotropic velocity distribution in the lab frame, the effective cross section averaged over the direction $\hat{\mathbf{n}}_2$ of \mathbf{v}_2 is

$$v_1 \sigma_{\Delta E}^{\text{eff}}(\mathbf{v}_1, \mathbf{v}_2) = \frac{1}{4\pi} \int d\hat{\mathbf{n}}_2 |\mathbf{v}_1 - v_2 \hat{\mathbf{n}}_2| \sigma_{\Delta E}(\mathbf{v}_1, \mathbf{v}_2). \quad (45.69)$$

If \mathbf{v}_1 is also isotropic, then the average of (45.69), together with (45.67), gives for the special case of a Coulomb potential

$$\sigma_{\Delta E}^{\text{eff}}(\mathbf{v}_1, \mathbf{v}_2) = \frac{\pi(Z_1 Z_2 e^2)^2}{4|\Delta E|^3 v_1^2 v_2} \left[(v_1^2 - v_2^2)(v_2'^2 - v_1'^2)(v_1^{-1} - v_u^{-1}) \right. \\ \left. + (v_1^2 + v_2^2 + v_1'^2 + v_2'^2)(v_u - v_\ell) - \frac{1}{3}(v_u^3 - v_\ell^3) \right], \quad (45.70)$$

$$\text{where } v_1' = (v_1^2 - 2\Delta E/m_1)^{1/2}, \quad (45.71)$$

$$v_2' = (v_2^2 + 2\Delta E/m_2)^{1/2}, \quad (45.72)$$

and v_u, v_ℓ are defined below for cases (1)–(4). With the definitions

$$\Delta \varepsilon_{12} = 4m_1 m_2 (E_1 - E_2)/M^2, \quad \Delta m_{12} = |m_1 - m_2|,$$

$$\Delta \tilde{\varepsilon}_{12} = \frac{4m_1 m_2}{M^2} \left(E_1 \frac{v_2}{v_1} - E_2 \frac{v_1}{v_2} \right),$$

the four cases are

$$(1) \quad \Delta E \geq \Delta \varepsilon_{12} + |\Delta \tilde{\varepsilon}_{12}| \geq 0, \text{ and } 2m_2 v_2 \geq \Delta m_{12} v_1:$$

$$v_\ell = v_2' - v_1', \quad v_u = v_1' + v_2', \quad \Delta E \geq 0; \quad (45.73a)$$

$$v_\ell = v_2 - v_1, \quad v_u = v_1 + v_2, \quad \Delta E \leq 0. \quad (45.73b)$$

If $2m_2 v_2 < \Delta m_{12} v_1$, then $\sigma_{\Delta E}^{\text{eff}}(\mathbf{v}_1, \mathbf{v}_2) = 0$,

$$(2) \quad \Delta \varepsilon_{12} - \Delta \tilde{\varepsilon}_{12} \leq \Delta E \leq \Delta \varepsilon_{12} + \Delta \tilde{\varepsilon}_{12}, \text{ and } m_1 > m_2:$$

$$v_\ell = v_2' - v_1', \quad v_u = v_1 + v_2, \quad \Delta E \geq 0; \quad (45.73c)$$

$$v_\ell = v_2 - v_1, \quad v_u = v_1' + v_2', \quad \Delta E \leq 0 \quad (45.73d)$$

$$(3) \quad \Delta E \leq \Delta \varepsilon_{12} - |\Delta \tilde{\varepsilon}_{12}| \leq 0, \text{ and } 2m_1 v_1 \geq \Delta m_{12} v_2:$$

$$v_\ell = v_1 - v_2, \quad v_u = v_1 + v_2, \quad \Delta E \geq 0; \quad (45.73e)$$

$$v_\ell = v_1' - v_2', \quad v_u = v_1' + v_2', \quad \Delta E \leq 0. \quad (45.73f)$$

If $2m_1 v_1 < \Delta m_{12} v_2$ then $\sigma_{\Delta E}^{\text{eff}}(\mathbf{v}_1, \mathbf{v}_2) = 0$,

(4) $\Delta\epsilon_{12} + \Delta\tilde{\epsilon}_{12} \leq \Delta E \leq \Delta\epsilon_{12} - \Delta\tilde{\epsilon}_{12}$, and $m_1 < m_2$:

$$v_l = v_1 - v_2, \quad v_u = v'_1 + v'_2, \quad \Delta E \geq 0; \quad (45.73g)$$

$$v_l = v'_1 - v'_2, \quad v_u = v_1 + v_2, \quad \Delta E \leq 0. \quad (45.73h)$$

If $2m_1v_1 < \Delta m_{12}v_2$ then $\sigma_{\Delta E}^{\text{eff}}(v_1, v_2) = 0$.

Since v'_1 and v'_2 , given by (45.71) and (45.72) respectively, must be real, $\sigma_{\Delta E}(v_1, v_2) = 0$ for ΔE outside the range

$$-\frac{1}{2}m_2v_2^2 \leq \Delta E \leq \frac{1}{2}m_1v_1^2, \quad (45.74)$$

which simply expresses the fact that the particle losing energy in the collision cannot lose more than its initial kinetic energy.

The cross section (45.70) must be integrated over the classically allowed range of energy transfer ΔE and averaged over a prescribed speed distribution $W(v_2)$ before comparison with experiment can be made. See Refs. [16, 34] for details.

Classical Removal Cross Section [17]. The cross section for removal of an electron from a shell is given by

$$\sigma_r(V) = \int_0^\infty f(v) \sigma_{\Delta E}(v_1, v_2) dv. \quad (45.75)$$

Total Removal Cross Section [17]. In an independent electron model,

$$\sigma_r^{\text{total}}(V) = N_{\text{shell}} \sigma_r(V), \quad (45.76)$$

where N_{shell} is the number of equivalent electrons in a shell. In a shielding model,

$$\sigma_r^{\text{total}}(V) = \left[1 - \frac{(N_{\text{shell}} - 1)}{4\pi\bar{r}^2} \sigma_r(V) \right] N_{\text{shell}} \sigma_r(V), \quad (45.77)$$

where \bar{r}^2 is the root mean square distance between electrons within a shell. Experiment [18] favors (45.77) over (45.76). See Fig. 4a-e of Ref. [17] for details.

Classical trajectory and Monte-Carlo methods are covered in Chap. ??.

45.6 WORKING FORMULAE FOR RYDBERG COLLISIONS

45.6.1 Inelastic n, ℓ -Changing Transitions

$$A^*(n\ell) + B \rightarrow A^*(n') + B + \Delta E_{n',n\ell}, \quad (45.78)$$

where $\Delta E_{n',n\ell} = E_{n'} - E_{n\ell}$ is the energy defect. The cross section for (45.78) in the *quasi-free electron model* [19] is

$$\sigma_{n',n\ell}(V) = \frac{2\pi a_s^2}{(V/v_B)^2 n'^3} f_{n',n\ell}(\lambda), \quad \ell \ll n, \quad (45.79)$$

where a_s is the scattering length for $e^- + B$ scattering, $\lambda = n^* a_0 \omega_{n',n\ell} / V$, $\omega_{n',n\ell} = |\Delta E_{n',n\ell}| / \hbar$, $E_{n'} = -R_\infty / n'^2$, and $E_{n\ell} = -R_\infty / n^2$, with $n^* = n - \delta_\ell$. Also, v_B is the atomic unit of velocity, and

$$f_{n',n\ell}(\lambda) = \frac{2}{\pi} \left[\tan^{-1} \left(\frac{2}{\lambda} \right) - \frac{\lambda}{2} \ln \left(1 + \frac{4}{\lambda^2} \right) \right]. \quad (45.80)$$

Limiting cases: $f_{n',n\ell}(\lambda) \rightarrow 1$ as $\lambda \rightarrow 0$, and $f_{n',n\ell}(\lambda) \sim 8/(3\pi\lambda^3)$ for $\lambda \gg 1$. Then

$$\sigma_{n',n\ell} \sim \begin{cases} \frac{2\pi a_s^2}{(V/v_B)^2 n'^3}, & \lambda \rightarrow 0 \\ \frac{16a_s^2 V n^3}{3v_B |\delta_\ell + \Delta n|^3}, & \lambda \gg 1 \end{cases} \quad (45.81)$$

Rate Coefficients:

$$\langle \sigma_{n',n\ell}(V) \rangle \equiv \langle V \sigma_{n',n\ell}(V) \rangle / \langle V \rangle \quad (45.82a)$$

$$= \frac{2\pi a_s^2}{(V_T/v_B)^2 n'^3} \varphi_{n',n\ell}(\lambda_T), \quad (45.82b)$$

where $V_T = \sqrt{2k_B T / \mu}$, $\lambda_T = n^* a_0 \omega_{n',n\ell} / V_T$, $\Delta n = n' - n$, and μ is the reduced mass of $A-B$. The function $\varphi_{n',n\ell}(\lambda_T)$ in (45.82b) is given by

$$\varphi_{n',n\ell}(\lambda_T) = e^{\lambda_T^2/4} \text{erfc} \left(\frac{1}{2} \lambda_T \right) - \frac{\lambda_T}{\pi} \int_0^\infty \frac{du}{\sqrt{u}} e^{-u} \ln \left(1 + \frac{4}{\lambda_T^2} \right) \quad (45.83a)$$

$$= \begin{cases} 1 - \frac{\lambda_T}{\sqrt{\pi}} \ln(1/\lambda_T^2), & \lambda_T \rightarrow 0 \\ 2/(\sqrt{\pi}\lambda_T^3), & \lambda_T \gg 1 \end{cases} \quad (45.83b)$$

and $\text{erfc}(x)$ is the complementary error function.

45.6.2 Inelastic $n \rightarrow n'$ Transitions

$$A^*(n) + B \rightarrow A^*(n') + B + \Delta E_{n',n}. \quad (45.84)$$

(A) Cross Sections:

$$\sigma_{n'n} = \sum_{\ell'} \frac{(2\ell + 1)}{n^2} \sigma_{n'\ell',n\ell}, \quad (45.85)$$

$$\sigma_{n',n}(V) = \frac{2\pi a_s^2}{(V/v_B)^2 n'^3} F_{n',n}(\lambda), \quad (45.86)$$

where $\lambda = n a_0 \omega_{n',n} / V = |\Delta n| v_B / (n^2 V)$, and

$$F_{n',n}(\lambda) = \frac{2}{\pi} \left[\tan^{-1} \left(\frac{2}{\lambda} \right) - \frac{2\lambda(3\lambda^2 + 20)}{3(4 + \lambda^2)^2} \right]. \quad (45.87)$$

Limiting cases:

$$\sigma_{n'n} \sim \begin{cases} \frac{2\pi a_s^2}{(V/v_B)^2 n'^3}, & \lambda \ll 1 \\ \frac{256\sigma_{e-B}^{\text{elastic}}(V/v_B)^3 n^7}{15\pi |\Delta n|^5}, & \lambda \gg 1 \end{cases} \quad (45.88)$$

where $\sigma_{e^-B}^{\text{elastic}}$ is the elastic cross section for $e^- + B$ scattering.

(B) Rate Coefficients:

$$K_{n'l',nl}(T) = \langle V \sigma_{n'l',nl} \rangle, \quad (45.89a)$$

$$K_{n'n}(T) = \sum_{l,l'} \frac{(2l+1)}{n^2} K_{n'l',nl}, \quad (45.89b)$$

$$K_{n'n}(T) = \frac{v_B \sigma_{e^-B}^{\text{elastic}}}{\sqrt{\pi} n^3 (V_T/v_B)} \Phi_{n'n}(\lambda_T), \quad (45.89c)$$

where

$$\Phi_{n'n}(\lambda_T) = e^{\lambda_T^2/8} \left\{ e^{\lambda_T^2/8} \text{erfc}\left(\frac{1}{2}\lambda_T\right) - \frac{\lambda_T^2}{\sqrt{2\pi}} D_{-3}\left(\frac{\lambda_T}{2}\right) - \frac{5\lambda_T}{\sqrt{\pi}} D_{-4}\left(\frac{\lambda_T}{\sqrt{2}}\right) \right\} \quad (45.90a)$$

$$\sim \begin{cases} 1 - 8\lambda_T/3\sqrt{\pi}, & \lambda_T \ll 1 \\ 2^6/(\sqrt{\pi}\lambda_T^5), & \lambda_T \gg 1 \end{cases}, \quad (45.90b)$$

where $D_{-\nu}(y)$ denotes the parabolic cylinder function.

Limiting cases:

$$K_{n'n}(T) \sim \begin{cases} \left(\frac{\mu R_\infty}{\pi m_e k_B T} \right)^{1/2} \frac{v_B \sigma_{e^-B}^{\text{elastic}}}{n^3}, & \lambda_T \rightarrow 0 \\ \frac{2^6 v_B \sigma_{e^-B}^{\text{elastic}} n^7}{\pi |\Delta n|^5} \left(\frac{2k_B T}{\mu v_B^2} \right)^2, & \lambda_T \gg 1. \end{cases} \quad (45.91)$$

Born Results:

$$\sigma_{n'n} = \frac{8\pi}{k^2} \frac{1}{n^2} \int_{|k-k'|}^{k+k'} F_{n'n}(Q) \frac{d(Qa_0)}{(Qa_0)^3}. \quad (45.92)$$

(A) Electron-Rydberg Atom Collision:

$$\sigma_{n'n} = \frac{8\pi a_0^2 R_\infty}{Z^2 E n^2} \left\{ \left[1 - \frac{1}{4\Delta n} \right] \frac{(\varepsilon\varepsilon')^{3/2}}{(\Delta\varepsilon)^4} \ln(1 + \varepsilon_e/\varepsilon) + \left[1 - \frac{0.6}{\Delta n} \right] \frac{\varepsilon_e}{\varepsilon + \varepsilon_e} \frac{(\varepsilon')^{3/2}}{(\Delta\varepsilon)^2} \left[\frac{4}{3\Delta n} + \frac{1}{\varepsilon} \right] \right\} \quad (45.93)$$

for $n' > n$, where $\varepsilon_e = E/(Z^2 R_\infty)$, $\varepsilon = 1/n^2$, $\varepsilon' = 1/n'^2$, and $\Delta\varepsilon = \varepsilon - \varepsilon'$.

(B) Heavy Particle-Rydberg Atom Collision:

$$\sigma_{n'n} = \frac{8\pi a_0^2 Z^2}{Z^4 n^2 \varepsilon_e} \left\{ \left[1 - \frac{1}{4\Delta n} \right] \frac{(\varepsilon\varepsilon')^{3/2}}{(\Delta\varepsilon)^4} \ln(1 + \varepsilon_e/\varepsilon) + \left[1 - \frac{0.6}{\Delta n} \right] \frac{\varepsilon_e}{\varepsilon + \varepsilon_e} \frac{(\varepsilon')^{3/2}}{(\Delta\varepsilon)^2} \left[\frac{4}{3\Delta n} + \frac{1}{\varepsilon} \right] \right\}, \quad (45.94)$$

where $\varepsilon_e = m\varepsilon/MZ^2 R_\infty$ with heavy particle mass and charge denoted above by M and Z , respectively, and all other terms retain their meaning as in Eq. (45.93).

45.6.3 Quasi-elastic ℓ -Mixing Transitions

$$\sigma_{n\ell}^{(\ell\text{-mixing})} \equiv \sum_{\ell' \neq \ell} \sigma_{n'\ell',n\ell} \quad (45.95a)$$

$$\sim \begin{cases} \sigma_{\text{geo}} = 4\pi a_0^2 n^4, & n \ll n_{\text{max}} \\ 2\pi a_s^2 v_B^2 / V^2 n^3, & n \gg n_{\text{max}}. \end{cases} \quad (45.95b)$$

The two limits correspond to strong (close) coupling for $n \ll n_{\text{max}}$, and weak coupling for $n \gg n_{\text{max}}$, and expressions (45.95b) are valid when the quantum defect δ_ℓ of the initial Rydberg orbital $n\ell$ is small. n_{max} is the principal quantum number, where the ℓ -mixing cross section reaches a maximum [20],

$$n_{\text{max}} \sim \left(\frac{v_B |a_s|}{V a_0} \right)^{2/7}. \quad (45.96)$$

For Rydberg atom-Rare gas atom scattering, $n_{\text{max}} = 8 - 20$, while for Rydberg atom-alkali atom scattering $n_{\text{max}} = 15 - 30$.

45.6.4 Elastic $n\ell \rightarrow n'\ell'$ Transitions

$$A^*(n\ell) + B \rightarrow A^*(n'\ell') + B. \quad (45.97)$$

(A) Cross Sections:

$$\sigma_{n's}^{\text{elastic}}(V) = \frac{2\pi C_{ss} a_s^2}{(V/v_B)^2 n^{*4}}, \quad (45.98)$$

valid for $n^* \gg [v_B |a_s| / (4V a_0)]^{1/4}$ with

$$C_{ss} = \frac{8}{\pi^2} \int_0^{1/\sqrt{2}} [K(k)]^2 dk, \quad (45.99)$$

where $K(k)$ denotes the complete elliptic integral of the first kind.

(B) Rate Coefficients: [21] (3 Cases)

With the definitions

$$v_B = v_B/v_{\text{rms}}, \quad v_{\text{rms}} = \sqrt{(8k_B T)/\mu\pi}, \quad (45.100)$$

$$f(y) = y^{-1/2} (1 - (1-y)e^{-y}) + y^{3/2} \text{Ei}(y), \quad (45.101)$$

$$y = (\nu_B a_s)^2 / (4\pi a_0^2 n^{*8}), \quad (45.102)$$

$$n_1 = (|a_s| \nu_B / 4a_0)^{1/4}, \quad (45.103)$$

$$n_2 = 0.7 \left[|a_s| \nu_B^{5/6} / (\alpha_d a_0^3)^{1/6} \right]^{1/3}, \quad (45.104)$$

where α_d is the dipole polarizability of A^* , then

$$\langle \sigma_{n's}^{\text{el}} \rangle \sim \begin{cases} 8\pi a_0^2 n^{*4}, & n^* \leq n_1 \\ 4\pi^{1/2} a_0 |a_s| \nu_B f(y), & n_1 \leq n^* \leq n_2 \\ 7(\alpha_d \nu_B)^{2/3} + \frac{4a_s^2 \nu_B^2}{n^{*4}} - \frac{2.7 a_s^2 \nu_B^2 (\alpha_d \nu_B)^{1/3}}{a_0 n^{*6}}, & n^* \geq n_2. \end{cases} \quad (45.105)$$

45.6.5 Fine Structure $n\ell J \rightarrow n\ell J'$ Transitions

$$A^*(n\ell J) + B \rightarrow A^*(n\ell J') + B + \Delta E_{J'J}. \quad (45.106)$$

(A) Cross Sections: (Two cases)

$$\sigma_{n\ell J}^{n\ell J'}(V) = \frac{2J' + 1}{2(2\ell + 1)} c_{\text{norm}} 4\pi a_0^2 n^{*4}, \quad (45.107)$$

valid for $n^* \leq n_0(V)$, and

$$\sigma_{n\ell J}^{n\ell J'}(V) = \frac{2\pi C_{J'J}^{(\ell)} a_s^2 v_B^2}{V^2 n^{*4}} \varphi_{J'J}^{(\ell)}(\nu_{J'J}) \left[1 - \frac{n_0^8(V)}{2n^{*8}} \right], \quad (45.108)$$

valid for $n^* \geq n_0(V)$, where the quantity $n_0(V)$ is the effective principal quantum number such that the impact parameter ρ_0 of B (moving with relative velocity V) equals the radius $2n^{*2}a_0$ of the Rydberg atom A^* . $n_0(V)$ is given by the solution to the following transcendental equation

$$n_0^8(V) = \frac{(2\ell + 1)C_{J'J}^{(\ell)}}{2(2J' + 1)c_{\text{norm}}} \left(\frac{v_B a_s}{V a_0} \right)^2 \varphi_{J'J}^{(\ell)}(\nu_{J'J} [n_0(V)]). \quad (45.109)$$

The constant c_{norm} in (45.107) is equal to $5/8$ if $\sigma_{\text{geo}} = \pi \langle r^2 \rangle_{n\ell}$, or 1 if $\sigma_{\text{geo}} = 4\pi a_0^2 n^{*4}$. The function $\varphi_{J'J}^{(\ell)}(\nu_{J'J})$ in (45.108) is given in general by [22]

$$\varphi_{J'J}^{(\ell)}(\nu_{J'J}) = \xi_{J'J}^{(\ell)}(\nu_{J'J}) / \xi_{J'J}^{(\ell)}(0), \quad (45.110a)$$

$$\xi_{J'J}^{(\ell)}(\nu_{J'J}) = \sum_{s=0}^{\ell} A_{JJ',\ell}^{(2s)} \int_{\nu_{J'J}}^{\infty} j_s^2(z) J_s^2(z) z dz, \quad (45.110b)$$

$$\nu_{J'J} = |\delta_{JJ'} - \delta_{JJ}| \frac{v_B}{V n^*}, \quad (45.110c)$$

where $j_s(z)$ is the spherical Bessel function and the coefficients $C_{J'J}^{(\ell)}$ and $A_{JJ',\ell}^{(2s)}$ in (45.108) and (45.110b), respectively, are given in table 5.1 of Beigman and Lebedev [1]. The quantum defect of Rydberg state $n\ell J$ is $\delta_{\ell J}$. For elastic scattering, $\nu_{JJ} = 0$, and $\varphi_{JJ}^{(\ell)}(0) = 1$.

Symmetry Relation:

$$\xi_{J'J}^{(\ell)}(\nu_{J'J}) = \frac{2J + 1}{2J' + 1} \xi_{JJ'}^{(\ell)}(\nu_{JJ'}). \quad (45.111)$$

(B) Rate Coefficients:

$$\langle \sigma_{n\ell J}^{n\ell J'} \rangle = \left[\frac{c_{\text{norm}} (2J' + 1) C_{J'J}^{(\ell)}}{2(2\ell + 1)} \right]^{1/2} \times \pi a_0^2 F(\zeta) \left(\frac{v_B |a_s|}{V_T a_0} \right), \quad (45.112)$$

where $\zeta = n_0^8(V_T)/n^{*8}$, and

$$F(\zeta) \equiv \sqrt{\zeta} \left[E_2(\zeta) + \frac{1}{\zeta} (1 - e^{-\zeta}) \right], \quad (45.113)$$

where $E_2(x)$ is an exponential integral.

Limiting cases:

$$\langle \sigma_{n\ell J}^{n\ell J'} \rangle = \begin{cases} \frac{2J' + 1}{2(2\ell + 1)} c_{\text{norm}} 4\pi a_0^2 n^{*4}, & n^* \ll n_{\text{max}}^* \\ \frac{2\pi C_{J'J}^{(\ell)} a_s^2 v_B^2}{V_T^2 n^{*4}}, & n^* \gg n_{\text{max}}^* \end{cases} \quad (45.114)$$

where $n_{\text{max}}^* = (3/2)^{1/8} n_0(V)$ if $\nu_{J'J} \ll 1$.

45.7 IMPULSE APPROXIMATION

45.7.1 Quantal Impulse Approximation

Basic Formulation [23]

Consider a Rydberg collision between a projectile (1) of charge Z_1 and a target with a valence electron (3) in orbital ψ_i bound to a core (2). The full three-body wave function for the system of projectile + target is denoted by Ψ_i . The relative distance between 1 and the center-of-mass of 2-3 is denoted by σ , while the separation of 2 from the center-of-mass of 1-3 is ρ .

Formal Scattering Theory:

$$\Psi_i^{(+)} = \Omega^{(+)} \psi_i, \quad (45.115)$$

where the Möller scattering operator $\Omega^{(+)} = 1 + G^+ V_i$, and $V_i = V_{12} + V_{13}$.

Let χ_m be a complete set of free-particle wave functions satisfying

$$(H_0 - E_m) \chi_m = 0, \quad (45.116)$$

and define operators $\omega_{ij}^{\pm}(m)$ by

$$\omega_{ij}^{\pm}(m) \chi_m = \left(1 + \frac{1}{E_m - H_0 - V_{ij} + i\epsilon} V_{ij} \right) \chi_m, \quad (45.117)$$

where V_{ij} denotes the pairwise interaction potential between particles i and j ($i, j = 1, 2, 3$). Then the action of the full Green's function G^+ on the two-body potential V_{ij} is

$$G^+ V_{ij} = [\omega_{ij}^+(m) - 1] + G^+ \{ (E_m - E) + V_{12} + V_{13} + V_{23} - V_{ij} \} \times [\omega_{ij}^+(m) - 1]. \quad (45.118)$$

Projection Operators:

$$b_{ij}^+(m) = \omega_{ij}^+(m) - 1, \quad (45.119a)$$

$$b_{ij}^+ = \sum_m b_{ij}^+(m) |\chi_m\rangle \langle \chi_m|, \quad \omega_{ij}^+ = b_{ij}^+ + 1. \quad (45.119b)$$

$$G^+ V_{ij} |\psi_i\rangle = \sum_m G^+ V_{ij} |\chi_m\rangle \langle \chi_m | \psi_i\rangle \quad (45.120a)$$

$$= \{b_{ij}^+ + G^+ [V_{23}, b_{ij}^+]\} |\psi_i\rangle + G^+ [V_{12} + V_{13} - V_{ij}] b_{ij}^+(m) |\psi_i\rangle. \quad (45.120b)$$

Möller Scattering Operator:

$$\Omega^+ = (\omega_{13}^+ + \omega_{12}^+ - 1) + G^+ [V_{23}, (b_{13}^+ + b_{12}^+)] + G^+ (V_{13} b_{12}^+ + V_{12} b_{13}^+). \quad (45.121)$$

Exact T-matrix:

$$T_{if} = \langle \psi_f | V_f | (\omega_{13}^+ + \omega_{12}^+ - 1) \psi_i \rangle + \langle \psi_f | V_f | G^+ [V_{23}, (b_{13}^+ + b_{12}^+)] \psi_i \rangle + \langle \psi_f | V_f | G^+ (V_{13} b_{12}^+ + V_{12} b_{13}^+) \psi_i \rangle. \quad (45.122)$$

The impulse approximation to the exact T-matrix element (45.122) is obtained by ignoring the second term involving the commutator of V_{23} .

$$\Psi_i \longrightarrow \Psi_i^{\text{imp}} = (\omega_{13}^+ + \omega_{12}^+ - 1) \psi_i. \quad (45.123)$$

Impulse Approximation: Post Form.

$$T_{if}^{\text{imp}} = \langle \psi_f | V_f | (\omega_{13}^+ + \omega_{12}^+ - 1) \psi_i \rangle. \quad (45.124)$$

The impulse approximation can also be expressed using incoming-wave boundary conditions by making use of the prior operators

$$\omega_{ij}^-(m) \chi_m = \left(1 + \frac{1}{E_m - H_0 - V_{ij} - i\epsilon} V_{ij} \right) \chi_m, \quad (45.125a)$$

$$\omega_{ij}^- = \sum_m \omega_{ij}^-(m) |\chi_m\rangle \langle \chi_m|. \quad (45.125b)$$

The impulse approximation (45.124) is exact if $V_{23} = \text{const.}$ since the commutator of V_{23} vanishes in that case.

Applications [23]

(1) **Electron Capture:** $X^+ + H(i) \rightarrow X(f) + H^+$.

$$T_{if}^{\text{imp}} = \langle \psi_f | V_{12} + V_{23} (\omega_{12}^+ + \omega_{13}^+ - 1) \psi_i \rangle. \quad (45.126)$$

Wave functions: $\psi_i = e^{i\mathbf{k}_i \cdot \mathbf{r}} \varphi_i(\mathbf{r})$, $\psi_f = e^{i\mathbf{k}_f \cdot \mathbf{r}} \varphi_f(\mathbf{r})$, $\chi_m = (2\pi)^{-3} \exp[i(\mathbf{K} \cdot \mathbf{x} + \mathbf{k} \cdot \rho)]$, where the φ_n are hydrogenic wave functions.

If X above is a heavy particle, the V_{12} term in (45.126) may be omitted due to the difference in mass between the

projectile 1 and the bound Rydberg electron 3. See [23] and references therein for details. With the definitions

$$\begin{aligned} z &= \frac{4\alpha\delta^2}{(T-2\delta)(T-2\alpha\delta)}, & T &= \beta^2 + P^2 \\ \delta &= i\beta K - \mathbf{p} \cdot \mathbf{K}, & \nu &= aZ_1/K \\ \mathbf{t}_1 &= \mathbf{K}/a + \mathbf{v}, & N(\nu) &= e^{\pi\nu/2} \Gamma(1-i\nu) \\ a &= \frac{M_1}{M_1 + m_e}, & b &= \frac{M_2}{M_2 + m_e} \\ \mathbf{k} &= a\mathbf{k}_2 - (1-a)\mathbf{k}_f, & \mathbf{K} &= a\mathbf{k}_1 - (1-a)\mathbf{k}_i, \\ \mathbf{t} &= (\mathbf{K} - \mathbf{p})/a, & \mathbf{p} &= a\mathbf{k}_f - \mathbf{k}_i. \end{aligned}$$

the impulse approximation to the T-matrix becomes, in this case,

$$T_{if}^{\text{imp}} \sim \langle \psi_f | V_{23} | \omega_{13}^+ \psi_i \rangle \quad (45.127)$$

$$= \frac{-1}{2\pi^2 a^3} \int \frac{d\mathbf{K}}{t^2} N(\nu) g_i(\mathbf{t}_1) \mathcal{F}(f, \mathbf{K}, \mathbf{p}), \quad (45.128)$$

where, for a general final s -state,

$$\mathcal{F}(f, \mathbf{K}, \mathbf{p}) = \int \varphi_f^*(\mathbf{x}) e^{i\mathbf{p} \cdot \mathbf{x}} F_1[i\nu, 1; i(Kx - \mathbf{K} \cdot \mathbf{x})] d\mathbf{x}. \quad (45.129)$$

where in (45.128) $g_i(\mathbf{t}_1)$ denotes the Fourier transform of the initial state. The normalization of the Fourier transform is chosen such that momentum and coordinate space hydrogenic wave functions are related, $\varphi_n(\mathbf{r}) = (2\pi)^{-3} \int \exp(i\mathbf{t}_1 \cdot \mathbf{r}) g_n(\mathbf{t}_1) d\mathbf{t}_1$, where n denotes the principal quantum number. Below the variable $\beta \equiv aZ_1/n$. For the case $f = 1s$,

$$\begin{aligned} \mathcal{F}(1s, \mathbf{K}, \mathbf{p}) &= -\frac{\beta^{3/2}}{\sqrt{\pi}} \frac{\partial}{\partial \beta} \mathcal{I}(\nu, 0, \beta, -\mathbf{K}, \mathbf{p}) \\ &= 8\sqrt{\pi} \beta^{3/2} \left[\frac{(1-i\nu)\beta}{T^2} + \frac{i\nu(\beta - iK)}{T(T-2\delta)} \left(\frac{T}{T-2\delta} \right)^{i\nu} \right] \end{aligned} \quad (45.130)$$

evaluated at $\beta = aZ_1$. For the case $f = 2s$,

$$\mathcal{F}(2s, \mathbf{K}, \mathbf{p}) = -\frac{\beta^{3/2}}{\sqrt{\pi}} \left[\left(\frac{\partial}{\partial \beta} + \beta \frac{\partial^2}{\partial \beta^2} \right) \mathcal{I}(\nu, 0, \beta, -\mathbf{K}, \mathbf{p}) \right] \quad (45.131)$$

evaluated at $\beta = aZ_1/2$. For a general final ns -state f ,

$$\begin{aligned} \mathcal{I}(\nu, \alpha, \beta, \mathbf{K}, \mathbf{p}) &= \frac{4\sqrt{\pi}}{T} \left(\frac{T-2\alpha\delta}{T-2\delta} \right)^{i\nu} \\ &\times (U \cosh \pi\nu \pm iV \sinh \pi\nu), \end{aligned} \quad (45.132)$$

where the complex quantity $U + iV$ is

$$U + iV = (4z)^{i\nu} \frac{\Gamma(\frac{1}{2} + i\nu)}{\Gamma(1 + i\nu)} {}_2F_1(-i\nu, -i\nu; 1 - 2i\nu; 1/z). \quad (45.133)$$

(2) Electron Impact Excitation:

$$e^- + H(i) \rightarrow e^- + H(f). \quad (45.134)$$

Neglecting V_{12} and exchange yields the approximate T-matrix element

$$\begin{aligned} T_{if}^{\text{imp}} &\sim \langle \psi_f | V_{13} | \omega_{13}^+ \psi_i \rangle \quad (45.135) \\ &= \frac{-Z_1}{(2\pi a)^3} \int d\mathbf{x} \int d\mathbf{r} e^{i\mathbf{q} \cdot \mathbf{r}} \varphi_f^*(\mathbf{r}) \frac{1}{x} \\ &\quad \times \int d\mathbf{K} N(\nu) g_i(\mathbf{t}_1) e^{i\mathbf{t}_1 \cdot \mathbf{r}_1} F_1(i\nu, 1; i\mathbf{K} \cdot \mathbf{x} - i\mathbf{K} \cdot \mathbf{x}) \\ &= \frac{-Z_1}{(2\pi a)^3} \int d\mathbf{K} N(\nu) g_i(\mathbf{t}_1) g_f^*(\mathbf{t}_2) \mathcal{I}(\nu, 0, 0, -\mathbf{K}, -\mathbf{q}), \end{aligned} \quad (45.136)$$

where

$$\begin{aligned} \mathcal{I}(\nu, 0, 0, -\mathbf{K}, -\mathbf{q}) \\ = \lim_{\beta \rightarrow 0} \frac{4\pi}{\beta^2 + q^2} \left[\frac{\beta^2 + q^2}{\beta^2 + q^2 + 2\mathbf{q} \cdot \mathbf{K} - 2i\beta K} \right]^{i\nu} \quad (45.137) \\ = \frac{4\pi}{q^2} \left| 1 + \frac{2K}{q} \cos \theta \right|^{-i\nu} A(\cos \theta), \end{aligned} \quad (45.138)$$

with

$$A(\cos \theta) = \begin{cases} 1, & \cos \theta > -q/2K \\ e^{-\pi\nu}, & \cos \theta < -q/2K \end{cases} \quad (45.139)$$

and $\cos \theta = \hat{\mathbf{K}} \cdot \hat{\mathbf{q}}$, $\mathbf{t}_2 = \mathbf{t}_1 + b\mathbf{q}$ and $\mathbf{q} = \mathbf{k}_i - \mathbf{k}_f$.

(3) Heavy Particle Excitation: [24]

$$H^+ + H(1s) \rightarrow H^+ + H(2s). \quad (45.140)$$

$$\begin{aligned} T_{if}^{\text{imp}} &= -\frac{Z_1 2^{15/2} b^5}{\pi a^3 q^2} \int_0^\infty dK N(K) K^2 \int_{-1}^1 d(\cos \theta) \\ &\quad \times \left| 1 + \frac{2K}{q} \cos \theta \right|^{-i\nu} \tilde{A}(\cos \theta), \end{aligned} \quad (45.141)$$

where

$$\begin{aligned} \tilde{A}(\cos \theta) &= \frac{2\pi}{D^4} \left[\frac{\alpha D(D - 2b^2)}{(\alpha^2 - \beta^2)^{3/2}} + \frac{8(3b^2 - D)}{(\alpha^2 - \beta^2)^{1/2}} \right. \\ &\quad \left. - \frac{48\gamma^2 D^2 b^2}{(\gamma^2 - \delta^2)^{5/2}} + \frac{16D[\gamma D - (3\gamma + 4\alpha)b^2]}{(\gamma^2 - \delta^2)^{3/2}} \right. \\ &\quad \left. + \frac{32(D - 3b^2)}{(\gamma^2 - \delta^2)^{1/2}} \right] A(\cos \theta), \end{aligned} \quad (45.142)$$

with $A(\cos \theta)$ given by (45.139), and

$$\alpha = b^2 + v^2 + \frac{K^2}{a^2} + \frac{K}{aq} \left(\frac{q^2}{\mu} + \Delta E \right) \cos \theta, \quad (45.143a)$$

$$\beta = \frac{K}{aq} \sin \theta \left[4v^2 q^2 - \left(\frac{q^2}{\mu} + \Delta E \right)^2 \right]^{1/2}, \quad (45.143b)$$

$$\delta = 4\beta, \quad \gamma = 4\alpha + D, \quad (45.143c)$$

$$D = \frac{4bq}{a} (q + 2K \cos \theta), \quad (45.143d)$$

while ν and $N(\nu)$ retain their meaning from (45.128).

(4) Ionization: $e^- + H(i) \rightarrow e^- + H^+ + e^-$.

$$T_{if}^{\text{imp}} \sim -\frac{4\pi}{q^2} N(\nu) g_i(\mathbf{k} - b\mathbf{q}) \left(\frac{q^2}{q^2 - 2\mathbf{q} \cdot \mathbf{K}} \right)^{i\nu}, \quad (45.144)$$

where $\mathbf{K} = a(\mathbf{k} - b\mathbf{q} - \mathbf{v})$ and $\mathbf{q} = \mathbf{k}_i - \mathbf{k}_f$ and exchange and V_{12} are neglected.

(5) Rydberg Atom Collisions: [11, 25]

$$A + B(n) \rightarrow A + B(n') \quad (45.145)$$

$$\rightarrow A + B^+ + e^-. \quad (45.146)$$

Consider a Rydberg collision between a projectile (3) and a target with an electron (1) bound in a Rydberg orbital to a core (2) (see [11, 25] for details).

Full T-matrix element:

$$\begin{aligned} T_{fi}(\mathbf{k}_3, \mathbf{k}'_3) \\ = \langle \phi_f(\mathbf{r}_1) e^{i\mathbf{k}'_3 \cdot \mathbf{r}_3} | V(\mathbf{r}_1, \mathbf{r}_3) | \Psi_i^{(+)}(\mathbf{r}_1, \mathbf{r}_3; \mathbf{k}_3) \rangle, \end{aligned} \quad (45.147)$$

with primes denoting quantities *after* the collision, and where the potential V is

$$V(\mathbf{r}_1, \mathbf{r}_3) = V_{13}(\mathbf{r}) + V_{3C}(\mathbf{r}_3 + a\mathbf{r}_1), \quad \mathbf{r} = \mathbf{r}_1 - \mathbf{r}_3, \quad (45.148)$$

with $a = M_1/(M_1 + M_2)$, while the subscript C labels the core. The impulse approximation to the full, outgoing wave function $\Psi_i^{(+)}$ is written

$$\Psi_i^{\text{imp}} = (2\pi)^{3/2} \int g_i(\mathbf{k}_1) \Phi(\mathbf{k}_1, \mathbf{k}_3; \mathbf{r}_1, \mathbf{r}_3) d\mathbf{k}_1, \quad (45.149)$$

$$g_i(\mathbf{k}_1) = \frac{1}{(2\pi)^{3/2}} \int \phi_i(\mathbf{r}_1) e^{-i\mathbf{k}_1 \cdot \mathbf{r}_1} d\mathbf{r}_1. \quad (45.150)$$

Impulse approximation:

$$\begin{aligned} T_{fi}^{\text{imp}}(\mathbf{k}_3, \mathbf{k}'_3) &= \int d\mathbf{k}_1 \int d\mathbf{k}'_1 g_f^*(\mathbf{k}'_1) g_i(\mathbf{k}_1) T_{13}(\mathbf{k}, \mathbf{k}') \\ &\quad \times \delta[\mathbf{P} - (\mathbf{k}'_1 - \mathbf{k}_1)], \end{aligned} \quad (45.151)$$

where T_{13} is the exact off-shell T-matrix for 1-3 scattering,

$$T_{13}(\mathbf{k}, \mathbf{k}') = \langle \exp(i\mathbf{k}' \cdot \mathbf{r}) | V_{13}(\mathbf{r}) | \psi(\mathbf{k}, \mathbf{r}) \rangle. \quad (45.152)$$

The delta function in (45.151) ensures linear momentum, $\mathbf{K} = \mathbf{k}_1 + \mathbf{k}_3 = \mathbf{k}'_1 + \mathbf{k}'_3$, is conserved in 1-3 collisions, with

$$\mathbf{k}'_1 = \mathbf{k}_1 + (\mathbf{k}_3 - \mathbf{k}'_3) \equiv \mathbf{k}_1 + \mathbf{P}, \quad (45.153a)$$

$$\mathbf{k}' = \frac{M_3}{M_1 + M_3} (\mathbf{k}_1 + \mathbf{k}_3) - \mathbf{k}'_3 = \mathbf{k} + \mathbf{P}. \quad (45.153b)$$

Elastic scattering:

$$T_{ii}(\mathbf{k}_3, \mathbf{k}_3) = \int g_f^*(\mathbf{k}_1) g_i(\mathbf{k}_1) T_{13}(\mathbf{k}, \mathbf{k}) d\mathbf{k}_1, \quad (45.154)$$

where $\mathbf{k} = (M_3/M)\mathbf{k}_1 + (M_1/M)\mathbf{k}_3$ and $M = M_1 + M_3$.
Integral cross section: for 3-(1,2) scattering,

$$\sigma_{if}(k_3) = \left(\frac{M_{AB}}{M_{13}} \right)^2 \frac{k'_3}{k_3} \int |\langle g_f(\mathbf{k}_1 + \mathbf{P}) | \times f_{13}(\mathbf{k}, \mathbf{k}') | g_i(\mathbf{k}_1) \rangle|^2 d\hat{\mathbf{k}}'_3, \quad (45.155)$$

where M_{AB} is the reduced mass of the 3-(1,2) system, M_{13} the reduced mass of 1-3. The 1-3 scattering amplitude f_{13} is given by

$$f_{13}(\mathbf{k}, \mathbf{k}') = -\frac{1}{4\pi} \left(\frac{2M_{13}}{\hbar^2} \right) T_{13}(\mathbf{k}, \mathbf{k}'). \quad (45.156)$$

Six Approximations to Eq. (45.151)

(1) Optical Theorem:

$$\begin{aligned} \sigma_{\text{tot}}(k_3) &= \frac{1}{k_3} \frac{2M_{AB}}{\hbar^2} T_{ii}(\mathbf{k}_3, \mathbf{k}'_3) \\ &= \frac{1}{v_3} \int |g_i(\mathbf{k}_1)|^2 [v_{13} \sigma_{13}^T(v_{13})] d\mathbf{k}_1, \end{aligned} \quad (45.157)$$

where σ_{13}^T is the total cross section for 1-3 scattering at relative speed v_{13} . The resultant cross section (45.157) is an upper limit and contains no interference terms.

(2) Plane-wave Final State:

$$\phi_f(\mathbf{r}_1) = (2\pi)^{-3/2} \exp(i\kappa'_1 \cdot \mathbf{r}_1), \quad (45.158)$$

$$g_f(\mathbf{k}'_1) = \delta(\mathbf{k}'_1 - \kappa'_1), \quad (45.159)$$

$$T_{fi}(\mathbf{k}_3, \mathbf{k}'_3) = g_i(\mathbf{k}_1) T_{13}(\mathbf{k}, \mathbf{k}'), \quad \mathbf{k}_1 = \kappa_1 - \mathbf{P}, \quad (45.160)$$

$$\frac{d\sigma_{if}}{d\hat{\mathbf{k}}'_3 d\mathbf{k}'_1} = \left(\frac{M_{AB}}{M_{13}} \right)^2 \frac{k'_3}{k_3} |g_i(\mathbf{k}_1)|^2 |f_{13}(\mathbf{k}, \mathbf{k}')|^2 \quad (45.161)$$

(3) Closure:

$$\sum_f g_f(\mathbf{k}'_1) g_f^*(\mathbf{k}''_1) = \delta(\mathbf{k}'_1 - \mathbf{k}''_1), \quad (45.162)$$

$$\frac{d\sigma_i^T}{d\hat{\mathbf{k}}'_3} = \frac{k'_3}{k_3} \left(\frac{M_{AB}}{M_{13}} \right)^2 \int |g_i(\mathbf{k}_1)|^2 |f_{13}(\mathbf{k}, \mathbf{k}')|^2 d\mathbf{k}_1, \quad (45.163)$$

where $\mathbf{k}'_1 = (M_3/M)(\mathbf{k}_1 + \mathbf{k}_3) - \mathbf{k}'_3$.

Conditions for validity of (45.163): (a) k_3 is high enough to excite all atomic bound and continuum states, and (b) $k_3'^2 = (k_3^2 - 2\varepsilon_{fi}/M_{AB})$ can be approximated by k_3 , or by an averaged wavenumber $\bar{k}_3 = (k_3^2 - 2\bar{\varepsilon}_{fi}/M_{AB})^{1/2}$, where the averaged excitation energy is

$$\bar{\varepsilon}_{fi} = \ln \langle \varepsilon_{fi} \rangle = \sum_j f_{ij} \ln \varepsilon_{ij} \left(\sum_j f_{ij} \right)^{-1}, \quad (45.164)$$

and the f_{ij} are the oscillator strengths.

(4) Peaking Approximation:

$$T_{fi}^{\text{peak}}(\mathbf{k}_3, \mathbf{k}'_3) = F_{fi}(\mathbf{P}) T_{13}(\mathbf{k}, \mathbf{k}'), \quad (45.165)$$

where F_{fi} is the inelastic form factor

$$F_{fi}(\mathbf{P}) = \int g_f^*(\mathbf{k}_1 + \mathbf{P}) g_i(\mathbf{k}_1) d\mathbf{k}_1 \quad (45.166)$$

$$= \langle \psi_f(\mathbf{r}) | \exp(i\mathbf{P} \cdot \mathbf{r}) | \psi_i(\mathbf{r}) \rangle. \quad (45.167)$$

(5) $T_{13} = T_{13}(\mathbf{P})$:

$$T_{fi}(\mathbf{k}_3, \mathbf{k}'_3) = T_{13}(\mathbf{P}) F_{fi}(\mathbf{P}). \quad (45.168)$$

(6) $T_{13} = \text{constant}$:

$f_{13} \equiv a_s = \text{constant scattering length.}$

$$\sigma_{if}(k_3) = \frac{2\pi a_s^2}{k_3^2} \left(\frac{M_{AB}}{M_{13}} \right)^2 \int_{\mathbf{k}_3 - \mathbf{k}'_3}^{\mathbf{k}_3 + \mathbf{k}'_3} |F_{fi}(\mathbf{P})|^2 P dP \quad (45.169)$$

$$\sigma_{\text{tot}}(k_3) = \begin{cases} 4\pi a_s^2, & v_3 \gg v_1 \\ \langle v_1 \rangle 4\pi a_s^2 / v_3, & v_3 \ll v_1. \end{cases} \quad (45.170)$$

Validity Criteria

(A) Intuitive Formulation: [25]

(i) Particle 3 scatters separately from 1 and 2, i.e. $r_{12} \gg A_{1,2}$; the relative separation of (1,2) \gg the scattering lengths of 1 and 2.

(ii) $\lambda_{13} \ll r_{12}$, i.e., the reduced wavelength for 1-3 relative motion $\ll r_{12}$. Interference effects of 1 and 2 can be ignored and 1, 2 treated as *independent* scattering centers.

(iii) 2-3 collisions do not contribute to inelastic 1-3 scattering.

(iv) Momentum impulsively transferred to 1 during collision (time τ_{coll}) with $3 \gg$ Momentum transferred to 1 due to V_{12} i.e.,

$$P \gg \langle \psi_{n\ell} | -\nabla V_{12} | \psi_{n\ell} \rangle \tau_{\text{coll}}. \quad (45.171)$$

For a precise formulation of Validity Criteria based upon the Two-Potential Formula see the Appendix of Ref. [25].

Two classes of interaction in $A-B(n)$ Rydberg collisions justify use of the impulse approximation for the T-matrix for 1-3 collisions: (i) Quasiclassical binding: $V_{\text{core}} = \text{const.}$ (ii) Weak binding:

$$E_3 \gg \Delta E_c \sim \langle \psi_n(\mathbf{r}) | V_{1C}(\mathbf{r}) | \psi_n(\mathbf{r}) \rangle \quad (45.172a)$$

$$\langle \psi_n(\mathbf{r}_1) | -\frac{\hbar^2}{2M_{12}} \nabla_1^2 | \psi_n(\mathbf{r}_1) \rangle \sim |\varepsilon_n|, \quad (45.172b)$$

where E_3 is the kinetic energy of relative motion of 3, and ΔE_c is the energy shift in the core. The fractional error is [26]

$$\frac{f_{13}}{\lambda} \frac{\Delta E_c}{\hbar} \left(\frac{\hbar}{E_3} + \tau_{\text{delay}} \right) \ll 1, \quad (45.173)$$

where $\lambda \sim k_3^{-1}$ is the reduced wavelength of 3, f_{13} is the scattering amplitude for 1-3 collisions and τ_{delay} is the time delay associated with 1-3 collisions.

Special Case: for nonresonant scattering with $\tau_{\text{delay}} = 0$

$$\frac{f_{13}}{\lambda} \frac{|\varepsilon_n|}{E_3} \ll 1, \quad (45.174)$$

which follows from (45.173) upon identifying the shift in the core energy ΔE_c with the binding energy $|\varepsilon|$.

Condition (45.174) is less restrictive than (45.172a) or (45.172b) since f_{13} can be either less than or greater than λ .

45.7.2 Classical Impulse Approximation

(A) Ionization: For electron impact on heavy particles [27], the cross section for ionization of a particle moving with velocity t by a projectile with velocity s is

$$Q(s, t) = \frac{1}{u^2} \frac{2s}{m_2} \int_1^{s^2} \frac{dz}{z^2} \left[\frac{A(z)}{z} + B(z) \right], \quad (45.175)$$

where

$$A(z) = \frac{1}{2st^3} \left[\frac{1}{3}(x_{02}^{3/2} - x_{01}^{3/2}) - 2(s^2 + t^2)(x_{02}^{1/2} - x_{01}^{1/2}) \right. \\ \left. - \frac{(s^2 - t^2)^2}{2ts^3}(x_{02}^{-1/2} - x_{01}^{-1/2}) \right] \quad (45.176a)$$

$$B(z) = \frac{1}{2m_2st^3} \left[(m_1 + m_2)(s^2 - t^2)(x_{02}^{-1/2} - x_{01}^{-1/2}) \right. \\ \left. - (m_2 - m_1)(x_{02}^{1/2} - x_{01}^{1/2}) \right]. \quad (45.176b)$$

For electron impact, (45.176b) is evaluated at $m_1 = 1$. The remaining terms above are given by

$$s^2 = v_2^2/v_0^2, \quad t^2 = v_1^2/v_0^2 = E_1/u, \quad E_2 = m_2v_2^2,$$

$$u = v_0^2 = \text{Ionization potential of target},$$

$$x_{0i} = (s^2 + t^2 - 2st \cos \theta_i), \quad i=1,2,$$

$$\cos \theta_i = \begin{cases} \kappa_0 \pm \kappa_1, & |\kappa_0 \pm \kappa_1| \leq 1 \\ 1, & \kappa_0 \pm \kappa_1 > 1 \\ -1, & \kappa_0 \pm \kappa_1 < -1 \end{cases},$$

$$\kappa_0 \pm \kappa_1 = -\frac{1}{2} \left(1 - \frac{m_1}{m_2} \right) \frac{z}{st} \pm \sqrt{\left(1 + \frac{z}{t^2} \right) \left(1 - \frac{z}{s^2} \right)}.$$

Equal Mass Case: ($m_1 = m_2$)

$$Q(s, t) = \begin{cases} \frac{4}{3s^2} \frac{1}{u^2} \frac{2(s^2 - 1)^{3/2}}{t}, & 1 \leq s^2 \leq t^2 + 1 \\ \frac{4}{3s^2} \frac{1}{u^2} \left[2t^2 + 3 - \frac{3}{s^2 - t^2} \right], & s^2 \geq t^2 + 1. \end{cases} \quad (45.177)$$

Integrating over the speed distribution (see Sect. 45.4),

$$Q(s) = \frac{32}{\pi} \frac{1}{u^2} \int_0^\infty \frac{Q(s, t) t^2 dt}{(t^2 + 1)^4}, \quad (45.178)$$

which is then numerically evaluated. For electrons, the integral can be done analytically with the result

$$Q(y) = \frac{8}{3\pi y^2 (y+1)^4} \\ \times \left[(5y^4 + 15y^3 - 3y^2 - 7y + 6)(y-1)^{1/2} \right. \\ \left. + (5y^5 + 17y^4 + 15y^3 - 25y^2 + 20y) \times \tan^{-1}(y-1)^{1/2} \right. \\ \left. - 24y^{3/2} \ln \left| \frac{\sqrt{y} + \sqrt{y-1}}{\sqrt{y} - \sqrt{y-1}} \right| \right], \quad (45.179)$$

with $y = s^2$.

Thomson's Result:

$$Q_T(y) = \frac{4}{y} \frac{1}{u^2} \left(1 - \frac{1}{y} \right). \quad (45.180)$$

(B) Electron Loss Cross Section: [17]

$$A(V) + B(u) \rightarrow A^+ + e^- + B(f), \quad (45.181)$$

where $B(f)$ denotes that the target B is left in any state (either bound or free) after the collision with the projectile A . The initial velocity of the projectile is V while the velocity of the Rydberg electron relative to the core is u , and the ionization potential of the target B is I .

$$\sigma_{\text{loss}} = \frac{1}{3\pi\nu^2} \int_{\tau/4\nu}^\infty dx \sigma_T(x\bar{u}) \left[\frac{8\nu x - 1 - (\nu - x)^2 - 2\tau}{[1 + (\nu - x)^2]^3} \right. \\ \left. + \frac{1}{[1 + (\nu + x)^2 - \tau]^2} \right], \quad (45.182)$$

where $\nu = V/\bar{u}$, $\tau = I/\frac{1}{2}m_e\bar{u}^2$, $\bar{u} = \sqrt{2I/m_e}$, and σ_T is the total electron scattering cross section at speed $x\bar{u}$. The cross section (45.182) is valid only for particles being stripped (or lost from the projectile) which are not strongly bound. See Refs. [17, 28, 29] for details and numerous results.

(C) Capture Cross Section from Shell i : [17]

$$\sigma_{\text{capture}}^i(V) = \frac{2^{5/2} N_i \pi}{3V^7} \int_0^{r_i} dr \int_{C(-1)}^{C(+1)} d(\cos \eta') [P_i(r)]^2 \\ \times \frac{\sqrt{1+y^2} [4\varepsilon^2 - (\varepsilon^2 - y^2)(1 + \varepsilon^2 + a^2 - y^2)]}{r^{3/2} \varepsilon^{9/2} (1 + a^2)^3 \sqrt{y^2 - a^2}} \quad (45.183)$$

where C denotes that the integration range $[-1, +1]$ is restricted such that the integrand is real and positive and that $|1 - \varepsilon| < \sqrt{y^2 - a^2}$. The dimensionless variables a and y above are defined,

$$y^2 = \frac{2}{m_e} |V(R)| V^2, \quad a^2 = \frac{2}{m_e} I_i V^2, \quad (45.184)$$

and with $P_i(r)/r$ representing the Hartree-Fock-Slater radial wave function for shell i , with normalization

$$\int_0^{r_i} [P_i(r)]^2 dr = 1. \quad (45.185)$$

The ionization potential and number of electrons in shell i are denoted above, respectively, by I_i and N_i .

(D) Total Capture Cross Section: [17]

$$\sigma_{\text{capture}}^{\text{total}}(V) = \sum_i \sigma_{\text{capture}}^i. \quad (45.186)$$

(E) Universal Capture Cross Section: [17]

A universal curve independent of projectile mass M and charge Z is obtained from the above expressions for the capture cross section by plotting the scaled cross section

$$\tilde{\sigma}_{\text{capture}}^{\text{total}} = \frac{E^{11/4}}{M^{11/4} Z^{7/2} \lambda^{3/4}} \sigma_{\text{capture}}^{\text{total}} \quad (45.187)$$

versus the scaled energy

$$\tilde{E} = \frac{m_e}{M} \frac{E}{I}, \quad (45.188)$$

where m_e is the mass of the particle captured, which is usually taken to be a single electron, and I is the ionization potential of the target. The term λ in (45.187) is the coupling constant in the target potential, $V(R) = m_e \lambda / R^2$, which the electron being captured experiences during the collision. See Fig. 11 of [17] for details.

45.7.3 Semiquantal Impulse Approximation

Basic Expression: [25, 30]

$$\frac{d\sigma}{d\epsilon dP dk_1 dk d\phi_1} = \frac{k_1'^2 k_3'}{J_{55} k_3} \left(\frac{M_3}{M_{13}} \right)^2 |g_i(\mathbf{k}_1)|^2 |f_{13}(\mathbf{k}, \mathbf{k}')|^2. \quad (45.189)$$

J_{55} is the 5-dimensional Jacobian of the transformation

$$(P, \epsilon, k_1, k, \phi_1) \rightarrow (\hat{\mathbf{k}}_3', \mathbf{k}_1'), \quad (45.190a)$$

$$J_{55} = \frac{\partial(P, \epsilon, k_1, k, \phi_1)}{\partial(\cos \theta_3' \phi_3', k_1', \cos \theta_1', \phi_1')}. \quad (45.190b)$$

Expression for Elemental Cross Section: [25]

In the $(P, \epsilon, k_1, k, \phi_1)$ representation,

$$d\sigma = \frac{d\epsilon dP}{M_{13}^2 v_3^2} \left[\frac{|g_i(\mathbf{k}_1)|^2 k_1^2 dk_1 d\phi_1}{v_1} \right] \frac{|f_{13}(\mathbf{k}, \mathbf{k}')|^2 dg^2}{\sqrt{(g_+^2 - g^2)(g^2 - g_-^2)}} \quad (45.191)$$

Where $g_{\pm}^2 = \frac{1}{2} B \pm \sqrt{\frac{1}{4} B^2 - C}$, and

$$B = B(\epsilon, P, v_1; v_3) = \frac{a}{(1+a)^2} \frac{P^2}{M_{13}^2} + \left(v_1^2 + v_1'^2 + v_3^2 + v_3'^2 + \frac{2\Delta_3}{M_{13}} \right) - \frac{4\epsilon(\epsilon + \Delta_3)}{P^2},$$

$$C = C(\epsilon, P, v_1; v_3) = \frac{v_1^2 + a v_3^2}{1+a} \frac{P^2}{M_{13}^2} + (v_1^2 - v_3^2)(v_1'^2 - v_3'^2) + \frac{2\Delta_3}{M_{13}}(v_1^2 + v_3^2) + \frac{4\Delta_3}{P^2} [v_1^2(\epsilon + \Delta_3) - \epsilon v_3^2],$$

$$a = \frac{M_2 M_3}{M_1(M_1 + M_2 + M_3)},$$

$$\tilde{M}_1 = M_1(1 + M_1/M_2),$$

$$v_1'^2 = v_1^2 + \frac{2\epsilon}{\tilde{M}_1}, \quad v_3'^2 = v_3^2 - \frac{2(\epsilon + \Delta_3)}{M_{AB}},$$

and Δ_3 is the change in internal energy of particle 3, while ϵ denotes the energy change in the target 1-2.

Hydrogenic Systems: $g_i(\mathbf{k}_1) = g_{nl}(k_1) Y_{lm}(\theta_1, \phi_1)$.

The g_{nl} are the hydrogenic wave functions in momentum space See Chap. ?? for details on hydrogenic wave functions.

Elemental Cross Sections: (m -averaged and ϕ_1 -integrated)

$$d\sigma = \frac{d\epsilon dP}{M_{13}^2 v_3^2} \frac{W_{nl}(v_1) dv_1}{2v_1} \frac{|f_{13}(P, g)|^2 dg^2}{\sqrt{(g_+^2 - g^2)(g^2 - g_-^2)}}, \quad (45.192)$$

where the speed distribution W_{nl} is given by (45.58).

Two Representations for 1-3 Scattering Amplitude: [25]

(i) $f_{13} = f_{13}(P, g)$ is a function of momentum transferred and relative speed. Then

$$\sigma(v_3) = \frac{1}{M_{13}^2 v_3^2} \int_{\epsilon_1}^{\epsilon_2} d\epsilon \int_{v_{10}}^{\infty} \frac{W_{nl}(v_1) dv_1}{v_1} \int_{P^-}^{P^+} dP \times \int_{g_-}^{g_+} \frac{|f_{13}(P, g)|^2 dg^2}{\sqrt{(g_+^2 - g^2)(g^2 - g_-^2)}}, \quad (45.193)$$

where $v_{10}^2(\epsilon) = \max[0, (2\epsilon/M)]$, and the limits to the P integral are

$$P^+ = P^+(\epsilon, v_1; v_3) = \min[M(v_1' + v_1), M_{AB}(v_3' + v_3)], \quad (45.194a)$$

$$P^- = P^-(\epsilon, v_1; v_3) = \max[M|v_1' - v_1|, M_{AB}|v_3' - v_3|], \quad (45.194b)$$

and unless $P^+ > P^-$, the P integral is zero.

(ii) $f_{13} = f_{13}(g, \psi)$ is a function of relative speed and scattering angle. Then

$$\sigma(v_3) = \frac{1}{v_3^2} \int_{\epsilon_1}^{\epsilon_2} d\epsilon \int_{v_{10}}^{\infty} \frac{W_{nl}(v_1) dv_1}{v_1} \int_{g_-}^{g_+} \frac{g dg}{S(v_1, g; v_3)} \times \int_{\psi^-}^{\psi^+} \frac{|f_{13}(g, \psi)|^2 d(\cos \psi)}{\sqrt{(\cos \psi^+ - \cos \psi)(\cos \psi - \cos \psi^-)}}, \quad (45.195)$$

where

$$S(v_1, g; v_3) = \frac{M_{13}}{1+a} [(1+a)(v_1^2 + av_3^2) - ag^2]^{1/2}.$$

Scattering angle ψ -limits,

$$\cos \psi^\pm = \cos \psi^\pm(\epsilon, v_1, g; v_3) \quad (45.196)$$

$$= \frac{g}{g' \alpha^2 + \beta^2} \left\{ \alpha(\alpha + \bar{\epsilon}) \pm \beta [\omega^2(\alpha^2 + \beta^2) - (\alpha + \bar{\epsilon})^2]^{1/2} \right\}, \quad (45.197)$$

where

$$\alpha = \alpha(v_1, g; v_3) = \frac{1}{2} M_{13} \left[v_1^2 - v_3^2 + \left(\frac{1-a}{1+a} \right) g^2 \right],$$

$$\beta = \beta(v_1, g; v_3) = \frac{1}{2} M_{13} [(2v_1^2 + 2v_3^2 - g^2)g^2 - (v_1^2 - v_3^2)^2]^{1/2},$$

$$\omega = g'/g, \quad \bar{\epsilon} = \epsilon + \frac{a}{1+a} \Delta_3.$$

Special Case: $f_{13} = f_{13}(P)$

$$\sigma(v_3) = \frac{\pi}{M_{13}^2 v_3^2} \int_{\epsilon_1}^{\epsilon_2} d\epsilon \int_{v_{10}}^{\infty} \frac{W_{nl}(v_1) dv_1}{v_1} \times \int_{P^-}^{P^+} |f_{13}(P)|^2 dP. \quad (45.198)$$

45.8 BINARY ENCOUNTER APPROXIMATION

The basic assumption of the binary encounter approximation is that an excitation or ionization process is caused solely by the interaction of the incoming charged or neutral projectile with the Rydberg electron bound to its parent ion. If, for example, the cross section depends only on the momentum transfer P to the Rydberg electron (as in the Born approximation), then the total cross section is obtained by integrating σ_P over the momentum distribution of the Rydberg electron. The basic cross sections required are given in the following section. For further details see [31] and references therein.

45.8.1 Differential Cross Sections

Cross Section per Unit Momentum Transfer

Let the masses, velocities and charges of the particles be $(m_1, \mathbf{v}_1, Z_1, e)$ and $(m_2, \mathbf{v}_2, Z_2, e)$, with $\mathbf{v} = |\mathbf{v}_1 - \mathbf{v}_2|$ denoting the relative velocity and quantities *after* the collision are denoted by primes. Then for distinguishable particles,

$$\sigma_P = \frac{8\pi Z_1^2 Z_2^2 e^4 P}{v^2} \left| \frac{\exp(i\eta_P)}{P^2} \right|^2, \quad (45.199)$$

where the phase shift η_P is

$$\eta_P = -2\gamma \ln(P/2\mu v) + 2\eta_0 + \pi, \quad (45.200)$$

and with

$$\mu = \frac{m_1 m_2}{m_1 + m_2}, \quad \gamma = \frac{Z_1 Z_2 e^2}{\hbar v}, \quad e^{2i\eta_0} = \frac{\Gamma(1+i\gamma)}{\Gamma(1-i\gamma)}. \quad (45.201)$$

For identical particles,

$$\sigma_P^\pm = \frac{8\pi Z_1^2 Z_2^2 e^4 P}{v^2} \left| \frac{e^{i\eta_P}}{P^2} \pm \frac{e^{i\eta_S}}{S^2} \right|^2, \quad (45.202)$$

where η_P is given by (45.200) and η_S is

$$\eta_S = -2\gamma \ln(S/2\mu v) + 2\eta_0 + \pi, \quad (45.203)$$

while η_0 is given by (45.201). The momenta \mathbf{P} and \mathbf{S} transferred by direct and exchange collisions, respectively are given by

$$\mathbf{P} = m_1(\mathbf{v}_1 - \mathbf{v}_1') = m_2(\mathbf{v}_2 - \mathbf{v}_2'), \quad (45.204a)$$

$$\mathbf{S} = m_1(\mathbf{v}_1 - \mathbf{v}_2') = m_2(\mathbf{v}_1' - \mathbf{v}_2). \quad (45.204b)$$

The collision rates (in cm³/s) are

$$\hat{\alpha}_P = v_1 \sigma_P, \quad \hat{\alpha}_P^\pm = v_1 \sigma_P^\pm. \quad (45.205)$$

Cross Section per Unit Momentum Transferred per Unit Steradian

Differential relationships:

$$\alpha_{E,P} = \frac{d^2 \alpha}{dP dE} = \frac{d^2 \alpha}{dP d\varphi} \frac{d\varphi}{dE} = \alpha_{P,\varphi} \frac{d\varphi}{dE}. \quad (45.206)$$

For distinguishable particles,

$$\alpha_P = 2\pi v_1 \sigma_{P,\varphi} = 2\pi \alpha_{P,\varphi}, \quad (45.207a)$$

$$\alpha_{P,\varphi} = \frac{4Z_1^2 Z_2^2 e^4 P}{v} \left| \frac{e^{i\eta_P}}{P^2} \right|^2, \quad (45.207b)$$

$$\alpha_{E,P} = v_1 \sigma_{E,P} = \frac{8Z_1^2 Z_2^2 e^4}{v_1 v_2 \sqrt{X}} \left| \frac{e^{i\eta_P}}{P^2} \right|^2. \quad (45.207c)$$

For identical particles,

$$\alpha_{P,\varphi}^{\pm} = \frac{4Z_1^2 Z_2^2 e^4 P}{v} \left| \frac{\exp(i\eta_P)}{P^2} \pm \frac{\exp(i\eta_S)}{S^2} \right|^2, \quad (45.208a)$$

$$\alpha_{E,P}^{\pm} = v_1 \sigma_{E,P}^{\pm} = \frac{8Z_1^2 Z_2^2 e^4}{v_1 v_2 \sqrt{X}} \left| \frac{e^{i\eta_P}}{P^2} \pm \frac{e^{i\eta_S}}{S^2} \right|^2, \quad (45.208b)$$

where

$$X = -\cos^2 \phi + 2(\hat{v}_1 \cdot \hat{P})(\hat{v}_2 \cdot \hat{P}) \cos \phi + 1 - (\hat{v}_1 \cdot \hat{P})^2 - (\hat{v}_2 \cdot \hat{P})^2 \quad (45.209a)$$

$$= (\cos \phi_{\min} - \cos \phi)(\cos \phi - \cos \phi_{\max}) \quad (45.209b)$$

$$= \left(\frac{v}{v_1 v_2 P} \right)^2 (E_{\max} - E)(E - E_{\min}), \quad (45.209c)$$

with ϕ being the angle between the velocity vectors \mathbf{v}_1 and \mathbf{v}_2 .

For the special case where the target particle (2) is an electron in a Rydberg orbital, $m_2 = m_e$, $Z_2 = -1$, and

$$\sigma_{E,P}(\phi) = \frac{8Z_1^2 e^4}{v_1^2 v_2 P^4 \sqrt{X}}, \quad (45.210)$$

$$\sigma_{E,P}^{\pm}(\phi) = \frac{8e^4}{v_1^2 v_2 \sqrt{X}} \left[\frac{1}{P^4} + \frac{1}{S^4} \pm \frac{2 \cos(\eta_P - \eta_S)}{P^2 S^2} \right], \quad (45.211)$$

where $\eta_P - \eta_S = -2\gamma \ln(P/S) = (2e^2/\hbar v) \ln(S/P)$, and X is given by (45.209b).

Integrated Cross Sections

For incident heavy particles:

$$\sigma_{E,P} = \int_0^\pi \sigma_{E,P}(\phi) \frac{1}{2} \sin \phi d\phi = \frac{4\pi Z_1^2 e^4}{v_1^2 v_2 P^4}. \quad (45.212)$$

For incident electrons:

$$\sigma_{E,P}^{\pm} = \int_0^\pi \sigma_{E,P}^{\pm}(\phi) \frac{1}{2} \sin \phi d\phi \quad (45.213a)$$

$$= \frac{4\pi e^4}{v_1^2 v_2} \left[\frac{1}{P^4} + \frac{v_1^2 + v_2^2 - P^2/2m_e^2 - 2E^2/P^2}{m_e^4 |v_1^2 - v_2^2 - 2E/m_e|^3} \pm \frac{2\Phi}{m_e^2 P^2 |v_1^2 - v_2^2 - 2E/m_e|} \right], \quad (45.213b)$$

where Φ can be approximated [32] by

$$\Phi \sim \cos \left(\left| \frac{R_\infty}{E_3 - E_2} \right|^{1/2} \ln \left| \frac{E}{E_3 - E_2 - E} \right| \right). \quad (45.214)$$

and E_3 is defined in ref. [32].

Cross Sections per Unit Energy

For incident heavy particles (3 cases):

$$\sigma_E = \frac{2\pi Z_1^2 e^4}{m_e v_1^2} \left(\frac{1}{E^2} + \frac{2m_e v_2^2}{3E^2} \right), \quad (45.215)$$

which is valid for $2v_1 \geq v_2 + v'_2$, $E \leq 2m_e v_1(v_1 - v_2)$, or

$$\sigma_E = \frac{\pi Z_1^2 e^4}{3v_1^2 v_2 E^3} \left[4v_1^3 - \frac{1}{2}(v'_2 - v_2)^2 \right], \quad (45.216)$$

which is valid for $v'_2 - v_2 \leq 2v_1 \leq v'_2 + v_2$, $2m_e v_1(v_1 - v_2) \leq E \leq 2m_e v_1(v_1 + v_2)$, or otherwise, $\sigma_E = 0$ for $E \geq m_e v_1(v'_2 + v_2)$.

For incident electrons (2 cases):

$$\sigma_E^{\pm} = \frac{2\pi e^4}{m_e v_1^2} \left[\frac{1}{E^2} + \frac{2m_e v_2^2}{3E^3} + \frac{1}{D^2} + \frac{2m_e v_2^2}{3D^3} \pm \frac{2\Phi}{ED} \right], \quad (45.217)$$

which is valid for $m_e(v_1 - v'_1) \leq m_e(v'_2 - v_2)$, $m_e(v'_2 + v_2) \leq m_e(v_1 + v'_1)$, $D \geq 0$, or

$$\sigma_E = \frac{2\pi e^4}{m_e v_1^2} \left[\frac{1}{E^2} + \frac{2m_e v_1'^2}{3E^3} + \frac{1}{D^2} + \frac{2m_e v_1'^2}{3|D|^3} \pm \frac{2\Phi}{E|D|} \right] \frac{v'_1}{v_1}, \quad (45.218)$$

which is valid for $m_e(v'_2 - v_2) \leq m_e(v_1 - v'_1)$, $m_e(v_1 + v'_1) \leq m_e(v'_2 + v_2)$, $D \leq 0$.

In the expressions above, the exchange energy D transferred during the collision is

$$D = \frac{1}{2} m_e v_1^2 - \frac{1}{2} m_e v_2'^2 = \frac{1}{2} m_e v_1^2 - \frac{1}{2} m_e v_2^2 - E. \quad (45.219)$$

45.8.2 Integral Cross Sections

$$e^-(T) + A(E_2) \rightarrow e^-(E) + A^+ + e^-, \quad (45.220)$$

where T is the initial kinetic energy of the projectile electron, while the Rydberg electron, initially bound in potential U_i to the core A^+ , has kinetic energy E_2 . The cross section per unit energy E is denoted below by σ_E . See the review by Vriens [31] for details.

For electron impact, there are two collision models: the *unsymmetrical collision model* of Thomson and Gryzinski assumes that the incident electron has zero potential energy, and the *symmetrical collision model* of Thomas and Burgess assumes that the incident electron is accelerated initially by the target (and thereby gains kinetic energy) while losing an equal amount of potential energy.

Unsymmetrical model (2 cases):

$$\sigma_E = \frac{\pi e^4}{T} \left[\frac{1}{E^2} + \frac{4E_2}{3E^3} + \frac{1}{D^2} + \frac{4E_2}{3D^3} - \frac{\Phi}{ED} \right], \quad (45.221)$$

which is valid for $D = T - E_2 - E \geq 0$ or,

$$\sigma_E = \frac{\pi e^4}{T} \left[\frac{1}{E^2} + \frac{4T'}{3E^3} + \frac{1}{D^2} + \frac{4T'}{3|D|^3} - \frac{\Phi}{E|D|} \right] \left(\frac{T'}{E_2} \right)^{1/2} \quad (45.222)$$

which is valid for $D \leq 0$ and $T \geq E$; and where $T' \equiv T - E$.

Symmetrical model (2 cases):

$$\sigma_E = \frac{\pi e^4}{T_i} \left[\frac{1}{E^2} + \frac{4E_2}{3E^3} + \frac{1}{X_i^2} + \frac{4E_2}{3X_i^3} - \frac{\Phi}{EX_i} \right], \quad (45.223)$$

which is valid for $X_i \equiv T + U_i - E \geq 0$, with $T_i \equiv T + U_i + E_2$, and

$$\sigma_E = \frac{\pi e^4}{T_i} \left[\frac{1}{E^2} + \frac{4T'_i}{3E^3} + \frac{1}{X_i^2} + \frac{4T'_i}{3|X_i|^3} - \frac{\Phi}{E|X_i|} \right] \left(\frac{T'_i}{E_2} \right)^{1/2} \quad (45.224)$$

which is valid for $0 \leq T'_i \leq E_2$, $T \geq 0$, with $T'_i \equiv T_i - E$, and where Φ is given by (45.214).

For incident heavy particles, the unsymmetrical model (45.221) should be used.

Single Particle Ionization

The total ionization cross section per atomic electron for incident heavy particles is

$$Q_i = \frac{2\pi Z_i^2 e^4}{m_e v_i^2} \left[\frac{1}{U_i} + \frac{m_e v_2^2}{3U_i^2} - \frac{1}{2m_e(v_1^2 - v_2^2)} \right], \quad (45.225)$$

which is valid for $U_i \leq 2m_e v_1(v_1 - v_2)$, or

$$Q_i = \frac{\pi Z_i^2 e^4}{m_e v_i^2} \left\{ \frac{1}{2m_e v_2(v_1 + v_2)} + \frac{1}{U_i} + \frac{m_e}{3v_2 U_i^2} [2v_1^3 + v_2^3 - \left(\frac{2U_i}{m_e} + v_2^2 \right)^{3/2}] \right\}, \quad (45.226)$$

which is valid for $2m_e v_1(v_1 - v_2) \leq U_i \leq 2m_e v_1(v_1 + v_2)$, or otherwise $Q_i = 0$ for $U_i \geq 2m_e v_1(v_1 + v_2)$.

For electron impact,

$$Q_i = \frac{1}{2} [Q_i^{\text{dir}} + Q_i^{\text{ex}} + Q_i^{\text{int}}]. \quad (45.227)$$

In the unsymmetrical model, Q_i^{ex} diverges, hence the exchange and interference terms above are omitted in the unsymmetrical model for electrons to obtain

$$Q_i^{\text{dir}} = \frac{\pi e^4}{T} \left[\frac{1}{U_i} + \frac{2E_2}{3U_i^2} - \frac{1}{T - E_2} \right], \quad (45.228)$$

which is valid for $T \geq E_2 + U_i$, or

$$Q_i^{\text{dir}} = \frac{2\pi e^4}{3T} \frac{(T - U_i)^{3/2}}{U_i^2 \sqrt{E_2}}, \quad (45.229)$$

which is valid for $U_i \leq T \leq E_2 + U_i$.

In the symmetrical model,

$$Q_i^{\text{dir}} = Q_i^{\text{ex}} = \frac{\pi e^4}{T_i} \left[\frac{1}{U_i} - \frac{1}{T} + \frac{2}{3} \left(\frac{E_2}{U_i^2} - \frac{E_2}{T^2} \right) \right], \quad (45.230)$$

$$Q_i^{\text{int}} = -\frac{\pi e^4}{T_i} \left[\frac{2\Phi'}{T + U_i} \ln \frac{T}{U_i} \right], \quad (45.231)$$

where Φ' can be approximated by [32]

$$\Phi' = \cos \left[\left(\frac{R_\infty}{E_1 + U_i} \right)^{1/2} \ln \frac{E_1}{U_i} \right]. \quad (45.232)$$

and E_1 is defined in [32].

The sum of (45.230) and (45.231) yields

$$Q_i = \frac{\pi e^4}{T_i} \left[\frac{1}{U_i} - \frac{1}{T} + \frac{2}{3} \left(\frac{E_2}{U_i} - \frac{E_2}{T^2} \right) - \frac{\Phi'}{T + U_i} \ln \frac{T}{U_i} \right], \quad (45.233)$$

which is also obtained by integrating the expression (45.224) for σ_E ,

$$Q_i = \int_{U_i}^{\frac{1}{2}(T+U_i)} \sigma_E dE. \quad (45.234)$$

Ionization Rate Coefficients. For heavy particle impact [27],

$$\langle Q \rangle = \frac{a_0^2}{\kappa^2} \left\{ \frac{128}{9} (\kappa^3 b^3 - b^{3/2}) + \frac{1}{3} \lambda b (35 - \frac{58}{3} b - \frac{8}{3} b^2) + \frac{2}{3} \kappa a b [(5 - 4\kappa^2)(3a^2 + \frac{3}{2} a b + b^2) - \lambda \kappa (\frac{15}{2} + 9a + 5b)] - 16\kappa a^4 \ln(4\kappa^2 + 1) + \theta [\frac{35}{6} - \kappa^2 a (\frac{5}{2} + 3a + 4a^2 + 8a^3)] \right\}, \quad (45.235)$$

where

$$\kappa = v_1/v_0, \quad \lambda = \kappa - (4\kappa)^{-1}, \quad \theta = \pi + 2 \tan^{-1} \lambda, \quad (45.236)$$

$$a = (1 + \kappa^2)^{-1}, \quad b = (1 + \lambda^2)^{-1}, \quad (45.237)$$

$$\langle \sigma_{E,P} dP dE \rangle = \frac{64e^4 v_0^5}{3v_i^2 P^4} \left(\left| \frac{E}{P} - \frac{P}{2m_e} \right|^2 + v_0^2 \right)^{-3} dP dE, \quad (45.238)$$

where $\frac{1}{2} m_e v_0^2$ is the ionization energy of H(1s).

Scaling Laws. Given the binary encounter cross section for ionization by protons of energy E_1 of an atom with binding energy u_a , the cross section for ionization of an atom with different binding energy u_b and scaled proton energy E'_1 can be determined to be [17]

$$\sigma_{\text{ion}}(E'_1, u_b) = \left(\frac{u_a^2}{u_b^2} \right) \sigma_{\text{ion}}(E_1, u_a), \quad (45.239)$$

$$E'_1 = (u_b/u_a)E_1, \quad (45.240)$$

where $\sigma_{\text{ion}}(E, u)$ is the ionization cross section for removal of a single electron from an atom with binding energy u by impact with a proton with initial energy E .

Double Ionization: See Ref. [33] for binary encounter cross section formulae for the direct double ionization of two-electron atoms by electron impact.

Excitation

Excitation is generally less violent than ionization and hence binary encounter theory is less applicable. Binary encounter theory can be applied to *exchange excitation* transitions e.g., $e^- + \text{He}(n^1L) \rightarrow e^- + \text{He}(n'^3L)$, with the restriction of large incident electron velocities. The cross section is

$$Q_e^{\text{ex}} = \int_{U_n}^{U_{n+1}} \sigma_{E,\text{ex}} dE \\ = \frac{\pi e^4}{T_i} \left\{ \frac{1}{T_{n+1}} - \frac{1}{T_n} + \frac{2}{3} \left[\frac{E_2}{T_{n+1}^2} - \frac{E_2}{T_n^2} \right] \right\}, \quad (45.241)$$

valid for $T \geq U_{n+1}$, with $T_n \equiv T + U_i - U_n$ and $T_{n+1} \equiv T + U_i + U_{n+1}$, or

$$Q_e^{\text{ex}} = \int_{U_n}^T \sigma_{E,\text{ex}} dE \\ = \frac{\pi e^4}{T_i} \left\{ \frac{1}{U_i} - \frac{1}{T_n} + \frac{2}{3} \left[\frac{E_2}{U_i^2} - \frac{E_2}{T_n^2} \right] \right\}, \quad (45.242)$$

valid for $U_n \leq T \leq U_{n+1}$. U_n and U_{n+1} denote the excitation energies for levels n and $n+1$, respectively.

45.8.3 Classical Ionization Cross Section

Applying the classical energy-change cross section result (45.70) of Gerjuoy [16] to the case of electron-impact ionization yields the four cases [34]

$$\sigma_{\text{ion}}(v_1, v_2) \sim \int_{\Delta E_l}^{\Delta E_u} \sigma_{\Delta E}^{\text{eff}}(v_1, v_2; m_1/m_2) d(\Delta E) \\ = \frac{\pi(Z_1 Z_2 e^2)^2}{3v_1^2 v_2} \left[\frac{-2v_2^3}{(\Delta E)^2} - \frac{6v_2}{m_2 \Delta E} \right], \quad (45.243)$$

which is valid for $0 < \Delta E < b$, or

$$\sigma_{\text{ion}}(v_1, v_2) \\ = \frac{\pi(Z_1 Z_2 e^2)^2}{3v_1^2 v_2} \left[\frac{4(v_1 - 2v'_1)}{m_1^2(v_1 - v'_1)^2} + \frac{4(v_2 - 2v'_2)}{m_2^2(v_2 - v'_2)^2} \right], \quad (45.244)$$

which is valid for $b < \Delta E < a$, or

$$\sigma_{\text{ion}}(v_1, v_2) = \frac{\pi(Z_1 Z_2 e^2)^2}{3v_1^2 v_2} \left[\frac{-2v_1^3}{(\Delta E)^2} \right], \quad (45.245)$$

which is valid for $\Delta E > a$, $2m_2 v_2 > |m_1 - m_2|v_1$, or otherwise is zero for $\Delta E > a$, $2m_2 v_2 < |m_1 - m_2|v_1$.

The limits $\Delta E_{l,u}$ to the ΔE integration in each of the four cases is indicated in the appropriate validity conditions. The constants a and b above are given by

$$a = \frac{4m_1 m_2}{(m_1 + m_2)^2} [E_1 - E_2 + \frac{1}{2} v_1 v_2 (m_1 - m_2)], \\ b = \frac{4m_1 m_2}{(m_1 + m_2)^2} [E_1 - E_2 - \frac{1}{2} v_1 v_2 (m_1 - m_2)].$$

The expressions above for $\sigma_{\text{ion}}(v_1, v_2)$ must be averaged over the speed distribution of v_2 before comparison with experiment. See [34] for explicit formulae for the case of a delta function speed distribution.

45.8.4 Classical Charge Transfer Cross Section

Applying the classical energy-change cross section result (45.70) of Gerjuoy [16] to the case of charge-transfer yields the four cases [34]

$$\sigma_{\text{CX}}(v_1, v_2) \sim \int_{\Delta E_l}^{\Delta E_u} \sigma_{\Delta E}^{\text{eff}}(v_1, v_2) d\Delta E \\ = \frac{\pi e^4}{3v_1^2 v_2} \left[-\frac{2v_2^3}{(\Delta E)^2} - \frac{6v_2/m_2}{\Delta E} \right] \quad (45.246)$$

which is valid for $0 < \Delta E < b$, or

$$\sigma_{\text{CX}}(v_1, v_2) = \frac{\pi e^4}{3v_1^2 v_2} \left[3 \frac{v_1/m_1 - v_2/m_2}{\Delta E} + \frac{(v_2^3 - v_1^3) - (v_1^3 + v_2^3)}{(\Delta E)^2} \right], \quad (45.247)$$

which is valid for $b < \Delta E < a$, or

$$\sigma_{\text{CX}}(v_1, v_2) = \frac{\pi e^4}{3v_1^2 v_2} \left(-\frac{2v_1^2}{(\Delta E)^2} \right), \quad (45.248)$$

which is valid for $\Delta E > a$, $m_e v_2 > (m_1 - m_e)v_1$, or otherwise $\sigma_{\text{CX}} = 0$ when $\Delta E > a$, $m_e v_2 < (m_1 - m_e)v_1$. The above expressions for $\sigma_{\text{CX}}(v_1, v_2)$ must be averaged over the speed distribution $W(v_2)$ before comparison with experiment. See [34] for details. The constants a and b above are as defined in Sect. 45.8.3, and the limits $\Delta E_{l,u}$ are given by

$$\Delta E_l = \frac{1}{2} m_e v_1^2 + U_A - U_B, \quad (45.249a)$$

$$\Delta E_u = \frac{1}{2} m_e v_1^2 + U_A + U_B, \quad (45.249b)$$

$$v_2 = \sqrt{2U_A/m_e}, \quad (45.249c)$$

where $U_{A,B}$ are the binding energies of atoms A and B . The expressions above for σ_{CX} diverges for some $v_1 > 0$ if $U_A < U_B$. If $U_A = U_B$ then σ_{CX} diverges at $v_1 = 0$. To avoid the divergence, employ Gerjuoy's modification, $\Delta E_l = \frac{1}{2} m_e v_1^2 + U_A$.

45.9 BORN APPROXIMATION

See reviews [35, 36], as well as any standard textbook on scattering theory, for background details on the Born approximation, and [37–40] for extensive tables of Born cross sections.

45.9.1 Form Factors

The basic formulation of the first Born approximation for high energy heavy particle scattering is discussed in Sect. ????. For the general atom-atom or ion-atom scattering process

$$A(i) + B(i') \rightarrow A(f) + B(f'), \quad (45.250)$$

with nuclear charges Z_A and Z_B respectively, let $\hbar\mathbf{K}_i$ and $\hbar\mathbf{K}_f$ be the initial and final momenta of the projectile A , and $\hbar\mathbf{q} = \hbar\mathbf{K}_f - \hbar\mathbf{K}_i$ be the momentum transferred to the target. Then Eq. (???) can be written in the generalized form

$$\sigma_{if}^{i'f'} = \frac{8\pi a_0^2}{s^2} \int_{t_-}^{t_+} \frac{dt}{t^3} |Z_A \delta_{if} - F_{if}^A(t)|^2 \times |Z_B \delta_{i'f'} - F_{i'f'}^B(t)|^2, \quad (45.251)$$

where the momentum transfer is $t = qa_0$, and $s = v/v_B$ is the initial relative velocity in units of v_B . The form factors are

$$F_{if}^A(t) = \left\langle \Phi_f^A \left| \sum_{k=1}^{N_A} \exp(it \cdot \mathbf{r}_k/a_0) \right| \Phi_i^A \right\rangle, \quad (45.252)$$

where N_A is the number of electrons associated with atom A , and similarly for $F_{i'f'}^B(t)$. The limits of integration are $t_{\pm} = |K_f \pm K_i|a_0$. For heavy particle collisions, $t_{+} \sim \infty$ and

$$t_- = (K_i - K_f)a_0 \simeq \frac{\Delta E_{if}}{2s} \left(1 + \frac{m_e \Delta E_{if}}{4Ms^2} \right), \quad (45.253)$$

where $M = M_A M_B / (M_A + M_B)$.

Limiting Cases. As discussed in Sect. ???, for the case $i = f$, $F_{if}^A(t) \rightarrow N_A$ as $t \rightarrow 0$, so that $Z_A - F_{if}^A(t) \rightarrow Z_A - N_A$. For the case $i \neq f$, $F_{if}^A(t) \rightarrow 0$ as $t \rightarrow 0$ and $t \rightarrow \infty$.

45.9.2 Hydrogenic Form Factors

Bound-Bound Transitions: In terms of $\tau = t/Z$,

$$|F_{1s,1s}| = \frac{16}{(4 + \tau^2)^2} \quad (45.254a)$$

$$|F_{1s,2s}| = 2^{17/2} \frac{\tau^2}{(4\tau^2 + 9)^3} \quad (45.254b)$$

$$|F_{1s,2p}| = 2^{15/2} \frac{3\tau}{(4\tau^2 + 9)^3} \quad (45.254c)$$

$$|F_{1s,3s}| = 2^4 3^{7/2} \frac{(27\tau^2 + 16)\tau^2}{(9\tau^2 + 16)^4} \quad (45.254d)$$

$$|F_{1s,3p}| = 2^{11/2} 3^3 \frac{(27\tau^2 + 16)\tau}{(9\tau^2 + 16)^4} \quad (45.254e)$$

$$|F_{1s,3d}| = 2^{17/2} 3^{7/2} \frac{\tau^2}{(9\tau^2 + 16)^4} \quad (45.254f)$$

Bound-Continuum Transitions: In terms of the scaled wave vector $\kappa = ka_0/Z$ for the ejected electron,

$$|F_{1s,\kappa}|^2 = \frac{2^8 \kappa \tau^2 (1 + 3\tau^2 + \kappa^2) \exp(-2\theta/\kappa)}{3 [1 + (\tau - \kappa)^2]^3 [1 + (\tau + \kappa)^2]^3 (1 - e^{-2\pi/\kappa})} \quad (45.255)$$

where $\theta = \tan^{-1}[2\kappa/(1 + \tau^2 - \kappa^2)]$. Expressions for the bound-continuum Form Factors for the L-shell ($2\ell \rightarrow \kappa$) and M-shell ($3\ell \rightarrow \kappa$) transitions can be found in Refs. [41] and [42], respectively. See also §4 of [43] for further details.

General Expressions and Trends:

For final ns states

$$|F_{1s,ns}|^2 = \frac{2^4 n [(n-1)^2 + n^2 \tau^2]^{n-1}}{\tau^2 [(n+1)^2 + n^2 \tau^2]^{n+1}} \times \sin^2(n \tan^{-1} x + \tan^{-1} y), \quad (45.256)$$

where

$$x = \frac{2\tau}{n(\tau^2 + 1 - n^{-2})}, \quad y = \frac{2\tau}{\tau^2 - 1 + n^{-2}}. \quad (45.257)$$

For final $n\ell$ states [46]

$$F_{1s,n\ell}(\tau) = (i\tau)^{\ell} 2^{3(\ell+1)} \sqrt{2\ell+1} (\ell+1)! \left(\frac{(n-\ell-1)!}{(n+\ell)!} \right)^{1/2} \times n^{\ell+1} \frac{[(n-1)^2 + n^2 \tau^2]^{(n-\ell-3)/2}}{[(n+1)^2 + n^2 \tau^2]^{(n+\ell+3)/2}} \left\{ a_{n\ell} C_{n-\ell-1}^{(\ell+2)}(x) - b_{n\ell} C_{n-\ell-2}^{(\ell+2)}(x) + c_{n\ell} C_{n-\ell-3}^{(\ell+2)}(x) \right\}, \quad (45.258)$$

with coefficients $a_{n\ell}$, $b_{n\ell}$ and $c_{n\ell}$ given by

$$a_{n\ell} = (n+1) [(n-1)^2 + n^2 \tau^2], \quad (45.259a)$$

$$b_{n\ell} = 2n \sqrt{[(n-1)^2 + n^2 \tau^2][(n+1)^2 + n^2 \tau^2]}, \quad (45.259b)$$

$$c_{n\ell} = (n-1) [(n+1)^2 + n^2 \tau^2], \quad (45.259c)$$

and argument

$$x = \frac{n^2 - 1 + n^2 \tau^2}{\sqrt{[(n+1)^2 + n^2 \tau^2][(n-1)^2 + n^2 \tau^2]}}.$$

Summation over final ℓ states

$$|F_{1s,n}|^2 = \sum_{\ell} |F_{1s,n\ell}|^2 = 2^8 n^7 \tau^2 \left[\frac{1}{3}(n^2 - 1) + n^2 \tau^2 \right] \times \frac{[(n-1)^2 + n^2 \tau^2]^{n-3}}{[(n+1)^2 + n^2 \tau^2]^{n+3}}. \quad (45.260)$$

which becomes for large n ,

$$|F_{1s,n}|^2 \sim \frac{2^8 \tau^2 (3\tau^2 + 1)}{3n^3 (\tau^2 + 1)^6} \exp\left(\frac{-4}{(\tau^2 + 1)}\right). \quad (45.261)$$

For initial $2s$ and $2p$ states,

$$|F_{2s,n}|^2 = 2^4 n^7 \tau^2 \left[-\frac{1}{3} + \frac{1}{2}n^2 - \frac{3}{16}n^4 + \frac{1}{48}n^6 + n^2 \tau^2 \left(\frac{1}{3} - \frac{2}{3}n^2 + \frac{19}{48}n^4 \right) + n^4 \tau^4 \left(\frac{5}{3} - \frac{7}{6}n^2 \right) + n^6 \tau^6 \right] \frac{[(\frac{1}{2}n-1)^2 + n^2 \tau^2]^{n-4}}{[(\frac{1}{2}n+1)^2 + n^2 \tau^2]^{n+4}}, \quad (45.262)$$

$$|F_{2p,n}|^2 = \frac{2^4 n^9 \tau^2}{3} \left[\frac{1}{4} - \frac{7}{24}n^2 + \frac{11}{192}n^4 - n^2 \tau^2 \left(\frac{5}{6} - \frac{23}{24}n^2 \right) + \frac{1}{4}n^4 \tau^4 \right] \times \frac{[(\frac{1}{2}n-1)^2 + n^2 \tau^2]^{n-4}}{[(\frac{1}{2}n+1)^2 + n^2 \tau^2]^{n+4}}. \quad (45.263)$$

Power Series Expansion: $\tau^2 \ll 1$ [4]

$$|F_{1s,n}(\tau)|^2 = A(n)\tau^4 + B(n)\tau^6 + C(n)\tau^8 + \dots, \quad (45.264)$$

where

$$A(n) = \frac{2^8 n^9 (n-1)^{2n-6}}{3^2 (n+1)^{2n+6}},$$

$$B(n) = -\frac{2^9 n^{11} (n^2 + 11)(n-1)^{2n-8}}{3^2 5 (n+1)^{2n+8}},$$

$$C(n) = -\frac{2^8 n^{13} (313n^4 - 1654n^2 - 2067)(n-1)^{2n-10}}{3^2 5^2 7 (n+1)^{2n+10}}.$$

For analytical expressions for $A(n)$, $B(n)$ and $C(n)$ for final np and nd states see Refs. [44, 45].

General Trends in Hydrogenic Form Factors: [47]

The inelastic form factor $|F_{n\ell \rightarrow n'\ell'}|$ oscillates with ℓ' on an increasing background until the value

$$\ell'_{max} = \min \left\{ (n' - 1), n \left(\frac{2(n+3)}{(n+1)} \right)^{1/2} - \frac{1}{2} \right\} \quad (45.265)$$

is reached, after which a rapid decline for $\ell > \ell'_{max}$ occurs. See [47] for illustrative graphs.

45.9.3 Excitation Cross Sections

Atom-Atom Collisions [48]

Single Excitation. For the process

$$A(i) + B \rightarrow A(f) + B, \quad (45.266)$$

Eq. (45.251) reduces to

$$\sigma_{if} = \frac{8\pi a_0^2}{s^2} \int_{t_-}^{\infty} \frac{dt}{t^3} |F_{if}^A|^2 |Z_B - F_{if}^{B'}|^2. \quad (45.267)$$

Double Excitation. For the process

$$H(1s) + H(1s) \rightarrow H(n\ell) + H(n'\ell'), \quad (45.268)$$

$$\sigma_{1s,n\ell}^{1s,n'\ell'} = \frac{8\pi a_0^2}{s^2} \int_{t_-}^{\infty} \frac{dt}{t^3} |F_{1s,n\ell}|^2 |F_{1s,n'\ell'}|^2. \quad (45.269)$$

Special cases are [49]

$$\sigma_{1s,2s}^{1s,2s} = \frac{2^{30} \pi a_0^2 (880t_-^4 + 396t_-^2 + 81)}{495s^2 (4t_-^2 + 9)^{11}}, \quad (45.270a)$$

$$\sigma_{1s,2p}^{1s,2p} = \frac{2^{30} 3^4 \pi a_0^2}{11s^2 (4t_-^2 + 9)^{11}}, \quad (45.270b)$$

$$\sigma_{1s,2s}^{1s,2p} = \frac{2^{29} 3^2 (44t_-^2 + 9)}{55s^2 (4t_-^2 + 9)^{11}}, \quad (45.270c)$$

with $t_-^2 = [9/(16s^2)][1 + 3m_e/(4Ms^2) + \dots]$.

Ion-Atom Collisions.

For the proton impact process

$$H^+ + H(1s) \rightarrow H^+ + H(n\ell), \quad (45.271)$$

Eq. (45.251) reduces to

$$\sigma_{1s,n\ell} = \frac{8\pi a_0^2}{s^2} \int_{t_-}^{\infty} \frac{dt}{t^3} |F_{1s,n\ell}(t)|^2 \quad (45.272)$$

with $t_- = (1 - n^{-2})/(2s)$.

Asymptotic Expansions:

$$\sigma_{1s,ns} = \frac{4\pi a_0^2 (n^2 - 1) |X_{1s \rightarrow ns}|^2}{24s^2 n^2} \left[C_s(n) - \frac{1}{s^2} + \frac{n^2 + 11}{20n^2 s^4} + \frac{313n^4 - 1654n^2 - 2067}{8400n^4 s^6} \right], \quad (45.273)$$

$$\sigma_{1s,np} = \frac{2^{10} \pi a_0^2 n^7 (n-1)^{2n-5}}{3s^2 (n+1)^{2n+5}} \left[C_p(n) + \ln s^2 + \frac{n^2 + 11}{10n^2 s^2} + \frac{313n^4 - 1654n^2 - 2067}{5600n^4 s^4} \right], \quad (45.274)$$

$$\sigma_{1s,nd} = \frac{2^{11} \pi a_0^2 (n^2 - 4)n^5 (n^2 - 1)^2 (n-1)^{2n-7}}{3^2 5s^2 (n+1)^{2n+7}} \times \left[C_d(n) - \frac{1}{s^2} + \frac{11n^2 + 13}{28n^2 s^4} \right], \quad (45.275)$$

where $C_s(2) = 16/5$, $C_s(3) = 117/32$, $C_s(4) \approx 3.386$, and

$$\gamma_n C_p(n) = \frac{1.3026}{n^3} + \frac{1.7433}{n^5} + \frac{16.918}{n^7}, \quad (45.276)$$

$$\gamma_n C_d(n) = \frac{2.0502}{n^3} + \frac{7.6125}{n^5}, \quad (45.277)$$

with

$$\gamma_n \equiv \frac{2^8 n^7 (n-1)^{(2n-5)}}{3(n+1)^{(2n+5)}}. \quad (45.278)$$

Further asymptotic expansion results can be found in Refs. [3-6].

A general expression for Born excitation and ionization cross sections for hydrogenic systems in terms of a parabolic coordinate representation (see Chap. ??) is given in Ref. [50].

Number of Independent Transitions \mathcal{N}_i between levels n and n' : [50]

$$\mathcal{N}_i = n^2 \left[n' - \left(\frac{n}{3} \right) \right] + \left(\frac{n}{3} \right) \quad (45.279)$$

Validity Criterion: The Born approximation is valid provided that [51]

$$nE \gg \ln \left(\frac{4E}{J_n} \right) \quad (45.280)$$

for transitions $n \rightarrow n'$ when $n, n' \gg 1$ and $|n - n'| \sim 1$. The constant J_n is undetermined (see [51] for details) but is generally taken to be the ionization potential of level n .

45.9.4 Ionization Cross Sections

$$e^-(k) + H \rightarrow e^-(k') + H^+ + e^-(\kappa) \quad (45.281)$$

The general expression for the Born differential ionization cross section can be evaluated in closed form using screened hydrogenic wave functions. The differential cross section per incident electron scattered into solid angle $d\Omega_{k'}$, integrated over directions κ for the ejected electron (treated as distinguishable) is [52, 53]

$$I(\theta, \phi) d\Omega_{k'} d\kappa' = \frac{4k'}{kq^4 a_0 \tilde{Z}_B^4} |F_{n\ell, \kappa'}(q)|^2 d\Omega_{k'} d\kappa', \quad (45.282)$$

where the form factor is given by Eq. (45.256) for the case $n\ell = 1s$, with the ejected electron wavenumber κ and momentum transferred q in the collision, $\kappa' = \kappa a_0 / \tilde{Z}_B$, $q = (\mathbf{k}' - \mathbf{k})a_0 / \tilde{Z}_B$, being scaled by the screened nuclear charge \tilde{Z}_B appropriate to the $n\ell$ -shell from which the electron is ejected. The total Born ionization cross section per electron is

$$\sigma_{\text{ion}}^B = \int_0^{\kappa_{\text{max}}} d\kappa' \int_{\mathbf{k}-\mathbf{k}'}^{\mathbf{k}+\mathbf{k}'} I(q, \kappa') dq \quad (45.283)$$

which is generally evaluated numerically.

Table 45.2. Coefficients $C(n_i \ell_i \rightarrow n_f \ell_f)$ in the Born capture cross section formula (45.288).

$n_f \ell_f$	$C(1s \rightarrow n_f \ell_f)$
1s	$2^8 Z_A^5 Z_B^5$
2s	$2^5 Z_A^5 Z_B^5$
2p	$2^5 Z_A^5 Z_B^7$
3s	$2^8 Z_A^5 Z_B^5 / 3^3$
3p	$2^{13} Z_A^5 Z_B^7 / 3^6$
3d	$2^{15} Z_A^5 Z_B^9 / 3^9$
4s	$2^2 Z_A^5 Z_B^5$
4p	$5 Z_A^5 Z_B^7$
4d	$Z_A^5 Z_B^9$
4f	$Z_A^5 Z_B^{11} / 20$
<hr/>	
$C(2s \rightarrow n_f \ell_f) = C(1s \rightarrow n_f \ell_f) / 8$	
$C(2p \rightarrow n_f \ell_f) = C(1s \rightarrow n_f \ell_f) / 24$	
<hr/>	

45.9.5 Capture Cross Sections

Electron Capture:

$$A^+ + B(n\ell) \rightarrow A(n'\ell') + B^+. \quad (45.284)$$

In the Ochkur-Brinkmann-Kramer (OBK) approximation [54],

$$\sigma_{n\ell, n'\ell'} = \frac{M^2}{2\pi\hbar^3} \frac{v_f}{v_i} \int_{-1}^1 d(\cos\theta) |F_{n\ell \rightarrow n'\ell'}|^2, \quad (45.285)$$

where $\mathbf{v}_i = v_i \hat{\mathbf{n}}_i$, $\mathbf{v}_f = v_f \hat{\mathbf{n}}_f$, θ is the angle between $\hat{\mathbf{n}}_i$ and $\hat{\mathbf{n}}_f$, $M = M_A M_B / (M_A + M_B)$, and

$$|F_{n\ell, n'\ell'}| = \int \int dr ds \varphi_i(\mathbf{r}) \varphi_f^*(\mathbf{s}) \left(\frac{Z_A e^2}{r} \right) e^{i(\alpha \cdot \mathbf{r} + \beta \cdot \mathbf{s})}, \quad (45.286)$$

with

$$\begin{aligned} \alpha &= k_f \hat{\mathbf{n}}_f + k_i \hat{\mathbf{n}}_i \frac{M_A}{M_A + m_e}, \\ \beta &= -k_i \hat{\mathbf{n}}_i - k_f \hat{\mathbf{n}}_f \frac{M_B}{M_B + m_e}, \\ k_i &= \frac{v_f}{\hbar} \frac{M_B (M_A + m_e)}{(M_A + M_B + m_e)}, \\ k_f &= \frac{v_f}{\hbar} \frac{(M_B + m_e) M_A}{(M_A + M_B + m_e)}. \end{aligned}$$

The Jackson-Schiff correction factor [55] is

$$\begin{aligned} \gamma_{\text{JS}} &= \frac{1}{192} \left(127 + \frac{56}{p^2} + \frac{32}{p^4} \right) \\ &\quad - \frac{\tan^{-1} \frac{1}{2} p}{48p} \left(83 + \frac{60}{p^2} + \frac{32}{p^4} \right) \end{aligned}$$

Table 45.3. Functions $F(n_i \ell_i \rightarrow n_f \ell_f; x)$ in the Born capture cross section formula (45.288).

$n_f \ell_f$	$F(n_i \ell_i, n_f \ell_f; x)$
1s	x^{-6}
2s	$(x - 2b^2)^2 x^{-8}$
2p	$(x - b^2)x^{-8}$
3s	$(x^2 - \frac{16}{3}b^2x + \frac{16}{3}b^4)^2 x^{-10}$
3p	$(x - b^2)(x - 2b^2)^2 x^{-10}$
3d	$(x - b^2)^2 x^{-10}$
4s	$(x - 2b^2)^2 (x^2 - 8b^2x + 8b^4)^2 x^{-12}$
4p	$(x - b^2)(x^2 - \frac{24}{5}b^2x + \frac{24}{5}b^4)^2 x^{-12}$
4d	$(x - b^2)^2 (x - 2b^2)^2 x^{-12}$
4f	$(x - b^2)^3 x^{-12}$
<hr/>	
$F(2s, n_f \ell_f; x) = (x - 2a^2)^2 x^{-2} F(1s, n_f \ell_f; x)$	
$F(2p, n_f \ell_f; x) = (x - a^2)x^{-2} F(1s, n_f \ell_f; x)$	
<hr/>	

$$+ \frac{(\tan^{-1} \frac{1}{2}p)^2}{24p^2} \left(31 + \frac{32}{p^2} + \frac{16}{p^4} \right), \quad (45.287)$$

and the capture cross section is

$$\sigma(n_i \ell_i, n_f \ell_f) = \frac{\gamma_{JS} \pi a_0^2}{p^2} C(n_i \ell_i, n_f \ell_f) \times \int_x^\infty F(n_i \ell_i, n_f \ell_f; x) dx, \quad (45.288)$$

with

$$p = \frac{mv_i}{\hbar}, \quad a = \frac{Z_A}{n_i}, \quad b = \frac{Z_B}{n_f},$$

$$x = [p^2 + (a + b)^2] [p^2 + (a - b)^2] / 4p^2.$$

The coefficients C in Eq. (45.288) are given in Table 45.2, while the functions F are given in Table 45.3 [54]. In Table 45.3, the appropriate value of a and b is indicated by the quantum numbers n_i , ℓ_i and n_f , ℓ_f .

Acknowledgments

The author thanks Prof. M. R. Flannery for many helpful discussions and Prof. E. W. McDaniel for access to his collection of reprints. The author would also like to thank Dr. D. R. Schultz of ORNL for the time necessary to complete this work.

This work was begun at the Georgia Institute of Technology (GIT) and completed at the Controlled Fusion Atomic Data Center at Oak Ridge National Laboratory (ORNL). The work at GIT was supported by US AFOSR grant No. F49620-94-1-0379. The work at ORNL was supported by the Office of Fusion Energy, US

DOE contract No. DE-AC05-84OR21400 with Lockheed-Martin Energy Systems, Inc. and by ORNL Research Associates Program administered jointly by ORNL and ORISE.

REFERENCES

1. I. L. Beigman and V. S. Lebedev, *Phys. Rep.* **250**, 95 (1995).
2. H. A. Bethe and E. E. Salpeter, *Quantum Mechanics of One- and Two-Electron Atoms* (Springer-Verlag, Berlin, 1957).
3. G. S. Khandelwal and B. H. Choi, *J. Phys. B* **1**, 1220 (1968).
4. G. S. Khandelwal and E. E. Fitchard, *J. Phys. B* **2**, 1118 (1969).
5. G. S. Khandelwal and J. E. Shelton, *J. Phys. B* **4**, L109 (1971).
6. G. S. Khandelwal and B. H. Choi, *J. Phys. B* **2**, 308 (1969).
7. W. Gordon, *Ann. Phys. (Leipzig)* **2**, 1031 (1929).
8. V. A. Davidkin and B. A. Zon, *Opt. Spectrosc.* **51**, 25 (1981).
9. L. A. Bureeva, *Astron. Zh.* **45**, 1215 (1968).
10. H. Griem, *Astrophys. J.* **148**, 547 (1967).
11. M. R. Flannery, in *Rydberg States of Atoms and Molecules*, edited by R. F. Stebbings and F. B. Dunning (Cambridge University Press, 1983), ch. 11.
12. A. Burgess and I. C. Percival, *Adv. At. Mol. Phys.* **4**, 109 (1968).
13. I. C. Percival, in *Atoms and Molecules in Astrophysics*, edited by T. R. Carson and M. J. Roberts (Academic Press, New York, 1972), p. 65.
14. I. C. Percival and D. Richards, *Adv. At. Mol. Phys.* **11**, 1 (1975).
15. M. Matsuzawa, *J. Phys. B* **8**, 2114 (1975).
16. E. Gerjuoy, *Phys. Rev.* **148**, 54 (1966).
17. D. R. Bates and A. E. Kingston, *Adv. At. Mol. Phys.* **6**, 269 (1970).
18. J. M. Khan and D. L. Potter, *Phys. Rev.* **133**, A890 (1964).
19. V. S. Lebedev and V. S. Marchenko, *Sov. Phys. JETP* **61**, 443 (1985).
20. A. Omont, *J. de Phys.* **38**, 1343 (1977).
21. B. Kaulakys, *J. Phys. B* **17**, 4485 (1984).
22. V. S. Lebedev, *J. Phys. B: At. Mol. Opt. Phys.* **25**, L131 (1992); *Soviet Phys. (JETP)* **76**, 27 (1993).
23. J. P. Coleman, in *Case Studies in Atomic Collision Physics I* edited by E. W. McDaniel and M. R. C. McDowell, (North Holland, Amsterdam, 1969), ch. 3.
24. J. P. Coleman, *J. Phys. B* **1**, 567 (1968).
25. M. R. Flannery, *Phys. Rev. A* **22**, 2408 (1980).
26. M. L. Goldberger and K. M. Watson, *Collision Theory*, (Wiley, New York, 1964), ch. 11.

27. M. R. C. McDowell, Proc. Phys. Soc. **89**, 23 (1966).
28. D. R. Bates and J. C. G. Walker, Planetary Spac. Sci. **14**, 1367 (1966).
29. D. R. Bates and J. C. G. Walker, Proc. Phys. Soc. **90**, 333 (1967).
30. M. R. Flannery, Ann. Phys. (NY) **61**, 465 (1970), *ibid.*, **79**, 480 (1973).
31. L. Vriens, in *Case Studies in Atomic Collision Physics I*, edited by E. W. McDaniel and M. R. C. McDowell, (North Holland, Amsterdam, 1969), ch. 6.
32. L. Vriens, Proc. Phys. Soc. **89**, 13 (1966).
33. B. N. Roy and D. K. Rai, J. Phys. B **5**, 816 (1973).
34. J. D. Garcia, E. Gerjuoy, and J. E. Welker, Phys. Rev. **165**, 66 (1968).
35. A. R. Holt and B. Moiseiwitsch, Adv. At. Mol. Phys. **4**, 143 (1968).
36. K. L. Bell and A. E. Kingston, Adv. At. Mol. Phys. **10**, 53 (1974).
37. L. C. Green, P. P. Rush, and C. D. Chandler, Astrophys. J. Suppl. Ser. **3**, 37 (1957).
38. W. B. Sommerville, Proc. Phys. Soc. **82**, 446 (1963).
39. A. Burgess, D. G. Hummer, and J. A. Tully, Phil. Trans. Roy. Soc. A **266**, 255 (1970).
40. C. T. Whelan, J. Phys. B **19**, 2343 and 2355 (1986).
41. M. C. Walske, Phys. Rev. **101**, 940 (1956).
42. G. S. Khandelwal and E. Merzbacher, Phys. Rev. **144**, 349 (1966).
43. E. Merzbacher and H. W. Lewis, *Handbuch der Physik. 34/2 X-ray Production by Heavy Charged Particles*, pp. 166, Springer-Verlag (1958).
44. M. Inokuti, Argonne Nat. Lab. Radio Phys. Div. A Report No. ANL-7220, (1965), pp. 1-10.
45. M. Inokuti, Rev. Mod. Phys. **43**, 297 (1971).
46. H. Bethe, *Handbuch der Physik. 24/1 Quantenmechanik der Ein- und Zwei-Elektronenprobleme*, pp. 502, Springer-Verlag (1933).
47. M. R. Flannery and K. J. McCann, Astrophys. J. **236**, 300 (1980).
48. D. R. Bates and G. Griffing, Proc. Phys. Soc. **66A**, 961 (1953), *ibid.* **67A**, 663 (1954).
49. D. R. Bates and A. Dalgarno, Proc. Phys. Soc. **65A**, 919 (1952).
50. K. Omidvar, Phys. Rev. **140**, A26 and A38 (1965).
51. A. N. Starostin, Sov. Phys. JETP **25**, 80 (1967).
52. E. H. S. Burhop, Proc. Camb. Phil. Soc. **36**, 43 (1940); J. Phys. B **5**, L241 (1972).
53. N. F. Mott and H. S. W. Massey, *The Theory of Atomic Collisions* (Clarendon Press, Oxford, 1965), pp. 489-490.
54. D. R. Bates and A. Dalgarno, Proc. Phys. Soc. **66A**, 972 (1953).
55. J. D. Jackson and H. Schiff, Phys. Rev. **89**, 359 (1953).

XI. Appendix E:

Elastic Scattering: Classical, Quantal and Semiclassical

by

M. R. Flannery

School of Physics

Georgia Institute of Technology

Atlanta, Georgia 30332

Elastic Scattering: Classical, Quantal and Semiclassical

M. R. Flannery

School of Physics, Georgia Institute of Technology, Atlanta, Georgia 30332-0430

46.1	CLASSICAL SCATTERING FORMULAE	2
46.1.1	Deflection Functions	2
46.1.2	Elastic Scattering Cross Section	3
46.1.3	Center-of-Mass to Laboratory Coordinate Conversion	3
46.1.4	Glories and Rainbow Scattering	4
46.1.5	Orbiting and Spiraling Collisions	4
46.1.6	Quantities Derived from Classical Scattering	4
46.1.7	Collision Action	5
46.2	QUANTAL SCATTERING FORMULAE	5
46.2.1	Basic Formulae	5
46.2.2	Identical Particles: Symmetry Oscillations	7
46.2.3	Partial Wave Expansion	8
46.2.4	Scattering Length and Effective Ranges	8
46.2.5	Logarithmic Derivatives	10
46.2.6	Coulomb Scattering	11
46.2.7	Resonance Scattering	11
46.2.8	Integral Equation for Phase Shift	12
46.2.9	Variable Phase Method	13
46.2.10	General Amplitudes	13
46.3	SEMICLASSICAL SCATTERING FORMULAE	14
46.3.1	Scattering Amplitude: Exact Poisson Sum Representation	14
46.3.2	Semiclassical Procedure	14
46.3.3	Semiclassical Amplitudes: Integral Representation	15
46.3.4	Semiclassical Amplitudes and Cross Sections	16
46.3.5	Diffraction and Glory Amplitudes	18
46.3.6	Small-Angle (Diffraction) Scattering	18
46.3.7	Small-Angle (Glory) Scattering	19
46.3.8	Oscillations in Elastic Scattering	21
46.4	ELASTIC SCATTERING IN REACTIVE SYSTEMS	21
46.4.1	Quantal Elastic, Absorption and Total Cross Sections	21
46.5	RESULTS FOR MODEL POTENTIALS	22
46.5.1	Born Amplitudes and Cross Sections for Model Potentials	25
46.6	GENERAL REFERENCES	26

46.1 CLASSICAL SCATTERING FORMULAE

Central Field: The total energy $E > 0$ and orbital angular momentum L of relative planar motion are conserved. For a particle of mass M with coordinates (R, ψ) , a symmetric potential $V(R)$, and asymptotic speed v ,

$$E = \frac{p^2(R)}{2M} + V(R) + \frac{L^2}{2MR^2} = \frac{1}{2}Mv^2 = \text{constant}, \quad (46.1)$$

$$L^2 = (2ME)b^2 = M^2v^2b^2 = [MR^2(t)\dot{\psi}(t)]^2 = \text{constant}. \quad (46.2)$$

Equation (46.2) implies constant areal velocity.

Radial momentum $p(R)$:

$$p(R; E, b) = (2ME)^{1/2} \left[1 - \frac{V(R)}{E} - \frac{b^2}{R^2} \right]^{1/2}. \quad (46.3)$$

Effective potential:

$$V_{\text{eff}}(R) = V(R) + \frac{L^2}{2MR^2} = V(R) + \frac{b^2}{R^2}E. \quad (46.4)$$

The turning points $R_i(E, b)$ are the roots of $E = V_{\text{eff}}(R)$. The smallest R_i is the distance of closest approach $R_c(E, b)$ at the pericenter. The maximum impact parameter b_X and angular momentum L_X for approach to within a distance R_X are

$$b_X^2 = R_X^2 [1 - V(R_X)/E], \quad (46.5a)$$

$$L_X^2 = 2MR_X^2 [E - V(R_X)]. \quad (46.5b)$$

The trajectory is defined by $R = R(t; E, b)$, $\psi = \psi(t; E, b)$, where R is the distance from the scattering center O and ψ is measured with respect to the apse line OA joining O to the pericenter R_c . Taking $t = 0$, Eq. (46.1) implies

$$t(R) = \left[\frac{M}{2E} \right]^{1/2} \int_{R_c}^R \left[1 - \frac{V(R)}{E} - \frac{b^2}{R^2} \right]^{1/2} dR, \quad (46.6)$$

which implicitly provides $R = R(t; E, b)$.

$$\begin{aligned} \psi(t; E, b) &= \frac{L}{M} \int_0^t R^{-2}(t) dt \\ &= \frac{(2MEb^2)^{1/2}}{M} \int_0^t R^{-2}(t) dt. \end{aligned} \quad (46.7)$$

Orbit integral ($0 \leq \psi \leq \pi$): ψ is symmetrical about and measured from the apse line joining O and R_c .

$$\psi(R; E, b) = b \int_{R_c}^R \frac{dR/R^2}{[1 - V(R)/E - b^2/R^2]^{1/2}} \quad (46.8)$$

$$= -\frac{\partial}{\partial b} \int_{R_c}^R \left[1 - \frac{V(R)}{E} - \frac{b^2}{R^2} \right]^{1/2} dR. \quad (46.9)$$

For large b and/or small $V(R)/E \ll 1$, (46.9) reduces to

$$\psi(R; E, b) = \frac{\pi}{2} - \sin^{-1} \frac{b}{R} + \frac{1}{2E} \frac{\partial}{\partial b} \int_b^R \frac{V(R) dR}{[1 - b^2/R^2]^{1/2}}, \quad (46.10)$$

$$\psi(R \rightarrow \infty; E, b) = \frac{\pi}{2} + \frac{b}{2E} \int_b^\infty \left(\frac{dV}{dR} \right) \frac{dR}{(R^2 - b^2)^{1/2}}. \quad (46.11a)$$

For a straight-line path, $R^2 = b^2 + Z^2$, where Z is the distance along the scattering axis, and

$$\psi(R \rightarrow \infty; E, b) = \frac{\pi}{2} + \frac{1}{4E} \frac{\partial}{\partial b} \int_{-\infty}^\infty V(b, Z) dZ. \quad (46.11b)$$

46.1.1 Deflection Functions

The deflection function $\chi(E, b)$ ($-\infty \leq \chi < \pi$) is defined to be $\chi(E, b) = \pi - 2\psi(R \rightarrow \infty; E, b)$. Then

$$\begin{aligned} \chi(E, b) &= \pi - 2b \int_{R_c}^\infty \frac{dR/R^2}{[1 - V(R)/E - b^2/R^2]^{1/2}}, \quad (46.12) \\ &= \pi - 2 \int_0^1 \left[\left\{ \frac{1 - V(R_c/x)/E}{1 - V(R_c)/E} \right\} - x^2 \right]^{-1/2} dx. \end{aligned} \quad (46.13)$$

An expression which avoids spurious divergences is

$$\chi(E, b) = \pi + 2 \frac{\partial}{\partial b} \int_{R_c}^\infty [1 - V(R)/E - b^2/R^2]^{1/2} dR. \quad (46.14)$$

Small-angle scattering, $V(R_c)/E \ll 1$, $b \sim R_c$:

$$\chi(E, b) = \left(\frac{R_c}{E} \right) \int_{R_c}^\infty \frac{[V(R_c) - V(R)] R dR}{(R^2 - R_c^2)^{3/2}} \quad (46.15a)$$

$$= \frac{1}{E} \int_0^1 \frac{[V(R_c) - V(R_c/x)] dx}{(1 - x^2)^{3/2}}, \quad (46.15b)$$

where $x = R_c/R$. From (46.10)-(46.11b), other forms are

$$\chi(E, b) = -\frac{1}{E} \frac{\partial}{\partial b} \int_{R_c}^\infty \frac{V(R) dR}{(1 - b^2/R^2)^{1/2}} \quad (46.16a)$$

$$= -\frac{b}{E} \int_b^\infty \left(\frac{dV}{dR} \right) \frac{dR}{(R^2 - b^2)^{1/2}} \quad (46.16b)$$

$$= -\frac{1}{2E} \frac{\partial}{\partial b} \int_{-\infty}^\infty V(b, Z) dZ. \quad (46.16c)$$

For straight-line paths $R^2 = b^2 + v^2 t^2$, Eq. (46.12) yields the impulse-momentum result

$$\chi(E, b) = (Mv)^{-1} \int_{-\infty}^{\infty} F_{\perp}(t) dt = \Delta p_{\perp} / p_{\infty}, \quad (46.17)$$

where Δp_{\perp} is the momentum transferred perpendicular to the incident direction and $F_{\perp} = -(\partial V / \partial R)(b/R)$ is the impulsive force causing scattering. Special cases are

Head-on collisions ($b = 0$):	$\chi(E, 0) = \pi$.
Overall repulsion:	$0 < \chi \leq \pi$.
Overall Attraction:	$-\infty \leq \chi \leq 0$.
Forward Glory:	$\chi = 0, -(2n-1)\pi,$ $n = 0, 2, \dots$
Backward Glory:	$\chi = -2n\pi, n = 1, 2, \dots$
Rainbow Scattering:	$(d\chi/db) = 0$ at $\chi_r < 0$.
Deflection Range:	$\chi_r \leq \chi \leq \pi$.
Orbiting Collisions:	cf. Eq. (46.34).
Diffraction Scattering:	$\chi \rightarrow 0$ as $b \rightarrow \infty$.

The scattered particle may wind or spiral many times around ($\chi \rightarrow -\infty$) the scattering center. The experimentally observed quantity is the scattering angle θ ($0 \leq \theta \leq \pi$) which is associated with various deflections

$$\chi_i = +\theta, -\theta, -2\pi \pm \theta, -4\pi \pm \theta, \dots (i = 1, 2, \dots, n)$$

resulting from n different impact parameters b_i .

Gauss-Mehler Quadrature Evaluation of the Deflection Function.

$$\chi(E, b) = \pi \left[1 - \left(\frac{b}{R_c} \right) \frac{1}{n} \sum_{j=1}^n a_k g(a_j) \right], \quad (46.18)$$

where

$$a_k = \cos \left(\frac{2j-1}{4n} \pi \right), \quad k = n+1-j, \text{ and}$$

$$g(x) = [1 - V(R_c/x)/E - b^2 x^2 / R_c^2]^{-1/2}, \quad 0 \leq x \leq 1.$$

46.1.2 Elastic Scattering Cross Section

Differential cross section:

$$\frac{d\sigma(\theta, E)}{d\Omega} \equiv I(\theta; E) \equiv \sigma(\theta; E),$$

$$\sigma(\theta, E) = \sum_{i=1}^n \left| \frac{b_i db_i}{d(\cos \chi_i)} \right| = \sum_{i=1}^n I_i(\theta). \quad (46.19)$$

Integral cross section for scattering by angles $\theta \geq \theta_0$:

$$\sigma_0(E) = 2\pi \int_{\theta_0}^{\pi} I(\theta; E) d(\cos \theta) = 2\pi \int_0^{b_0(\theta_0)} b db, \quad (46.20)$$

where θ_0 results from one $b_0 = b(\theta_0)$. When θ results from three impact parameters b_1, b_2, b_3 , for example, then

$$\sigma_0(E) = 2\pi \int_0^{b_1} b db + 2\pi \int_{b_2}^{b_3} b db = \pi [b_1^2 + b_3^2 - b_2^2]. \quad (46.21)$$

Diffusion (momentum-transfer) cross section:

$$\sigma_d(E) = 2\pi \int_0^{\pi} [1 - \cos \theta(E, b)] I(\theta) d(\cos \theta), \quad (46.22a)$$

$$= 2\pi \int_0^{\infty} [1 - \cos \theta(E, b)] b db, \quad (46.22b)$$

$$= 4\pi \int_0^{\infty} \sin^2 \left[\frac{1}{2} \theta(E, b) \right] b db. \quad (46.22c)$$

Viscosity cross section:

$$\sigma_v(E) = 2\pi \int_0^{\pi} [1 - \cos^2 \theta(E, b)] I(\theta) d(\cos \theta), \quad (46.23a)$$

$$= 2\pi \int_0^{\infty} [1 - \cos^2 \theta(E, b)] b db, \quad (46.23b)$$

$$= 2\pi \int_0^{\infty} [\sin^2 \theta(E, b)] b db. \quad (46.23c)$$

Small-Angle Diffraction Scattering. The small-angle scattering regime is defined by the conditions $V(R_c)/E \ll 1$, $b \geq R_c$, where $\theta = |\chi|$. The main contribution to $d\sigma/d\Omega$ for small-angle scattering arises from the asymptotic branch of the deflection function χ at large impact parameters b , and is primarily determined by the long-range (attractive) part of the potential $V(R)$ (see Sect. 46.3.6).

Large-Angle Scattering. The main contribution to $d\sigma/d\Omega$ for large-angle scattering arises from the positive branch of χ at small b and is mainly determined by the repulsive part of the potential.

46.1.3 Center-of-Mass to Laboratory Coordinate Conversion

Let ψ_1, ψ_2 be the angles for scattering and recoil, respectively, of the projectile by a target initially at rest in the lab frame. Then

$$\sigma_1(\psi_1) d\Omega_1 = \sigma_2(\psi_2) d\Omega_2 = \sigma_{cm}^{(1,2)}(\theta) d\Omega_{cm}, \quad 0 \leq \theta \leq \pi; \quad (46.24)$$

$$\sigma_{cm}^{(2)}(\theta, \phi) = \sigma_{cm}^{(1)}(\pi - \theta, \phi + \pi). \quad (46.25)$$

(A) Two-body elastic scattering process without conversion of translational kinetic energy into internal energy: $(1) + (2) \rightarrow (1) + (2)$.

$$\sigma_1(\psi_1) = \sigma_{cm}(\theta) \frac{(1 + 2x \cos \theta + x^2)^{3/2}}{|1 + x \cos \theta|}; \quad (46.26)$$

$$\sigma_2(\psi_2) = \sigma_{cm}(\theta) |4 \sin \frac{1}{2} \theta|;$$

$$\psi_2 = \frac{1}{2}(\pi - \theta), \quad 0 \leq \psi_2 \leq \frac{1}{2}\pi; \quad (46.27)$$

$$\tan \psi_1 = \frac{\sin \theta}{(x + \cos \theta)}, \quad x = M_1/M_2. \quad (46.28)$$

$$\begin{aligned}
M_1 > M_2: & \text{As } 0 \leq \theta \leq \theta_c = \cos^{-1}(-M_2/M_1), \\
& 0 \leq \psi_1 \rightarrow \psi_1^{\max} = \sin^{-1}(M_2/M_1) < \frac{1}{2}\pi. \\
& \text{As } \theta_c \leq \theta \rightarrow \pi, \psi_1^{\max} \leq \psi_1 \rightarrow 0. \\
& \theta \text{ is a double-valued function of } \psi. \\
M_1 = M_2: & \sigma_1(\psi_1) = (4 \cos \psi_1) \sigma_{\text{cm}}(\theta = 2\psi_1), \\
& 0 \leq \psi_1 \leq \frac{1}{2}\pi, \psi_1 + \psi_2 = \frac{1}{2}\pi; \\
& \text{no backscattering.} \\
M_1 \ll M_2: & \sigma_1(\psi_1) = \sigma_{\text{cm}}(\theta = \psi_1) \\
& \text{lab and c.m. frames identical.}
\end{aligned}$$

(B) Two-body elastic scattering process with conversion of translational kinetic energy into internal energy: (1) + (2) \rightarrow (3) + (4). For conversion of internal energy ϵ_i so that kinetic energy of relative motion (in the c.m. frame) increases from E_i to $E_f = E_i + \epsilon_i$. For $j = 3, 4$,

$$\begin{aligned}
\sigma_j(\psi_j) &= \sigma_{\text{cm}}(\theta) \frac{[1 + 2x_j \cos \theta + x_j^2]^{3/2}}{|1 + x_j \cos \theta|}, \quad (46.29) \\
x_3 &= \left[\frac{M_1 M_3 E_i}{M_2 M_4 E_f} \right]^{1/2}, \quad x_4 = - \left[\frac{M_1 M_4 E_i}{M_2 M_3 E_f} \right]^{1/2}, \\
\tan \psi_3 &= \frac{\sin \theta}{(x_3 + \cos \theta)}, \quad \tan \psi_4 = \frac{\sin \theta}{(|x_4| - \cos \theta)}.
\end{aligned}$$

46.1.4 Glories and Rainbow Scattering

Glory: The deflection function χ passes through $-2n\pi$ (forward glory) or $-(2n+1)\pi$ (backward glory) at finite impact parameters b_g . Then $\sin \theta \rightarrow 0$ as $\theta \rightarrow \theta_g$ so that classical cross section diverges as

$$\sigma(E, \theta) = \left(\frac{2b_g}{\sin \theta} \right) \left| \frac{db}{d\chi} \right|_{\theta_g} \quad \text{as } \theta \rightarrow \theta_g. \quad (46.30)$$

Rainbow: The deflection function χ passes through a negative minimum at $b = b_r$; $(d\chi/db)_r \rightarrow 0$ so that

$$\chi(b) = \chi(b_r) + \omega_r(b - b_r)^2, \quad (46.31)$$

$$\omega_r = \frac{1}{2} \left(\frac{d^2\chi}{db^2} \right)_{b_r} > 0. \quad (46.32)$$

The classical cross section diverges as

$$\sigma(E, \theta) = \frac{b_r}{2 \sin \theta} [\omega_r(\theta_r - \theta)]^{-1/2}, \quad \theta < \theta_r, \quad (46.33)$$

and is augmented by the contribution from the positive branch of $\chi(b)$.

46.1.5 Orbiting and Spiraling Collisions

Attractive interactions $V(R) = -C/R^n$ ($n \geq 2$) can support quasibound states with positive energy within the angular momentum barrier. Particles with $b < b_0$ spiral towards the scattering center. Those with $b = b_0$ are in unstable circular orbits of radius R_0 . The radius R_0 is determined from the two conditions

$$\left(\frac{dV_{\text{eff}}}{dR} \right)_{R_0} = 0, \quad E = V_{\text{eff}}(R_0), \quad (46.34)$$

which when combined, yields

$$E = V_{\text{eff}}(R_0) = V(R_0) + \frac{1}{2} R_0 \left(\frac{dV}{dR} \right)_{R_0}. \quad (46.35)$$

The angular momentum L_0 of the circular orbit is

$$L_0^2 = (2ME)b_0^2 = 2MR_0^2[E - V(R_0)]. \quad (46.36)$$

Thus $b_0^2 = R_0^2 F$, where

$$F = 1 - \frac{V(R_0)}{E} = \frac{1}{2} \left(\frac{R_0}{E} \right) \left(\frac{dV}{dR} \right)_{R_0} \quad (46.37)$$

is the *focusing factor*. The orbiting and spiraling cross section is then

$$\sigma_{\text{orb}}(E) = \pi b_0^2 = \pi R_0^2 F. \quad (46.38)$$

46.1.6 Quantities Derived from Classical Scattering

The semiclassical phase $\eta(E, b) \equiv \eta(E, \lambda)$, with $\lambda = (\ell + \frac{1}{2}) = kb$ is a function of b or λ . The quantities $p(R) \equiv p(R; E, L)$ and $p_0(R) \equiv p_0(R; E, L)$ are radial momenta in the presence and absence of the potential $V(R)$, respectively.

$$\eta^{\text{SC}}(E, b) = \frac{1}{\hbar} \left[\int_{R_c}^{\infty} p(R) dR - \int_b^{\infty} p_0(R) dR \right] \quad (46.39)$$

$$\begin{aligned}
&= k \int_{R_c}^{\infty} [1 - V/E - b^2/R^2]^{1/2} dR \\
&- k \int_b^{\infty} [1 - b^2/R^2]^{1/2} dR. \quad (46.40)
\end{aligned}$$

Asymptotic speed v : $E = \frac{1}{2} M v^2 = \hbar^2 k^2 / 2M$, $k/2E = 1/\hbar v$.

Jeffrey-Born phase function:

For small V/E and $b \sim R_c$,

$$\eta_{\text{JB}}(E, b) = -\frac{k}{2E} \int_b^{\infty} \frac{V(R) dR}{(1 - b^2/R^2)^{1/2}}. \quad (46.41)$$

Eikonal phase function:

For small V/E and a linear trajectory $R^2 = b^2 + Z^2$,

$$\eta_E(E, b) = -\frac{k}{4E} \int_{-\infty}^{\infty} V(b, Z) dZ. \quad (46.42)$$

Semiclassical cross sections:

$$\sigma(E) = 8\pi \int_0^{\infty} [\sin^2 \eta(E, b)] b db, \quad (46.43)$$

$$= (8\pi/k^2) \int_0^{\infty} \sin^2 \eta(E, \lambda) \lambda d\lambda. \quad (46.44)$$

Landau-Lifshitz cross section:

$$\sigma_{LL}(E) = 8\pi \int_0^\infty [\sin^2 \eta_{JB}(E, b)] b db. \quad (46.45)$$

Massey-Mohr cross section:

$$\eta(E, b_0) = \frac{1}{2}, \quad \langle \sin^2 \eta(E, b < b_0) \rangle = \frac{1}{2}, \quad (46.46)$$

$$\sigma_{MM}(E) = 2\pi b_0^2 + 8\pi \int_{b_0}^\infty \eta_{JB}^2(E, b) b db. \quad (46.47)$$

Schiff cross section:

$$\sigma_c(E) = 4 \int_{-\infty}^\infty dX \int_{-\infty}^\infty dY [4 \sin^2 \eta_E(X, Y)] \quad (46.48)$$

This reduces to (46.45) for spherical $V(\mathbf{R})$.

Random-phase approximation (RPA):

For angle α ,

$$4\pi \int_0^\infty P(b) \sin^2 \alpha(b) b db = 2\pi \int_0^{b_c} P(b) b db, \quad (46.49)$$

where $\alpha(b_c) = 1/\pi$.

Collision delay time function:

$$\tau(E, \lambda) = 2\hbar \frac{\partial \eta(E, \lambda)}{\partial E} = \frac{2}{v} \frac{\partial \eta_\ell(k)}{\partial k}. \quad (46.50)$$

Deflection-angle phase function relation:

$$\chi(E, \lambda) = \frac{2}{k} \frac{\partial \eta(E, b)}{\partial b} = 2 \frac{\partial \eta(E, \lambda)}{\partial \lambda}. \quad (46.51)$$

46.1.7 Collision Action

The classical collision action along a classical path with deflection $\chi = \chi(E, L)$, measured relative to the action along the path of the undeflected particle, is

$$S^C(E, L; \chi) = S_R(E, L) - L\chi(E, L) \quad (46.52a)$$

$$= 2\eta^{SC}(E, L)\hbar - L\chi. \quad (46.52b)$$

Radial component of collision action S^C :

$$S_R(E, L) = 2 \int_{R_c(E, L)}^\infty p(R) dR - 2 \int_{b(E, L)}^\infty p_0(R) dR \quad (46.53a)$$

$$= 2\eta^{SC}(E, L)\hbar \quad (46.53b)$$

Collision delay time function:

$$\tau(E, L) = 2M \left[\int_{R_c}^\infty \frac{dR}{p(R)} - \int_b^\infty \frac{dR}{p_0(R)} \right] \quad (46.54a)$$

$$= \left(\frac{\partial S_R}{\partial E} \right)_L. \quad (46.54b)$$

Deflection angle function:

$$\chi(E, L) = \pi - 2L \int_{R_c}^\infty \frac{dR/R^2}{p(R)} \quad (46.55a)$$

$$= \left(\frac{\partial S_R}{\partial L} \right)_E. \quad (46.55b)$$

Radial collision action change:

$$dS_R = \tau(E, L)dE + \chi(E, L)dL = 2\hbar d\eta^{SC} \quad (46.56)$$

46.2 QUANTAL SCATTERING FORMULAE

The basic quantity in *quantal* elastic scattering is the complex scattering amplitude $f(E, \theta)$, expressed in terms of the phase shifts $\eta_\ell(E)$ associated with scattering of the ℓ th partial wave. Derived quantities are the diagonal elements of the scattering matrix S , transition matrix T and reactance matrix K .

Reduced Energy: $k^2 = (2M/\hbar^2)E$.

Reduced Potential: $U(R) = (2M/\hbar^2)V(R)$.

46.2.1 Basic Formulae

Wave function: As $R \rightarrow \infty$,

$$\Psi(\mathbf{R}) \rightarrow \exp(ikZ) + \frac{1}{R} f(\theta) \exp(ikR) \quad (46.57)$$

for symmetric interactions $V = V(R)$.

Elastic scattering differential cross sections (DCS):

$$\frac{d\sigma}{d\Omega} = I(\theta) = |f(\theta)|^2. \quad (46.58)$$

Scattering, transition and reactance matrix elements in terms of η_ℓ :

$$S_\ell(k) = \exp(2i\eta_\ell), \quad (46.59a)$$

$$T_\ell(k) = \sin \eta_\ell \exp(i\eta_\ell), \quad (46.59b)$$

$$K_\ell(k) = \tan \eta_\ell. \quad (46.59c)$$

Scattering amplitudes $f(\theta)$:

$$f(\theta) = \frac{1}{2ik} \sum_{\ell=0}^\infty (2\ell+1) [\exp(2i\eta_\ell) - 1] P_\ell(\cos \theta) \\ = \sum_{\ell=0}^\infty f_\ell(\theta), \quad (46.60a)$$

$$f(\theta) = \frac{1}{2ik} \sum_{\ell=0}^\infty (2\ell+1) [S_\ell(k) - 1] P_\ell(\cos \theta), \quad (46.60b)$$

$$f(\theta) = \frac{1}{k} \sum_{\ell=0}^\infty (2\ell+1) T_\ell(k) P_\ell(\cos \theta), \quad (46.60c)$$

$$f(\theta) = \frac{1}{2ik} \sum_{\ell=0}^\infty S_\ell(k) P_\ell(\cos \theta), \quad \theta \neq 0, \quad (46.60d)$$

$$= \frac{1}{k} \sum_{\ell=0}^\infty (2\ell+1) T_\ell(k), \quad \theta = 0. \quad (46.60e)$$

Integral cross sections $\sigma(E)$:

$$\sigma(E) = 2\pi \int_0^\pi I(\theta) d(\cos \theta), \quad (46.61a)$$

$$= \frac{4\pi}{k^2} \sum_{\ell=0}^{\infty} (2\ell+1) \sin^2 \eta_\ell. \quad (46.61b)$$

Optical theorem:

$$\sigma(E) = (4\pi/k) \Im f(0). \quad (46.62)$$

Partial cross sections $\sigma_\ell(E)$:

$$\sigma(E) = \sum_{\ell=0}^{\infty} \sigma_\ell(E) \quad (46.63)$$

$$\sigma_\ell(E) = \frac{4\pi}{k^2} (2\ell+1) \sin^2 \eta_\ell \quad (46.64a)$$

$$= \frac{4\pi}{k^2} (2\ell+1) |T_\ell|^2 = \frac{2\pi}{k} (2\ell+1) [1 - \Re S_\ell] \quad (46.64b)$$

Upper limit:

$$\sigma_\ell(E) \leq (4\pi/k^2)(2\ell+1).$$

Unitarity, flux conservation, η_ℓ is real:

$$|S_\ell|^2 = 1, \quad |T_\ell|^2 = \Im T_\ell.$$

Differential cross sections (DCS):

$$\frac{d\sigma(E, \theta)}{d\Omega} = |f(\theta)|^2 = I(\theta) = A(\theta)^2 + B(\theta)^2, \quad (46.65a)$$

$$A(\theta) = \Re f(\theta) = \frac{1}{2k} \sum_{\ell=0}^{\infty} (2\ell+1) \sin 2\eta_\ell P_\ell(\cos \theta), \quad (46.65b)$$

$$B(\theta) = \Im f(\theta) = \frac{1}{2k} \sum_{\ell=0}^{\infty} (2\ell+1) [1 - \cos 2\eta_\ell] P_\ell(\cos \theta). \quad (46.65c)$$

$$\int A(\theta)^2 d\Omega = \frac{4\pi}{k^2} \sum_{\ell=0}^{\infty} (2\ell+1) \sin^2 \eta_\ell \cos^2 \eta_\ell \quad (46.66a)$$

$$\int B(\theta)^2 d\Omega = \frac{4\pi}{k^2} \sum_{\ell=0}^{\infty} (2\ell+1) \sin^4 \eta_\ell \quad (46.66b)$$

$$\frac{d\sigma(E, \theta)}{d\Omega} = \frac{1}{k^2} \sum_{L=0}^{\infty} a_L(E) P_L(\cos \theta) \quad (46.67a)$$

$$a_L = \sum_{\ell=0}^{\infty} \sum_{\ell'=\ell-L}^{\ell+L} (2\ell+1)(2\ell'+1) (\ell\ell'00 | \ell\ell' L0)^2 \times \sin \eta_\ell \sin \eta_{\ell'} \cos(\eta_\ell - \eta_{\ell'}) \quad (46.67b)$$

where $(\ell\ell' mm' | \ell\ell' LM)$ are the Clebsch-Gordon Coefficients.

Three-Term Expansion:

$$\frac{d\sigma(E, \theta)}{d\Omega} = \frac{1}{k^2} \left[(a_0 - \frac{1}{2}a_2) + a_1 \cos \theta + \frac{3}{2}a_2 \cos^2 \theta \right] \quad (46.68)$$

$$a_0(E) = \sum_{\ell=0}^{\infty} (2\ell+1) \sin^2 \eta_\ell, \quad (46.69a)$$

$$a_1(E) = 6 \sum_{\ell=0}^{\infty} (\ell+1) \sin \eta_\ell \sin \eta_{\ell+1} \times \cos(\eta_{\ell+1} - \eta_\ell), \quad (46.69b)$$

$$a_2(E) = 5 \sum_{\ell=0}^{\infty} [b_\ell \sin^2 \eta_\ell + c_\ell \sin \eta_\ell \sin \eta_{\ell+2} \times \cos(\eta_{\ell+2} - \eta_\ell)] . \quad (46.69c)$$

with coefficients

$$b_\ell = \frac{\ell(\ell+1)(2\ell+1)}{(2\ell-1)(2\ell+3)}, \quad (46.70a)$$

$$c_\ell = \frac{3(\ell+1)(\ell+2)}{(2\ell+3)}. \quad (46.70b)$$

S, P wave ($\ell = 0, 1$) net contribution:

$$\frac{d\sigma}{d\Omega} = \frac{1}{k^2} [\sin^2 \eta_0 + [6 \sin \eta_0 \sin \eta_1 \cos(\eta_1 - \eta_0)] \cos \theta + 9 \sin^2 \eta_1 \cos^2 \theta], \quad (46.71)$$

$$\sigma(E) = \frac{4\pi}{k^2} [\sin^2 \eta_0 + 3 \sin^2 \eta_1]. \quad (46.72)$$

For pure S -wave scattering, the DCS is isotropic. For pure P -wave scattering, the DCS is symmetric about $\theta = \pi/2$, where it vanishes; the DCS rises to equal maxima at $\theta = 0, \pi$. For combined S - and P -wave scattering, the DCS is asymmetric with forward-backward asymmetry.

Transport cross sections ($n \geq 1$):

$$\sigma^{(n)}(E) = 2\pi \left[1 - \frac{1 + (-1)^n}{2(n+1)} \right]^{-1} \times \int_0^\pi [1 - \cos^n \theta] I(\theta) d(\cos \theta). \quad (46.73)$$

The diffusion and viscosity cross sections (46.22a) and (46.23a) are given by the transport cross sections $\sigma^{(1)}$ and $\frac{2}{3}\sigma^{(2)}$, respectively.

$$\sigma^{(1)}(E) = \frac{4\pi}{k^2} \sum_{\ell=0}^{\infty} (\ell+1) \sin^2(\eta_\ell - \eta_{\ell+1}) \quad (46.74a)$$

$$\sigma^{(2)}(E) = \frac{4\pi}{k^2} \left(\frac{3}{2} \right) \sum_{\ell=0}^{\infty} \frac{(\ell+1)(\ell+2)}{(2\ell+3)} \sin^2(\eta_\ell - \eta_{\ell+2}),$$

(46.74b)

$$\sigma^{(3)}(E) = \frac{4\pi}{k^2} \sum_{\ell=0}^{\infty} \frac{(\ell+1)}{(2\ell+5)} \left[\frac{(\ell+2)(\ell+3)}{(2\ell+3)} \sin^2(\eta_{\ell} - \eta_{\ell+3}) + \frac{3(\ell^2+2\ell-1)}{(2\ell-1)} \sin^2(\eta_{\ell} - \eta_{\ell+1}) \right], \quad (46.74c)$$

$$\sigma^{(4)}(E) = \frac{4\pi}{k^2} \left(\frac{5}{4} \right) \sum_{\ell=0}^{\infty} \frac{(\ell+1)(\ell+2)}{(2\ell+3)(2\ell+7)} \times \left[\frac{(\ell+3)(\ell+4)}{(2\ell+5)} \sin^2(\eta_{\ell} - \eta_{\ell+4}) + \frac{2(2\ell^2+6\ell-3)}{(2\ell-1)} \sin^2(\eta_{\ell} - \eta_{\ell+2}) \right]. \quad (46.74d)$$

Collision integrals: Averages of $\sigma^{(n)}(E)$ over a Maxwellian distribution at temperature T are

$$\Omega^{(n,s)}(T) = [(s+1)!(kT)^{s+2}]^{-1} \int_0^{\infty} \sigma^{(n)}(E) \times \exp(-E/kT) E^{s+1} dE. \quad (46.75)$$

Normalization factors are chosen so that the above expressions for $\sigma^{(n)}$ and $\Omega^{(n,s)}$ reduce to πd^2 for classical rigid spheres of diameter d .

Mobility: The mobility K of ions of charge e in a gas of density N is given by the Chapman-Enskog Formula

$$K = \frac{3e}{16N} \left(\frac{\pi}{2MkT} \right)^{1/2} [\Omega^{(1,1)}(T)]^{-1}. \quad (46.76)$$

Phase shifts η_{ℓ} can be determined from the numerical solution of the radial Schrödinger equation (46.91), from an integral equation (46.177b), from solving a nonlinear first-order differential equation (46.177a), from Logarithmic Derivatives (see Sect. 46.2.5) or from variational techniques (see Sect. ???.??).

46.2.2 Identical Particles: Symmetry Oscillations

Colliding Particles, each with spin s , in a Total Spin S , Resolved State in the Range ($0 \rightarrow 2s$).

Particle Interchange: $\Psi(\mathbf{R}) = (-1)^{S_i} \Psi(-\mathbf{R})$

$$I_{A,S}(\theta) = \frac{1}{2} |f(\theta) \mp f(\pi - \theta)|^2, \quad (46.77)$$

$$\Psi_{A,S}(\mathbf{R}) \rightarrow [\exp(ikZ) \mp \exp(-ikZ)] + \frac{1}{R} [f(\theta) \mp f(\pi - \theta)] \exp(ikR), \quad (46.78)$$

$$I_{A,S}(\theta) = \frac{1}{4k^2} \left| \sum_{\ell=0}^{\infty} \omega_{\ell}(2\ell+1) [\exp 2i\eta_{\ell} - 1] P_{\ell}(\cos \theta) \right|^2, \quad (46.79)$$

$$\sigma_{A,S}(E) = \frac{4\pi}{k^2} \sum_{\ell=0}^{\infty} \omega_{\ell}(2\ell+1) \sin^2 \eta_{\ell}, \quad (46.80)$$

where A and S denote antisymmetric and symmetric wave functions (with respect to particle interchange) for collisions of identical particles with odd and even total spin S_i .

A: S_i odd $\omega_{\ell} = 0$ (ℓ even); $\omega_{\ell} = 2$ (ℓ odd);
B: S_i even $\omega_{\ell} = 2$ (ℓ even); $\omega_{\ell} = 0$ (ℓ odd).

Spin-States S_i Unresolved. S/A combination:

$$I(\theta) = g_A I_A(\theta) + g_S I_S(\theta), \quad (46.81)$$

$$\sigma(E) = g_A \sigma_A(E) + g_S \sigma_S(E). \quad (46.82)$$

where g_A and g_S are the fractions of states with odd and even total spins $S_i = 0, 1, 2, \dots, 2s$. For Fermions (F) with half integer spin s , and Bosons (B) with integral spin s

F: $g_A = (s+1)/(2s+1)$; $g_S = s/(2s+1)$;

B: $g_A = s/(2s+1)$; $g_S = (s+1)/(2s+1)$.

so that (46.81) and (46.82) have the alternative forms

$$I(F) = |f(\theta)|^2 + |f(\pi - \theta)|^2 - \mathcal{I}, \quad (46.83a)$$

$$\sigma(F) = \frac{1}{2} [\sigma_S + \sigma_A] - \frac{1}{2} [\sigma_S - \sigma_A] / (2s+1) \quad (46.83b)$$

$$I(B) = |f(\theta)|^2 + |f(\pi - \theta)|^2 + \mathcal{I}, \quad (46.83c)$$

$$\sigma(B) = \frac{1}{2} [\sigma_S + \sigma_A] + \frac{1}{2} [\sigma_S - \sigma_A] / (2s+1). \quad (46.83d)$$

where the interference term is

$$\mathcal{I} = \left(\frac{2}{2s+1} \right) \Re [f(\theta) f^*(\pi - \theta)]. \quad (46.84)$$

Example: For fermions with spin 1/2,

$$\sigma(E) = \frac{2\pi}{k^2} \left[\sum_{\ell=\text{even}}^{\infty} (2\ell+1) \sin^2 \eta_{\ell} + 3 \sum_{\ell=\text{odd}}^{\infty} (2\ell+1) \sin^2 \eta_{\ell} \right]. \quad (46.85)$$

Symmetry oscillations originate from the interference between unscattered incident particles in the forward ($\theta = 0$) direction and backward scattered particles ($\theta = \pi, \ell = 0$). Symmetry oscillations are sensitive to the repulsive wall of the interaction.

Resonant Charge Transfer and Transport Cross Sections for ($A^+ - A$) Collisions:

The phase shifts for elastic scattering by the gerade (g) and ungerade (u) potentials of A_2^+ are, respectively, η_{ℓ}^g and η_{ℓ}^u . The charge transfer (X) and transport cross sections are

$$\sigma_X(E) = \frac{\pi}{k^2} \sum_{\ell=0}^{\infty} (2\ell+1) \sin^2(\eta_{\ell}^g - \eta_{\ell}^u) \quad (46.86a)$$

$$\sigma_{A,S}^{(1)}(E) = \frac{4\pi}{k^2} \sum_{\ell=0}^{\infty} (\ell+1) \sin^2(\beta_{\ell} - \beta_{\ell+1}) \quad (46.86b)$$

$$\sigma_{A,S}^{(2)}(E) = \frac{4\pi}{k^2} \left(\frac{3}{2} \right) \sum_{\ell=0}^{\infty} \frac{(\ell+1)(\ell+2)}{(2\ell+3)} \sin^2(\beta_{\ell} - \beta_{\ell+2}). \quad (46.86c)$$

A: $\beta_\ell = \eta_\ell^g$ (ℓ even), or η_ℓ^u (ℓ odd)

S: $\beta_\ell = \eta_\ell^u$ (ℓ even), or η_ℓ^g (ℓ odd)

$\sigma_{A,S}^{(1)}$ contains (g/u) interference; $\sigma_{A,S}^{(2)}$ does not. When nuclear spin degeneracy is acknowledged the cross sections $\sigma_{A,S}$ are summed according to (46.83b) or (46.83d).

Since there is no coupling between molecular states of different electronic angular momentum, the scattering by the $^2\Sigma_{g,u}$ pair and the $^2\Pi_{g,u}$ pair of Ne_2^+ potentials (for example) is independent and

$$\sigma_X(E) = \frac{1}{3}\sigma_\Sigma(E) + \frac{2}{3}\sigma_\Pi(E) \quad (46.87)$$

Singlet-triplet spin flip cross section:

$$\sigma_{ST}(E) = \frac{\pi}{k^2} \sum_{\ell=0}^{\infty} (2\ell+1) \sin^2(\eta_\ell^s - \eta_\ell^t), \quad (46.88)$$

where $\eta_\ell^{s,t}$ are the phase shifts for individual scattering by the singlet and triplet potentials, respectively.

46.2.3 Partial Wave Expansion

$$\Psi(R) = \frac{1}{kR} \sum_{\ell=0}^{\infty} A_\ell v_\ell(kR) P_\ell(\cos \theta), \quad (46.89)$$

$$A_\ell = i^\ell (2\ell+1) \exp(i\eta_\ell). \quad (46.90)$$

Radial Schrödinger equation (RSE):

$$\frac{d^2 v_\ell}{dR^2} + \left[k^2 - U(R) - \frac{\ell(\ell+1)}{R^2} \right] v_\ell(R) = 0 \quad (46.91)$$

where v_ℓ is normalized so that

$$\begin{aligned} v_\ell(R) &\stackrel{R \gg R_0}{\sim} \cos \eta_\ell F_\ell(kR) + \sin \eta_\ell G_\ell(kR) \\ &\rightarrow \sin(kR - \frac{1}{2}\ell\pi + \eta_\ell) \text{ as } R \rightarrow \infty \end{aligned} \quad (46.92)$$

The regular (nonsingular) solution (zero at $R=0$) of the field-free RSE (46.91) with $U(R)=0$ is

$$F_\ell(kR) = (kR) j_\ell(kR) = \left(\frac{1}{2}\pi kR\right)^{1/2} J_{\ell+1/2}(kR) \quad (46.93)$$

$$\rightarrow \begin{cases} (kR)^{\ell+1}/(2\ell+1)!!, & R \rightarrow 0 \\ \sin(kR - \frac{1}{2}\ell\pi), & R \rightarrow \infty, \end{cases} \quad (46.94)$$

where j_ℓ is the spherical Bessel function. Equation (46.89) with $v_\ell = F_\ell$ is the partial-wave expansion for the incident plane-wave $\exp(ikZ)$.

The irregular solution (divergent at $R=0$) of the field-free RSE is

$$\begin{aligned} G_\ell(kR) &= -(kR) n_\ell(kR) \\ &= \left(\frac{1}{2}\pi kR\right)^{1/2} J_{-(\ell+1/2)}(kR) \end{aligned} \quad (46.95)$$

$$\rightarrow \begin{cases} (2\ell-1)!!/(kR)^\ell, & R \rightarrow 0 \\ \cos(kR - \frac{1}{2}\ell\pi), & R \rightarrow \infty, \end{cases} \quad (46.96)$$

where n_ℓ is the spherical Neumann function.

The full asymptotic scattering solution is the combination (46.92) of the regular and irregular solutions. The mixture depends upon:

Forms of Normalization for v_ℓ . In Eq. (46.89), possible choices of normalization are:

$$(a) \quad A_\ell = i^\ell (2\ell+1) \exp i\eta_\ell, \quad (46.97a)$$

$$v_\ell(R) \sim \sin(kR - \frac{1}{2}\ell\pi + \eta_\ell); \quad (46.97b)$$

$$(b) \quad A_\ell = i^\ell (2\ell+1) \cos \eta_\ell, \quad (46.98a)$$

$$v_\ell(R) \sim \sin(kR - \frac{1}{2}\ell\pi) + K_\ell \cos(kR - \frac{1}{2}\ell\pi); \quad (46.98b)$$

$$(c) \quad A_\ell = i^\ell (2\ell+1), \quad (46.99a)$$

$$v_\ell(R) \sim \sin(kR - \frac{1}{2}\ell\pi) + T_\ell e^{i(kR - \ell\pi/2)}; \quad (46.99b)$$

$$(d) \quad A_\ell = \frac{1}{2} i^{\ell+1} (2\ell+1), \quad (46.100a)$$

$$v_\ell(R) \sim e^{-i(kR - \ell\pi/2)} - S_\ell e^{i(kR - \ell\pi/2)}; \quad (46.100b)$$

$$S_\ell = 1 + 2iT_\ell; \quad K_\ell = T_\ell/(1 + iT_\ell); \quad (46.101)$$

$$T_\ell = \sin \eta_\ell e^{i\eta_\ell}; \quad 1 + iT_\ell = \cos \eta_\ell e^{i\eta_\ell}. \quad (46.102)$$

Significance of η_ℓ , K_ℓ , T_ℓ , and S_ℓ . The effect of scattering is therefore to: (1) introduce a phase shift η_ℓ in Eq. (46.97b) to the regular standing wave, (2) leave the regular standing wave alone and introduce either an irregular standing wave of real amplitude K_ℓ in Eq. (46.98b) or, a spherical outgoing wave of amplitude T_ℓ in Eq. (46.99b), and (3) to convert in Eq. (46.100b) an incoming spherical wave of unit amplitude to an outgoing spherical wave of amplitude S_ℓ .

Levinson's Theorem. A local potential $U(R)$ can support n_ℓ bound states of angular momentum ℓ and energy E_n such that

$$\lim_{k \rightarrow 0} \eta_0(k) = \begin{cases} n_0\pi, & E_n < 0 \\ (n_0 + \frac{1}{2})\pi, & E_{n+1} = 0, \end{cases} \quad (46.103)$$

$$\lim_{k \rightarrow 0} \eta_\ell(k) = n_\ell\pi, \quad \ell > 0. \quad (46.104)$$

46.2.4 Scattering Length and Effective Ranges

Blatt-Jackson Effective Range Formula. For short-range potentials,

$$k \cot \eta_0 = -\frac{1}{A} + \frac{1}{2} R_e k^2 + \mathcal{O}(k^4). \quad (46.105)$$

Effective range:

$$R_e = 2 \int_0^\infty [u_0^2(R) - v_0^2(R)] dR, \quad (46.106)$$

where $u_0 = \sin(kR + \eta_0)/\sin \eta_0$ is the $k=0$ limit of the potential-free $\ell=0$ radial wave function and normalized so that $u_0(R)$ goes to unity as $k \rightarrow 0$. The potential

distorted $\ell = 0$ radial function v_0 is normalized at large R to $u_0(R)$. The effective range is a measure of the distance over which v_0 differs from u_0 . The outside factor of 2 in Eq. (46.106) is chosen such that $R_e = a$ for a square well of range a .

Scattering length:

$$a_s = -\lim_{k \rightarrow 0} f(\theta). \quad (46.107)$$

Relation with $k \rightarrow 0$ elastic cross section.

$$\sigma(k \rightarrow 0) = \frac{4\pi}{k^2} \sin^2 \eta_0$$

$$= 4\pi a_s^2 \left\{ \left[1 - \frac{1}{2} k^2 a_s R_e \right]^2 + k^2 a_s^2 \right\}^{-1} \quad (46.108)$$

$$\sim 4\pi a_s^2 [1 + a_s k^2 (R_e - a_s)] \quad (46.109)$$

Relation with Bound Levels. If a $\ell = 0$ bound level of energy $E_n = -\hbar^2 k_n^2 / 2M$ lies sufficiently near the dissociation limit the effective range and scattering lengths, R_e and a_s , respectively, are related by,

$$-\frac{1}{a_s} = -k_n + \frac{1}{2} R_e k_n^2 + \dots \quad (46.110)$$

Wigner Causality Condition. If η_ℓ provides the dominant contribution to $f(\theta)$ then

$$\frac{\partial \eta_\ell(k)}{\partial k} \geq -a_s \quad (46.111)$$

where a_s is the scattering length ($\ell = 0$) and is a measure of the range of the interaction.

Effective Range Formulae. [1-5] The Blatt-Jackson formula must be modified for long-range interactions as follows.

(1) Modified Coulomb potential: $V(R) \sim Z_1 Z_2 e^2 / R$

$$2(K/a_0) = -(1/a_s) + \frac{1}{2} R_e k^2 \quad (46.112)$$

$$K = \frac{\pi \cot \eta_0}{e^{2\pi\alpha} - 1} - \ln \beta - 0.5772$$

$$+ \beta^2 \sum_{n=1}^{\infty} [n(n^2 + \beta^2)]^{-1} \quad (46.113)$$

where $\beta = Z_1 Z_2 e^2 / \hbar v = Z_1 Z_2 / (ka_0)$.

(2) Polarization potential: $V(R) = -\alpha_d e^2 / 2R^4$

$$\tan \eta_0 = -a_s k - \frac{\pi}{3} C_4 k^2 - \frac{4}{3} C_4 a_s k^3 \ln(ka_0) + Dk^3 + Fk^4, \quad (46.114)$$

$$\tan \eta_1 = \frac{\pi}{15} C_4 k^2 - a_s^{(1)} k^3, \quad (46.115)$$

$$\tan \eta_\ell = \frac{\pi C_4 k^2}{(2\ell + 3)(2\ell + 1)(2\ell - 1)} + O(k^{2\ell+1}), \quad (46.116)$$

for $\ell > 1$, where

$$C_4 = \frac{2M}{\hbar^2} \left(\frac{\alpha_d e^2}{2} \right) = \left(\frac{\alpha_d}{a_0} \right) \left(\frac{M}{m_e} \right). \quad (46.117)$$

Example: e^- -Ar low energy collisions: The values

$$a_s = -1.459a_0; \quad D = 68.93a_0^3$$

$$a_s^{(1)} = 8.69a_0^3; \quad F = -97a_0^4$$

provide an accurate fit to recent measurements [6] of (46.74a) for the diffusion cross section σ_d .

(3) Van der Waals potential: $V(R) = -C/R^6$

$$k \cot \eta_0 = -\frac{1}{a_s} + \frac{1}{2} R_e k^2 - \frac{\pi}{15a_s^2} \left[\frac{2MC}{\hbar^2} \right] k^3$$

$$- \frac{4}{15a_s} \left[\frac{2MC}{\hbar^2} \right] k^4 \ln(ka_0) + O(k^4) \quad (46.118)$$

e-Atom Collisions with Polarization Attraction. As $k \rightarrow 0$, the differential cross section is

$$\frac{d\sigma}{d\Omega} = a_s^2 \left[1 + \frac{C_4}{a_s} k \sin \frac{\theta}{2} + \frac{8}{3} C_4 k^2 \ln(ka_0) + \dots \right] \quad (46.119)$$

and the elastic and diffusion cross sections are

$$\sigma(k \rightarrow 0) = 4\pi a_s^2 \left[1 + \frac{2\pi C_4 k}{3a_s} + \frac{8}{3} C_4 k^2 \ln(ka_0) + \dots \right] \quad (46.120)$$

$$\sigma_d(k \rightarrow 0) = 4\pi a_s^2 \left[1 + \frac{4\pi C_4 k}{5a_s} + \frac{8}{3} C_4 k^2 \ln(ka_0) + \dots \right] \quad (46.121)$$

For e^- -noble gas collisions, the scattering lengths are

	He	Ne	Ar	Kr	Xe
$a_s (a_0)$	1.19	0.24	-1.459	-3.7	-6.5

For atoms with $a_s < 0$, a Ramsauer-Townsend minimum appears in both σ and σ_d at low energies, provided that scattering from higher partial waves can be neglected, because from Eq. (46.114), $\eta_0 \simeq 0$ at $k = -3a_s/\pi C_4$.

Semiclassical Scattering Lengths. For heavy particle collisions, $\eta^{SC}(E \rightarrow 0, b)$ tends to

$$\eta_0^{SC} = \left(\frac{2M}{\hbar^2} \right)^{1/2} \int_{R_0}^{\infty} |V(R)|^{1/2} dR. \quad (46.122)$$

(a) Hard-core + well:

$$V(R) = \begin{cases} \infty, & R < R_0 \\ -V_0, & R_0 \leq R < R_1 \\ 0, & R_1 < R \end{cases}$$

$$a_s = [1 - \tan \eta_0^{SC} / (kR_1)] R_1 \quad (46.123)$$

$$\eta_0^{SC} = k(R_1 + R_0), \quad k^2 = 2MV_0/\hbar^2. \quad (46.124)$$

The phase-averaged scattering length is $\langle a_s \rangle = R_1$.

(b) Hard-core + power-law ($n > 2$):

$$V(R) = \begin{cases} \infty, & R < R_0 \\ \pm C/R^n, & R > R_0 \end{cases} \quad (46.125)$$

Repulsion (+): with $\gamma^2 = 2MC/\hbar^2$

$$a_s^{(+)} = \left(\frac{\gamma}{n-2} \right)^{2/(n-2)} \Gamma \left(\frac{n-3}{n-2} \right) / \Gamma \left(\frac{n-1}{n-2} \right). \quad (46.126)$$

Attraction (-): with $\theta_n = \pi/(n-2)$,

$$a_s^{(-)} = a_s^{(+)} [1 - \tan \theta_n \tan (\eta_0^{\text{SC}} - \frac{1}{2}\theta_n)] \cos \theta_n, \quad (46.127)$$

$$\eta_0^{\text{SC}} = \gamma \int_{R_0}^{\infty} R^{-n/2} dR = \frac{2\gamma R_0^{1-n/2}}{n-2}, \quad (46.128)$$

$$\langle a_s^{(-)} \rangle = a_s^{(+)} \cos \theta_n. \quad (46.129)$$

Number of bound states:

$$N_b = \text{int} \left\{ \frac{1}{\pi} \left[\eta_0^{\text{SC}} - \frac{1}{2}(n-1)\theta_n \right] \right\} + 1, \quad (46.130)$$

where $\text{int}[x]$ denotes the largest integer of the real argument x . For integer x , $a_s^{(-)}$ is infinite and a new bound state appears at zero energy.

46.2.5 Logarithmic Derivatives

Phase shift calculations can be based on the logarithmic derivative at $R = a$ separating internal and external regions. Two equivalent forms using sets (R_ℓ, j_ℓ, n_ℓ) or (v_ℓ, F_ℓ, G_ℓ) when $R_\ell = v_\ell/kR$ are

$$K_\ell(k) = \frac{kj'_\ell(ka) - \gamma_\ell(k)j_\ell(ka)}{kn'_\ell(ka) - \gamma_\ell(k)n_\ell(ka)} = \tan \eta_\ell, \quad (46.131a)$$

$$= -\frac{kF'_\ell(ka) - L_\ell(k)F_\ell(ka)}{kG'_\ell(ka) - L_\ell(k)G_\ell(ka)}, \quad (46.131b)$$

where the logarithmic derivative of the internal solution at $R = a$ appropriate to either set, is

$$\gamma_\ell = [R_\ell^{-1} dR_\ell/dR]_{R=a}, \quad (46.132)$$

or alternatively, $L_\ell = [v_\ell^{-1} dv_\ell/dR]_{R=a}$. The primes denote differentiation with respect to the argument, i.e.

$$B'_\ell(ka) = \left[\frac{dB_\ell(x)}{dx} \right]_{x=ka} = \frac{1}{k} \left[\frac{dB_\ell(kR)}{dR} \right]_{R=a}, \quad (46.133)$$

where B_ℓ denotes the functions F_ℓ , G_ℓ , j_ℓ , and n_ℓ .

Decomposition of the S-Matrix Element:

$$S_\ell(k) = e^{2i\eta_\ell} = \left[\frac{\gamma_\ell - (r_\ell - is_\ell)}{\gamma_\ell - (r_\ell + is_\ell)} \right] e^{2i\eta_\ell^H}, \quad (46.134)$$

where

$$\eta_\ell^H(k) = -\frac{j_\ell(ka) - in_\ell(ka)}{j_\ell(ka) + in_\ell(ka)}, \quad (46.135)$$

$$r_\ell + is_\ell = k \left[\frac{j'_\ell(ka) + in'_\ell(ka)}{j_\ell(ka) + in_\ell(ka)} \right]. \quad (46.136)$$

Decomposition of the Phase Shift:

$$\eta_\ell = \eta_\ell^H + \delta_\ell, \quad (46.137)$$

where η_ℓ^H is determined by (46.135), and where δ_ℓ is determined by

$$\tan \delta_\ell = \frac{s_\ell}{\gamma_\ell - r_\ell}, \quad (46.138)$$

which depends on the shape of U via the logarithmic derivative γ_ℓ of Eq. (46.132), and can vary rapidly with k , thereby giving rise to resonances.

Examples:

(1) Hard sphere: if $V(R) = \infty$ for $R < a$, and $V(R) = 0$ for $R > a$, then $\gamma_\ell = \infty$, and

$$K_\ell^{\text{(HS)}} = \tan \eta_\ell^{\text{(HS)}}(k) = \frac{j_\ell(ka)}{n_\ell(ka)} \quad (46.139)$$

$$\rightarrow \begin{cases} -(ka)^{2\ell+1} / [(2\ell+1)!!(2\ell-1)!!], & ka \ll 1 \\ -\tan(ka - \frac{1}{2}\ell\pi), & ka \gg 1 \end{cases} \quad (46.140)$$

$$S_\ell^{\text{(HS)}} = \exp [2i\eta_\ell^{\text{(HS)}}] = -\frac{j_\ell(ka) - in_\ell(ka)}{j_\ell(ka) + in_\ell(ka)} = 1 + 2iT_\ell^{\text{(HS)}}. \quad (46.141)$$

The phase shift η_ℓ^H in the decomposition (46.137) is therefore identified as $\eta_\ell^{\text{(HS)}}$ for hard sphere scattering.

$$\sigma(E \rightarrow 0) = 4\pi a^2. \quad (46.142)$$

Diffraction pattern: As $E \rightarrow \infty$,

$$\frac{d\sigma}{d\Omega} \rightarrow \frac{1}{4}a^2 [1 + \cot^2(\frac{1}{2}\theta) J_1^2(ka \sin \theta)], \quad (46.143)$$

$$\sigma(E) \rightarrow 2\pi a^2. \quad (46.144)$$

Classical hard sphere scattering and diffraction about the sharp edge each contribute πa^2 to σ .

(2) Spherical Well: if $U(R) = -U_0$ for $R \leq a$, and $U(R) = 0$ for $R > a$, then

$$\gamma_\ell(k) = \kappa \frac{j'_\ell(\kappa a)}{j_\ell(\kappa a)}; \quad \kappa^2 = U_0 + k^2 \equiv k_0^2 + k^2. \quad (46.145)$$

S-wave ($\ell = 0$) properties:

$$\eta_0(k) = -ka + \tan^{-1} [(k/\kappa) \tan \kappa a]. \quad (46.146)$$

As $k \rightarrow 0$, $\sigma_0(E) \rightarrow 4\pi A_0^2$, where the scattering length is

$$A_0 = [1 - \tan(k_0 a)/(k_0 a)] a. \quad (46.147)$$

For a shallow well $k_0 a \ll 1$: $\sigma_0(E) = (4\pi/9)U_0^2 a^6$, which agrees with the Born result (46.169) as $k \rightarrow 0$.

The condition for $\ell = 0$ bound state with energy $E_n = -(\hbar^2 k_n^2/2M)$ is

$$k_n \tan \kappa' a = -\kappa', \quad \kappa'^2 = k_0^2 - k_n^2. \quad (46.148)$$

As the well is further deepened, $\sigma_0(E)$ oscillates between zero, where $\tan k_0 a = k_0 a$, and ∞ , where $k_0 a = n\pi/2$, the condition both for appearance of a new level n at energy E and for $a_0 \rightarrow \infty$. In the neighborhood of these infinite resonances,

$$\sigma_0(E) = \frac{4\pi}{k^2 + \kappa'^2}, \quad (46.149)$$

where $\kappa' = \kappa / \tan \kappa a$.

46.2.6 Coulomb Scattering

Direct solution of RSE (46.91) yields

$$v_l \sim \sin(kR - \frac{1}{2}\ell\pi + \eta_l^{(C)} - \beta \ln 2kR), \quad (46.150)$$

$$\beta = Z_1 Z_2 e^2 / \hbar v = Z_1 Z_2 / (ka_0). \quad (46.151)$$

Coulomb phase shift:

$$\eta_l^{(C)} = \arg \Gamma(\ell + 1 + i\beta) = \Im \ln \Gamma(\ell + 1 + i\beta). \quad (46.152)$$

Coulomb S -matrix element:

$$S_l^{(C)} = \exp[2i\eta_l^{(C)}] = \frac{\Gamma(\ell + 1 + i\beta)}{\Gamma(\ell + 1 - i\beta)}. \quad (46.153)$$

Coulomb scattering amplitude:

$$f_C(\theta) = -\frac{\beta \exp[2i\eta_l^{(C)} - i\alpha \ln(\sin^2 \frac{1}{2}\theta)]}{2k \sin^2 \frac{1}{2}\theta}. \quad (46.154)$$

Coulomb differential cross section:

$$\frac{d\sigma}{d\Omega} = \frac{\beta^2}{4k^2 \sin^4 \frac{1}{2}\theta} = \frac{Z_1^2 Z_2^2 e^4}{16E^2} \csc^4 \frac{1}{2}\theta, \quad (46.155)$$

which is the Rutherford scattering cross section.

Mott Formula: For the Coulomb scattering of two identical particles: From (46.83a) and (46.83c)

(a) spin-zero bosons (e.g. ${}^4\text{He} - {}^4\text{He}$):

$$\frac{d\sigma}{d\Omega} = \frac{\beta^2}{4k^2} [\csc^4 \frac{1}{2}\theta + \sec^4 \frac{1}{2}\theta + 2 \csc^2 \frac{1}{2}\theta \sec^2 \frac{1}{2}\theta \cos \Gamma], \quad (46.156)$$

(b) spin- $\frac{1}{2}$ fermions (e.g. $\text{H}^+ - \text{H}^+$, $e^\pm - e^\pm$)

$$\frac{d\sigma}{d\Omega} = \frac{\beta^2}{4k^2} [\csc^4 \frac{1}{2}\theta + \sec^4 \frac{1}{2}\theta - \csc^2 \frac{1}{2}\theta \sec^2 \frac{1}{2}\theta \cos \Gamma], \quad (46.157)$$

where $\Gamma = 2\beta \ln(\tan \frac{1}{2}\theta)$.

46.2.7 Resonance Scattering

Zero-Energy Broad Resonances. The spherical well example (46.145) serves to illustrate broad resonances. When the well depth U_0 is strong enough to accommodate the $(n_0 + 1)$ th energy level at zero energy, the bound state condition (46.148) implies that $\eta_0(k \rightarrow 0) = (n_0 + 1)\pi$, illustrating Levinson's theorem (46.103). As k increases, η_0 generally decreases through either $(2n-1)\pi/2$, or $(n-1)\pi$, where σ_0 has, respectively, a maximum value $4\pi/k^2$ and a minimum value of zero. If the phase shifts η_ℓ for $\ell > 0$ are small, then a nonzero minimum value in $\sigma(E)$ is evident. This is the *Ramsauer-Townsend minimum* manifest when the potential is just strong enough to introduce one or more wavelengths into the well with no observable scattering. Since the rate of decrease of η_0 cannot be arbitrarily rapid, [cf. Eq. (46.103)], broad resonances will be exhibited in contrast to narrow (Breit-Wigner) resonances when η_ℓ increases rapidly through $(2n-1)\pi/2$ over a small energy range ΔE .

Narrow Resonances. The general decomposition (46.137) can be used to analyze narrow resonances. When η_ℓ varies rapidly within an energy width Γ about a resonance energy E_r then δ_ℓ increases through odd multiples of $\pi/2$ and

$$\delta_\ell = \delta_\ell^r = \tan^{-1} \frac{\Gamma}{2(E_r - E)}, \quad (46.158)$$

so that (46.60a) with (46.59a) and (46.59b) is

$$f_\ell = \frac{(2\ell + 1)}{k} \left[T_\ell^{(\text{HS})} + S_\ell^{(\text{HS})} \frac{\Gamma/2}{E_r - E - \frac{i}{2}\Gamma} \right] P_\ell(\cos \theta). \quad (46.159)$$

Breit-Wigner Formula. For a pure resonance with no background phase shift, $S_\ell^{(\text{HS})} = 1$ and the cross section has the Lorentz shape

$$\sigma(E) = \frac{4\pi(2\ell + 1)}{k^2} \left[\frac{\Gamma^2/4}{(E - E_r)^2 + \Gamma^2/4} \right]. \quad (46.160)$$

Shape Resonances. (Also called quasibound state or tunneling resonances). At very low impact energies near or below the energy threshold for orbiting, sharp spikes superimposed on the glory oscillations may be evident in the E -dependence of $\sigma(E)$. These are due to quasibound states with positive energy $E_{n\ell}$ supported by the effective potential $V(r) + L^2/(2Mr^2)$. In heavy particle collisions, quasibound levels are the continuation of the bound rotational levels to positive energies $E_{n\ell} > 0$.

Systems in quasibound states ($n\ell$), with nonresonant eigenenergy $E_{n\ell}$ and phase shift $\eta_\ell^{(0)}$, have

$$E = E_{nl} - \frac{i}{2} \Gamma_{nl}, \quad (46.161a)$$

$$\eta_l = \eta_l^{(0)} + \eta_l^{(r)}, \quad (46.161b)$$

$$\eta_l = \eta_l^{(0)} + \tan^{-1} \frac{\Gamma_{nl}}{2(E_{nl} - E)}; \quad (46.161c)$$

$$S_l(E) = e^{2i\eta_l} = \left[\frac{E - E_{nl} - \frac{i}{2} \Gamma_{nl}}{E - E_{nl} + \frac{i}{2} \Gamma_{nl}} \right] e^{2i\eta_l^{(0)}}. \quad (46.162)$$

The phase shift $\eta_l^{(r)}$ increases by π as E increases through E_{nl} at a rate determined by Γ_{nl} . The dominant amplitude shifts from the external to the quasibound internal regions at $E = E_{nl}$.

Partial-Wave Scattering Amplitude.

$$\begin{aligned} f_l(\theta) &= \frac{1}{2ik} (2\ell + 1) \exp(2i\eta_l^{(0)}) P_\ell(\cos \theta) \\ &\times \left[1 - \frac{i\Gamma_{nl}}{(E - E_{nl} + \frac{i}{2} \Gamma_{nl})} \right]; \quad (46.163) \\ &= \text{background potential scattering amplitude} \\ &\quad + \text{resonance scattering amplitude.} \end{aligned}$$

The partial-wave cross section is composed of the following: potential resonance and interference contributions to $\sigma_l = |f_l(\theta)|^2$:

$$\begin{aligned} \sigma_l &= \frac{4\pi}{k^2} (2\ell + 1) \left[\sin^2 \eta_l^{(0)} \right. \\ &\quad \left. + \frac{\Gamma_{nl}^2 \cos 2\eta_l^{(0)} + 2\Gamma_{nl}(E_{nl} - E) \sin 2\eta_l^{(0)}}{4(E - E_{nl})^2 + \Gamma_{nl}^2} \right] \quad (46.164a) \end{aligned}$$

$$\begin{aligned} &= \frac{4\pi}{k^2} (2\ell + 1) \left\{ \sin^2 \eta_l^{(0)} \left[\frac{(E - E_{nl})^2}{(E - E_{nl})^2 + (\Gamma_{nl}/2)^2} \right] \right. \\ &\quad + \cos^2 \eta_l^{(0)} \left[\frac{(\Gamma_{nl}/2)^2}{(E - E_{nl})^2 + (\Gamma_{nl}/2)^2} \right] \\ &\quad \left. + \sin 2\eta_l^{(0)} \left[\frac{(\Gamma_{nl}/2)(E_{nl} - E)}{(E - E_{nl})^2 + (\Gamma_{nl}/2)^2} \right] \right\} \quad (46.164b) \end{aligned}$$

$$\sigma(E) = \sum_{l=0}^{\infty} \sigma_l = \sigma_0(E) + \sigma_{\text{res}}(E) \quad (46.164c)$$

Resonance Shapes. Resonance shapes depend on the value of the background phase shift $\eta_l^{(0)}$. The case $\eta_l^{(0)} = 0$ gives a Lorentz line shape through the Breit-Wigner formula

$$\sigma_l = \frac{4\pi(2\ell + 1)}{k^2} \frac{\Gamma_{nl}^2/4}{(E - E_{nl})^2 + \Gamma_{nl}^2/4}. \quad (46.165)$$

The other cases from Eq. (46.164b) are

$$\begin{aligned} \eta_l^{(0)} &= n\pi && \text{Large positive spike;} \\ \eta_l^{(0)} &= (n + \frac{1}{2})\pi && \text{Large negative spike;} \\ n\pi &< \eta_l^{(0)} < (n + \frac{1}{2})\pi && \text{Positive then negative;} \\ (n + \frac{1}{2})\pi &< \eta_l^{(0)} < (n + 1)\pi && \text{Negative then positive.} \end{aligned} \quad (46.166)$$

Time Delay.

$$\tau = 2\hbar \left(\frac{\partial \eta_l}{\partial E} \right)_l = 2\hbar \left(\frac{\partial \eta_l^{(0)}}{\partial E} \right) + \frac{4\hbar}{\Gamma_{nl}}. \quad (46.167)$$

The time for capture into quasibound levels is $\tau_c = 4\hbar/\Gamma_{nl}$, and the capture frequency is $\nu_c = \Gamma_{nl}/4\hbar$.

46.2.8 Integral Equation for Phase Shift

$$\sin \eta_l = -\frac{1}{k} \int_0^\infty F_l(kR) U(R) v_l^{(A)}(kR) dR, \quad (46.168a)$$

$$K_l = \tan \eta_l = -\frac{1}{k} \int_0^\infty F_l(kR) U(R) v_l^{(B)}(kR) dR, \quad (46.168b)$$

$$T_l = e^{i\eta_l} \sin \eta_l = -\frac{1}{k} \int_0^\infty F_l(kR) U(R) v_l^{(C)}(kR) dR, \quad (46.168c)$$

$$\begin{aligned} S_l - 1 &= \exp(2i\eta_l) - 1 \\ &= -\frac{1}{k} \int_0^\infty F_l(kR) U(R) v_l^{(D)}(kR) dR, \quad (46.168d) \end{aligned}$$

where $v_l^{(A)}, v_l^{(B)}, v_l^{(C)}, v_l^{(D)}$ are so chosen to have asymptotes prescribed by Eqs. (46.97b)–(46.100b), respectively.

Born Approximation for Phase Shifts. Set $v_l = F_l$ in Eqs. (46.168a)–(46.168d) to obtain

$$\tan \eta_l^B(k) = -k \int_0^\infty U(R) [j_\ell(kR)]^2 R^2 dR. \quad (46.169)$$

For $\lambda = (\ell + 1/2) \gg ka$, substitute

$$\langle k^2 R^2 [j_\ell(kR)]^2 \rangle = \frac{1}{2} [1 - \lambda^2/k^2 R^2]^{-1/2}. \quad (46.170)$$

For the Jeffrey-Born (JB) phase shift function, $\ell \gg ka$,

$$\tan \eta_{\text{JB}}(\lambda) = -\frac{k}{2E} \int_{\lambda/k}^\infty \frac{V(R) dR}{[1 - \lambda^2/(kR)^2]^{1/2}}, \quad (46.171)$$

which agrees with (46.41) since $bk = \ell + \frac{1}{2} = \lambda$. For linear trajectories $R^2 = b^2 + Z^2$, the eikonal phase (46.42) is recovered.

Born S-wave Phase Shift.

$$\tan \eta_0^B(k) = -\frac{1}{k} \int_0^\infty U(R) \sin^2(kR) dR \quad (46.172)$$

Examples: (i) $U = U_0 \frac{e^{-\alpha R}}{R}$, (ii) $U = \frac{U_0}{(R^2 + R_0^2)^2}$;

$$(i) \tan \eta_0^B = -\frac{U_0}{4k} \ln [1 + 4k^2/\alpha^2], \quad (46.173)$$

$$(ii) \tan \eta_0^B = -\frac{\pi U_0}{4kR_0^3} [1 - (1 + 2kR_0)e^{-2kR_0}] \quad (46.174)$$

Born Phase Shifts (Large ℓ). For $\ell \gg ka$,

$$\tan \eta_\ell^B = -\frac{k^{2\ell+1}}{[(2\ell+1)!!]^2} \int_0^\infty U(R) R^{2\ell+2} dR, \quad (46.175)$$

valid only for finite range interactions $U(R > a) = 0$.

Example: $U = -U_0$, $R \leq a$ and $U = 0$, $R > a$.

$$\tan \eta_\ell^B (\ell \gg ka) = U_0 a^2 \frac{(ka)^{2\ell+1}}{[(2\ell+1)!!]^2 (2\ell+3)}. \quad (46.176)$$

For $\ell \gg ka$, $\eta_{\ell+1}/\eta_\ell \sim (ka/2\ell)^2$.

46.2.9 Variable Phase Method

The phase function $\eta_\ell(R)$ is defined to be the scattering phase shift produced by the part of the potential $V(R)$ contained within a sphere of radius R . It satisfies the nonlinear differential equation for $\eta_\ell(R)$

$$\frac{d\eta_\ell}{dR} = -kR^2 U(R) [\cos \eta_\ell(R) j_\ell(kR) - \sin \eta_\ell(R) n_\ell(kR)]^2. \quad (46.177a)$$

The corresponding integral equation for $\eta_\ell(R)$ is

$$\eta_\ell(R) = -k \int_0^R [\cos \eta_\ell(R) j_\ell(kR) - \sin \eta_\ell(R) n_\ell(kR)]^2 U(R) R^2 dR. \quad (46.177b)$$

The Born approximation (46.169) is recovered by substituting $\eta_\ell = 0$ on the RHS of Eq. (46.177b) as $R \rightarrow \infty$.

46.2.10 General Amplitudes

For a general potential $V(\mathbf{R})$, define the reduced potential $U(\mathbf{R}) = (2M/\hbar^2)V(\mathbf{R})$. The plane wave scattering states are

$$\phi_{\mathbf{k}}(\mathbf{R}) = \exp(i\mathbf{k} \cdot \mathbf{R}) = \phi_{-\mathbf{k}}^*(\mathbf{R}) \quad (46.178)$$

and the full scattering solutions have the form

$$\Psi_{\mathbf{k}}^{(\pm)}(\mathbf{R}) \sim \phi_{\mathbf{k}}(\mathbf{R}) + \frac{f(\mathbf{k}, \mathbf{k}')}{R} \exp(\pm i k R), \quad (46.179)$$

where the scattering amplitude is

$$f(\mathbf{k}, \mathbf{k}') = -\frac{1}{4\pi} \langle \phi_{\mathbf{k}'}(\mathbf{R}) | U(\mathbf{R}) | \Psi_{\mathbf{k}}^{(+)}(\mathbf{R}) \rangle \quad (46.180a)$$

$$= -\frac{1}{4\pi} \langle \Psi_{\mathbf{k}'}^{(-)}(\mathbf{R}) | U(\mathbf{R}) | \phi_{\mathbf{k}}(\mathbf{R}) \rangle \quad (46.180b)$$

$$\equiv -\frac{1}{4\pi} \langle \phi_{\mathbf{k}'}(\mathbf{R}) | T | \phi_{\mathbf{k}}(\mathbf{R}) \rangle \quad (46.180c)$$

The last equation defines the T -matrix element.

First Born Approximation.

Set $\Psi_{\mathbf{k}}^+ = \phi_{\mathbf{k}}$ in (46.180a). Then

$$f_B(K) = -\frac{1}{4\pi} \int U(\mathbf{R}) \exp(i\mathbf{K} \cdot \mathbf{R}) d\mathbf{R}, \quad (46.181)$$

where the momentum change is $\mathbf{K} = \mathbf{k} - \mathbf{k}'$, and $K = 2k \sin \frac{1}{2}\theta$. For a symmetric potential,

$$f_B(K) = -\int \frac{\sin KR}{KR} U(R) R^2 dR. \quad (46.182)$$

Connection with partial wave analysis:

$$\frac{\sin KR}{KR} = \sum_{\ell=0}^{\infty} (2\ell+1) [j_\ell(kR)]^2 P_\ell(\cos \theta). \quad (46.183)$$

which is consistent with (46.169).

The static e^- -atom scattering potential and Born scattering amplitude are

$$V(R) = -\frac{Ze^2}{R} + e^2 \int \frac{|\psi(\mathbf{r})|^2 d\mathbf{r}}{|\mathbf{R} - \mathbf{r}|}, \quad (46.184)$$

$$f_B(K) = \frac{2Me^2}{\hbar^2} \frac{[Z - F(K)]}{K^2}. \quad (46.185)$$

where the elastic form factor is $F(K) = \int |\psi(\mathbf{r})|^2 \exp(i\mathbf{K} \cdot \mathbf{r}) d\mathbf{r}$. For a pure Coulomb field, $F(K) = 0$ and $\sigma_B(\theta, E) = |f_B(K)|^2$ reduces to Eq. (46.155).

Two Potential Formulae. For scattering from the combined potential $U(\mathbf{R}) = U_0(\mathbf{R}) + U_1(\mathbf{R})$,

$$f(\mathbf{k}, \mathbf{k}') = -\frac{1}{4\pi} \left[\langle \phi_{\mathbf{k}'}(\mathbf{R}) | U_0(\mathbf{R}) | \chi_{\mathbf{k}}^{(+)}(\mathbf{R}) \rangle + \langle \chi_{\mathbf{k}'}^{(-)}(\mathbf{R}) | U_1(\mathbf{R}) | \Psi_{\mathbf{k}}^{(+)} \rangle \right] \quad (46.186a)$$

where $\chi_{\mathbf{k}}^{(\pm)}(\mathbf{R})$ and $\Psi_{\mathbf{k}}^{(\pm)}(\mathbf{R})$ are full solutions for scattering by V_0 and $V_0 + V_1$, respectively. For symmetric interactions,

$$f(\theta) = \frac{1}{k} \sum_{\ell=0}^{\infty} (2\ell+1) [T_\ell^{(0)} + T_\ell^{(1)}] P_\ell(\cos \theta) \quad (46.187)$$

$$T_\ell^{(0)} = \exp[i\eta_\ell^{(0)}] \sin \eta_\ell^{(0)}; \quad (46.188a)$$

$$T_\ell^{(0)} = -\frac{1}{k} \int_0^\infty dR [F_\ell(R) U_0(R) u_\ell(R)]. \quad (46.188b)$$

$$T_\ell^{(1)} = \exp[2i\eta_\ell^{(0)}] \exp[i\eta_\ell^{(1)}] \sin \eta_\ell^{(1)}, \quad (46.189a)$$

$$T_\ell^{(1)} = -\frac{1}{k} \int_0^\infty dR [u_\ell(R) U_1(R) v_\ell(R)]. \quad (46.189b)$$

where u_ℓ and v_ℓ are the radial wave functions in (46.91), with phase-shifts $\eta_\ell^{(0)}$ and $\eta_\ell = \eta_\ell^{(0)} + \eta_\ell^{(1)}$, for scattering

by V_0 and $V_0 + V_1$, respectively, normalized according to (46.99b).

Distorted-Wave Approximation.

$$\begin{aligned} \Psi_{\mathbf{k}}^{(+)}(\mathbf{R}) &\sim \chi_{\mathbf{k}}^{(+)}(\mathbf{R}) \\ f(\mathbf{k}, \mathbf{k}') &= -\frac{1}{4\pi} \left[\langle \phi_{\mathbf{k}'}(\mathbf{R}) | U_0(\mathbf{R}) | \chi_{\mathbf{k}}^{(+)}(\mathbf{R}) \rangle \right. \\ &\quad \left. + \langle \chi_{\mathbf{k}'}^{(-)}(\mathbf{R}) | U_1(\mathbf{R}) | \chi_{\mathbf{k}}^{(+)}(\mathbf{R}) \rangle \right]. \end{aligned} \quad (46.190)$$

46.3 SEMICLASSICAL SCATTERING FORMULAE

46.3.1 Scattering Amplitude: Exact Poisson Sum Representation

Poisson Sum Formula: $\lambda = \ell + \frac{1}{2}$

$$\sum_{\ell=0}^{\infty} F\left(\ell + \frac{1}{2}\right) = \sum_{m=-\infty}^{\infty} (-1)^m \int_0^{\infty} F(\lambda) e^{i2m\pi\lambda} d\lambda. \quad (46.191)$$

When applied to (46.60b),

$$\begin{aligned} f(\theta) &= (ik)^{-1} \sum_{m=-\infty}^{\infty} (-1)^m \int_0^{\infty} \lambda \left[e^{2i\eta(\lambda)} - 1 \right] \\ &\quad \times P_{\lambda-\frac{1}{2}}(\cos \theta) e^{i2m\pi\lambda} d\lambda, \end{aligned} \quad (46.192)$$

where $\eta(\lambda)$ and $P_{\lambda-1/2} \equiv P(\lambda, \theta)$ are now phase functions and Legendre functions of the *continuous* variable λ , being interpolated from discrete to continuous ℓ . This *infinite-sum-of-integrals* representation for $f(\theta)$ is in principle exact. It is the appropriate technique for conversion from a sum over (quantal) discrete values of a variable to a continuous integration over that variable which classically can assume any value. The particular merit here is that the index m labels the classical paths that have encircled the (attractive) scattering center m times, and that the terms with $m < 0$ have no regions of stationary phase (SP). For deflections χ in the range $-\pi < \chi < \pi$, the only SP contribution is the $m = 0$ term.

46.3.2 Semiclassical Procedure

Semiclassical analysis [7-9] involves reducing (46.192) by the three approximations represented by cases A to C below. Since the integrands can oscillate very rapidly over large regions of λ , the main contributions to the integrals arise from points λ_i of stationary phase of each integrand. The amplitude can then be evaluated by the *method of stationary phase*, the basis of semiclassical analysis.

A. Legendre Function Asymptotic Expansions

Main range: $\sin \theta > \lambda^{-1}$, θ not within λ^{-1} of zero or π .

$$P_{\ell}(\cos \theta) = [2/(\pi \lambda \sin \theta)]^{1/2} \cos[\lambda \theta - \pi/4]. \quad (46.193)$$

Forward formula: θ within λ^{-1} of zero.

$$P_{\ell}(\cos \theta) = [\theta/\sin \theta]^{1/2} J_0(\lambda \theta), \quad (46.194a)$$

$$J_0(\lambda \theta) = \frac{1}{\pi} \int_0^{\pi} e^{-i\lambda \theta \cos \phi} d\phi. \quad (46.194b)$$

Backward formula: θ within λ^{-1} of π .

$$P_{\ell}(\cos \theta) = \left[\frac{\pi - \theta}{\sin \theta} \right]^{1/2} J_0[\lambda(\pi - \theta)] e^{-i\pi(\lambda-1/2)}. \quad (46.195)$$

Equations (46.193)–(46.195) are useful for analysis of caustics (rainbows), diffraction and forward and backward glories, respectively. Also, a useful identity is

$$\sum_{\ell=0}^{\infty} (2\ell+1) P_{\ell}(\cos \theta) = \begin{cases} 4\delta(1 - \cos \theta), & \theta > 0 \\ 0, & \theta = 0 \end{cases}$$

where $\delta(x)$ is the Dirac delta function.

B. JWKB Phase Shift Functions

$$\eta(\lambda) = \int_{R_c}^{\infty} k_{\lambda}(R) dR - \int_{\lambda/k}^{\infty} \left[k^2 - \frac{\lambda^2}{R^2} \right]^{1/2} dR \quad (46.196a)$$

$$= \lim_{R \rightarrow \infty} \left[\int_{R_c}^{\infty} k_{\ell}(R') dR' - kR \right] + \frac{1}{2} \lambda \pi. \quad (46.196b)$$

Local wave number:

$$k_{\lambda}^2(R) = k^2 - U(R) - \lambda^2/R^2, \quad (46.197)$$

with the *Langer modification*:

$$b = \frac{\sqrt{\ell(\ell+1)}}{k} = \frac{\ell+1/2}{k} = \frac{\lambda}{k}. \quad (46.198)$$

Useful Identity:

$$\begin{aligned} \sin \left\{ \int_{\lambda/k}^R [k^2 - \lambda^2/R^2]^{1/2} dR + \frac{\pi}{4} \right\} \\ \rightarrow \sin \left(kR - \frac{1}{2} \ell \pi \right) \text{ as } R \rightarrow \infty. \end{aligned} \quad (46.199)$$

JWKB phase functions are valid when variation of the potential over the local wavenumber $k_{\ell}^{-1}(R)$ is a small fraction of the available kinetic energy $E - V(R)$. Many wavelengths can then be accommodated within a range ΔR for a characteristic potential change ΔV . The classical method is valid when $(1/k)(dV/dR) \ll (E - V)$.

Phase-Deflection Function Relation.

$$\chi(\lambda) = 2 \frac{\partial \eta(\lambda)}{\partial \lambda} \quad (46.200)$$

C. Stationary Phase Approximations (SPA) to Generic Integrals

$$A^\pm(\theta) = \int_{-\infty}^{\infty} g(\theta; \lambda) \exp[\pm i\gamma(\theta; \lambda)] d\lambda \quad (46.201)$$

for parametric θ . In cases where the phase function γ has two stationary points, a phase minimum γ_1 at λ_1 and a phase maximum γ_2 at λ_2 , then $\gamma'_i = 0$, $\gamma''_1 > 0$, $\gamma''_2 < 0$ where $\gamma'_i = (d\gamma/d\lambda)$ at λ_i and $\gamma''_i = (d^2\gamma/d\lambda^2)$ for $i = 1, 2$. Since g is real, $A^- = (A^+)^*$, $g_i(\theta) = g(\theta, \lambda_i)$.

Uniform Airy result.

$$A^+(\theta) = a_1(\theta)e^{i(\gamma_1 + \pi/4)}F^*(\gamma_{21}) + a_2(\theta)e^{i(\gamma_2 - \pi/4)}F(\gamma_{21}), \quad (46.202)$$

$$a_i(\theta) = [2\pi/|\gamma''_i|]^{1/2} g_i(\theta), \quad i = 1, 2, \quad (46.203)$$

$$\gamma_{21}(\theta) = \gamma_2 - \gamma_1 \equiv \frac{4}{3}|z(\theta)|^{3/2} > 0, \quad (46.204)$$

$$F[\gamma_{21}(\theta)] = \left[z^{1/4} \text{Ai}(-z) + iz^{-1/4} \text{Ai}'(-z) \right] \sqrt{\pi} \times e^{-i(\gamma_{21}/2 - \pi/4)}, \quad (46.205)$$

where Ai and Ai' are the Airy function and its derivative.

This result holds for all separations $(\lambda_2 - \lambda_1)$ in location of stationary phases including a caustic (or rainbow), which is a point of inflection in γ , i.e. $\gamma_1 = \gamma_2$, $\gamma'_i = 0 = \gamma''_i$. An equivalent expression is [9]

$$A^+(\theta) = \left[(a_1 + a_2)z^{1/4} \text{Ai}(-z) - i(a_1 - a_2)z^{-1/4} \text{Ai}'(-z) \right] \sqrt{\pi} e^{i\bar{\gamma}}, \quad (46.206)$$

where the mean phase is $\bar{\gamma} = \frac{1}{2}(\gamma_1 + \gamma_2)$. The first form (46.202) is useful for analysis of widely separated regions of stationary phase when $\gamma_{21} \gg 0$ and $F \rightarrow 1$. The equivalent second form (46.206) is valuable in the neighborhood of caustics or rainbows when the stationary phase regions coalesce as $a_1 \rightarrow a_2$.

Primitive result. For widely separated regions λ_1 and λ_2 , $F \rightarrow 1$ and

$$A^\pm(\epsilon) = [a_1(\epsilon) \mp ia_2(\epsilon)e^{\pm i\gamma_{21}}] e^{\pm i(\gamma_1 + \pi/4)}, \quad (46.207a)$$

$$A^\pm(\epsilon) = a_1(\epsilon) \exp\left[\pm i\left(\gamma_1 + \frac{\pi}{4}\right)\right] + a_2(\epsilon) \exp\left[\pm i\left(\gamma_2 - \frac{\pi}{4}\right)\right]. \quad (46.207b)$$

Note that the minimum phase γ_1 is increased by $\pi/4$ and the maximum phase γ_2 is reduced by $\pi/4$.

Transitional Airy result. In the neighborhood of a caustic or rainbow where $\gamma'' = 0$, at the inflexion point $\lambda_1 = \lambda_2 = \lambda_r$, then

$$A^\pm(\theta) = 2\pi \left| \frac{2}{\gamma'''(\lambda_r)} \right|^{1/3} g(\theta; \lambda_r) \text{Ai}(-z) e^{\pm i\gamma(\theta; \lambda_r)} \quad (46.208)$$

$$z = \left| \frac{2}{\gamma'''(\lambda_r)} \right|^{1/3} \gamma'(\theta; \lambda_r). \quad (46.209)$$

Only over a very small angular range does this result agree in practice with the uniform result (46.202), which uniformly connects Eqs. (46.207a) and (46.208). These stationary-phase formulae are not only applicable to integrals involving (λ, θ) but also to (t, E) and (R, p) combinations which occur in the Method of Variation of Constants and in Franck-Condon overlaps of vibrational wave functions, respectively.

46.3.3 Semiclassical Amplitudes: Integral Representation

A. Off-Axis Scattering: $\sin \theta > \lambda^{-1}$.

Except in the forward and backward directions, Eq. (46.192) with (46.193) reduces to

$$f(\theta) = -\frac{1}{k(2\pi \sin \theta)^{1/2}} \sum_{m=-\infty}^{\infty} (-1)^m \int_0^{\infty} d\lambda \lambda^{1/2} \times \left[e^{i\Delta^+(\lambda, m)} - e^{i\Delta^-(\lambda, m)} \right], \quad (46.210)$$

$$\Delta^\pm(\lambda; m) = 2\eta(\lambda) + 2m\pi\lambda \pm \lambda\theta \pm \pi/4 \quad (46.211)$$

$$\equiv S^C \pm \pi/4, \quad (46.212)$$

where S^C is the classical action (46.52b) divided by \hbar .

The stationary phase condition $d\Delta^\pm/d\lambda = 0$ yields the deflection function χ to scattering angle θ relation

$$\chi(\lambda_i) = \mp\theta - 2m\pi, \quad (46.213)$$

where λ_i are points of stationary phase (SP). Since $\pi \geq \chi \geq -\infty$, integrals with $m < 0$ have no SP's and vanish under the SPA. For cases involving no orbiting (where $\chi \rightarrow -\infty$) and when $\pi > \chi > -\pi$, then integrals with $m > 0$ also vanish under SPA so that the only remaining contribution from $m = 0$ to (46.212) is

$$f(\theta) = -\frac{1}{k(2\pi \sin \theta)^{1/2}} \int_0^{\infty} \lambda^{1/2} \left[e^{i\Delta^+(\lambda)} - e^{i\Delta^-(\lambda)} \right] d\lambda, \quad (46.214)$$

$$\Delta^\pm(\lambda) = 2\eta(\lambda) \pm \lambda\theta \pm \pi/4. \quad (46.215)$$

The attractive branch Δ^+ contributes only negative deflections and the repulsive branch Δ^- contributes only positive deflections and has one SP point at λ_1 where Δ^- is maximum.

Rainbow angle θ_r : $(\Delta^+)''_{\lambda_r} = 0$, so that $\chi'(\lambda_r) = 0$ and $\chi(\lambda_r) < 0$ has reached its most negative.

$\theta < \theta_r$: Δ^+ has two SP points $\lambda_{2,3}$;
a maximum at λ_2 and
a minimum at λ_3 .
 $\theta = \theta_r$: $\lambda_2 = \lambda_3$: SP's coalesce.
 $\theta > \theta_r$: no classical attractive scattering.
 Δ^+ has no SP points.

B. Forward Amplitude: $\sin \theta \sim \theta < \lambda^{-1}$.

$$f(\theta) = \frac{1}{ik} \left(\frac{\theta}{\sin \theta} \right)^{1/2} \sum_{m=-\infty}^{\infty} e^{-im\pi} \int_0^{\infty} \lambda J_0(\lambda\theta) \times [e^{2i\eta(\lambda)} - 1] e^{2im\pi\lambda} d\lambda. \quad (46.216)$$

Stationary phase points: $\gamma'(\lambda_m) = 0$.

$$\chi(\lambda_m) = 2 \left(\frac{\partial \eta}{\partial \lambda} \right) = -2m\pi. \quad (46.217)$$

Terms with $m < 0$ therefore make no SP contribution to $f(\theta)$ since $\chi \leq \pi$. The $m = 0$ term provides diffraction due to $\chi \rightarrow 0$, $\chi' \rightarrow 0$ at long range, and a forward glory due to $\chi \rightarrow 0$ at a finite λ_g and nonzero χ'_g .

C. Backward Amplitude: $\theta \sim \pi - \mathcal{O}(\lambda^{-1})$.

$$f(\theta) = \frac{1}{k} \left(\frac{\pi - \theta}{\sin \theta} \right)^{1/2} \sum_{m=-\infty}^{\infty} e^{im\pi} \int_0^{\infty} \lambda J_0[\lambda(\pi - \theta)] \times e^{i[2\eta(\lambda) + (2m-1)\pi\lambda]} d\lambda. \quad (46.218)$$

Stationary phase points:

$$\chi(\lambda_m) = 2 \left(\frac{\partial \eta}{\partial \lambda} \right) = -(2m-1)\pi. \quad (46.219)$$

There are no SP for $m < 0$. The $m = 0$ term provides a normal backward amplitude due to repulsive collisions ($\chi = \pi$), and $m > 0$ terms are due to attractive half-windings.

D. Eikonal Amplitude.

The $m = 0$ term of Eq. (46.216) gives

$$f_E(\theta) = \frac{1}{ik} \int_0^{\infty} \lambda [e^{2i\eta(\lambda)} - 1] J_0(\lambda\theta) d\lambda \quad (46.220a)$$

$$= -ik \int_0^{\infty} [e^{2i\eta(b)} - 1] J_0(kb\theta) b db. \quad (46.220b)$$

From the optical theorem,

$$\sigma_E(E) = 8\pi \int_0^{\infty} \sin^2 \eta(b, E) b db \quad (46.221)$$

For potentials with cylindrical symmetry, $kb\theta$ can be replaced by $2kb \sin \frac{1}{2}\theta = \mathbf{K} \cdot \mathbf{b}$, and

$$f_E(\theta) = -\frac{ik}{2\pi} \int [e^{2i\eta(b)} - 1] J_0(\mathbf{K} \cdot \mathbf{b}) d\mathbf{b}. \quad (46.222)$$

46.3.4 Semiclassical Amplitudes and Cross Sections

Amplitude addition:

$$f(\theta) = \sum_{j=1}^N f_j(\theta), \quad (46.223)$$

where each classical path $b_j = b_j(\theta)$ or SP-point $\lambda_j = \lambda_j(\theta)$ contributes.

Primitive amplitudes:

$$f_j(\theta) = -i\alpha_j \beta_j \sigma_j^{1/2}(\theta) \exp[iS_j^C(\theta)] \quad (46.224)$$

$$\chi_j' = (d\chi/d\lambda)_j \quad (46.225)$$

$$\alpha_j = e^{\pm i\pi/4}; \quad (+)\chi_j' > 0; \quad (-)\chi_j' < 0; \quad (46.226a)$$

$$\beta_j = e^{\pm i\pi/4}; \quad (+)\chi_j > 0; \quad (-)\chi_j < 0. \quad (46.226b)$$

Classical cross section:

$$\sigma_j(\theta) = \left| \frac{bdb}{d(\cos \chi)} \right|_{\chi_j} = \frac{1}{k^2} \frac{\lambda_j}{\sin \theta |\chi_j'|}. \quad (46.227)$$

N classical deflections χ_j provide the same θ :

$$\chi_j = \chi(\lambda_j) = \theta, -\theta, -2\pi \pm \theta, -4\pi \pm \theta, \dots \quad (46.228)$$

Classical collision action $S^C(E, L; \chi)/\hbar$:

$$S_j^C = 2\eta(\lambda_j) - \lambda_j \chi(\lambda_j) \quad (46.229a)$$

$$= 2\eta(\lambda_j) - \lambda_j \theta, \quad 0 \leq \chi \leq \pi \quad (46.229b)$$

$$= 2\eta(\lambda_j) + \lambda_j \theta - m\pi, \quad \chi < 0, \quad (46.229c)$$

where $m = 0, 1, 2, \dots$ is the number of times the ray has traversed the backward direction during its attractive windings about the scattering center.

A. Amplitude Addition: For three well separated regions of stationary phase

$$\lambda_1 < \lambda_2 < \lambda_3$$

A scattering angle θ in the range $0 < \theta < \theta_r$ (rainbow angle) typically results from deflections χ_j at three impact parameters b (or λ): $\theta = \{\chi(b_1), -\chi(b_2), -\chi(b_3)\} \equiv \{\chi_j\}$. Scattering in the range $\theta_r \leq \theta < \pi$ results from one deflection at b_1 . b_1 is in the positive branch (inner repulsion) and $b_{2,3}$ are in the negative branch (outer attraction) of the deflection function $\chi(b)$ such that $b_1 < b_2 < b_3$. $kb = (\ell + 1/2) = \lambda$. Thus

$$f(\theta) = \sum_{j=1}^3 f_j(\theta) = \sum_{j=1}^3 [\sigma_j(\theta)]^{1/2} \exp(iS_j), \quad (46.230)$$

where the overall phases of each f_j are

$$S_1 = 2\eta(\lambda_1) - \lambda_1\theta - \pi/2, \quad (46.231a)$$

$$S_2 = 2\eta(\lambda_2) + \lambda_2\theta - \pi, \quad (46.231b)$$

$$S_3 = 2\eta(\lambda_3) + \lambda_3\theta - \pi/2, \quad (46.231c)$$

which are appropriate, respectively, to deflections $\chi_1 = \theta$ at λ_1 , $\chi_2 = -\theta$ at λ_2 and $\chi_3 = -\theta$ at λ_3 , within the range $-\pi \leq \chi \leq \pi$.

The elastic differential cross section

$$\begin{aligned} \sigma(\theta) &= \sum_{j=1}^3 \sigma_j(\theta) + 2 \sum_{i<j}^3 [\sigma_i(\theta)\sigma_j(\theta)]^{1/2} \cos(S_i - S_j) \\ &\equiv \sigma_c(\theta) + \Delta\sigma(\theta) \end{aligned} \quad (46.232)$$

exhibits interference effects. The first term σ_c is the classical background DCS with no oscillations. The second term $\Delta\sigma$ provides the oscillatory structure which originates from interference between classical actions associated with the different trajectories resulting in a given θ . The part of $S_{ij} = S_i - S_j$ most rapidly varying with θ are the angular action changes $(\lambda_1 + \lambda_2)\theta$, $(\lambda_1 + \lambda_3)\theta$ and $(\lambda_2 - \lambda_3)\theta$. Interference oscillations between the action phases S_1 and S_2 or between S_1 and S_3 then have angular separations

$$\Delta\theta_{1,(2,3)} = \frac{2\pi n}{(\lambda_1 + \lambda_{2,3})}, \quad (46.233)$$

which are much smaller than the separation

$$\Delta\theta_{2,3} = \frac{2\pi n}{(\lambda_2 - \lambda_3)} \quad (46.234)$$

for interference between phases S_2 and S_3 . The oscillatory structure in $\Delta\sigma(\theta)$ is composed therefore of *supernumerary rainbow* oscillations with large angular separations $\Delta\theta_{2,3}$ from S_2 and S_3 interference, with superimposed rapid oscillations with smaller separation $\Delta\theta_{1,(2,3)}$ from interference between S_1 and S_2 or S_1 and S_3 .

For deflections $\chi_j = \theta, -\theta, -2\pi \mp \theta, -4\pi \mp \theta, \dots$, then the Δ^+ -branch of (46.210) provides additional contributions to (46.230) with phases

$$S_{2m}^\pm = 2\eta(\lambda_{2m}) \pm \lambda_{2m}\theta - 2m\pi - \pi, \quad (46.235a)$$

$$S_{3m}^\pm = 2\eta(\lambda_{3m}) \pm \lambda_{3m}\theta - 2m\pi - \pi/2, \quad (46.235b)$$

for $m = 1, 2, 3, \dots$

B. Uniform Airy Result: For two regions of stationary phase which can coalesce

The combined contribution $f_{23}(\theta)$ from the λ_2 and λ_3 attractive regions in Δ^+ branch is

$$f_{23}(\theta) = \sigma_2^{1/2} e^{iS_2} F_{23} + \sigma_3^{1/2} e^{iS_3} F_{23}^*, \quad (46.236a)$$

$$F_{23} = [A + iB] e^{-i(S_{23}/2)}, \quad (46.236b)$$

$$S_{23} = S_2 - S_3$$

$$= 2(\eta_2 - \eta_3) + (\lambda_2 - \lambda_3)\theta - \frac{1}{2}\pi, \quad (46.236c)$$

$$A(z) = \pi^{1/2} z^{1/4} \text{Ai}(-z), \quad (46.236d)$$

$$B(z) = \pi^{1/2} z^{-1/4} \text{Ai}'(-z), \quad (46.236e)$$

$$\frac{4}{3}|z|^{3/2} = S_2^C - S_3^C = S_{23} + \frac{1}{2}\pi. \quad (46.236f)$$

The amplitude f_{23} tends to the primitive result $f_2(\theta) + f_3(\theta)$ in the limit of well-separated regions ($z \gg 1$) when $F_{23} \rightarrow 1$. An equivalent form of (46.236a) is

$$f_{23}(\theta) = [A(\sigma_2^{1/2} + \sigma_3^{1/2}) + iB(\sigma_2^{1/2} - \sigma_3^{1/2})] \exp(i\bar{S}), \quad (46.237)$$

where the mean phase $\bar{S} = \frac{1}{2}(S_2 + S_3)$. This form is useful for analysis of caustic regions at $\theta \sim \theta_r$ where $z \rightarrow 0$.

C. Transitional Result: Neighborhood of Caustic or Rainbow at $(\theta_r, b_r, \lambda_r)$

In the vicinity of rainbow angle $\theta \approx \theta_r$,

$$\chi' = \frac{\partial \chi}{\partial \ell} = [2(\theta_r - \theta)\chi''(\lambda_r)]^{1/2} \quad (46.238)$$

$$z = (\theta_r - \theta)[2/\chi''(\lambda_r)]^{1/3} > 0 \quad (46.239)$$

$$S_r = \frac{1}{2}(S_1 + S_2) = 2\eta(\lambda_r) + \lambda_r\theta_r - \frac{3}{4}\pi. \quad (46.240)$$

The scattering amplitude

$$f_{23}(\theta_r) = \left[\frac{2\pi\lambda_r}{k^2 \sin \theta_r} \right]^{1/2} \left[\frac{2}{\chi''(\lambda_r)} \right]^{1/3} \text{Ai}(-z) e^{iS_r}, \quad (46.241)$$

is finite at the rainbow angle θ_r . In Eq. (46.237), the $(\theta_r - \theta)^{-1/4}$ divergence in $|\chi'|^{1/2}$ of Eq. (46.238) arising in the constructive interference term $(\sigma_2^{1/2} + \sigma_3^{1/2})$ is exactly balanced by the $z^{1/4}$ term of $A(z)$. Also $(\sigma_2^{1/2} - \sigma_3^{1/2}) \rightarrow 0$ in (46.237) more rapidly than $z^{-1/4}$ in $B(z)$ so that (46.237) at θ_r is finite and reproduces (46.241).

The uniform semiclassical DCS

$$\frac{d\sigma}{d\Omega} = \left| \sigma_1^{1/2}(\theta) e^{iS_1} + \sigma_2^{1/2}(\theta) F_{23} e^{iS_2} + \sigma_3^{1/2} F_{23}^* e^{iS_3} \right|^2 \quad (46.242)$$

contains, in addition to the S_i/S_j interference oscillations in the primitive result (46.232), the θ -variation of the Airy Function $|\text{Ai}(z)|^2$, which has a principal finite (rainbow) maximum at $\theta \leq \theta_r$, the classical rainbow angle, and subsidiary maxima (supernumerary rainbows) at smaller angles. The DCS decreases exponentially as θ increases past θ_r into the classical forbidden region and tends to $\sigma_1(\theta)$ at larger angles. For $\theta_r < \theta < \pi$,

$$f(\theta) = \sigma_1^{1/2}(\theta) \exp(iS_1). \quad (46.243)$$

46.3.5 Diffraction and Glory Amplitudes

Diffraction. Diffraction arises from the outer (attractive) part of the potential. Many contributions arise from the attractive Δ^+ branch appropriate for negative χ at large b where η is small. Here χ, χ' both tend to zero.

Glory. The deflection function χ passes through zero at a finite λ_g . A confluence of the two maxima of each phase shift from the positive and negative branches of $\chi(b)$ occurs at $b_1 = b_2 = b_g = \lambda_g/k$. η_g is maximum for $\chi = 0$. In general $\chi(b_m) = -2m\pi$ (forward glory); $\chi(b_m) = -(2m-1)\pi$ (backward glory); $m = 0, 1, 2, \dots$. There is only a forward glory at $\chi = 0$ when the deflection at the rainbow is $|\chi_r| < 2\pi$. In contrast to diffraction, the glory contribution can be calculated by the *stationary phase approximation*.

Transitional Results for Forward and Backward Glories

Forward Glories. Contributions arise from $\chi = \pm\theta, -2\pi \pm \theta, \dots, -2m\pi \pm \theta$ as $\theta \rightarrow 0$. The stationary phase points λ_m are located at

$$\chi(\lambda_m) = \chi_m = -2m\pi; \quad m \geq 0. \quad (46.244)$$

The phase function in the neighborhood of a glory is

$$\eta(\lambda) = \eta_m - m\pi(\lambda - \lambda_m) + \frac{1}{4}\chi'_m(\lambda - \lambda_m)^2. \quad (46.245)$$

The $m = 0$ term provides zero deflection χ due to a net balance of attractive and repulsive scattering for a finite impact parameter b_g or λ_g where $\eta(\lambda)$ attains its maximum value η_m . The glories at θ are due to a confluence of the two contributions from the deflections $\chi_m = -2m\pi \pm \theta$ at the stationary phase points $\lambda_{m1} = \lambda_{m1}$ and λ_{m2} . SP integration of (46.216) with (46.245) yields the forward glory amplitude

$$f_{FG} = \frac{1}{k} \sum_{n=1}^2 \sum_{m=0}^{\infty} \lambda_{mn} \left[\frac{2\pi}{|\chi'_m|} \right]^{1/2} J_0(\lambda_{mn}\theta) e^{iS_{mn}^{(g)}}, \quad (46.246)$$

$$S_{mn}^{(g)} = 2\eta(\lambda_{mn}) + m\pi(\lambda_{mn} - 1) - \frac{3}{4}\pi. \quad (46.247)$$

Backward Glories. Contributions arising from $\chi = -\pi \pm \alpha, -3\pi \pm \alpha, \dots, -(2m-1)\pi \pm \alpha$ coalesce as $\alpha \equiv \pi - \theta \rightarrow 0$. The phase function near a backward glory is

$$\eta(\lambda) = \eta(\lambda_m) + \frac{1}{2}\chi_m(\lambda - \lambda_m) + \frac{1}{4}\chi'_m(\lambda - \lambda_m)^2. \quad (46.248)$$

The $m = 0$ term provides the normal backward amplitude due to head-on ($b = 0$) repulsive collisions. $m > 0$

terms provide contributions from attractive collisions for which there are two points λ_{mn} of stationary phase for each m in $\chi_m = -(2m-1)\pi \pm \alpha$.

The backward glory amplitude at $\theta = \pi - \alpha$ is

$$f_{BG} = \frac{1}{k} \sum_{n=1}^2 \sum_{m=0}^{\infty} \lambda_{mn} \left[\frac{2\pi}{|\chi'_m|} \right]^{1/2} J_0(\lambda_{mn}\alpha) e^{iS_{mn}^{(g)}}, \quad (46.249)$$

$$S_{mn}^{(g)} = 2\eta(\lambda_{mn}) + \pi(2m-1)(\lambda_{mn} - \frac{1}{2}) - \frac{3}{4}\pi. \quad (46.250)$$

In contrast to the Bessel amplitudes (below), these transitional formulae do not uniformly connect with the primitive semiclassical results for $(f_1 + f_2)$ away from the critical glory angles.

Uniform Bessel Amplitude for Glory Scattering

The combined contributions from $\chi_1 = -N\pi + \theta$ and $\chi_2 = -N\pi - \theta$, where $N = 2m$, for forward and $N = 2m-1$ for backward scattering, yield [9]

$$f_G(\theta) = \frac{\alpha_j}{2i} e^{-iN\pi/2} \left[\pi S_{21}^{(C)} \right]^{1/2} \exp i\bar{S}^{(C)}(\theta) \times \left[(\sigma_1^{1/2} + \sigma_2^{1/2}) J_0 \left(\frac{1}{2} S_{21}^{(C)} \right) - i(\sigma_1^{1/2} - \sigma_2^{1/2}) J_1 \left(\frac{1}{2} S_{21}^{(C)} \right) \right], \quad (46.251)$$

where $S_{21}^{(C)}$ is,

$$S_{21}^{(C)}(\theta) = S_2^{(C)} - S_1^{(C)}, \quad (46.252)$$

the difference of the collision actions (46.229a)

$$S_i^{(C)}(\theta) = 2\eta(\lambda_i) - \lambda_i \chi_i, \quad i = 1, 2, \quad (46.253)$$

with mean

$$\bar{S}_{21}^{(C)}(\theta) = \frac{1}{2} [S_2^{(C)} + S_1^{(C)}], \quad (46.254)$$

and phases

$$\alpha_j = e^{\pm i\pi/4}; \quad (+)\chi'_j > 0; \quad (-)\chi'_j < 0, \quad (46.255)$$

and the ordinary Bessel functions $J_n(Z)$ satisfy the relationships $J_1(z) = -J'_0(z)$, $J_1(-z) = -J_1(z)$. This formula, valid for both forward ($\theta \sim 0$) and backward ($\theta \sim \pi$) glories, does uniformly connect the *primitive result* for $(f_1 + f_2)$, valid when $S_{21}^{(C)} \gg 1$ to the *transitional results* (46.246) and (46.249), valid only in the vicinity of the glories.

46.3.6 Small-Angle (Diffraction) Scattering

Diffraction originates from scattering in the forward direction by the long-range attractive tail of $V(R)$ where

χ , χ' and $\eta \rightarrow 0$. The main contributions to (46.220a) arise from a large number of small $\eta(\lambda)$ at large λ . The Jeffrey-Born phase function (46.171) can therefore be used in (46.220b) for $f(\theta)$ and in (46.45) and (46.47), respectively, for $\sigma(E)$. A finite forward diffraction peak as $\theta \rightarrow 0$ is obtained for $f(\theta)$ in contrast to the classical infinite result.

Integral Cross Sections

For $V(R) = -C/R^n$, the Landau-Lifshitz (LL) and Massey-Mohr (MM) cross sections are [cf. Equation (46.346)]

$$\sigma_{LL}(E) = \pi \left[\frac{2CF(n)}{(n-1)\hbar v} \right]^{2/(n-1)} \times \pi \left[\sin \left(\frac{\pi}{n-1} \right) \Gamma \left(\frac{2}{n-1} \right) \right]^{-1} \quad (46.256)$$

$$\sigma_{MM}(E) = \pi \left[\frac{2CF(n)}{(n-1)\hbar v} \right]^{2/(n-1)} \left(\frac{2n-3}{n-2} \right) \quad (46.257)$$

where $F(n) = \sqrt{\pi} \Gamma(\frac{1}{2}n + \frac{1}{2}) / \Gamma(\frac{1}{2}n)$ and v is the relative speed. For σ_{MM} , the phases are $\eta(\lambda) = \frac{1}{2}$ ($0 < \lambda < \lambda_0$) and $\eta(\lambda) = \eta_{JB}$ ($\lambda > \lambda_0$). For σ_{LL} , phases are η_{JB} for all λ . Both σ_{LL} and σ_{MM} have the general form

$$\sigma_D(E) = \gamma \left(\frac{C}{\hbar v} \right)^{2/(n-1)} \quad (46.258)$$

Ion-Atom Collisions. For $n = 4$ attraction at low energy, $\sigma_D \sim v^{-2/3}$. $\gamma_{LL} = 11.373$, $\gamma_{MM} = 10.613$. For $n = 12$ repulsion at high energy, $\sigma_D \sim v^{-2/11}$. $\gamma_{LL} = 6.584$, $\gamma_{MM} = 6.296$.

Atom-Atom Collisions. For $n = 6$ (attraction), $\sigma_D \sim v^{-2/5}$, $\gamma_{LL} = 8.083$, $\gamma_{MM} = 7.547$ (see Fig. 46.1).

Exact numerical calculations favor σ_{LL} over σ_{MM} (see Ref. [10], pp. 1325 for details).

Differential Cross Section

$$\frac{d\sigma}{d\Omega} = f_i^2(\theta) + f_r^2(\theta), \quad (46.259a)$$

$$f_i = \frac{2}{k} \int_0^\infty \lambda \sin^2 \eta(\lambda) \left[1 - \frac{1}{4} \lambda^2 \theta^2 \right] d\lambda \quad (46.259b)$$

$$f_i = \frac{k\sigma_D(E)}{4\pi} \left[1 - \left(\frac{k^2\sigma_D}{16\pi} \right) g_1(n)\theta^2 \right], \quad (46.259c)$$

$$f_r = \frac{1}{k} \int_0^\infty \lambda \sin 2\eta(\lambda) \left[1 - \frac{1}{4} \lambda^2 \theta^2 \right] d\lambda \quad (46.259d)$$

$$f_r = \frac{k\sigma_D(E)}{4\pi} \left[1 - \left(\frac{k^2\sigma_D}{16\pi} \right) g_2(n)\theta^2 \right] \tan \left(\frac{\pi}{n-1} \right) \quad (46.259e)$$

and where σ_D is given by (46.258) and where

$$g_j(n) = \pi^{-1} \tan \left[\frac{j\pi}{n-1} \right] \frac{\{\Gamma[2/(n-1)]\}^2}{\Gamma[4/(n-1)]}. \quad (46.260)$$

The optical theorem (46.62) is satisfied, and

$$f_D(\theta \sim 0) = \sigma_D^{1/2}(E) e^{iS_D(n)}, \quad (46.261)$$

where the (energy-independent) phase is

$$S_D(n) = \frac{\pi(n-3)}{2(n-1)}. \quad (46.262)$$

46.3.7 Small-Angle (Glory) Scattering

Amplitude and Cross Section. The other contribution to forward scattering is the forward glory, which originates from the combined null effect of attraction and repulsion at a specified glory impact parameter $b_g = \lambda_g/k$, where $\eta(\lambda)$ attains a maximum value of η_g . The $m = 0$ term of (46.246) yields

$$f_G(\theta) = \sigma_G^{1/2}(\theta) \exp[iS_G(E)], \quad (46.263a)$$

$$\sigma_G(\theta) = \frac{\lambda_g^2}{k^2} \left(\frac{2\pi}{|\chi'_g|} \right) J_0^2(\lambda_g \theta), \quad (46.263b)$$

$$S_G(E) = 2\eta_g(E) - \frac{3}{4}\pi, \quad (46.263c)$$

where $J_0^2(x) \sim 1 - \frac{1}{4}x^2 + \dots$. The classical result (46.30) is recovered by averaging (46.263b) over several oscillations with $\langle J_0^2(x) \rangle = (\pi x)^{-1}$.

Diffraction-Glory Oscillations.

$$\sigma(E) = \frac{4\pi}{k} \Im [f_D(0) + f_G(0)] \quad (46.264a)$$

$$= \sigma_D(E) + \Delta\sigma_G(E), \quad (46.264b)$$

where the diffraction cross section is (46.258), and where

$$\Delta\sigma_G(E) = \frac{2\pi}{k^2} \lambda_g |\chi'_g| \cos(2\eta_g - \frac{1}{4}\pi) \quad (46.265a)$$

$$= \frac{4\pi}{k^2} \lambda_g \left[\frac{2\pi}{|\chi'_g|} \right]^{1/2} \sin(2\eta_g(E) - \frac{3}{4}\pi) \quad (46.265b)$$

oscillates with E .

For sufficiently deep attractive wells, the phase shift η_g successively decreases with increasing E through a series of multiples of $\pi/2$. Writing $\eta_g(E) = \pi(N - \frac{3}{8})$, maxima appear at $N = 1, 2, \dots$, and minima at $N = \frac{3}{2}, \frac{5}{2}, \frac{7}{2}, \dots$. The glories are indexed by N in order of appearance, starting at high energies. $\eta_g(E \rightarrow 0)$ is related to the number n of bound states by Levinson's theorem: $\eta_0(E \rightarrow 0) = (n + \frac{1}{2})\pi$. Diffraction-glory oscillations also occur in the DCS at a frequency governed entirely by the energy variation of $\eta_g(E)$ and n of (46.262).

JWKB Formulae for Shape Resonances and Tunneling Predissociation

For the three classical turning points $R_1 < R_2 < R_3$ at energies E below the orbiting threshold V_{\max} at R_X , the JWKB phase shift

$$\eta_l = \left[\eta_l^{(0)} - \frac{1}{2} \phi(\gamma_l) \right] + \eta_l^{(r)} \quad (46.266)$$

is composed of (a) the phase shift

$$\eta_l^{(0)} = \lim_{R \rightarrow \infty} \left[\int_{R_3}^{\infty} k(R) dR - kR + \frac{1}{2}(\ell + \frac{1}{2})\pi \right] \quad (46.267)$$

appropriate to one turning point at R_3 , (b) a contribution $\eta_l^{(r)}$ arising from the region between the two inner turning points R_2 and R_3 due to penetration of the centrifugal barrier and given by

$$\tan \eta_l^{(r)}(E) = \left[\frac{\{1 + \exp(-2\gamma_l)\}^{1/2} - 1}{\{1 + \exp(-2\gamma_l)\}^{1/2} + 1} \right] \tan(\alpha_l - \frac{1}{2}\phi_l), \quad (46.268)$$

and (c) a phase correction factor

$$\phi_l(\gamma_l) = \arg \Gamma(\frac{1}{2} + i\epsilon) - \epsilon \ln |\epsilon| + \epsilon, \quad (46.269)$$

where $\epsilon = -\gamma_l/\pi$. The radial action $J_R(E)$ is $2\hbar\alpha_l(E)$. For motion within the potential well α_l is

$$\alpha_l(E) = \int_{R_1}^{R_2} k(R) dR, \quad (46.270)$$

and is

$$\gamma_l(E < E_{\max}) = \int_{R_2}^{R_3} |k(R)| dR \quad (46.271)$$

in the classically forbidden region of the potential hump.

The above expressions also hold for energies $E > V_{\max}$, except that (46.271) is replaced by

$$\gamma_l(E > E_{\max}) = -i \int_{R_-}^{R_+} k(R) dR, \quad (46.272)$$

where R_{\pm} are the complex roots of $k_l(R) = 0$. For the quadratic form

$$V(R) = V_{\max} - \frac{1}{2} M \omega_*^2 (R - R_{\max})^2, \quad (46.273)$$

appropriate in the vicinity of the potential hump, γ for both cases reduces to

$$\gamma = \pi(V_{\max} - E)/\hbar\omega_*. \quad (46.274)$$

The deflection function $\chi_l = 2(\partial\eta_l/\partial\ell)$ no longer diverges at the orbiting angular momentum ℓ_0 or impact

parameter b_0 . The singularities in η_l of Eq. (46.51) are exactly canceled by $-\frac{1}{2}(\partial\phi/\partial\ell)$ in Eq. (46.269).

Limiting cases:

(a) $E \gg V_{\max}$. Then $\gamma_l \rightarrow -\infty$ and $\phi \rightarrow -(\pi/24\gamma_l) \rightarrow 0$, so that $\eta_l^{(r)} \rightarrow \alpha_l$ and η_l reduces to the single turning point result (46.267) with $R_3 = R_1$.

(b) $E \ll V_{\max}$. Then $\gamma_l \gg 1$ and

$$\eta_l^{(r)}(E) = \tan^{-1} \left[\frac{1}{2} e^{-2\gamma_l} \tan(\alpha_l - \frac{1}{2}\phi_l) \right], \quad (46.275)$$

which remains negligible except for those energies E close to quasibound energy levels E_{nl} determined via the *Bohr quantization condition*

$$\alpha_l(E) - \frac{1}{2}\phi_l(E) = (n + \frac{1}{2})\pi. \quad (46.276)$$

As E increases past each E_{nl} , $\eta_l^{(r)}$ increases rapidly by π . Since $(\partial J/\partial E)_{nl} = \nu_{nl}^{-1} = 2\pi/\omega_{nl}$, the time period for radial oscillation within the potential barrier, the level spacing is $\hbar\omega_{nl} = \hbar\nu_{nl} = \pi(\partial E/\partial\alpha)_{nl}$.

Shape Resonance. In the neighborhood of $E_{nl} \sim E$,

$$\alpha_l(E) = \alpha_{nl}(E_{nl}) + \left(\frac{\pi}{\hbar\omega_{nl}} \right) (E - E_{nl}), \quad (46.277)$$

and, under the assumption that the energy variation of ϕ_l can be neglected, (valid for E not close to V_{\max}), then η_l reduces to the Breit-Wigner form

$$\eta_l(E) = \eta_l^{(0)}(E) + \tan^{-1} \left[\frac{\Gamma_{nl}/2}{E_{nl} - E} \right], \quad (46.278)$$

with resonance width

$$\Gamma_{nl} = 2 \left(\frac{\hbar\omega_{nl}}{\pi} \right) \frac{[1 + \exp(-2\gamma_{nl})]^{1/2} - 1}{[1 + \exp(-2\gamma_{nl})]^{1/2} + 1}, \quad (46.279)$$

where $\gamma_{nl} = \gamma(E_{nl})$. The partial cross sections are then determined by (46.164a)–(46.164b) with $\eta_l^{(0)}$ replaced by $\eta_l^{(0)} - \frac{1}{2}\phi(\gamma)$ of (46.267).

Gamow's Result. For $E \ll V_{\max}$, $\gamma_{nl} \gg 1$, then

$$\Gamma_{nl} \xrightarrow{\gamma \gg 1} \left(\frac{\hbar\omega_{nl}}{2\pi} \right) \exp(-2\gamma_{nl}). \quad (46.280)$$

The probabilities of transmission through and reflection from a barrier for unit incident flux from the left are

Transmission Probability:

$$T = [1 + e^{2\gamma}]^{-1} \xrightarrow{\gamma \gg 1} e^{-2\gamma}. \quad (46.281)$$

Reflection Probability:

$$R = [1 + e^{-2\gamma}]^{-1} \xrightarrow{\gamma \gg 1} 1. \quad (46.282)$$

Frequency of leakage:

$$\nu_T = \Gamma_{nl}/\hbar = \left(\frac{\omega_{nl}}{2\pi} \right) e^{-2\gamma}. \quad (46.283)$$

$$S_\ell = A_\ell(k) \exp(2i\eta_\ell), \quad (46.287)$$

where the absorption (inelasticity) factor is

$$A_\ell = \exp(-2\gamma_\ell) \leq 1. \quad (46.288)$$

46.4.1 Quantal Elastic, Absorption and Total Cross Sections

$$f_{el}(\theta) = \frac{1}{2ik} \sum_{\ell=0}^{\infty} (2\ell+1) [A_\ell e^{2i\eta_\ell} - 1] P_\ell(\cos \theta), \quad (46.289a)$$

$$\sigma_{el}(k) = \frac{\pi}{k^2} \sum_{\ell=0}^{\infty} (2\ell+1) |A_\ell e^{2i\eta_\ell} - 1|^2, \quad (46.289b)$$

$$\sigma_{abs}(k) = \frac{\pi}{k^2} \sum_{\ell=0}^{\infty} (2\ell+1) [1 - |A_\ell|^2], \quad (46.289c)$$

$$\begin{aligned} \sigma_{tot}(k) &= \sigma_{el}(k) + \sigma_{abs}(k) \\ &= \frac{2\pi}{k^2} \sum_{\ell=0}^{\infty} (2\ell+1) [1 - A_\ell \cos 2\eta_\ell]. \end{aligned} \quad (46.289d)$$

Upper limits to the partial cross sections are

$$\sigma_\ell^{el} \leq \frac{4\pi}{k^2} (2\ell+1), \quad \sigma_\ell^{abs} \leq \frac{\pi}{k^2} (2\ell+1), \quad (46.290a)$$

$$\sigma_\ell^{tot} \leq \frac{4\pi}{k^2} (2\ell+1) = \frac{4\pi}{k} \Im f_\ell^{el}(\theta=0). \quad (46.290b)$$

For pure elastic scattering with no absorption, $A_\ell = 1$. All nonelastic processes ($0 \leq A_\ell < 1$) are always accompanied by elastic scattering, even in the ($A_\ell = 0$) limit of full absorption.

Eikonal Formulae for Forward Reactive Scattering.

$$f_{el}(\theta) = -ik \int_0^\infty [e^{2i\delta} - 1] J_0(2kb \sin \frac{1}{2}\theta) b db, \quad (46.291a)$$

$$\sigma_{el}(k) = 2\pi \int_0^\infty |1 - e^{-2\gamma} e^{2i\eta}|^2 b db, \quad (46.291b)$$

$$\sigma_{abs}(k) = 2\pi \int_0^\infty [1 - e^{-4\gamma}] b db, \quad (46.291c)$$

$$\sigma_{tot}(k) = 4\pi \int_0^\infty [1 - e^{-2\gamma} \cos^2 \eta] b db, \quad (46.291d)$$

where the phase shift function $\delta = \eta + \gamma$ at impact parameter b can be either the Jeffrey-Born phase

$$\delta_{JB}(b) = -\frac{1}{2k} \int_b^\infty \frac{U(R) dR}{(1 - b^2/R^2)^{1/2}}, \quad (46.292)$$

where $kb = \lambda = (\ell + 1/2)$, or the eikonal phase

$$\delta_E(b) = -\frac{1}{4k} \int_{-\infty}^\infty U(b, Z) dZ, \quad (46.293)$$

Figure 46.1. Illustration of all the various oscillatory effects for elastic scattering by a Lennard-Jones (12,6) potential of well depth ϵ and equilibrium distance R_e . Ordinate $\sigma^* = \sigma/(2\pi R_e^2)$, abscissa $v^* = \hbar v/(\epsilon R_e)$.

46.3.8 Oscillations in Elastic Scattering

Figure 46.1 is an illustration [11] of all the various oscillatory structure and effects — Ramsauer-Townsend minimum (see Sect. 46.2.4), orbiting resonances (46.340), diffraction-glory oscillations (46.264b) and symmetry oscillations (46.80) — for elastic scattering by a Lennard-Jones (12,6) potential. Note the shift of velocity dependence from $v^{-2/5}$ at low v to $v^{-2/11}$ at high v . $\sigma = 2\pi R_e^2$ is the averaged cross section $2\pi b_0^2$ in (46.47) at $b_0 = R_e$. The region $\sigma^* > 1$ probes the attractive part of the potential at low speeds and $\sigma^* < 1$ probes the repulsive part at high speeds. The four distinct types of structure originate from nonrandom behavior of $\sin^2 \eta$ in (46.45). Orbiting trajectories exist for $E < 0.8\epsilon$ (see Sect. 46.5).

46.4 ELASTIC SCATTERING IN REACTIVE SYSTEMS

All nonelastic processes (e.g. inelastic scattering and rearrangement collisions/chemical reactions) can be viewed as a net absorption from the incident beam current vector \mathbf{J} and modeled by a complex optical potential

$$V(R) = V_r(R) + iV_i(R). \quad (46.284)$$

The continuity equation is then

$$\nabla \cdot \mathbf{J} = -\frac{2}{\hbar} V_i(R) |\Psi(\mathbf{R})|^2, \quad (46.285)$$

so that particle absorption implies $V_i > 0$ and particle creation $V_i < 0$. Since particle conservation implies $|S_\ell|^2 = 1$, the phase shift

$$\delta_\ell(k) = \eta_\ell(k) + i\gamma_\ell(k) \quad (46.286)$$

is also complex since then

where the reduced interaction is $U = (2m/\hbar^2)V$.

Fraunhofer Diffraction by a Black Sphere. For a complex spherical well U

$$U = \begin{cases} U_r + iU_i, & R < a \\ 0, & R > a. \end{cases} \quad (46.294)$$

The eikonal phase function (46.42) is

$$\delta(b) = \begin{cases} (U/2k)(a^2 - b^2)^{1/2}, & 0 \leq b \leq a \\ 0 & b > a. \end{cases} \quad (46.295)$$

The absorption factor is

$$|A(b)|^2 \equiv e^{-4\gamma} = \exp \left[-2(a^2 - b^2)^{1/2}/\lambda \right], \quad (46.296)$$

where $\lambda = k/U_i$ is the mean free path towards absorption. For strong absorption, $\lambda \ll a$, so that

$$f_{el}(\theta) = ik \int_0^a J_0(2kb \sin \frac{1}{2}\theta) b db, \quad (46.297)$$

$$\frac{d\sigma_{el}}{d\Omega} = (ka)^2 \left[\frac{J_1(2ka \sin \frac{1}{2}\theta)}{2ka \sin \frac{1}{2}\theta} \right]^2 a^2, \quad (46.298)$$

which has a diffraction shaped peak of width $\sim \theta \leq (ka)^{-1}$ about the forward direction, and

$$\sigma_{tot} = \frac{4\pi}{k} \Im f_{el}(\theta = 0) = 2\pi a^2 \quad (46.299)$$

is composed of πa^2 for classical absorption and πa^2 for edge diffraction or shadow (nonclassical) elastic scattering. This result also holds for the perfectly reflecting sphere (πa^2 for classical elastic and πa^2 for edge diffraction).

46.5 RESULTS FOR MODEL POTENTIALS

Exact results for various quantities in classical, quantum, and semiclassical elastic scattering are obtained for the model potentials (a)–(s) in Table 46.1.

Classical Deflection Functions for Model Potentials

(a) Hard Sphere.

$$\theta(b; E) = \chi = \begin{cases} \pi - 2 \sin^{-1} b/a, & b \leq a; \\ 0, & b > a. \end{cases} \quad (46.300)$$

$$b(\theta) = a \cos \frac{1}{2}\theta, \quad (46.301)$$

$$\sigma(\theta) = \frac{d\sigma}{d\Omega} = \frac{1}{4}a^2; \quad \text{isotropic}, \quad (46.302)$$

$$\sigma = \pi a^2 = \text{geometric cross section}; \quad (46.303)$$

θ , $\sigma(\theta)$ and σ are all independent of energy E .

Table 46.1. Model interaction potentials.

Potential	$V(R)$
(a) Hard sphere	$\infty, R \leq a; 0, R > a$
(b) Barrier	$V_0, R \leq a; 0, R > a$
(c) Well	$-V_0, R \leq a; 0, R > a$
(d) Coulomb (\pm)	$\pm k/R$
(e) Finite-range Coulomb	$-k/R + k/R_s, R \leq R_s; 0, R > R_s$
(f) Pure dipole	$\pm \alpha/R^2$
(g) Finite-range dipole	$\pm \alpha \left(\frac{1}{R^2} - \frac{1}{a^2} \right), R \leq a; 0, R > a$
(h) Dipole + hard sphere	$\pm \alpha/R^2, R \leq a; 0, R > a$
(i) Power law attractive	$-C/R^n, (n > 2)$
(j) Fixed dipole + polarization	$-\frac{De \cos \theta_d}{R^2} - \frac{\alpha_d e^2}{2R^4}$
(k) Fixed dipole + Coulomb	$-\frac{De \cos \theta_d}{R^2} + \frac{e^2}{R}$
(l) Lennard-Jones ($n, 6$)	$\frac{\epsilon n}{n-6} \left[\frac{6}{n} \left(\frac{R_e}{R} \right)^n - \left(\frac{R_e}{R} \right)^6 \right]$
(m) Polarization ($n, 4$)	$\frac{\epsilon n}{n-4} \left[\frac{4}{n} \left(\frac{R_e}{R} \right)^n - \left(\frac{R_e}{R} \right)^4 \right]$
(n) Multiple-term power law	$\frac{C_m}{R^m} - \frac{C_n}{R^n} = V_m(R) - V_n(R)$
(o) Exponential	$V_0 \exp(-\alpha R)$
(p) Screened Coulomb	$V_0 \exp(-\alpha R)/R$
(q) Morse	$\epsilon \left[e^{2\beta(R_e-R)} - 2e^{\beta(R_e-R)} \right]$
(r) Gaussian	$V_0 \exp(-\alpha^2 R^2)$
(s) Polarization finite	$-V_0/(R^2 + R_0^2)^2$

(b) Potential Barrier.

For $E < V_0$, classical scattering is the same as for hard sphere reflection as given by Eqs. (46.300)–(46.303). For $E > V_0$ and $\theta = \chi$, define $n^2 = 1 - V_0/E$, $b_0 = na$. Then

$$\theta(b) = \begin{cases} 2 [\sin^{-1}(b/na) - \sin^{-1}(b/a)] & 0 \leq b \leq b_0 \\ \pi - 2 \sin^{-1}(b/a), & b_0 \leq b \leq a \end{cases} \quad (46.304)$$

and $\theta_{\max} = 2 \cos^{-1} n$. For a given θ , the two impact parameters which contribute are

$$b_1(\theta) = \frac{an \sin \frac{1}{2}\theta}{[1 - 2n \cos \frac{1}{2}\theta + n^2]^{1/2}}, \quad 0 < b_1 \leq b_0 \quad (46.305)$$

$$b_2(\theta) = a \cos \frac{1}{2}\theta, \quad b_0 < b_2 \leq a \quad (46.306)$$

For $0 \leq \theta \leq \theta_{\max}$,

$$\frac{d\sigma}{d\Omega} = \frac{1}{4}a^2 + \frac{a^2n^2(n \cos \frac{1}{2}\theta - 1)(n - \cos \frac{1}{2}\theta)}{4 \cos \frac{1}{2}\theta [1 + n^2 - 2 \cos \frac{1}{2}\theta]}, \quad (46.307)$$

and $d\sigma/d\Omega = 0$ for $\theta_{\max} \leq \theta \leq \pi$. Finally,

$$\sigma = \int_{\theta=0}^{\theta_{\max}} \left(\frac{d\sigma}{d\Omega} \right) d\Omega = \pi a^2. \quad (46.308)$$

(c) Potential Well.

Results are similar to the potential barrier case above, except that there is only a single scattering trajectory with $\theta = -\chi$, and $n = (1 + V_0/E)^{1/2}$ is the effective index of refraction for the equivalent problem in geometrical optics. Refraction occurs on entering and exiting the well. Then

$$\theta(b) = -2 [\sin^{-1}(b/na) - \sin^{-1}(b/a)], \quad (46.309)$$

$$\theta(b=a) = \theta_{\max} = 2 \cos^{-1}(1/n), \quad (46.310)$$

$$b(\theta) = \frac{-an \sin \frac{1}{2}\theta}{[1 - 2n \cos \frac{1}{2}\theta + n^2]^{1/2}}, \quad (46.311)$$

$$\frac{d\sigma}{d\Omega} = \frac{a^2n^2 [n \cos \frac{1}{2}\theta - 1] [n - \cos \frac{1}{2}\theta]}{4 \cos \frac{1}{2}\theta [n^2 + 1 - 2n \cos \frac{1}{2}\theta]^2}, \quad (46.312)$$

$$\sigma = \pi a^2 \quad (46.313)$$

(d) Rutherford or Coulomb.

$$\theta(b, E) = |\chi| = 2 \csc^{-1} [1 + (2bE/k)^2]^{1/2} \quad (46.314)$$

$$b(\theta, E) = (k/2E) \cot \frac{1}{2}\theta. \quad (46.315)$$

$$\sigma(\theta) = \frac{d\sigma}{d\Omega} = \left(\frac{k}{4E} \right)^2 \csc^4 \frac{1}{2}\theta. \quad (46.316)$$

(e) Finite Range Coulomb.

$$R_0(E) = \frac{k}{2E}, \quad \alpha(E) = R_0(E)/R_s, \\ \frac{d\sigma}{d\Omega} = \frac{R_0^2}{4} \left[\frac{1 + \alpha}{\alpha^2 + (1 + 2\alpha) \sin^2 \frac{1}{2}\theta} \right]^2. \quad (46.317)$$

(f) Pure Dipole. $R_0^2(E) = \alpha/E$.

Repulsion (+): $\chi > 0$, $\chi = \theta$.

$$b^2(\chi) = R_0^2 \left[\left(\frac{1}{\chi} + \frac{1}{2\pi - \chi} \right) \frac{\pi}{2} - 1 \right], \quad (46.318)$$

$$\frac{d\sigma}{d\Omega} = \frac{\pi R_0^2}{4 \sin \theta} \left| \frac{1}{\theta^2} - \frac{1}{(2\pi - \theta)^2} \right|. \quad (46.319)$$

Attraction (-): $\chi < 0$.

$$b^2(\chi) = R_0^2 \left[\left(\frac{1}{|\chi|} - \frac{1}{|\chi| + 2\pi} \right) \frac{\pi}{2} + 1 \right]. \quad (46.320)$$

There is an infinite number of (negative) deflections $\chi = \chi_n^\pm$ associated with a given scattering angle θ :

$$|\chi_n^+| = 2\pi n + \theta, \quad n = 0, 1, 2, \dots, \quad (46.321a)$$

$$|\chi_n^-| = 2\pi n - \theta, \quad n = 1, 2, 3, \dots \quad (46.321b)$$

The infinite sum over contributions from $b_n^\pm = b(\chi_n^\pm)$ for the attractive dipole yields

$$\frac{d\sigma}{d\Omega} = \frac{\pi R_0^2}{4 \sin \theta} \left| \frac{1}{\theta^2} + \frac{1}{(2\pi - \theta)^2} \right|. \quad (46.322)$$

(g) Finite Range Dipole Scattering.

$$R_0^2 = \alpha/E, \quad R_c^2 = b^2 \pm R_0^2, \quad b_0^2 = a^2 \pm R_0^2.$$

Repulsion (+): for $b \leq a$,

$$\chi(b) = \frac{\pi(R_c^+ - b)}{R_c^+} + \frac{2b}{R_c^+} \sin^{-1} \left(\frac{R_c^+}{b_0^+} \right) - 2 \sin^{-1} \left(\frac{b}{a} \right), \quad (46.323)$$

$$\chi(0) = \pi, \quad \chi(b \geq a) = 0, \quad \sigma = \pi a^2. \quad (46.324)$$

Attraction (-): for $b > R_0$,

$$\chi(b) = \frac{\pi(R_c^- - b)}{R_c^-} + \frac{2b}{R_c^-} \sin^{-1} \left(\frac{R_c^-}{b_0^-} \right) - 2 \sin^{-1} \left(\frac{b}{a} \right), \quad (46.325)$$

$$\chi(R_0) \rightarrow \infty, \quad \chi(b \geq a) = 0, \quad \sigma = \pi a^2.$$

(h) Dipole + Hard Sphere Scattering. $R_0^2 = \alpha/E$, $R_c^2 = b^2 \pm R_0^2$, $b_0^2 = a^2 \pm R_0^2$. Repulsion (+): for $0 \leq b \leq b_0$,

$$\chi(b) = \frac{\pi(R_c^+ - b)}{R_c^+} + \frac{2b}{R_c^+} \sin^{-1} \left(\frac{R_c^+}{a} \right) - 2 \sin^{-1} \left(\frac{b}{a} \right), \quad (46.326)$$

$$(46.327)$$

$$b_0 \leq b \leq a; \quad \chi(b) = \pi - 2 \sin^{-1}(b/a), \quad (46.328)$$

$$\chi(0) = \pi, \quad \chi(b \geq a) = 0, \quad \sigma = \pi a^2.$$

Attraction (-): for $b > R_0$,

$$\chi(b) = \frac{\pi(R_c^- - b)}{R_c^-} + \frac{2b}{R_c^-} \sin^{-1} \left(\frac{R_c^-}{a} \right) - 2 \sin^{-1} \left(\frac{b}{a} \right), \quad (46.329)$$

$$\chi(b) = \chi_{\min} \text{ at } b = a,$$

$$\chi(0) = \pi, \quad \chi(b \geq a) = 0, \quad \sigma = \pi a^2.$$

Orbiting or Spiraling Collisions

From Sect. 46.1.7, the parameters are

Orbiting radius: R_0 .

Focusing factor: $F = [1 - V(R_0)/E]$.

Orbiting cross section: $\sigma_{\text{orb}} = \pi R_0^2 F$.

(i) Attractive Power Law Potentials.

$$V_{\text{eff}}(R_0) = (1 - \frac{1}{2}n)V(R_0), \quad n > 2,$$

$$R_0(E) = \left[\frac{(n-2)C}{2E} \right]^{1/n}, \quad F = \left[\frac{n}{(n-2)} \right], \quad (46.330)$$

$$\sigma_{\text{orb}}(E) = \pi \left[\frac{n}{(n-2)} \right] \left[\frac{(n-2)C}{2E} \right]^{2/n}. \quad (46.331)$$

For the case $n = 4$ with $V(R) = -\alpha_d e^2 / 2R^4$, this gives the Langevin cross section

$$\sigma_L(E) = 2\pi R_0^2 = 2\pi \left(\frac{\alpha_d e^2}{2E} \right)^{1/2} \quad (46.332)$$

for orbiting collisions, and the Langevin rate

$$k_L = v\sigma_L(E) = 2\pi(\alpha_d e^2 / M)^{1/2}, \quad (46.333)$$

which is independent of E .

The case $n = 6$ with $V(R) = -C/R^6$ is the van der Waals potential for which

$$\sigma_{\text{orb}}(E) = \frac{3}{2}\pi R_0^2 = \frac{3}{2}\pi (2C/E)^{1/3}. \quad (46.334)$$

(j) Fixed Dipole plus Polarization Potential.

$$R_0^2(E) = \left(\frac{\alpha_d e^2}{2E} \right)^{1/2}, \quad (46.335)$$

$$\sigma_{\text{orb}}(E) = 2\pi \left(\frac{\alpha_d e^2}{2E} \right)^{1/2} + \left(\frac{\pi D e \cos \theta_d}{E} \right). \quad (46.336)$$

For a locked-in dipole, the orientation angle is $\theta_d = 0$, and $\sigma_{\text{orb}}(E) > 0$ for all θ_d when $E > E_c = (D^2/2\alpha_d)$.

On averaging over all θ_d from 0 to $\theta_{\text{max}} = [\frac{1}{2}\pi + \sin^{-1}(2ER_0^2/De)]$, which satisfies $\sigma_{\text{orb}}(E) > 0$ for all E , then

$$\langle \sigma_{\text{orb}}(E) \rangle_{\theta_d} = \pi \left[\left(\frac{\alpha_d e^2}{2E} \right)^{1/2} + \frac{\alpha_d e^2}{2E_0} \right] + \frac{\pi D e}{4E} \left[1 - \frac{E}{E_c} \right], \quad (46.337a)$$

$$\rightarrow \sigma_L(E) \text{ as } E \rightarrow E_c. \quad (46.337b)$$

(k) Fixed Dipole + Coulomb Repulsion.

$$R_0^2(E) = e^2/2E. \quad (46.338)$$

For all E and fixed rotations in the range $0 \leq \theta_d \leq \theta_{\text{max}} = \cos^{-1}(e^2/2De)$,

$$\sigma_{\text{orb}}(E) = (\pi D e \cos \theta_d)/E - \pi R_0^2(E). \quad (46.339)$$

(l) **Lennard-Jones ($n, 6$).** For the following two interactions, there are two roots of $E = V_{\text{eff}}(R_0) = V(R_0) + \frac{1}{2}R_0 V'(R_0)$. They correspond to stable and unstable circular orbits [with different angular momenta associated with the minimum and maxima of the different $V_{\text{eff}}(R)$]. Analytical expressions can only be derived for the orbiting cross section at the critical energy E_{max} above which no orbiting can occur.

For the Lennard-Jones ($n, 6$) potential, orbiting occurs for $E < E_{\text{max}} = 2\epsilon [4/(n-2)]^{6/(n-6)}$. The orbiting radius at E_{max} is

$$R_0(E_{\text{max}}) = R_e [(n-2)/4]^{1/(n-6)}.$$

The orbiting cross section at $E_{\text{max}} = 2\epsilon(R_e/R_0)^6$ is

$$\sigma_{\text{orb}}(E_{\text{max}}) = \pi b_0^2(E_{\text{max}}) = \frac{3}{2}\pi R_0^2 \left(\frac{n}{n-2} \right). \quad (46.340)$$

$$n = 12: E_{\text{max}} = 4\epsilon/5, R_0 = 1.165R_e, \sigma_{\text{orb}} = 2.4\pi R_e^2.$$

(m) **Polarization ($n, 4$).** As discussed for case (l),

$$E_{\text{max}} = \epsilon \left[\frac{2}{n-2} \right]^{4/(n-4)}, \quad (46.341)$$

$$R_0(E_{\text{max}}) = R_e \left[\frac{n-2}{2} \right]^{1/(n-4)}, \quad (46.342)$$

$$\sigma_{\text{orb}}(E_{\text{max}}) = 2\pi R_0^2 \frac{n}{(n-2)}, \quad (46.343)$$

$$n = 12: E_{\text{max}} = \epsilon/\sqrt{5}; R_0 = 1.22R_e; \sigma_{\text{orb}} = 3.6\pi R_e^2.$$

Small-Angle Scattering

For the power law potential $V(R) = -C/R^n$, Eq. (46.12) can be expanded in powers of $V(R)/E$ to obtain analytic expressions for χ and η_{JB} . The general form is

$$\chi(b) = \sum_{j=1}^{\infty} \left[\frac{V(b)}{E} \right]^j F_j(n), \quad (46.344)$$

$$F_j(n) = \frac{\pi^{1/2} \Gamma(\frac{1}{2}jn + \frac{1}{2})}{\Gamma(j+1) \Gamma(\frac{1}{2}jn - j + 1)}. \quad (46.345)$$

For the leading $j = 1$ term, $F_1(n) \equiv F(n)$, as defined following Eq. (46.256). Then to first order in V/E ,

$$\eta_{\text{JB}} = - \left(\frac{k}{2E} \right) \left[\frac{CF(n)}{n-1} \right] b^{1-n}, \quad (46.346)$$

$$\frac{d\sigma}{d\Omega} = I_c(\theta) = \left[\frac{CF(n)}{E\theta} \right]^{2/n} \frac{1}{n \sin \theta}. \quad (46.347)$$

From a log-log plot of $\sin \theta (d\sigma/d\Omega)$ versus E, C and n can both be determined.

The integral cross sections for scattering by $\theta \geq \theta_0$ is

$$\begin{aligned} \sigma(E) &= 2\pi \int_{\theta_0}^{\pi} I_c(\theta) d(\cos \theta) = 2\pi \int_0^{b_{\text{max}}} b db \\ &= \pi \left[\frac{CF(n)}{E\theta_0} \right]^{2/n}, \end{aligned} \quad (46.348)$$

where θ_0 is the smallest measured scattering angle corresponding to a trajectory with impact parameter, $b_{\text{max}} = [CF(n)/E\theta_0]^{1/n}$. A plot of $\ln \sigma(E)$ versus $\ln E$ is a straight line with slope $(-2/n)$.

The Landau-Lifshitz cross section (46.256) and the Massey-Mohr cross section (46.257) follow from use of the JB phases (46.346).

The diffusion cross section is

$$\sigma_d(E) = 4\pi \int_0^{b_c} \langle \sin^2 \theta/2 \rangle b db, \quad |\chi(b_c)| = \frac{2}{\pi}$$

$$= \pi(C/2E)^{2/n} [\pi F(n)]^{2/n}. \quad (46.349)$$

(n) Multiple-Term Power-Law Potentials.

$$\chi(E, b) = \frac{1}{E} [V_m(b)F(m) - V_n(b)F(n)]. \quad (46.350)$$

For example, a Lennard-Jones ($n, 6$) potential (see Table 46.5) has the following features:

Forward Glory: $\chi = 0$ when $b_g = \alpha_n^{1/(n-6)} R_e$.

Rainbow: $d\chi/db = 0$ at $b_r = (n\alpha_n/6)^{1/(n-6)} R_e$,

where $\alpha_n = 6F(n)/[nF(6)]$.

$$\omega_r = \frac{1}{2} (d^2\chi_r/db^2)_r = \frac{3n}{b_r^2} |\chi(b_r)| \quad (46.351)$$

(o) Exponential Potential.

$$\eta_{JB}(E, b) = -\frac{1}{2} kb \frac{V_0}{E} K_1(\alpha b) \xrightarrow{\text{large } b} -\frac{1}{2} kb \frac{V(b)}{E} \left(\frac{\pi b}{2\alpha} \right)^{1/2}.$$

(p) Screened Coulomb Potential.

$$\chi(E, b) = \alpha(V_0/E) K_1(\alpha b)$$

$$\rightarrow \left(\frac{1}{2} \pi \alpha b \right)^{1/2} V(b)/E, \quad (46.352)$$

$$\eta_{JB}(E, b) = -\frac{k}{2E} V_0 K_0(\alpha b)$$

$$\xrightarrow{\text{large } b} -\frac{k}{2E} V(b) \left(\frac{\pi b}{2\alpha} \right)^{1/2}. \quad (46.353)$$

(q) Morse Potential.

$$\chi(E, b) = (2\beta b) \left(\frac{\epsilon}{E} \right) [e^{2\beta R_e} K_0(2\beta b) - e^{\beta R_e} K_0(\beta b)],$$

$$\xrightarrow{\text{large } b} (\pi\beta b)^{1/2} \left(\frac{\epsilon}{E} \right) [e^{2\beta(R_e-b)} - \sqrt{2}e^{\beta(R_e-b)}], \quad (46.354)$$

$$b_r = R_e + (2\beta)^{-1} \ln 2,$$

$$\chi_r = -(\pi\beta b_r)^{1/2} (\epsilon/2E),$$

$$\omega_r = \beta^2 |\chi_r| R_e^2.$$

Large-Angle Scattering

For power law potentials $V(R) = C/R^n$,

$$\chi(b) = \pi - \sum_{j=1}^n \left[\frac{E}{V(b)} \right]^{(2j-1)/n} G_j(n), \quad (46.355)$$

$$G_j(n) = \frac{(-1)^{j-1}}{\Gamma(j)\Gamma(k)} \left(\frac{2\pi^{1/2}}{n} \right) \Gamma \left(\frac{2j-1}{n} \right), \quad (46.356)$$

with $k = [(2j-1)/n] - j - \frac{1}{2}$. For the $j = 1$ term,

$$\chi(b) = \pi - \left[\frac{E}{C_n} \right]^{1/n} G_1(n)b, \quad (46.357)$$

$$I_c(\theta) = \frac{d\sigma}{d\Omega} = \left[\frac{C_n}{E} \right]^{2/n} G_1^{-2}(n), \quad (46.358)$$

which is isotropic. Including both $j = 1$ and 2 terms provides a good approximation to the entire repulsive branch of the deflection function χ . Series (46.355) for large angles and (46.344) for small angles eventually diverge for impact parameters $b < b_c$ and $b > b_c$, respectively, where

$$b_c = n^{1/2} \left(\frac{C}{2E} \right)^{1/n} \frac{|n-2|^{1/n}}{|n-2|^{1/2}}.$$

46.5.1 Born Amplitudes and Cross Sections for Model Potentials

$$k^2 = 2ME/\hbar^2, \quad K = 2k \sin \frac{1}{2}\theta,$$

$$U_0 = 2MV_0/\hbar^2, \quad U_0/k^2 = V_0/E.$$

(a) Exponential: $V(R) = V_0 \exp(-\alpha R)$.

$$f_B(\theta) = -\frac{2\alpha U_0}{(\alpha^2 + K^2)^2}, \quad (46.359)$$

$$\sigma_B(E) = \frac{16}{3} \pi U_0^2 \left[\frac{3\alpha^4 + 12\alpha^2 k^2 + 16k^4}{\alpha^4(\alpha^2 + 4k^2)^3} \right]$$

$$\xrightarrow{E \rightarrow \infty} \frac{4}{3} \pi \left(\frac{V_0}{E} \right) \left(\frac{U_0}{\alpha^4} \right). \quad (46.360)$$

(b) Gaussian: $V(R) = V_0 \exp(-\alpha^2 R^2)$.

$$f_B(\theta) = -\left(\frac{\pi^{1/2} U_0}{4\alpha^2} \right) \exp(-K^2/4\alpha^2), \quad (46.361)$$

$$\sigma_B(E) = \left(\frac{\pi^2 U_0}{8\alpha^4} \right) \left(\frac{V_0}{E} \right) [1 - \exp(-2k^2/\alpha^2)]. \quad (46.362)$$

(c) Spherical well: $V(R) = V_0$ for $R < a$, $V(R) = 0$ for $R > a$.

$$f_B(\theta) = -\frac{U_0}{K^3} [\sin Ka - Ka \cos Ka], \quad (46.363)$$

$$\sigma_B(E) = \frac{\pi}{2} \frac{V_0}{E} (U_0 a^4) [1 - (ka)^{-2} + (ka)^{-3} \sin 2ka - (ka)^{-4} \sin^2 2ka]. \quad (46.364)$$

(d) Screened Coulomb: $V(R) = V_0 \exp(-\alpha R)/R$, $V_0 = Ze^2$, $U_0 = 2Z/a_0$.

$$f_B(\theta) = -\frac{U_0}{\alpha^2 + K^2}, \quad (46.365)$$

$$\sigma_B(E) = \frac{4\pi U_0^2}{\alpha^2(\alpha^2 + 4k^2)} \rightarrow \pi \left(\frac{V_0}{E} \right) \left(\frac{U_0}{\alpha^2} \right). \quad (46.366)$$

When $\alpha \rightarrow 0$, then $f_B(\theta) = -U_0/\alpha^2$.

(e) e^- -Atom:

$$V(R) = -Ne^2 [Z/a_0 + 1/R] \exp(-2ZR/a_0), \quad (46.367)$$

H(1s): $N = 1$, $Z = 1$; He(1s²): $N = 2$; $Z = 27/16$.

$$f_B(\theta) = \frac{2N}{a_0} \left[\frac{2\alpha^2 + K^2}{(\alpha^2 + K^2)^2} \right], \quad \alpha = 2Z/a_0, \quad (46.368)$$

$$\sigma_B(E) = \frac{\pi a_0^2 N^2 [12Z^4 + 18Z^2 k^2 a_0^2 + 7k^4 a_0^2]}{3Z^2(Z^2 + k^2 a_0^2)^3}. \quad (46.369)$$

Also, f_B decomposes as

$$f_B(K) = f_B^Z(K) + f_B^{ee}(K)F(K), \quad (46.370)$$

where f_B^{ij} are two-body Coulomb amplitudes for (i, j) scattering, and where

$$F(K) = \int |\Psi_0(\mathbf{R})|^2 \exp(i\mathbf{K} \cdot \mathbf{R}) d\mathbf{R} \quad (46.371)$$

is the elastic form factor.

(f) Dipole: $V(R) = V_0/R^2$.

$$f_B(\theta) = \pi U_0/2K. \quad (46.372)$$

(g) Polarization potential: $V(R) = V_0/(R^2 + R_0^2)^2$.

$$f_B(\theta) = -\frac{1}{4}\pi \left(\frac{U_0}{R_0} \right) \exp(-KR_0), \quad (46.373)$$

$$\sigma_B(E) = \left(\frac{\pi^3 U_0}{32R_0^4} \right) \left(\frac{V_0}{E} \right) [1 - (1 + 4kR_0) \exp(-4kR_0)]. \quad (46.374)$$

Acknowledgments

This research is supported by the U. S. Air Force Office of Scientific Research under Grant No. F49620-94-1-0379. I wish to thank Dr. E. J. Mansky for numerous discussions on the content and form of this chapter and without whose expertise in computer typesetting this chapter would not have been possible.

46.6 GENERAL REFERENCES

(A) Textbooks on Scattering Theory.

N. F. Mott and H. S. W. Massey, *The Theory of Atomic Collisions* (Clarendon Press, Oxford, 1965), 3rd ed., Chaps. 2-5.

R. G. Newton, *Scattering Theory of Waves and Particles* (McGraw-Hill, New York, 1966).

L. S. Rodberg and R. M. Thaler, *Introduction to the Quantum Theory of Scattering* (Academic Press, New York, 1967).

Electronic and Ionic Impact Phenomena, edited by H. S. W. Massey, E. H. S. Burhop, and H. B. Gilbody (Clarendon Press, Oxford, 1969-1974), Vols. 1-5.

M. R. C. McDowell and J. P. Coleman, *Introduction to the Theory of Ion-Atom Collisions* (North-Holland, Amsterdam, 1970).

M. S. Child, *Molecular Collision Theory* (Academic Press, New York, 1974).

C. J. Joachain, *Quantum Collision Theory* (North-Holland, Amsterdam, 1975).

L. D. Landau and E. M. Lifshitz, *Course of Theoretical Physics* (Pergamon Press, Oxford, 1976), 3rd ed., Vol. 1, Chap. 4, p. 41.

H. Eyring, S. H. Lin, and S. M. Lin, *Basic Chemical Kinetics* (Wiley, New York, 1980), Chap. 3, p. 81.

B. H. Bransden, *Atomic Collision Theory* (Benjamin-Cummings, Menlo Park, 1983), 2nd ed.

B. H. Bransden and C. J. Joachain, *Physics of Atoms and Molecules* (Wiley, New York, 1983).

E. E. Nikitin and S. Ya. Umanskiĭ, *Theory of Slow Atomic Collisions* (Springer-Verlag, Berlin, 1984).

E. W. McDaniel, *Atomic Collisions: Electron and Photon Projectiles* (Wiley, New York, 1989), Chaps. 3 and 4, p. 71.

M. S. Child, *Semiclassical Mechanics with Molecular Applications* (Clarendon Press, Oxford, 1991).

A. G. Sitenko, *Scattering Theory* (Springer-Verlag, Berlin, 1991).

E. W. McDaniel, J. B. A. Mitchell, and M. E. Rudd, *Atomic Collisions: Heavy Particle Projectiles* (Wiley, New York, 1993), Chap. 1, p. 1.

(B) Chapters in Edited Books.

E. H. Burhop, *Theory of Collisions*, in *Quantum Theory I. Elements*, edited by D. R. Bates (Academic Press, New York, 1961), Chap. 9, p. 300.

E. A. Mason and J. T. Vanderslice, *High-Energy Elastic Scattering of Atoms, Molecules and Ions*, in *Atomic and Molecular Processes*, edited by D. R. Bates (Academic Press, New York, 1962), Chap. 17, p. 663.

B. L. Moiseiwitsch, *Elastic Scattering of Electrons*, in *Atomic and Molecular Processes*, edited by D. R. Bates (Academic Press, New York, 1962), Chap. 9, p. 281.

A. Dalgarno, *Theory of Ion-Molecule Collisions*, in *Ion-Molecule Reactions*, edited by E. W. McDaniel, V. Čermák, A. Dalgarno, E. E. Ferguson, and L. Friedman (Wiley, New York, 1970) Chap. 3, p. 159.

K. W. Ford and J. A. Wheeler, *Semiclassical Description of Scattering*, *Ann. Phys. (NY)* **7**, 259 (1959).

K. W. Ford and J. A. Wheeler, *Applications of Semiclassical Scattering Analysis*, *ibid.* 287 (1959).

M. V. Berry and K. E. Mount, *Semiclassical Approximations in Wave Mechanics*, *Rep. Prog. Phys.* **35**, 315 (1972).

W. H. Miller, *Classical-Limit Quantum Mechanics*

and the Theory of Molecular Collisions, Adv. Chem. Phys. 25, 69 (1974).

W. H. Miller, *The Classical S-Matrix in Molecular Collisions*, Adv. Chem. Phys. 30, 77 (1975).

M. S. Child, *Semiclassical Methods in Molecular Collision Theory*, in *Dynamics of Molecular Collisions: Part B*, edited by W. H. Miller (Plenum Press, New York, 1976), Chap. 4, p. 171.

H. Pauly, *Elastic Scattering Cross Sections I: Spherical Potentials*, in *Atom-Molecule Collision Theory: A Guide for the Experimentalist*, edited by R. B. Bernstein (Plenum Press, New York, 1979), Chap. 4, p. 111.

S. Stolte and J. Reuss, *Elastic Scattering Cross Sections II: Noncentral Potentials in Atom-Molecule Collision Theory: A Guide for the Experimentalist*, edited by R. B. Bernstein (Plenum Press, New York, 1979), Chap. 5, p. 231.

J. N. L. Connor, *Semiclassical Theory of Elastic Scattering in Semiclassical Methods in Molecular Scattering and Spectroscopy*, edited by M. S. Child (D. Reidel, Boston, 1980), p. 45.

R. E. Johnson, *Atomic and Molecular Collisions in Encyclopedia of Physical Science and Technology* (Academic Press, New York, 1987), Vol. 2, p. 224.

U. Buck, *Elastic Scattering II: Differential Cross Sections in Atomic and Molecular Beam Methods*, edited by G. Scoles (Oxford University Press, New York, 1988), Vol. I, Chap. 20, p. 499.

J. J. H. van Biesen, *Elastic Scattering I: Integral Cross Sections*, *ibid.* Vol. I, Chap. 19, p. 472.

REFERENCES

1. T. F. O'Malley, L. Spruch and L. Rosenberg, J. Math. Phys. 2, 491 (1961).
2. T. F. O'Malley, Phys. Rev. 130, 1020 (1962).
3. L. M. Biberman and G. E. Norman, Soviet Phys. (JETP) 18, 1353 (1964).
4. O. Hinckelmann and L. Spruch, Phys. Rev. A 3, 642 (1971).
5. G. F. Gribakin and V. V. Flambaum, Phys. Rev. A 48, 546 (1993).
6. Z. L. Petović, T. F. O'Malley and R. W. Crompton, J. Phys. B: At. Mol. Opt. Phys. 28, 3309 (1995).
7. K. W. Ford and J. A. Wheeler, Ann. Phys. (NY) 7, 259 (1959).
8. K. W. Ford and J. A. Wheeler, *ibid.* 287 (1959).
9. M. V. Berry and K. E. Mount, Rep. Prog. Phys. 35, 315 (1972).
10. *Electronic and Ionic Impact Phenomena*, edited by H. S. W. Massey, E. H. S. Burhop, and H. B. Gilbody (Clarendon Press, Oxford, 1969-1974), Vols. 1-5.
11. E. W. McDaniel, J. B. A. Mitchell, and M. E. Rudd, *Atomic Collisions: Heavy Particle Projectiles* (Wiley, New York, 1993), Chap. 1, p. 1.